DISSERTATION

A HIGHLY ENANTIO- AND DIASTEREOSELECTIVE INTRAMOLECULAR STETTER REACTION CATALYZED BY CHIRAL TRIAZOLINYLIDENE CARBENES: CATALYST AND REACTION DEVELOPMENT PLUS MECHANISTIC STUDIES

Submitted by

Javier Read de Alaniz

Department of Chemistry

In partial fulfillment of the requirements

For the Degree of Doctor of Philosophy

Colorado State University

Fort Collins, Colorado

Summer 2006

Colorado State University

May 25, 2006

WE HEREBY RECOMMEND THAT THE DISSERTATION PREPARED UNDER OUR SUPERVISION BY JAVIER READ DE ALANIZ ENTITLED A HIGHLY ENANTIO- AND DIASTEREOSELECTIVE INTRAMOLECULAR STETTER REACTION CATALYZED BY CHIRAL TRIAZOLINYLIDENE CARBENES: CATALYST AND REACTION DEVELOPMENT PLUS MECHANISTIC STUDIES BE ACCEPTED AS FULFILLING IN PART REQUIREMENTS FOR THE DEGREE OF DOCTOR OF PHILOSOPHY

Committee on Graduate Work

Prof. Richard G. Finke

Prof. Alan J. Kennan

Prof. Thomas Meersmann

Prof. Michael R. McNeil

Advisor: Prof. Tomislav Rovis

Department Head: Prof. Anthony K. Rappé

Abstract of Dissertation

A HIGHLY ENANTIO- AND DIASTEREOSELECTIVE INTRAMOLECULAR STETTER REACTION CATALYZED BY CHIRAL TRIAZOLINYLIDENE CARBENES: CATALYST AND REACTION DEVELOPMENT PLUS MECHANISTIC STUDIES

A highly enantioselective intramolecular Stetter reaction has been developed with a new family of triazolinylidene carbenes. Subjection of α,α-disubstituted Michael acceptors to an asymmetric intramolecular Stetter reaction results in a highly enantioselective conjugate addition and a diastereoselective proton transfer. Available evidence suggests the diastereoselective protonation occurs via intramolecular delivery to the sterically more hindered face of the enolate. It was demonstrated that hexamethyldisilazane (HMDS) the conjugate acid of the base, the nature of catalyst, and concentration all affect the diastereoselectivity of the reaction. The substrate scope tolerates both aromatic and aliphatic aldehydes. A variety of electron rich and poor aromatic aldehydes afford the desired product in high enantiomeric excess and good yield. The nature of the Michael acceptor can include α,β-unsaturated esters, thioesters, ketones, amides, and aldehydes. Both five and six membered rings can be formed.

This reaction has been subject of mechanistic study; deuterium and ^{13}C kinetic isotope effects suggest that the rate-determining step is proton transfer when the intramolecular Stetter reaction is conducted in the presence of HMDS. The relative rate of the reaction is dependent on the nature of the aldehyde with electron deficient

aldehydes undergoing faster reactions. Studies on the resting state of the triazolinylidene carbene in the presence and absence of HMDS were elucidated with the aide of ^{13}C-labeled catalyst. Results from these studies have realized exogenous water or oxygen is detrimental to the active carbene species during the catalytic cycle.

New reaction pathways available to *in situ* generated acyl anion equivalents have been discovered utilizing chiral triazolinylidene carbenes. The use of chiral triazolium-derived carbenes allowed for the conversion of α-haloaldehydes to esters and *N*-tosylimines to nitriles. Investigations have begun on the synthesis of a new family of chiral triazolinylidene-gold(I) complexes and their reactivity has been illustrated.

Javier Read de Alaniz

Department of Chemistry

Colorado State University

Fort Collins, CO 80523

Summer 2006

ACKNOWLEDGEMENTS

This work is dedicated in loving memory of my grandmother Carolina Alaniz, my grandfather Henry Garland Read and my brother Pablo Read.

First, I would like to thank Tomislav Rovis for fostering an environment in the laboratory that has facilitated my growth as a scientist. He has also given me the opportunity to develop independently, which has been an invaluable experience. I truly appreciate our interactions over the years and the knowledge you have passed on to me. Thanks for giving me a chance to mature at my own rate.

Without the guidance of a few very important professors, I would not be here today. Specifically, I would like to thank Professor Ted Barlett and Ron Estler for their continuous support and advice over the past ten years. I would also like to thank Professor Lou Hegedus, Alan Kennan and Al Meyers for the taking the time to share their knowledge with me.

I would like to thank Chris Rithner, Donald L. Dick, and Susie Miller for all their assistance over the years.

Thanks to everyone in the Rovis Group past and present. I would especially like to thank Eric Bercot and Mark S. Kerr who were there from the beginning and made my daily life better. Thanks to Dr. Ernest Lee, Jennifer Moore, Dr. Arturo Orellana and Dr. Jeff Johnson for proofreading this dissertation. I want to thank all the friends I have made over the years who helped me keep my sanity and were my saving grace outside the lab, especially Annie for her friendship.

Last and most importantly I would like to thank my loving family. Without their support and guidance none of this would be possible. I have the highest regard

for each and every one of you (Mom, Dad, Pablo, Mariam, Angelina and David). I am honored to be your son and brother. My future wife Susanne, I can never thank you enough for being there with me through this experience. You are the person that keeps me going, makes me smile, picks me up and not enough can be said about how big and pure your heart is. You have taught me the most important lesson of all... "chemistry is not just a class".

Table of Contents

Chapter 4. Developing New Catalytic Reactions Utilizing Triazolinylidene Carbenes

LIST OF ABBREVIATIONS

AcOH	acetic acid
Boc_2O	di-*tert*-butyl dicarbonate
DABCO	1,4-diazabicyclo[2.2.2]octane
DBU	1,8-diazabicyclo[5.4.0]undec-7-ene
DCC	dicyclohexylcarbodiimide
DPPE	1,2-bis(diphenylphosphino)ethane
DMAP	4-(dimethylamino)pyridine
HMDS	hexamethyldisilazane
Hünigs Base	di-isopropylethyl amine
KIE	kinetic isotope effect
KHMDS	potassium bis(trimethylsilyl)amide
Pd_2dba_3	tris(dibenzylideneacetone)dipalladium(0)
TEA	trimethylamine
TFA	trifluoroacetic acid
TsOH	*para*-toluenesulfonic acid

Chapter 1

The Development of Chiral Bicyclic Triazolium Salts

1.1 Introduction

Beginning as an academic curiosity, carbenes have played an important role in organic chemistry. In the last 15 years, our understanding of carbene chemistry has advanced dramatically.[1] Carbenes are neutral compounds featuring a divalent carbon atom with only six electrons in its valence shell. Carbenes have two electrons that do not participate in bonding and can be spin-paired (singlet state **1**) or unpaired (triplet state **2**). Characteristically, carbenes are highly reactive intermediates typically used *in situ*, however, with appropriate substituents flanking the carbene carbon stable carbenes such as **3** or **4** can be isolated.

Scheme 1.

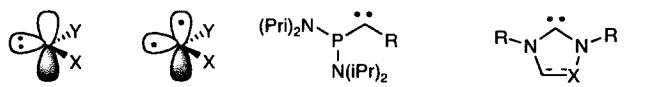

1 singlet carbene

2 triplet carbene

3 R = $SiMe_3$, CF_3, aryl (Bertrand)

4 R = alkyl, aryl; X = carbon or nitrogen; stable singlet carbene (Arduengo)

The study of stable nucleophilic carbenes has received considerable impetus since the first isolation of phosphanylsilycarbenes and imidazol-2-ylidenes by Bertrand[2] and Arduengo[3] in 1988 and 1991, respectively. These landmark papers solidified the *in situ* evidence first collected by Wanzlick[4] and others,[5] indicating that stable nucleophilic carbenes could be achieved from thiazole, benzothiazole, imidazolone and imidazole. The inherent stability of *N*-heterocyclic carbenes (NHCs) has been attributed to both electronic and steric effects. Arduengo carbenes

are stable singlet state carbenes that contain two nitrogen substituents on either side of the carbene carbon, they are nucleophilic in nature. The nucleophilic reactivity of the NHCs is attributed to the lone pair of electrons of the carbene found in the σ-orbital that lies perpendicular to the empty p-orbital. The lone pair of electrons on the two nitrogen substituents that sandwich the carbene center donate electron density into the empty p-orbital of the carbene, thus helping to stabilize the carbene intermediate. The bent geometry of NHCs increases the energy gap between the empty p-orbital and the σ-orbital, thus increasing the s character of the σ-orbital. The stabilization by the flanking nitrogen substituents and bent geometry combined favor the carbene in the singlet ground state (Scheme 2).[1]

Scheme 2.

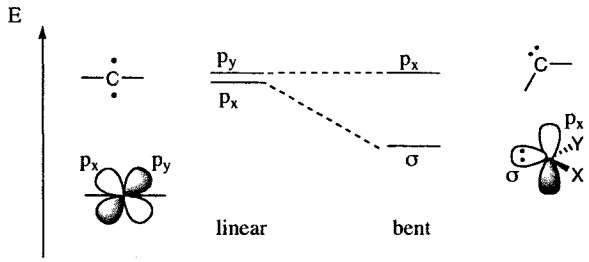

N-Heterocyclic carbenes have been a significant area of research since their description by Wanzlick and Arduengo. These compounds have found their primary utilization as ligands for various metal catalyzed transformations.[6] The use of NHCs as ligands has lead to major advances in the area of Ru-catalyzed alkene metathesis[7] and Pd-catalyzed carbon-carbon bond forming reactions.[8] These ligands are excellent σ-donors and can be used as surrogates for phosphines, in metal complexes. In most cases, NHC-metal complexes provide analogous stability and reactivity to phosphine-metal complexes. Moreover, in some cases NHCs have been shown to outperform

phosphine complexes.[9] Although the coordination chemistry and organometallic reactions of NHC-metal complexes have been studied extensively, their application as small molecule catalysts is a burgeoning field, one in which very little is known about their catalytic activity.[10] Reactions that are catalyzed by NHCs are an underdeveloped field that has a seemingly vast and untapped potential.

In the last five years there has been a surge of investigation directed toward their use as catalysts. The majority of studies have focused on the use of thiazolium salts and more recently on triazolium salts as pre-catalyst for a variety of organic transformations. The advantage of applying NHCs to catalyze carbon bond forming reactions is the potential for asymmetric induction. At the beginning of our studies we hypothesized that chiral bicyclic triazolium salts could serve as excellent pre-catalysts to *N*-heterocyclic carbenes. Consequently, we set out to synthesize a new family of chiral triazolinylidene carbenes and apply them to various asymmetric organic transformations. A long-term goal of this project was to understand the behavior of these new triazolium salts with an eye on developing new organic and transition-metal transformations.

1.1.1 History of *N*-Heterocyclic Carbenes

Although the isolation of the first stable *N*-heterocyclic carbene did not occur until 1990, research focused on the reactivity of *in situ* generated species dates back to 1943.[11] The reactivity of *N*-heterocyclic carbenes encompasses dipole-stabilized thiocarbonyl ylides and imidazol-2-ylidenes. A brief history of the chiral catalyst scaffolds that have been used to catalyze organic transformations will be presented first in order to fully understand our catalyst design. The benzoin reaction is used as

a model reaction to compare the different chiral scaffolds; however, a full evaluation of the catalytic potential of the NHCs will be outlined in subsequent chapters.

1.1.2 The Development of Chiral Thiazolium Salts

The catalytic reactivity of thiazolium salts originated in 1943 when Ukai *et al.*, reported that thiazolium salts catalyze the benzoin reaction in the presence of base.[12] In 1958 Breslow recognized the powerful implications of this reaction and elucidated the catalytic role of vitamin B_1 enzyme cofactor thiamine, a naturally occurring thiazolium salt.[13] In the presence of a base, thiamine **5** generates an active nucleophilic carbene species **5a** that reacts with an aldehyde and, after proton transfer, forms an acyl anion equivalent **6**, commonly known as the Breslow intermediate. Carbon-carbon bond formation results from nucleophilic attack of the Breslow intermediate with another aldehyde, resulting in the formation of α-hydroxy ketones (Scheme 3).

Scheme 3.

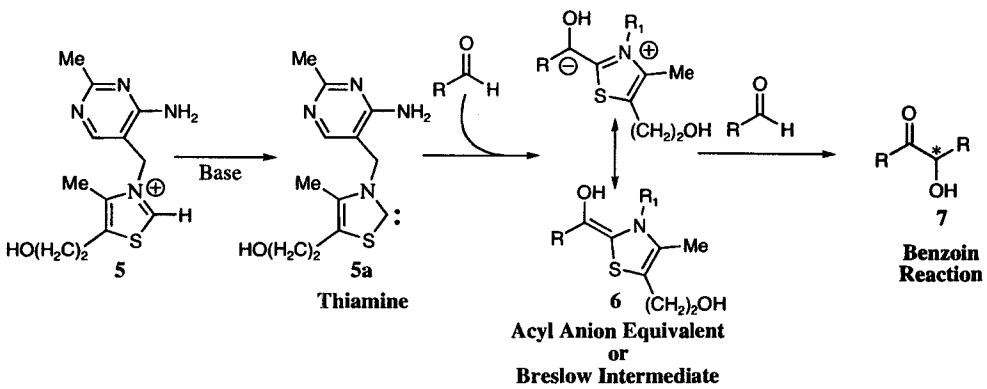

Thiazolium salts quickly became of interest because they facilitated the formation of carbon-carbon bonds and possess the potential for asymmetric catalysis. Sheehan and Hunneman first reported an asymmetric benzoin reaction that proceeded in modest enantioselectivity utilizing chiral thiazolium catalyst.[14] Two years later

Sheehan and Hara improved upon their own results and reported, for the time, an enantioselective benzoin reaction utilizing chiral thiazolium catalysts **10a-b** (Scheme 4).[15]

Scheme 4.

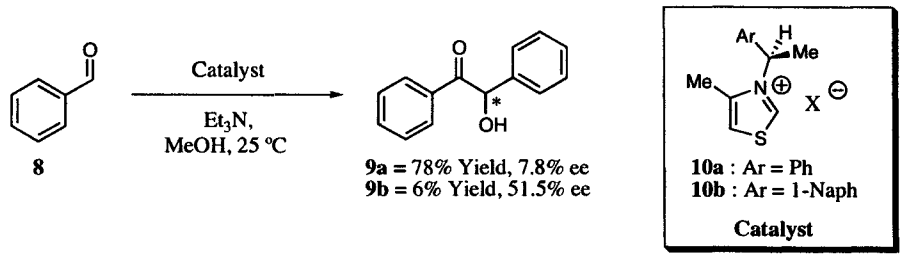

Over the next three decades numerous research groups tried to improve on Sheehan's initial asymmetric reaction of **9** utilizing a variety of chiral thiazolium salts. Despite a wide range of different chiral scaffolds (**11**,[16] **12**,[17] or **13**[18]) the reaction suffered from low reactivity and selectivity (Scheme 5, 18-35% ee).

Scheme 5.

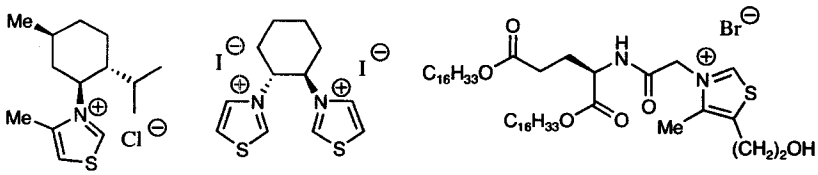

Enders and co-workers were able to increase the reactivity and selectivity (75% ee) of the benzoin reaction by employing triazolium salts (Scheme 6). They illustrated that triazolium salts such as **14** mimic the reactivity of thiazolium salts.[19]

Scheme 6.

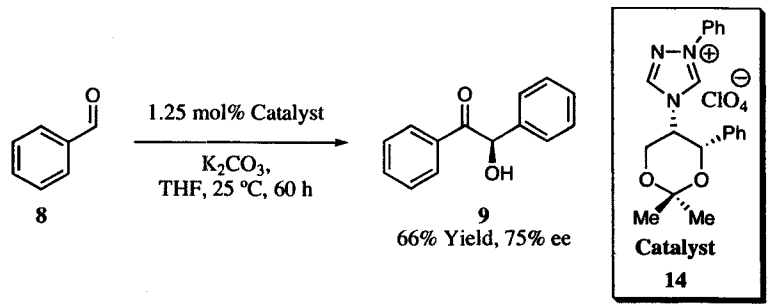

From 1966 to 1996, all chiral thiazolium and triazolium catalyst scaffolds reported shared the common feature of free rotation around the chiral center. Leeper and co-workers reasoned the low ee's obtained for the benzoin reactions were a result of free rotation available to the chiral side-chain. With this in mind, they synthesized two new families of chiral thiazolium salts: one, where the top face of the chiral bicyclic thiazolium salt is blocked by a bulky substituent (**15** and **16**),[20] and another where the chirality is fused into the backbone of a [2.2.2] bicyclic system (**17**).[21] Shortly after Leeper's initial report, Rawal and co-workers reported a new bicyclic chiral thiazolium salt **18** that they reasoned would increase the enantiomeric excess of the benzoin reaction by minimizing the number of possible transition states.[22]

Scheme 7.

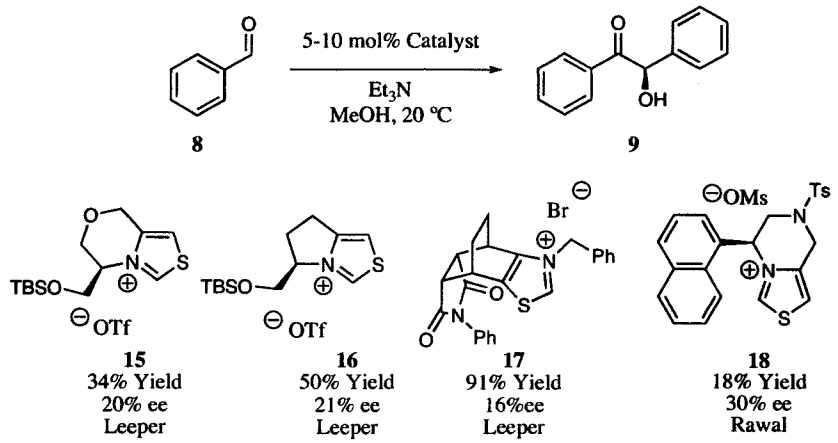

Unfortunately, only modest increases in enantioselectivity and reactivity were achieved with the bicyclic thiazolium salts. Leeper and co-workers were able to perform an enantioselective benzoin reaction in good ee's when they combined the increased reactivity of triazolium salts with the inherit rigidity of a fused bicyclic system (Scheme 8).[23]

Scheme 8.

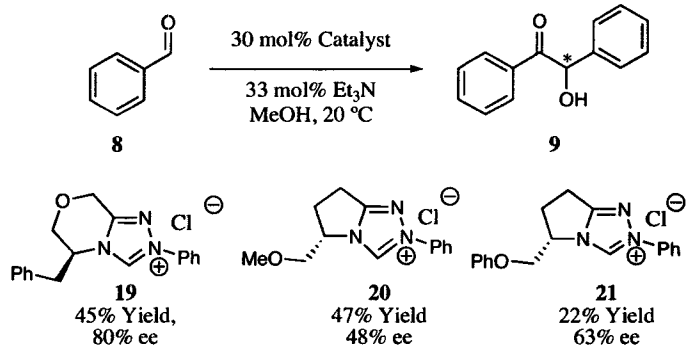

1.2 Development of a New Family of Chiral Triazolium Salts

To develop the utility of *N*-heterocyclic carbenes in asymmetric catalysis, we pursued a practical and efficient synthesis of a new family of triazolium salts. Our focus in the early stage of this research pivoted around the incorporation of easily

accessible chiral building blocks into a rigid framework that could be manipulated. Catalyst preparation from amino acid derivatives was desirable in order to take advantage of their diverse steric profile and availability. Two different chiral bicyclic cores (**22** and **23**) were envisioned to possess the qualities stated above (Scheme 9).

Scheme 9.

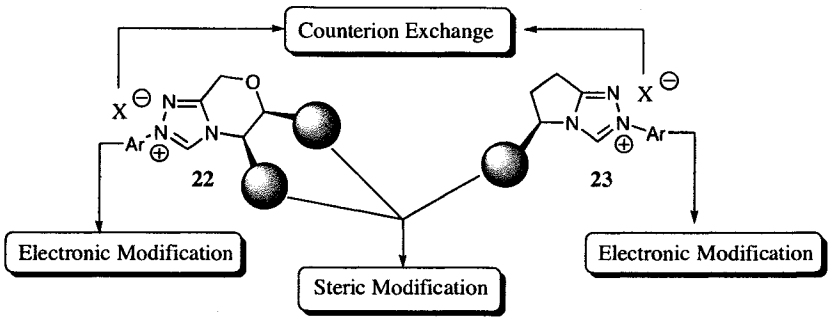

1.2.1 Changing the Steric Environment of the Triazolium Salts

Our investigations began with the synthesis of the requisite morpholinones and pyrrolidinones according to literature precedent.[24] Mark S. Kerr in the Rovis group pursued development of bicyclic core **22** while I pursued the synthesis of **23**. Independent synthesis of the two bicyclic cores led to the expedient development of two different chiral bicyclic catalysts.

Synthesis of enantiopure pyrrolidinone **27** began with Boc protection of *L*-phenylalanine according to Meyers' procedure (Scheme 10).[25] Meyers' protocol enables large quantities (~100 grams) of *N*-Boc protected phenylalanine to be prepared as a pure white crystalline solid. The synthesis of the pyrrolidinone core was realized according to literature precedent, commencing from the *N*-Boc protected phenylalanine.[26] Coupling of the Boc-protected amino acid with Meldrum's acid in the presence of DMAP and DCC affords the desired product that can be used without further purification. Reduction of the ketone with slow addition of 2.5 equivalents of

sodium borohydride at 0 °C over 3 hours, followed by stirring at 0 °C for 24 hours, provides the desired product as a yellow oil **26**. Initial attempts at using the resulting oil resulted in a complicated purification of the desired pyrrolidinone **27**. However, **26** can be recrystallized from diethyl ether affording an analytically pure white crystalline solid. Cyclization of **26** in toluene at 110 °C, followed by removal of the *N*-Boc protecting group with trifluoroacetic acid, gives the desired pyrrolidinone **27** as yellow oil that can be used without further purification. Pyrrolidinone **27** was reported to be a yellow solid;[18] however, we found a solid was only obtained after complete removal of the residual solvent *in vacuo*. The oil and the solid were indistinguishable spectroscopically and behave identically in the subsequent reactions; therefore, removal of residual solvent is unnecessary.

Scheme 10.

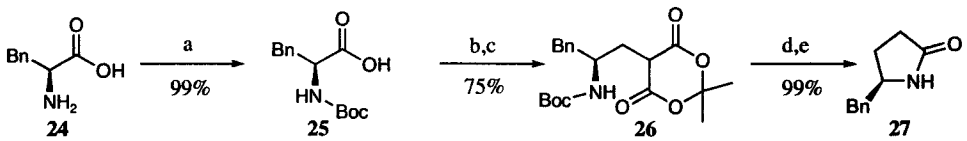

(a) Boc_2O, NaOH, THF/H_2O, 23 °C (b) Meldrum's acid, DMAP, DCC, CH_2Cl_2, 0 °C (c) AcOH, $NaBH_4$, CH_2Cl_2, 0 °C (d) Toluene, 110 °C (e) TFA, CH_2Cl_2, 0 °C.

With the pyrrolidinone **27** in hand, a one-pot modification of the Leeper synthesis was used for the three-step conversion into triazolium salt **28** (Scheme 11). O-Methylation of **27** with Meerwein's reagent produce the desired amidate **29**, which was treated in situ with phenylhydrazine to generate a red solution that corresponded to the desired cyclization precursor **30**. Final cyclization with trimethyl orthoformate at 80 °C in a 7:1 mixture of trimethyl orthoformate and methanol affords triazolium salt **28**. The triazolium salt was precipitated from ethyl acetate and then recrystallized from hot methanol affording a white crystalline solid that is air and water stable. The

synthesis of triazolium salt **28** is amenable to large-scale preparation without chromatography or deviation from the described procedure. The reaction commencing from 20 grams of *N*-Boc protected phenylalanine resulted in 16 grams of the desired triazolium salt.

Scheme 11.

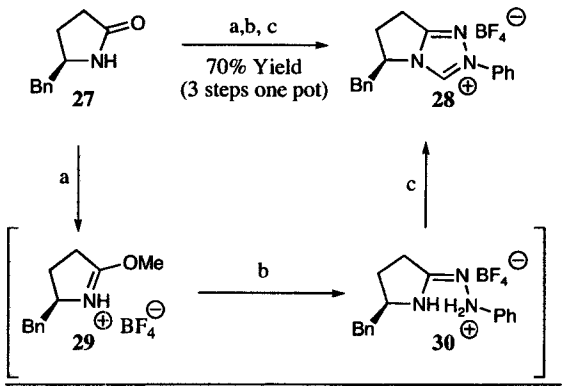

(a) $Me_3O^+BF_4^-$, CH_2Cl_2, 23 °C, 24 h (b) $PhNHNH_2$, CH_2Cl_2, 23 °C (c) $CH(OMe)_3$: MeOH (7 : 1), 80 °C

The synthesis of the chloride counter ion analogue of triazolium salt **28** was accomplished with the same protocol as above, but proved slightly more challenging (Scheme 12, path a). Formation of the phenylhydrazone tetrafluoroborate ($^-BF_4$) adduct was prepared as described above. Treatment with 10% HCl afforded the desired product **30** as the chloride salt after extraction with methylene chloride. Unfortunately, this procedure proved irreproducible and red oil was often obtained instead of the desired solid HCl salt. We hypothesized the desired product was too hygroscopic and removal of water was complicating the formation of the desired HCl salt. We therefore turned our attention to a new route that did not require the addition of 10% HCl for the generation of the chloride counter ion (Scheme 12, path b).

O-Methylation of pyrrolidinone **27** with Meerwein's reagent generates the amidate **29** after ice-cold aqueous sodium bicarbonate work-up. It is important to

note that hydrolysis of the amidate is not observed when exactly 3 mL of ice-cold aqueous sodium hydrogen carbonate is used per mmol of pyrrolidinone.[27] Addition of phenylhydrazine hydrogen chloride salt to the neutral amidate **29** afforded the desired hydrazone chloride salt **30** after 24 hours at room temperature. With **30** in hand, one could reproducibly obtain the desired triazolium chloride salt, **31**.

Scheme 12.

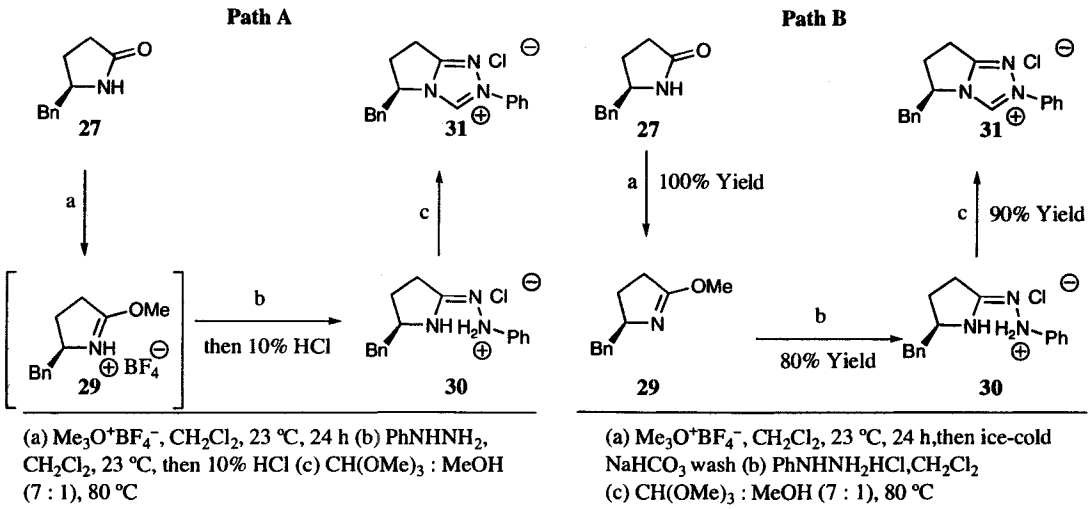

An X-ray crystal structure of the chloride salt **31** was obtained. The crystal structure shows that the two bicyclic rings are in plane as expected. Furthermore, the N(1)-Phenyl ring is only slightly twisted out of plane with the bicycle and the chiral benzyl scaffold is sitting above the plane of the bicyclic core. The angle between the N(3)-C(13)-N(1) was determined to be 106.5° (2) which is consistent with other known imidazolium and triazolium salts.

Scheme 13.

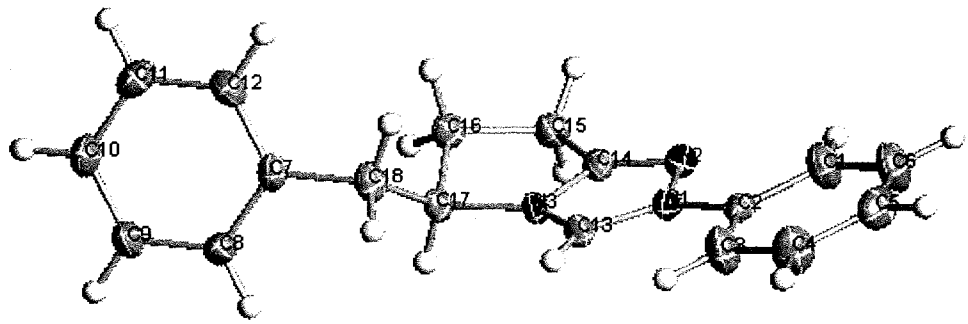

Distance	Å	Angle	
C(13)-N(1)	1.323 (3)	N(3)-C(13)-N(1)	106.5 ° (2)
C(13)-N(3)	1.319 (3)	N(2)-N(1)-C(2)	127.7 ° (17)
C(14)-N(2)	1.304 (3)	C(13)-N(1)-C(2)	127.7 ° (2)

With the successful conversion of phenylalanine into the triazolium salt, we began to incorporate other amino acid chiral scaffolds into triazolium salts. Valine, *tert*-leucine, and 2-phenylglycine were initially chosen to evaluate the steric effects of the triazolium salts. To our gratification the same route developed for the phenylalanine-derived pyrrolidinone could be applied to new amino acid derived pyrrolidinones in good overall yield. In addition, the new pyrrolidinones were highly crystalline and treatment of **47-49** with 10% HCl provided the corresponding chloride

salts as pure off-white solids that could be converted into the corresponding triazolium salts (Scheme 14).

Scheme 14.

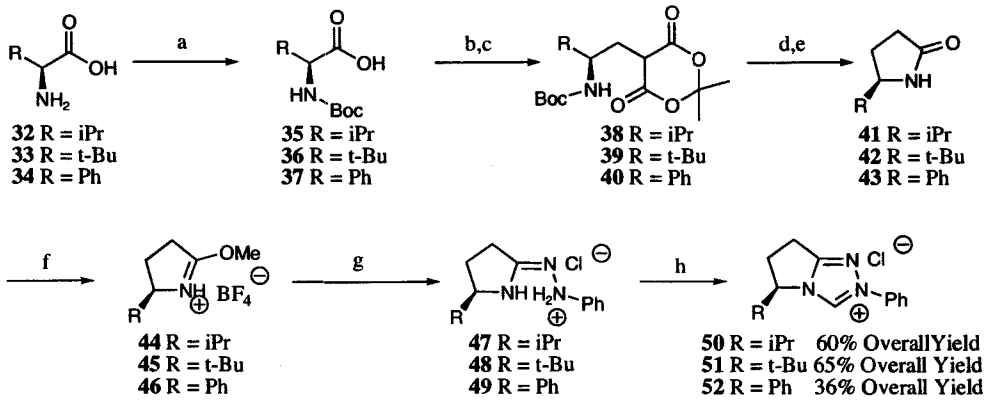

(a) Boc_2O, NaOH, THF/H_2O, 23 °C (b) Meldrum's acid, DMAP, DCC, CH_2Cl_2, 0 °C (c) AcOH, $NaBH_4$, CH_2Cl_2, 0 °C; (d) Toluene, 110 °C (e) TFA, CH_2Cl_2, 0 °C; (f) $Me_3O^+BF_4^-$, CH_2Cl_2, 23 °C, 24 h (g) $PhNHNH_2$,CH_2Cl_2, then washed with 10% HCl (h) $CH(OMe)_3$: MeOH (7 : 1), 80 °C.

Enantiopure pyrrolidinone derived from glutamic acid is commercially available as the oxygen protected tosylate **53** and can be easily converted into the desired triazolium chloride salt **54**, (Scheme 15), according to the previously described three step procedure (Scheme 12, path b). Unfortunately, the desired triazolium salt is isolated as yellow oil. In an attempt to obtain a solid triazolium salt, a counter-ion exchange reaction was performed. The oil was taken up in a biphasic 1:1 mixture of H_2O and CH_2Cl_2 in the presence of one equivalent of sodium tetraphenylborate and stirred overnight. The CH_2Cl_2 was separated, dried over $MgSO_4$ and the solvent removed *in vacuo* to afford the desired triazolium salt **54** as a yellow crystalline solid. Tetraphenylborate counter ion exchange is a valuable technique for obtaining crystalline material when the desired triazolium chloride or tetrafluoroborate salt is obtained as hygroscopic oil.

Scheme 15.

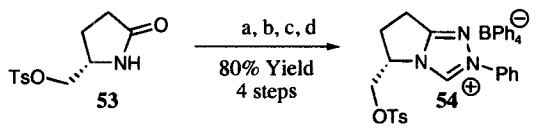

(a) $Me_3O^+BF_4^-$, CH_2Cl_2, 23 °C, 24 h, then ice-cold $NaHCO_3$ wash (b) PhNHNHHCl, CH_2Cl_2, 23 °C, (c) $CH(OMe)_3$: MeOH (7 : 1), 80 °C, (d) $Na^+BPh_4^-$, H_2O:CH_2Cl_2 (1:1), 24 h.

1.2.2 Tuning the Electronic Nature of the Triazolium Salts

With access to optically pure pyrrolidones, we turned our attention to the incorporation of electron rich or poor hydrazines. We reasoned that an increase in reactivity and stabilization of the carbene could be achieved through conjugation of the *N*-aryl substituent containing electron donating or withdrawing groups. Without a prior understanding of the electronic effects of the hydrazines, we decided to develop the synthesis of both types of catalyst.

Commencing with the phenylalanine-derived pyrrolidinone **27** we were able to synthesize four new chiral triazolium salts. The reaction proceeds uneventfully for the *p*-methoxyphenylhydrazine affording the desired product as an off white solid in 80% yield over three steps.

Scheme 16.

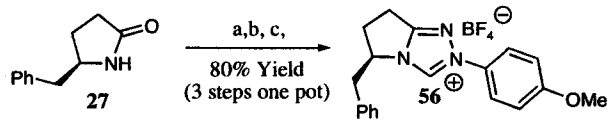

(a) $Me_3O^+BF_4^-$, CH_2Cl_2, 23 °C, 24 h (b) *p*-MeOPhNHNH$_2$, CH_2Cl_2, 23 °C (c) $CH(OMe)_3$: MeOH (7 : 1), 80 °C.

In contrast, electron withdrawing arylhydrazines were sluggish to cyclize with trimethylorthoformate:MeOH (7:1) at 80 °C and unreacted starting material was recovered. For this reason we switched to more forcing cyclization reaction conditions in order to obtain the desired product. Treatment of the arylhydrazone adduct with triethylorthoformate:MeOH (7:1) at 110 °C for 24 to 48 hours generated the desired triazolium salts in modest to good overall yield (Scheme 17).

Scheme 17.

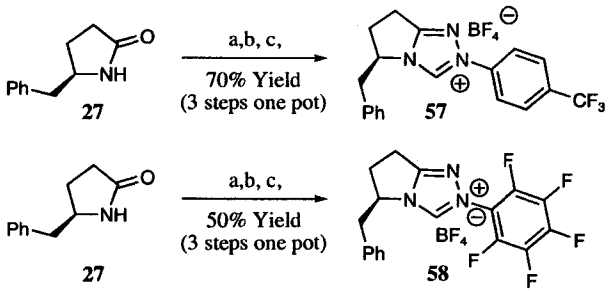

(a) $Me_3O^+BF_4^-$, CH_2Cl_2, 23 °C, 24 h, (b) *p*-CF_3PhNHNH$_2$ or F_5PhNHNH$_2$,CH_2Cl_2, 23 °C (c) $CH(OEt)_3$: MeOH (7 : 1), 110 °C.

In order to evaluate the steric effects of the substituent bound to the nitrogen of the chiral triazolium salt we prepared *N*-benzyl triazolium salt **60** according to the standard procedure (Scheme 11) in 77% yield over three steps (Scheme 18). All the triazolium salts prepared to date are air and water stable solids that can be stored

indefinitely on the benchtop without any special precaution. Hygroscopicity of the solid triazolium salts has not been observed.

Scheme 18.

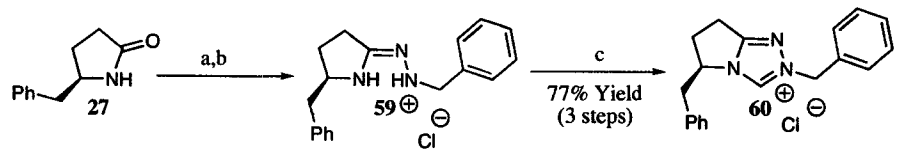

(a) $Me_3O^+BF_4^-$,, CH_2Cl_2, 23 °C, 24 h, (b) $PhCH_2NHNH_2$, CH_2Cl_2, 23 °C, then washed with 10% HCl
(c) $CH(OMe)_3$: MeOH (7 : 1), 80 °C.

1.2.3 pKa of Thiazolium, Imidazolium and Triazolium Salts

Even though it has been over 40 years since Breslow[28] and Olofson[29] discovered the facile deuterium exchange of the C(2)-protons of the thiamine and imidazolium cations in D_2O, respectively, only recently has effort been devoted to the correlation of structural features to carbene basicity.[30] To our knowledge there have been no studies directed toward the pKa of triazolium salts. In general, thiazolium salts have a lower pKa than imidazolium salts but there are only a few experimental calculations of these pKa values (**61**,[31] **62**,[32] **63**,[33] **64**,[29] **65**[34]) to base this generalization on (Scheme 19).

Scheme 19.

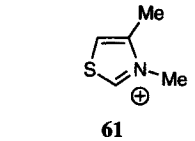

61
pKa (DMSO) = ~ 16.5

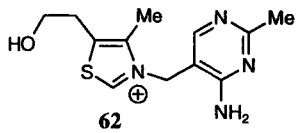

62
pKa (H_2O) = 18

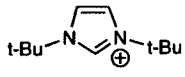

63
pKa (DMSO) = 23.04

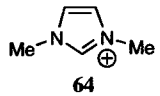

64
pKa (H_2O) = 23.0

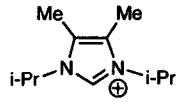

65
pKa (DMSO) = 24

The pKa values of a number of thiazolium and imidazolium salts have been computationally estimated.[35] Comparison of the experimental value and the calculated value are in general agreement; for example, Yates and co-workers obtained a pKa value of 22.6 ± 0.09 for the calculation of **63** in DMSO. Similarly, the basicity of 1,3-diisopropyl-4,5-dimethylimidazol-2-ylidene (**65**) was calculated to be 24.5 ± 0.15.

In a recent collaboration with Yates the calculated pKa of our triazolium salts was described in H_2O, and found to range between 16.9 and 20.7 (Scheme 20). The calculations support our hypothesis that basicity/nucleophilicity of the catalyst can be tuned by changing the electron donating or withdrawing nature of the *N*-aryl substituent (**66-69**). The size and nature of the bicyclic ring only shows a moderate effect on the pKa values of the triazolium salts (**66** and **70-73**).

Scheme 20.

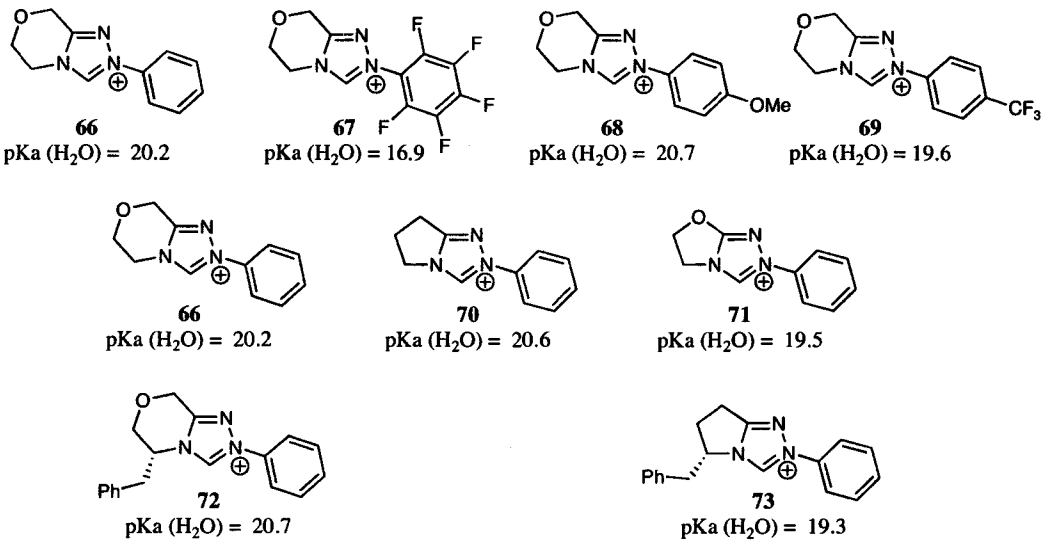

1.3 Conclusion

We developed a practical and efficient synthesis of a new family of chiral triazolium salts commencing from readily available amino acids. We can vary the counter ion of the triazolium salts by employing aryl hydrazine hydrogen chloride salts or, more conveniently, by counter ion exchange reactions. Furthermore the electronic nature of the triazolium salts can be tuned by a late stage variation of the aryl hydrazine. With access to a family of new chiral triazolium salts we set out to probe their ability to participate as nucleophilic catalysts with a variety of electrophilic species. In addition, the close analogy of NHCs to phosphine complexes makes them an attractive chiral ligand for metal catalyzed reactions. Our subsequent efforts focused on the realization of these goals.

References

[1] (a) Tomioka, H. *Acc. Chem. Res.* **1997**, *30*, 315-321. (b) Bourissou, D.; Guerret, O.; Gabbaï, F. P.; Bertrand, G. *Chem. Rev.* **2000**, *100*, 39-91.

[2] Igau, A.; Grutzmacher, H.; Baceiredo, A.; Bertrand, G. *J. Am. Chem Soc.* **1988**, *110*, 6463-6466.

[3] Arduengo, A. J.; Dias, R. L.; Harlow, R.; Kline, M. *J. Am. Chem. Soc.* **1991**, *113*, 361-363.

[4] (a) Wanzlick, H. W.; Kleiner, H. J. *Angew. Chem.* **1961**, *73*, 493. (b) Wanzlick, H. W. *Angew. Chem.* **1962**, *74*, 129. (c) Wanzlick, H. W.; Esser, T.; Kleiner, H. J. *Chem. Ber.* **1963**, *96*, 1208.

[5] For a review, see; Shvaika, O. P.; Korotkikh, N. I.; Aslanov, A. F. *Chemistry of Heterocyclic Compounds* **1992**, *9*, 1155.

[6] For a review, see; (a) Herrmann, W. A. *Angew. Chem., Int. Ed.* **2002**, *41*, 1290-1309. (b) Perry, M. C.; Burgess, K. *Tetrahedron: Asymmetry* **2003**, *14*, 951-961.

[7] (a) Trnka, T. M.; Grubbs, R. H. *Acc. Chem. Res.* **2001**, *34*, 18-29. (b) Jafarpour, L.; Nolan, S. P. *J. Organomet. Chem.* **2001**, *617-618*, 17-27.

[8] Hillier, A. C.; Grasa, G. A.; Viciu, M. S.; Lee, H. M.; Yang, C.; Nolan, S. P. *J. Organomet. Chem.* **2002**, *653*, 69-82.

[9] (a) Peris, E.; Loch, J. A.; Mata, J.; Crabtree, R. H. *Chem. Commun.* **2001**, 201-202. (b) Briot, A.; Bujard, M.; Gouverneur, V.; Nolan, S. P.; Mioskowski, C. *Org. Lett.* **2000**, *2*, 1517-1519.

[10] For reviews, see: (a) Enders, D.; Balensiefer, T. *Acc. Chem. Res.* **2004**, *37*, 534-541. (b) Johnson, J. S.; *Angew. Chem., Int. Ed.* **2004**, *43*, 1326-1328. (c) Pohl. M.; Lingen, B.; Muller, M. *Chem. Eur. J.* **2002**, *8*, 5288-5295.

[11] Ukai, T.; Tanaka, R.; Dokawa, T. *J. Pharm. Soc. Jpn.* **1943**, *63*, 296-300.

[12] See reference 11.

[13] Breslow, R. *J. Am. Chem. Soc.* **1958**, *80*, 3719-3726.

[14] Sheehan, J. C.; Hunneman, D. H. *J. Am. Chem. Soc.* **1966**, *88*, 3666-3667.

[15] Sheehan, J. C.; Hara, T. *J. Org. Chem.* **1974**, *39*, 1196-1199.

[16] Tagaki, W.; Tamura, Y.; Yano, Y. *Bull. Chem. Soc. Jpn.* **1980**, *53*, 478-480.

[17] Martí, J.; Castells, J.; López-Calahorra, F. *Tetrahedron Lett.* **1994**, *35*, 699-702.

[18] Yamashita, K.; Sasaki, S-I.; Osaki, T.; Nango, M.; Tsuda, K. *Tetrahedron Lett.* **1995**, *36*, 48-16-4820.

[19] Enders, D.; Breuer, K. *Helv. Chim. Acta* **1996**, *79*, 1217-1221.

[20] Knight, R. L.; Leeper, F. J. *Tetrahedron Lett.* **1997**, *38*, 3611-3614.

[21] Gerhard, A. U.; Leeper, F. J. *Tetrahedron Lett.* **1997**, *38*, 3615-3618.

[22] Dvorak, C. A.; Rawal, V. H. *Tetrahedron Lett.* **1998**, *39*, 2925-2928.

[23] Knight, R. L.; Leeper, F. J. *J. Chem. Soc., Perkin Trans. 1*, **1998**, 1891-1893.

[24] Kerr, M. S.; Read de Alaniz, J.; Rovis, T. *J. Org. Chem.* **2005**, *70*, 5725-5728.

[25] Meyers, A. I.; Tavares, F. X. *J. Org. Chem.* **1996**, *61*, 8207-8215.

[26] Smrcina, M.; Majer, P.; Majerová, E.; Guerassina, T.; Eissenstat, M. A. *Tetrahedron*, **1997** *53*, 12867-12874.

[27] Enders, D.; Kallfass, U. *Angew. Chem., Int. Ed.* **2002**, *41*, 1743-1745.

[28] Breslow, R. *J. Am. Chem. Soc.* **1958**, *80*, 3719-3726.

[29] Olofson, R. A.; Thompson, W. R.; Michelman, J. S. *J. Am. Chem. Soc.* **1964**, *86*, 1865-1866.

[30] Amyes, T. L.; Diver, S. T.; Richard, J. P.; Rivas, F. M.; Toth, K. *J. Am. Chem. Soc.* **2004**, *125*, 4366-4374 and references therein.

[31] Bordwell, F. G.; Satish, A. V. *J. Am. Chem. Soc.* **1991**, *113*, 985-990.

[32] Washabaugh, M. W.; Jencks, W. P. *Biochemistry* **1988**, *27*, 5044-5053.

[33] Kim, Y-J.; Streitwieser, A. *J. Am. Chem. Soc.* **2002**, *124*, 5757-5761.

[34] Alder, R. W.; Allen, P. R.; Williams, S. J. *J. Chem. Soc., Chem. Commun.* **1995**, 1267-1268.

[35] Magill, A. M.; Cavell, K. J.; Yates, B. F. *J. Am. Chem. Soc.* **2004**, *126*, 4366-4374.

Chapter 2

The Development of an Asymmetric Intramolecular Stetter Reaction Catalyzed by Chiral Triazolinylidene Carbenes.

2.1 Introduction

The increasing demand for efficient carbon-carbon bond forming reactions that result in the formation of asymmetric stereocenters has mandated the development of new reaction manifolds. The inversion of the normal mode of reactivity of aldehydes by cyanide or heteroazolium salt derived carbenes has emerged as a synthetically useful way of constructing carbon-carbon bonds. The catalytic version of this concept was first discovered in the context of the benzoin reaction and was later extended to the Stetter reaction.[1] The key element of the benzoin and Stetter reactions is the polarity reversal of the carbonyl initiated by nucleophilic attack of the catalyst to an aldehyde generating an acyl anion equivalent that can facilitate the formation of a carbon-carbon bond. The design of asymmetric catalytic systems that are capable of reversing aldehyde polarity is a fascinating area of research, due in part to their *in situ* ability to form acyl anion equivalents and the mild reaction conditions employed during the carbon bond-forming event. Traditional methods of forming umpolung reagents from aldehydes involve the use of dithianes or protected cyanohydrin derivatives.[2] These methods are stoichiometric and often require strong bases to generate the acyl anion equivalent.

The benzoin reaction has a long and illustrious history that dates back to 1832, when Wohler and Liebig demonstrated that cyanide anions catalyze the benzoin reaction.[3] Lapworth later proposed the currently accepted mechanism of the cyanide

anion catalyzed benzoin reaction in 1904.[4] In 1958 Breslow elucidated the mechanism of the benzoin reaction with thiazolium catalyst and showed the similarities between the active thiazolium catalyst and cyanide anion.[5] Breslow's discovery helped elucidate the catalytic role of vitamin B_1 enzyme cofactor thiamine, a naturally occurring thiazolium salt. In the enzymatic system, thiamine diphosphate adds to pyruvate to provide a stabilized intermediate that can permit facile loss of carbon dioxide and generate acetaldehyde.[6] It has been a long-standing goal of organic chemists to develop reaction systems that are capable of mimicking nature without the bulky protein around them to catalyze the reaction. Thiamine provided chemists with the platform to develop new chiral catalysts, where success is judged by their selectivity and reactivity.

2.2 The Accepted Mechanism of the Benzoin Reaction

The accepted mechanism for the benzoin reaction with cyanide anion or thiazolium derived carbenes was originally elucidated by Lapworth and Breslow, respectively. In the case of thiazolium salts the active catalyst is formed in situ by deprotonation of the thiazolium salt. The resulting thiazol-2-ylidene **I**, the active catalyst, then adds to the aldehyde to generate tetrahedral intermediate **II**. Proton transfer affords the acyl anion equivalent **III**, commonly known as the Breslow intermediate. Carbon-carbon bond formation occurs from nucleophilic attack of the Breslow intermediate with another molecule of aldehyde. A second proton transfer from intermediate **IV** followed by catalyst expulsion, closes the catalytic cycle (Scheme 1).

Scheme 1.

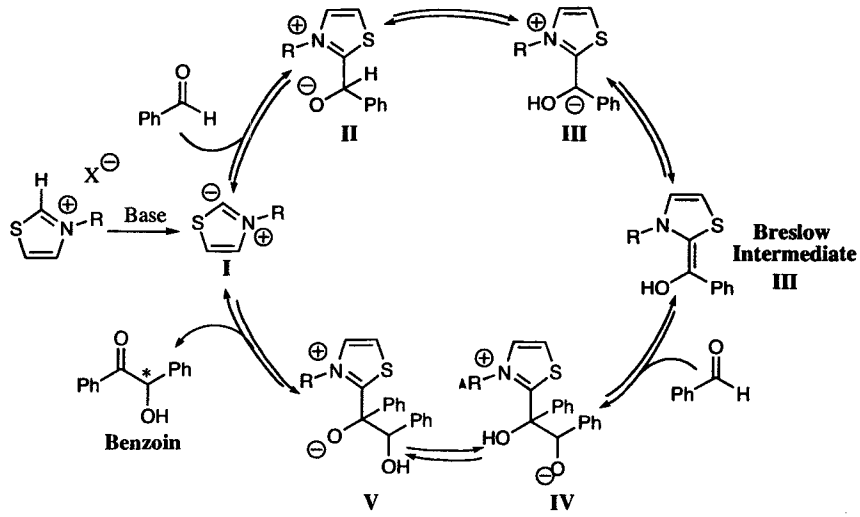

2.3 Asymmetric Benzoin Reaction

Since the discovery of the benzoin reaction the attention of many chemists has been devoted to trying to develop heteroazolium-catalyzed asymmetric nucleophilic acylation reactions, with the benzoin reaction serving as the testing platform. A variety of chiral thiazolium salts have seen extensive application in the asymmetric benzoin reaction. Unfortunately, the asymmetric benzoin reaction resulted in low reactivity and selectivity for 30 years (Scheme 2).

Scheme 2.

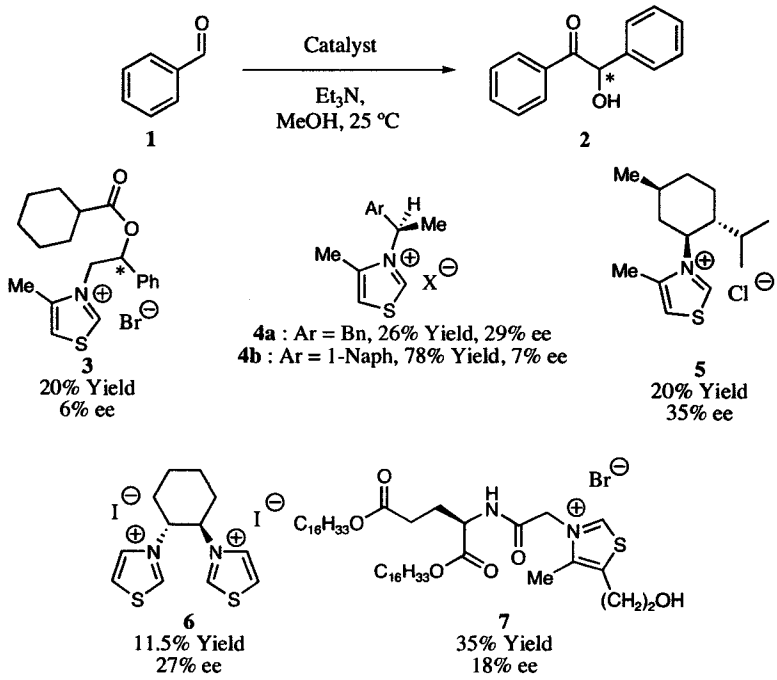

Following the pioneering work of Sheehan[7] and others[8], Enders and co-workers discovered a significant improvement in the reactivity and selectivity of the asymmetric benzoin reaction in 1996 by employing a chiral triazolinylidene carbene.[9] Utilizing only 1.25 mol% of catalyst **8** they were able to perform the asymmetric benzoin reaction in 75% ee and a satisfactory 66% yield (Scheme 3).

Scheme 3.

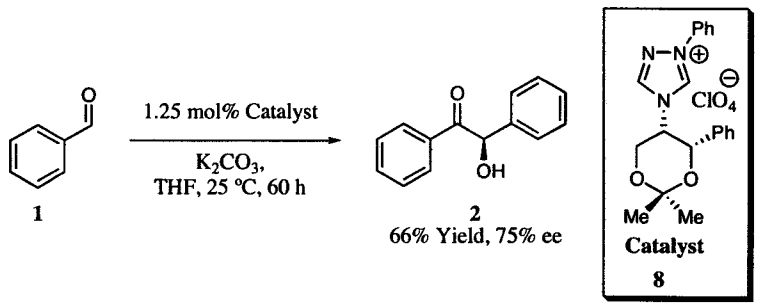

The second major breakthrough in the asymmetric benzoin reaction came from Leeper and Rawal who reasoned that the low ee's obtained in the benzoin

reaction resulted from free rotation available to the chiral side-chain (Scheme 4). They rationally designed chiral bicyclic thiazolium salts to address this problem.[10,11,12]

Scheme 4.

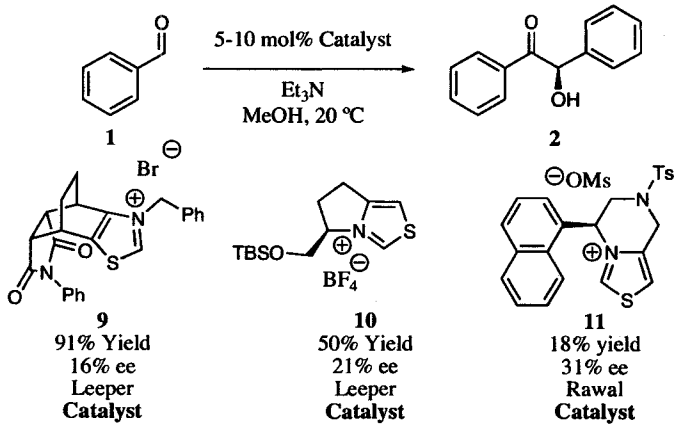

Although the application of these chiral bicyclic thiazolium salts did not lead to vast improvements in the asymmetric benzoin reaction, they did help lay the foundation for an important feature in future catalyst design. Later, Leeper and Knight were able to achieve enantioselectivity comparable to that observed by Enders utilizing a bicyclic triazolium catalyst.[13]

We reasoned that the increased reactivity of triazolinylidene carbenes combined with a bicyclic chiral scaffold would represent a powerful catalyst for the asymmetric benzoin reaction. Our initial experiments began with 5 mol% chiral triazolium salt **12** in the presence of 5 mol% TEA in MeOH. To our surprise the reaction proceeded in modest enantioselectivity and poor chemical yield (Scheme 5).

Scheme 5.

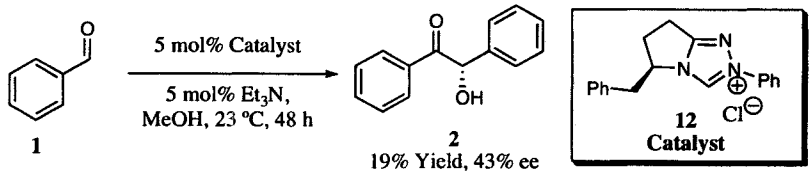

We in turn reasoned that the modest enantioselectivity could be a consequence of epimerization during the basic reaction conditions. In order to test this hypothesis we monitored enantioselectivity as a function of time and observed erosion of selectivity as the time of the reaction increased (Scheme 6).

Scheme 6.

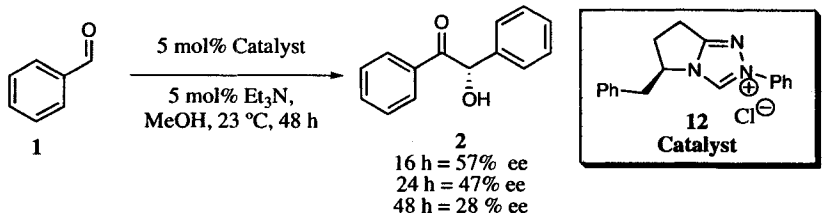

Discouraged by our initial result and cognizant of the fact that the benzoin reaction is often limited to homocoupling of two aldehydes, thereby limiting the synthetic utility, we turned our attention to another umpolung aldehyde reaction, the Stetter reaction.[14]

During this time, unbeknownst to us, Enders and co-workers were also working on an enantioselective benzoin reaction utilizing a chiral bicyclic triazolinylidene catalyst. Despite the similarities in catalyst architecture (**12**: Rovis, **13**: Enders) catalyst **13** provided a highly enantioselective benzoin reaction in 90% ee and 83% yield (Scheme 7).

Scheme 7.

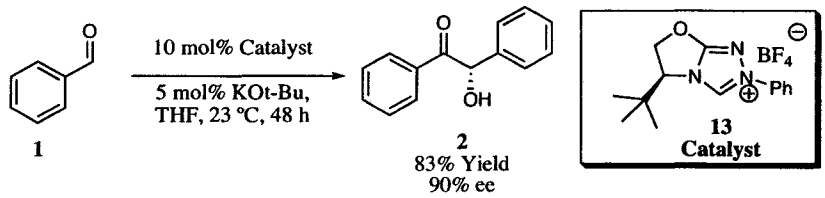

Recently, Dünkelmann *et al.* developed a donor-acceptor concept for an asymmetric enzymatic cross-benzoin reaction.[15] Under their reaction conditions, they are able to afford synthetically valuable α-hydroxy ketone building blocks from readily available starting material. Johnson and co-workers took a different approach toward addressing the limitation of homocoupling during the benzoin reaction by employing acyl silanes as aldehyde surrogates (Scheme 8). The kinetically controlled regiospecific cross silyl benzoin reaction between acylsilane **14** and aldehyde **15** can be catalyzed by KCN or asymmetrically by chiral phosphinate **17**.[16]

Scheme 8.

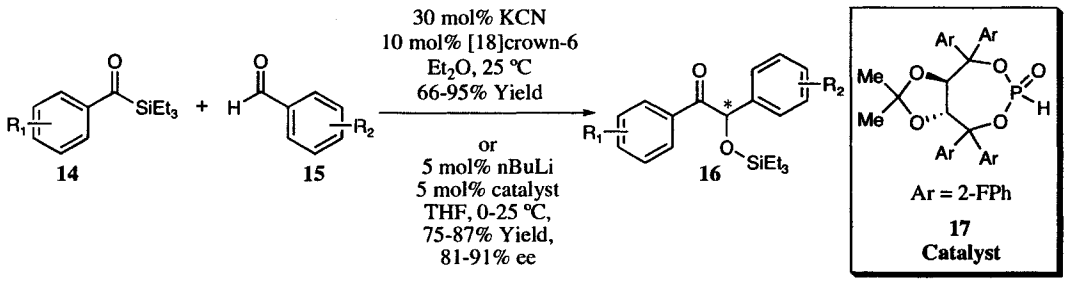

2.4 Asymmetric Stetter Reaction of α,β-Unsaturated Michael Acceptors

2.4.1 Introduction

In the early 1970's Stetter extended the synthetic utility of the Breslow intermediate by demonstrating that Michael acceptors can also be used as the electrophilic counterpart, affording 1,4-dicarbonyl compounds (Scheme 9).[17]

Scheme 9.

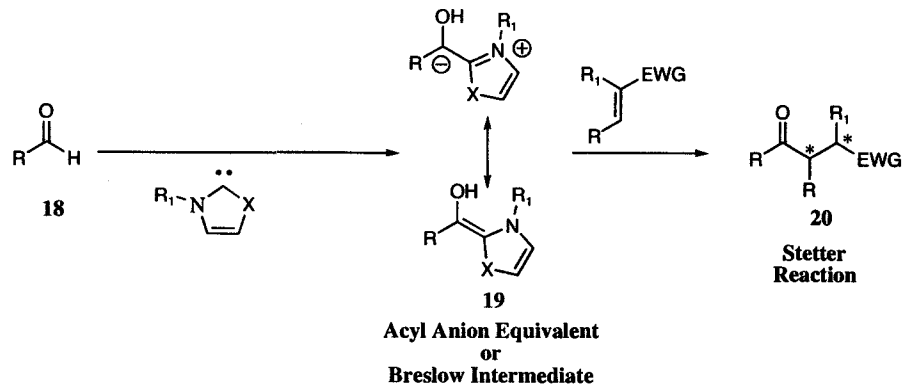

Stetter and co-workers demonstrated that a variety of aromatic and aliphatic aldehydes could participate in the intermolecular Stetter reaction catalyzed by cyanide anion or thiazolium derived carbenes. In addition, they were able to successfully employ a variety of different Michael acceptors with one major limitation. The Michael acceptors that contained a β-substituent often resulted in diminished reactivity and were generally limited to chalcones. Furthermore, unlike the intermolecular variant, the intramolecular Stetter reaction was not investigated until 1995 by Ciganek, possibly for the same reason.[18] Consequently, the asymmetric Stetter reaction has received little attention, with only a single example reported prior to 2002.[19] The Stetter reaction could provide a straightforward route to optically enriched 1,4-dicarbonyl compounds which are important building blocks for natural product synthesis, an underutilized approach at the time.

Enders and co-workers reported the first asymmetric intramolecular Stetter reaction in 1996 utilizing the increased reactivity of chiral triazolium carbene **23**, resulting in the synthesis of chromone-4-ones in modest enantioselectivity and yields (Scheme 10).[20]

Scheme 10.

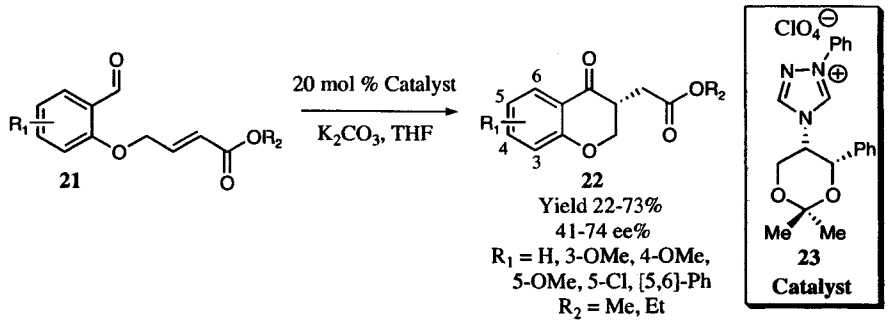

Two additional examples of an asymmetric intramolecular Stetter reaction have appeared subsequent to our initial contributions to this field.[21] Recently, Bach reported a unique, axially chiral thiazolium salt **26** that is capable of imparting modest enantioselectivity in the synthesis of **25** (Scheme 11).[22]

Scheme 11.

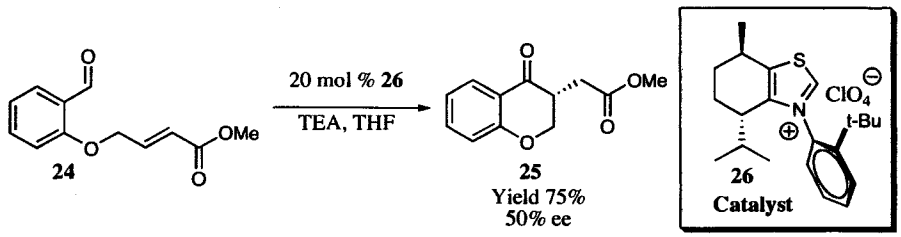

Miller and co-workers have extended their peptide bound catalyst research by attaching a terminal thiazolium salt to the peptide backbone (Scheme 12).[23] Miller observed substantial variation in the efficiency and selectivity of the reaction utilizing simple derivatives of a thiazolylalanine (Taz) derived catalyst. The highest selectivity was found by employing catalyst **29**, resulting in chromone **28** (R_1=H) in 80% ee and 40% yield. Embedding the thiazolium salt in the small peptide (**30**) increased the efficiency of the reaction to 67% isolated yield and the scope of the reaction was studied utilizing this optimized catalyst.

Scheme 12.

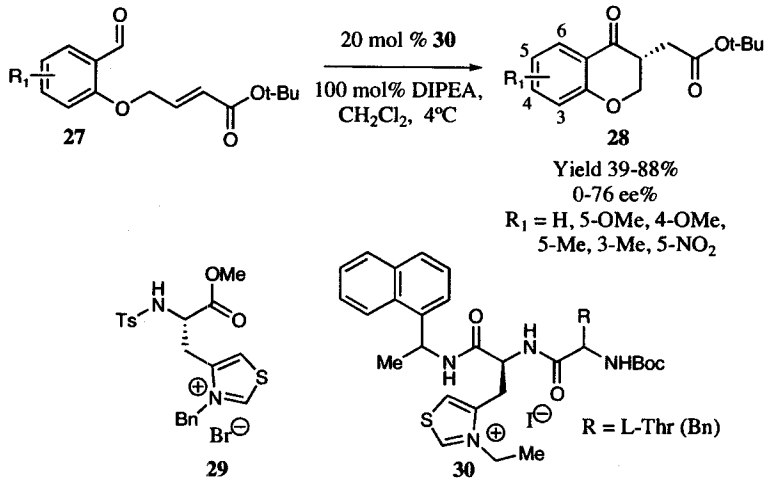

In addition to these two reports, since 2002 we have demonstrated the utility of chiral triazolium salts as precursors for nucleophilic carbenes in the formation of quaternary stereocenters,[24] contiguous stereocenters[25] and studied the effect of pre-existing stereocenters.[26]

2.4.2 Development of an Asymmetric Intramolecular Stetter Reaction

Our initial attempts at applying our chiral triazolium salts to the asymmetric benzoin reaction were met with little success and we therefore quickly turned our attention to the much more interesting problem of an enantioselective intramolecular Stetter reaction. The intramolecular variant of the Stetter reaction was chosen because the probability of a successful carbon-carbon bond cyclization would be greatly increased by tethering the Michael acceptor to the aldehyde. Another experimentally advantageous aspect of the intramolecular Stetter reaction is the fact that the starting materials are easy to handle, crystalline materials that can be purified by column chromatography. Furthermore, our initial hypothesis that the intramolecular Stetter reaction would be easier to perform has proven correct; to this

day we are unable to perform a highly enantioselective intermolecular Stetter reaction under our current reaction conditions.

Our initial investigations began with the aromatic aldehyde tethered to a Michael acceptor originally reported by Ciganek.[27] Recall that this process was later rendered asymmetric by Enders and co-workers (Scheme 10). We began with conditions typically employed in the asymmetric benzoin reaction and obtained the desired product in excellent yield, albeit in 4% ee (Scheme 13).

Scheme 13.

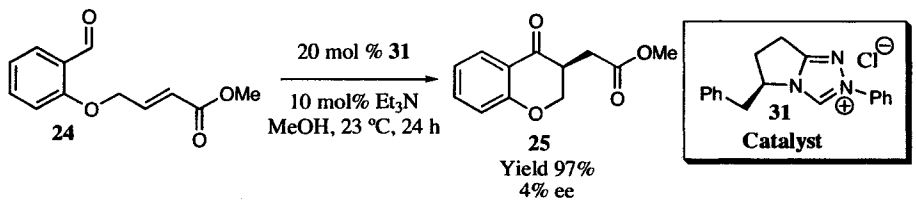

The enantioselectivity result was very disheartening, although we had achieved one of our original goals of developing a highly reactive triazolium catalyst. With this result in hand, our preliminary optimization efforts focused on increasing the selectivity of the reaction by varying the nature of the solvent and base. By simply switching the solvent from MeOH to THF, we were able to form the desired product **25** in 82% ee and 95% yield (Scheme 14).

Scheme 14.

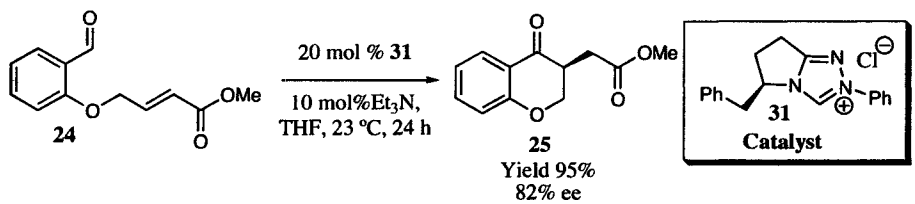

This exciting result provided the impetus for a complete solvent and base screen to determine the optimal reaction conditions. In our initial examination we screened a variety of bases with similar pKa values to TEA (Table 1). Hünigs base, DABCO, K_2CO_3 and proton sponge were investigated with TEA and Hünigs as the optimal base in THF for both selectivity and reactivity.

Table 1.

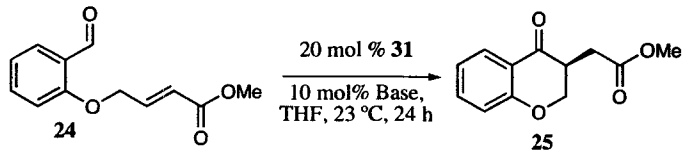

24 25

Base	% Yield	% ee
TEA	**95**	**82**
Hunigs	**95**	**83**
DABCO	40	65
K_2CO_3	95	75
Proton Sponge	0	NA

Triethyl amine was chosen as the optimal base for a solvent screen since it is readily available in most organic laboratories. A solvent screen commenced with anhydrous solvents that are available from our solvent system and once again our original solvent of THF was found to be the optimal solvent for selectivity and reactivity (Table 2).

Table 2.

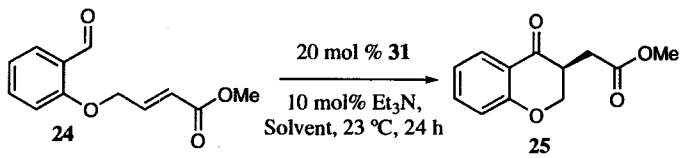

Solvent	% Yield	% ee
THF	**95**	**82**
MeOH	95	4
CH_2Cl_2	86	53
THF: Toluene	22	66

Unsatisfied with the current 82% selectivity, we performed a quick temperature study and found a dramatic effect on the reactivity of the reaction, but one that did not provide a practical solution to increasing the enantioselectivity. A modest increase in enantioselectivity was observed when the reaction was performed at 0 °C, however at the expense of reactivity which decreased to 30% yield over 48 hours (Table 3). Increasing the temperature resulted in an increase in reaction rate, but the enantioselectivity decreased to 79%.

Table 3.

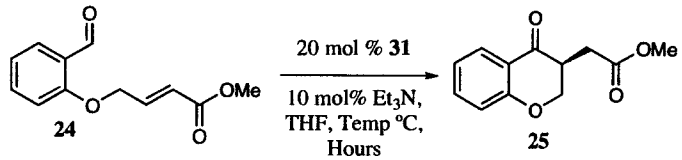

Temperature °C	Hours	% Yield	% ee
0	48	30	89
23	**24**	**95**	**82**
60	12	90	79

The next parameter we wanted to examine was the effect on selectivity and reactivity utilizing a different catalyst chiral scaffold. However, at this point the only other catalyst available was the valine-derived triazolium salt. Disappointingly,

application of the valine-derived catalyst **32** resulted in lower reactivity and enantioselectivity when compared to phenylalanine-derived catalyst **31**. In general the reaction proceeds slower with catalyst **32**, although the results follow the same trends with respect to base, solvent and temperature as the phenylalanine-derived catalyst (Table 4). Two important observations were made during this study despite the modest selectivity obtained. One, the rate and overall conversion of the reaction are drastically increased when the reaction is run in the presence of molecular sieves (Table 4, entry 4). We believe that exogenous water plays a role in shutting down the active catalyst during the reaction. Although not fully recognized at the time, exogenous water continues to play a similar, pragmatic role in the asymmetric Stetter reaction, especially with substrates that are difficult to cyclize. Employment of triazolium tetrafluoroborate ($^{-}BF_4$) salt resulted in recovered starting material with TEA base (Table 4, entry 5). Currently we believe this effect is simply due to the different solubility between the chloride and tetrafluoroborate catalysts. Apparently the chloride counter ion is slightly more soluble allowing for the formation of the active catalyst. We have not observed this effect with other bases.

Table 4.

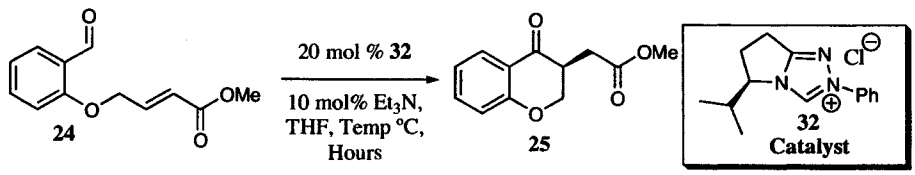

Entry	Temperature °C	Additives	Hours	% Yield	% ee
1	4	--	48	48	87
2	23	--	24	42	68
3	23	--	48	80	60
4	**23**	**molecular sieves**	**12**	**94**	**69**
5*	23	molecular sieves	48	0	NA

* The BF_4 counter ion of the triazolium catalsyt **32** was used.

2.4.3 Optimization of the Asymmetric Intramolecular Stetter Reaction

Up to this point optimization of the reaction conditions was based on literature precedent for the benzoin reaction, where it was believed that polar solvents with weak bases were optimal. Regrettably, these conditions led to only good enantioselectivity in the case of the Stetter reaction while we desired selectivity into the synthetically useful range of > 90% ee. Fortunately, my colleague Mark S. Kerr who was also working on the development of an asymmetric intramolecular Stetter utilizing a different chiral triazolium scaffold, discovered that strong bases in non-polar solvents afforded optimal results for his catalytic system. Armed with this knowledge, catalyst **31** was examined in the presence of potassium hexamethyldisilazane (KHMDS) and a mixture of xylenes:THF (10:0.5) (Scheme 15). To our delight the new reaction conditions afforded the desired product in 90% ee and 95% isolated yield.

Scheme 15.

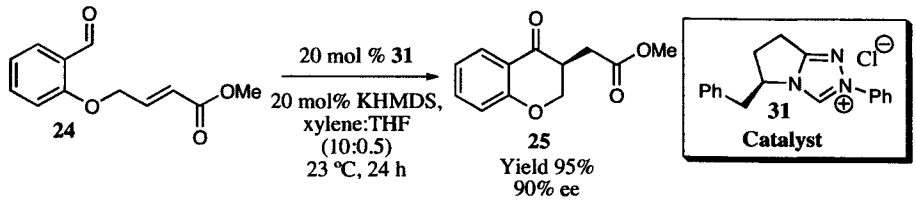

Regrettably, the reproducibility under these conditions was poor and the enantioselectivity varied from 67-91% depending on the work-up conditions employed. The reactions were worked up by directly placing the reaction mixture on a column after being judged complete by thin layer chromatography (TLC). The only two variables that were changing from reaction to reaction were the length of time the reaction was stirred prior to work-up and the length of time the product was on the column. Monitoring enantioselectivity of the reaction as a function of time revealed that there was no epimerization occurring during the reaction despite the basic conditions. Apparently the epimerization was occurring during column chromatography. A systematic evaluation of different work-up conditions revealed a simple reproducible solution, (Table 5, entry 5). Typically epimerization during column chromatography is a result of the acidic nature of silica gel. Treatment of the silica gel with 1% TEA is a standard technique used to address this problem. However, subjection of 90% enantioenriched product by HPLC to column chromatography containing 1% TEA pre-treated silica gel resulted in a drastic decrease in the ee of the product from 90% to 27% ee, (Table 5, entry 1). This surprising result led us to believe that maybe epimerization was base induced and was occurring when the product was concentrated down on the column in the presence of the basic carbene. To confirm this hypothesis we concentrated the reaction solution

down *in vacuo* after completion judged by TLC. Subjection of this material to HPLC revealed the enantioselectivity had decreased from 90% to 67%, thus supporting our hypothesis (Table 5, entry 2). Quenching the basic reaction with 1M HCl or saturated ammonium chloride (NH_4Cl) resulted in slight epimerization, 82% and 87% respectively, (entries 3-4). These results suggest that the basic carbene is only partly responsible for the epimerization and slight epimerization must be occurring on the silica gel. Indeed, simply pouring the reaction mixture on the column and quickly eluting the product with a 1:1 mixture of hexane to ethyl acetate (Table 5, entry 5) can afford the desired product with high enantioselectivity.

Table 5.

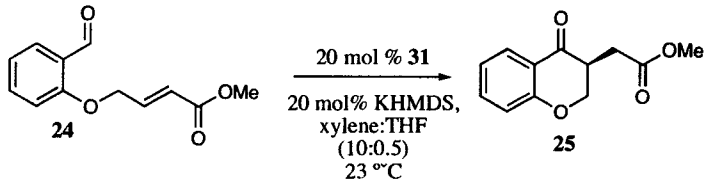

Entry	Work-up Conditions	% ee
1	Silica gel pre-treated with 1% TEA	27
2	Xylene:THF was removed *in vacuo*	67
3	Quenching with 1M HCl	82
4	Quenching with saturated NH_4Cl	87
5	**Quickly flashing through a column**	**90**

Epimerization during column chromatography became more apparent when we were investigating substrates that contained electron-withdrawing groups on the backbone of the aromatic aldehyde (section 2.4.5). At this point it became obvious that we needed a more general solution to the work-up procedures. Suppression of the epimerization is achieved by pre-treating the silica gel with 15% acetic acid (Scheme 16, entry 1). Apparently the silica gel that we employed is slightly basic. Epimerization from silica gel was confirmed by subjection of optically enriched

product to a solution of silica gel in toluene for four hours, which resulted in a decrease in ee from 90-69% ee when no acetic acid was present (Scheme 16, entry 2).

Scheme 16.

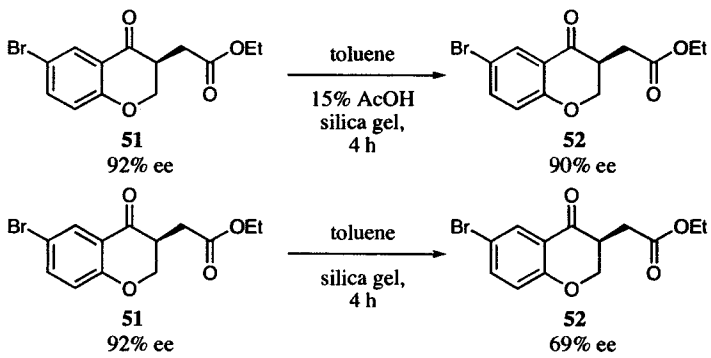

2.4.4 Optimization of Chiral Triazolium Catalyst

With optimized reaction conditions in hand we screened the entire family of chiral triazolium catalysts, Table 6. Comparing the steric effects of the chiral scaffold on reactivity and selectivity, entries 1a-d, it is obvious that the phenylalanine-derived chiral scaffold is optimal across this series. Increasing the chiral steric environment from benzyl to isopropyl to phenyl to tert-butyl decreases the reactivity of the catalyst from 100 to 0% conversion. Excellent enantioselectivity was observed when the electronics of the N-aryl substituent were varied from electron rich to electron poor (Table 2, entries 2a-d). However, the installation of an electron donating *p*-methoxy group resulted in decreased reactivity (Table, entry 2a). Only subtle differences exist between the neutral N-phenyl and the N-aryl substituents containing an electron-withdrawing group. The most dramatic effect on enantioselectivity arose from substitution of the N-aryl group with a benzyl substituent, entry 3b. Clearly, good enantioselectivity requires an aromatic substituent bound to the nitrogen of the bicyclic ring system. Not surprisingly catalyst **42**, which contains bulky oxygen

substituent, is also a competent catalyst under the current reaction conditions. From these results it is clear that an N-aryl group, preferably not an electron rich aryl group, must be present in order to obtain high enantioselectivity. It also appears that the chiral scaffold should possess a methine unit at the α position of the bicyclic ring system for optimal reactivity, entries 1a and 3c (Table 6). Lastly, under the current optimized reaction conditions there is no difference between the chloride and tetrafluoroborate counter ion, entries 1a and 2b (Table 6).

Table 6.

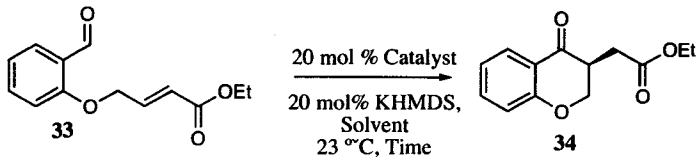

Entry	a	b	c	d
1[a]	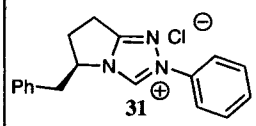 31	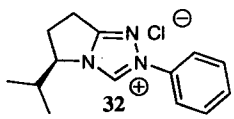 32	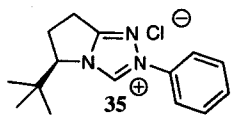 35	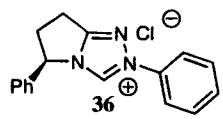 36
	95% Yield 90% ee 1h	43% Yield 88% ee 48h	0% Yield NA% ee 48h	41% Yield 58% ee 48h
2[b]	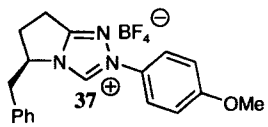 37	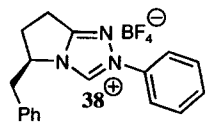 38	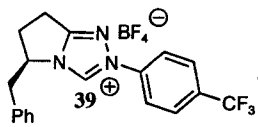 39	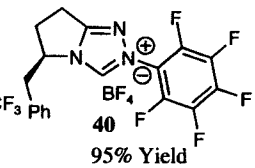 40
	60% Yield 86% ee 24h	95% Yield 90% ee 1h	95% Yield 92% ee 1h	95% Yield 91% ee 1h
3[b]		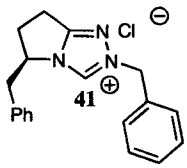 41	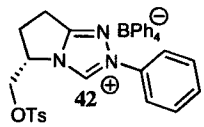 42	
		95% Yield 7% ee 24h	95% Yield 90% ee 1h	

[a] All reactions in column 1 were conduted in xylene:THF (10:0.5). [b] All reactions in column 2 and 3 were conducted in toluene.

2.4.5 Effects of the Aromatic Aldehyde

Based on our promising beginning we set out to test the scope of the intramolecular Stetter reaction by systematically investigating the different aspects that might influence the reaction. We began by changing the nature of the substituents around the aromatic aldehyde backbone. Subsequently we investigated a range of tethered Michael acceptors that were capable of participating in the intramolecular Stetter reaction. Finally we evaluated the effectiveness of aliphatic aldehydes tethered to different Michael acceptors.

Electron donating and electron withdrawing substituents were placed around the aromatic backbone of the aldehyde in an effort understand their effects on reactivity and selectivity, Table 7. Within this series, substitution of hydrogen at the 3 position of the aromatic ring by a larger group resulted in decreased selectivity, entries 1-4. The best results were obtained on substrates lacking steric bulk near the reactive site, entries 5-14. Electron donating groups (EDG) afforded higher enantioselectivity utilizing catalyst **38** relative to electron withdrawing groups (EWG) in the same position on the aromatic ring. Miller and co-workers reported similar trends with observed product racemization under the basic reaction conditions when the product contained an EWG on the backbone of the aromatic ring. We also observed that electron-withdrawing substituents lead to product racemization under the reaction conditions.[28] Low ee's can be avoided by the implementation of the less basic catalyst **39** or by immediate work-up after completion of the reaction.[29] Increasing the electron donating ability at the 4-position from methoxy to

diethylamino resulted in a decrease in reaction rate and an increase of an undesired aldol-elimination side reaction, generating seven-membered elimination products. Application of catalyst **39** completely suppresses the formation of the undesired side reaction and affords the desired products in higher yield with good enantioselectivity, entries 12 and 14 (Table 7).

Table 7.

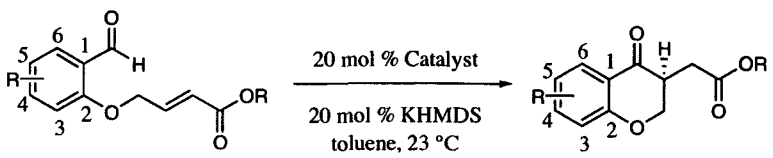

Entry	Substrate	Product	Catalyst	%Yield	% ee
1	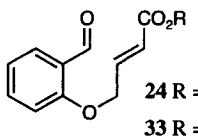 **24** R =Me	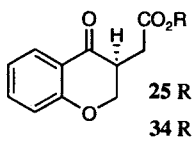 **25** R =Me	**38**	94	90
2	**33** R =Et	**34** R =Et	**38**	94	90
3	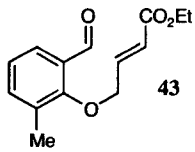 **43**	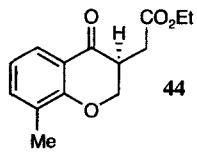 **44**	**38**	94	80
4	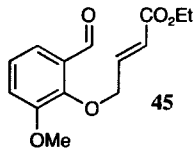 **45**	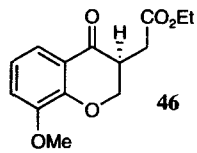 **46**	**38**	95	80
5	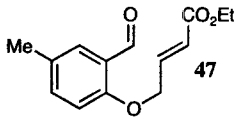 **47**	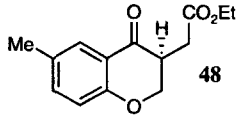 **48**	**38**	94	90
6	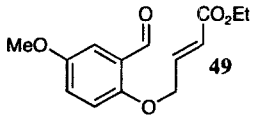 **49**	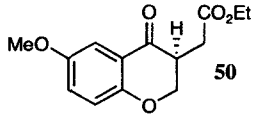 **50**	**38**	94	90
7	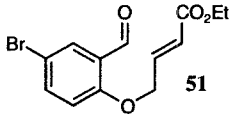 **51**	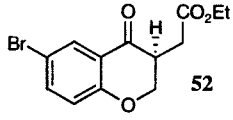 **52**	**38**	95	89
8			**39**	94	92
9	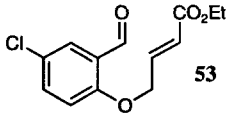 **53**	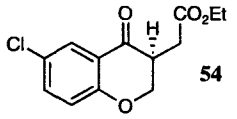 **54**	**38**	94	88
10			**39**	94	91
11	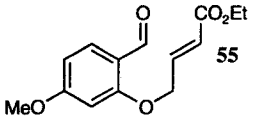 **55**	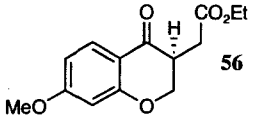 **56**	**38**	45	90
12			**39**	94	91
13	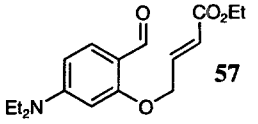 **57**	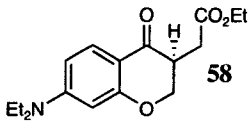 **58**	**38**	0	NA
14			**39**	55	95

We were interested in understanding the limitations of the intramolecular Stetter reaction and were intrigued with how the addition of an EDG at the 4-position lead to an aldol elimination product. The difference in product ratio is due to the basic nature of the triazolinylidene carbenes, which can be tuned to eliminate the undesired side reaction as seen in Table 7 (entry 11-14). For example, subjection of **57** to the reaction conditions in the absence of catalyst also affords the elimination product, suggesting a base induced aldol type mechanism (Scheme 17). However, a Baylis-Hillman reaction catalyzed by the nucleophilic carbene is also a possibility.

Scheme 17.

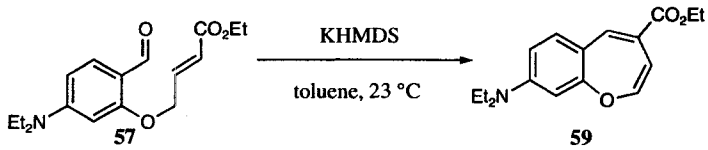

2.4.6 Effects of the Michael Acceptor

Mark S. Kerr initially investigated the effects of the Michael acceptor on the intramolecular Stetter reaction using catalyst **60**.[30] However catalyst **60** was unable to cyclize α,β-unsaturated aldehydes, amides or Michael acceptors that possessed *Z* alkenes. With access to a larger family of chiral catalysts we re-examined the effects of the Michael acceptor utilizing catalyst **61**. Catalyst **61** was initially chosen because it would allow us to compare our results to those previously obtained by my colleagues; in addition it was found that catalyst **61** affords higher reactivity and enantioselectivity across the entire range of different Michael acceptors.

Scheme 18.

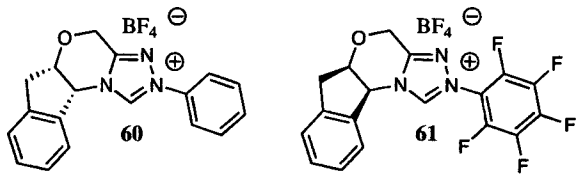

The reaction is remarkably broad with respect to the α,β-unsaturated Michael acceptor employed. Successful cyclizations of α,β-unsaturated aldehyde, amide, nitrile, esters, thioester, and ketones have been performed utilizing catalyst **61**. Increasing the steric bulk of the α,β-unsaturated esters from methyl to *tert*-butyl resulted in excellent enantioselectivity (Table 8, entries 1-3). To our gratification cyclization of the (*Z*)-α,β-unsaturated methyl ester **66** can now be achieved albeit in low enantioselectivity, entry 4. The cyclization of α,β-unsaturated ketones afforded the desired product in excellent overall yield; however, there was a decrease in selectivity from the α,β-unsaturated ethyl ketone **68** to the phenyl ketone **70** (entries 5-6). To our delight, the α,β-unsaturated thioesters **72** and amides **74** are tolerated in the intramolecular Stetter reaction, entries 7-8. Incorporation of the thioester and the Weinreb amide offer an excellent handle for further manipulations. The α,β-unsaturated aldehyde **78** affords the desired product in 50% isolated yield; however, the product is isolated in 30% ee. Interestingly α,β-unsaturated aldehyde **78** was re-isolated from the reaction as a 1:1 mixture of E:Z alkene isomers. This observation suggest that the low enantioselectivity observed could be a result of the unfavorable cyclization of the Z-α,β-unsaturated aldehyde which is formed in situ. Alkene isomerization could occur by a reversible formation of a homoenolate, which would result from an interaction of the carbene with the α,β-unsaturated aldehyde. The high

enantioselectivity obtained for a wide range of Michael acceptors illustrates that enantioselectivity is independent of the nature of the Michael acceptor when catalyst **62** is employed.

Table 8.

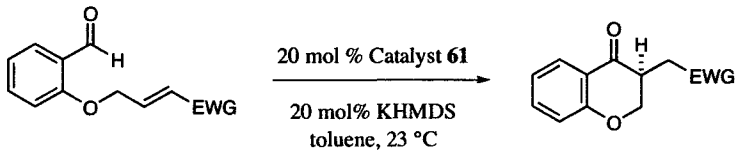

Entry	Substrate	Product	% Yield	% ee
1	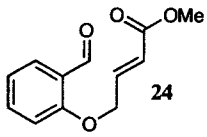 **24**	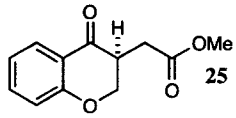 **25**	94	95
2	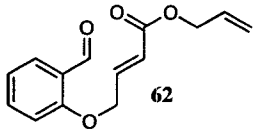 **62**	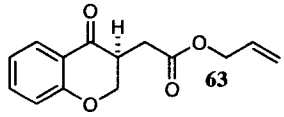 **63**	94	93
3	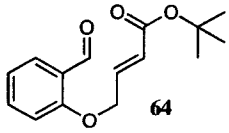 **64**	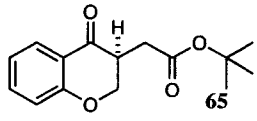 **65**	94	97
4	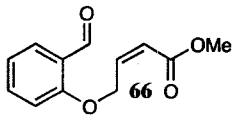 **66**	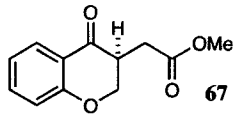 **67**	80	22
5	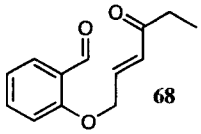 **68**	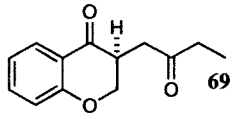 **69**	94	92
6	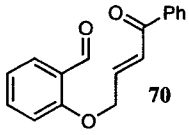 **70**	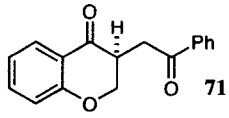 **71**	94	78
7	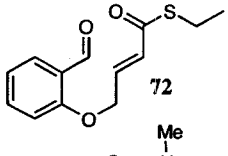 **72**	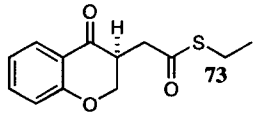 **73**	85	70
8	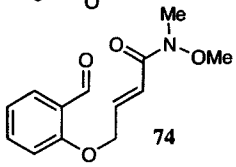 **74**	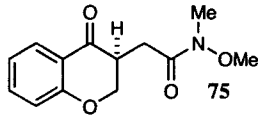 **75**	94	92
9[a]	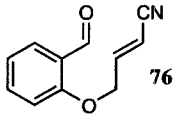 **76**	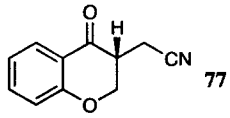 **77**	80	78
10	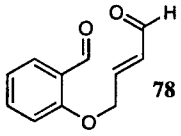 **78**	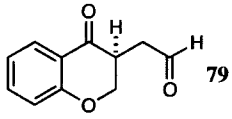 **79**	50	30

[a] Reaction was performed by Mark S. Kerr utilizing catalyst **60**.

During the preparation of starting material **76** an inseparable 1:1 mixture of *E/Z* olefin isomers was obtained. Initially we were hesitant to submit this material to reaction conditions for fear of obtaining low enantioselectivity. After failed attempts to separate the two alkene isomers the reaction was investigated with the inseparable 1:1 mixture of *E/Z* olefin isomers. To our surprise the reaction affords the desired product in good yield and 82% enantioselectivity. The enantioselectivity of the product was approximately identical to the reaction commencing from *(E)*-α,β-unsaturated nitrile (Scheme 19). This unexpected result clearly illustrates that *Z* olefin isomers are tolerated but the resulting enantioselectivity depends on the nature and size of the Michael acceptor.

Scheme 19.

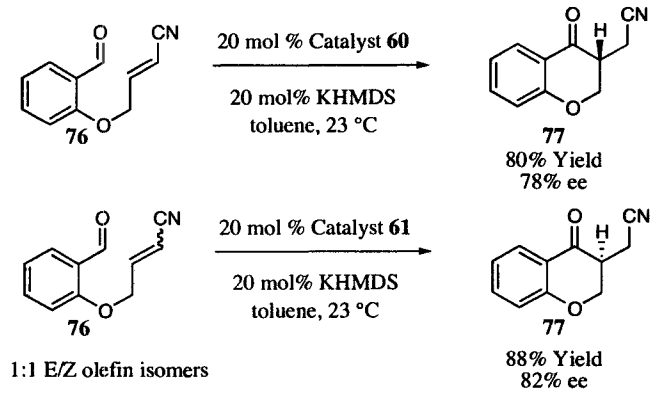

In order to garner further information about the differences and similarities between the two catalyst motifs (**38** and **61**) we evaluated the effects of the Michael acceptor utilizing catalyst **38** and **39** (Table 9). Unlike the results obtained in Table 8 utilizing catalyst **61,** employment of catalyst **38** or **39** shows a more dramatic effect on the enantioselectivity of the reaction depending on the nature of the Michael acceptor. These results are somewhat surprising and not completely consistent or

well understood. For example when comparing the α,β-unsaturated esters it is unclear why the α,β-unsaturated allyl ester **62** results in the lowest enantioselectivity since the α,β-unsaturated esters are electronically similar and the sterically largest ester is *t*-butyl ester **64**. Poor to moderate enantioselectivities were also observed for the (*Z*)-α,β-unsaturated methyl ester **66** and the α,β-unsaturated phenyl ketone **70** (Table 9, entries 4-6).

Table 9.

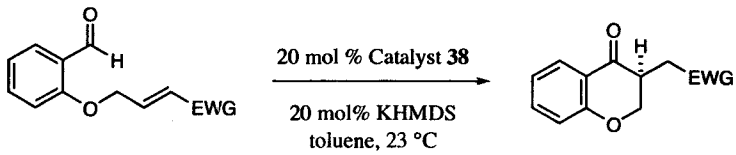

Entry	Substrate	Product	% Yield	% ee
1	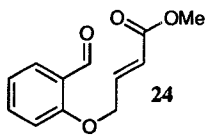 **24**	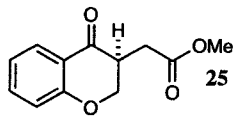 **25**	94	90
2	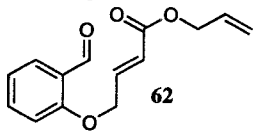 **62**	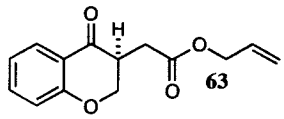 **63**	95	74
3	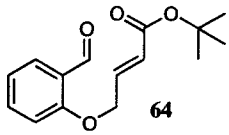 **64**	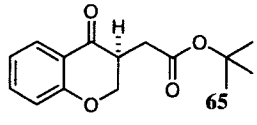 **65**	95	87
4	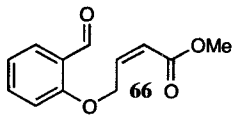 **66**	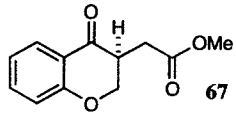 **67**	60	17
5[a]			95	21
6	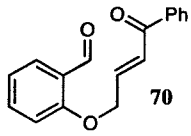 **70**	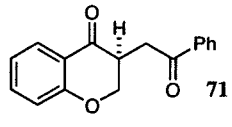 **71**	85	68
7[a]	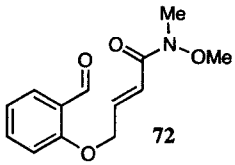 **72**	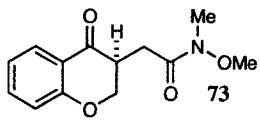 **73**	94	78

[a] Catalyst **39** was used.

Numerous biologically active natural products contain an indole scaffold. Catalyst **38** was examined for its performance in a highly enantioselective Stetter reaction on 2-indolecarboxaldehyde **80**. Treatment of **81** under standard reaction conditions affords the desired product in 80% isolated yield but a modest 65% ee (Scheme 20).

Scheme 20.

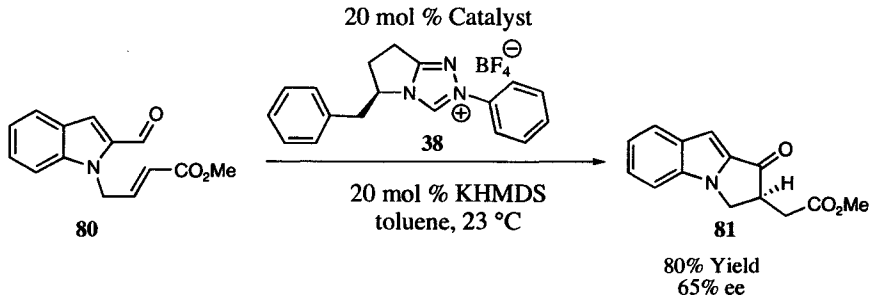

2.4.7 Expanding the Scope to Include Aliphatic Aldehydes

After successfully performing a highly enantioselective intramolecular Stetter reaction on a broad range of aromatic aldehydes, we turned our attention to the potentially more difficult aliphatic aldehydes. Aliphatic aldehydes bear acidic hydrogens α to the aldehyde and we were concerned that this could be a problem under our basic reaction conditions. To our gratification, aliphatic aldehydes that bear acidic hydrogens α to the aldehyde are well tolerated in the intramolecular Stetter reaction, Table 10. Cyclopentanone **81**, **83**, and **85** were each generated in excellent yield and selectivity (Table 10, entries 1-3). Nitrogen is tolerated in the tether affording the desired product in excellent enantiomeric excess. This offers a new approach towards optically enriched pyrolidinones **87** (Table10, entry 4).

The intramolecular Stetter reaction resulting in cyclohexanone products was more challenging and employment of α,β-unsaturated ethyl esters **88** resulted in only recovered starting material (Table 10, entries 5). However, increasing the electrophilic nature of the Michael acceptor resulted in successful cyclization of cychexanone **91** and **93** in moderate to good yield and enantioselectivity, entries 7-8.

Table 10.

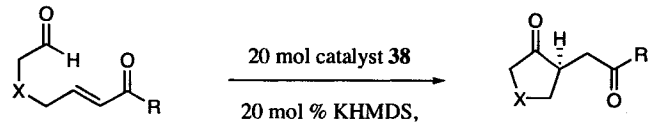

Entry	Substrate	Product	% Yield	% ee
1	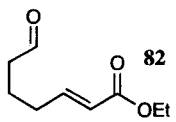 **82**	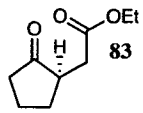 **83**	81	95
2	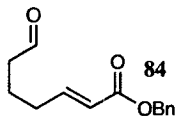 **84**	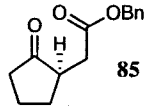 **85**	85	90
3	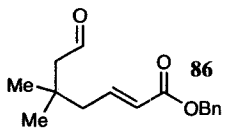 **86**	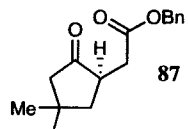 **87**	80	88
4	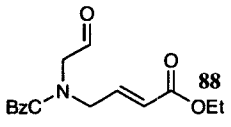 **88**	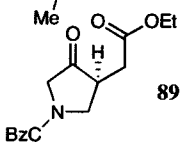 **89**	80	>99
5[a]	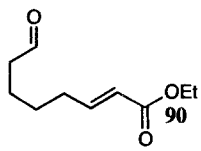 **90**	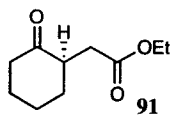 **91**	0	--
6	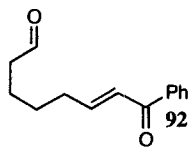 **92**	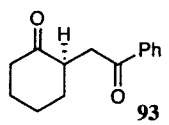 **93**	60	53
7	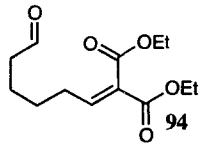 **94**	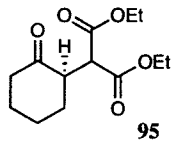 **95**	97	82

[a] Starting material recovered.

Extensive effort was directed to try and understand why increasing the length of tethered α-β-unsaturated ethyl ester resulted in no desired reaction. Regrettably, extensive experimentation did not provide definitive evidence for the disparity. A couple of experiments are worth comment. First, refluxing the reaction only resulted in a complex mixture of unidentifiable products. Second, monitoring the reaction by ^{1}H NMR showed a disappearance of aldehyde which does not coincide with any other changes to the NMR spectrum and we were unable to identify the product of this undesired reaction.

2.4.8 Stereochemical Model

Having determined the absolute sense of enantioinduction,[31] our working model to explain the outcome of the reaction is proposed by transition state B (Figure 1), operating under assumption that the carbon-carbon bond formation takes place from the *E* isomer of the Breslow intermediate. The proposed model is an adaptation of the transition state for the benzoin reaction with a related triazolinylidene carbene proposed by Dudding and Houk based on computational calculations.[32,33] According to Houk the *E* isomer of the Breslow intermediate is favored. The chiral residue sterically shields the *si* face of the Breslow intermediate thus causing the Michael acceptor to reside on the *re* face or opposite the chiral residue. The enantio-discriminating step would then result from attack on either the *re* or *si* face of the tethered Michael acceptor. Attack on the *re* face of the tethered Michael acceptor results in the observed stereochemistry as depicted by path B. It is not obvious from model A or B which transition state should be favored; however, experimental

evidence supports transition state B. For example, the *N*-phenyl group on the triazolinylidene is required for high selectivity (Table 6, entry 3b). Furthermore, higher ee's were obtained with β,β-disubstituted Michael acceptors when compared to corresponding β-monosubstituted Michael acceptor.[34] Changing the size of the β-substituent and the *N*-phenyl ring affects the ee's of the reaction. Therefore it is ressonable that transition state B is favored due to the minimized interaction between the β-substituent and the *N*-aryl group.

Figure 1.

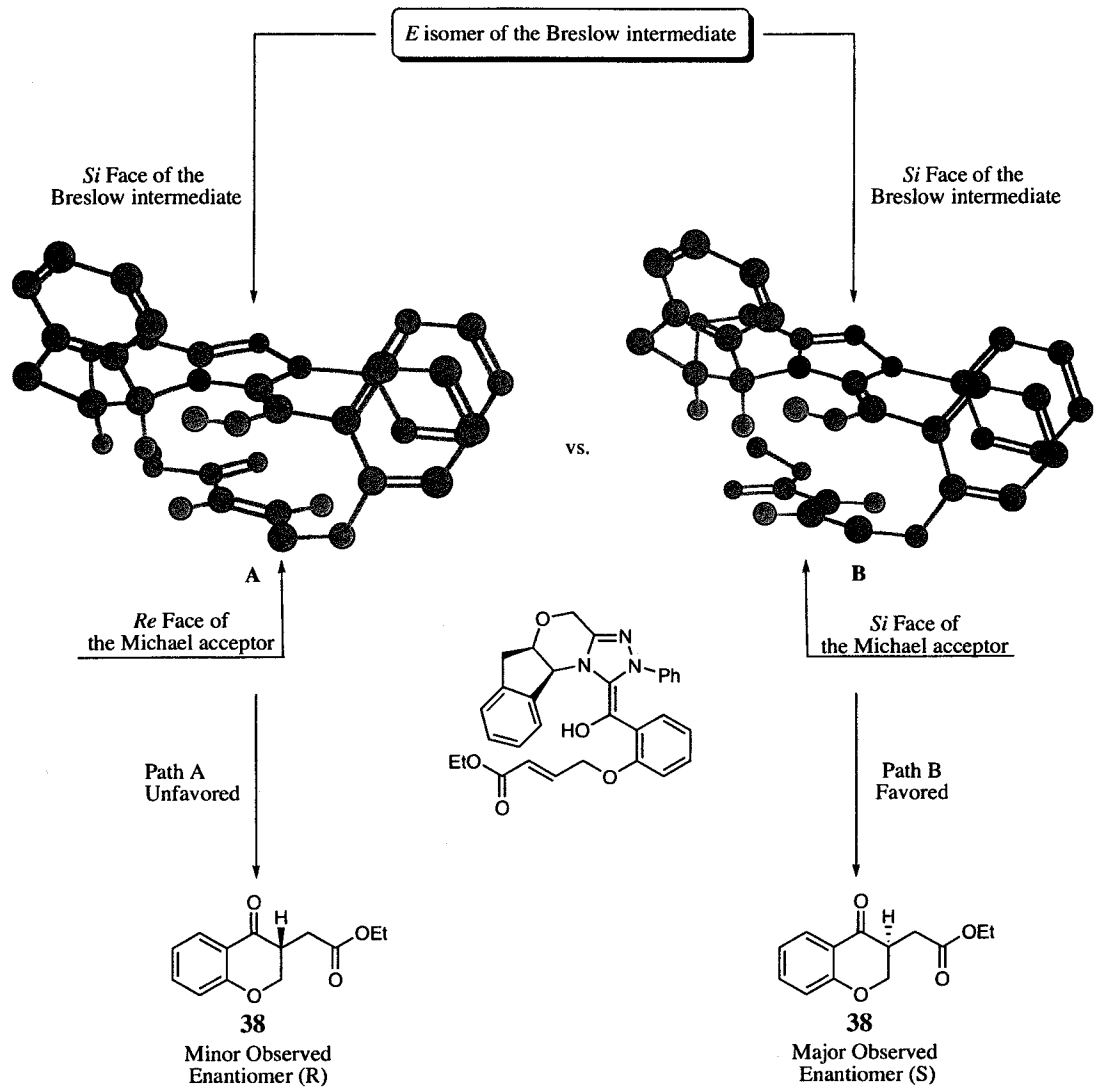

In conclusion of this chapter, we have developed a highly enantioselective intramolecular Stetter reaction of a broad range of aromatic and aliphatic aldehydes tethered to a variety of Michael acceptors. We have been able to garner information about the current limitations of the intramolecular Stetter reaction.

2.5 The Formation of Contiguous Stereocenters Via the Stetter Reaction

2.5.1 Introduction

Over the last 30 years the asymmetric conjugate addition of nucleophiles to α,β-unsaturated carbonyl compounds has played an important role in the development of asymmetric reactions.[35] More recently, the tandem reaction resulting from the conjugate addition of a nucleophile into a Michael acceptor followed by trapping of the anionic intermediate with an electrophile forming two contiguous stereocenters has been realized. A variety of compatible electrophiles have been demonstrated, including aldehydes, ketones, esters and nitriles, Pd-π-allyls, halides and tosylates, oxocarbenium ions and less frequently, a proton source.[36] Useful methods for forming two contiguous stereocenters in good levels of enantio- and diastereoselectivity include: the asymmetric 1,4-addition of organozinc reagents catalyzed by chiral copper complexes,[41] and 1,4-addition of organoboronic acids and derivatives catalyzed by chiral rhodium complexes.[37] Stoichiometric methods include the use of chiral auxiliaries,[38] chiral nucleophiles[39] and chiral radical sources.[40] However, the majority of these examples are confined to cyclic Michael acceptors in which the double bond is part of the ring. In these cases, the constraints imposed by the ring system govern the diastereoselective trapping reaction, in which the electrophile approaches from the less hindered face.

Extension of such protocols to include acyclic enones is limited, in part due to the lack of diastereocontrol resulting from the freely rotating acyclic system. The concerted addition of hydroxylamine to electron deficient alkenes is one elegant solution to this problem.[41] Despite the previous example, there are a few protocols that are able to control the absolute and relative stereochemistry of both new stereocenters in acyclic systems, with only two catalytic examples. Hoveyda and co-workers reported the Cu-catalyzed asymmetric conjugate addition of alkylzinc reagents to acyclic aliphatic enones.[6e] They observed excellent diastereoselectivity when an intramolecular trap is used to generate cyclic products; however, the use of benzyl bromide as the electrophilic trap for the zinc-enolate resulted in poor diastereoselectivity (3.2:1). The most general catalytic protocol was recently reported by Sibi and co-workers, who found that a variety of alkyl radicals add to α,β-disubstituted imide substrates in the presence of a chiral Lewis acid, followed by a diastereoselective hydrogen atom transfer.[42]

When a Michael acceptor bearing a single substituent alpha to the electron-withdrawing group is employed, an enantioselective protonation event may result in the control of α-stereocenters. Recently, tandem 1,4-addition/enantioselective protonation catalyzed by rhodium complexes has been reported.[43] In a related process, the radical conjugate addition to α-methylacrylates and α-methylacrylamides followed by an enantioselective hydrogen atom transfer has been developed.[44]

In the above examples it is believed that the diastereoselective transfer event is governed by the newly formed β-stereocenter, where the electrophile approaches from the less hindered face of the enolate. Zimmerman[45] and Fleming[46] have

examined electrophile additions to carbon-carbon double bonds adjacent to a stereogenic center, where the electrophile approaches from the less hindered face, according to the general model in Scheme 22.

Scheme 22.

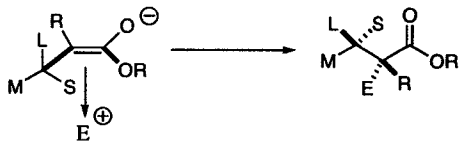

The development of new tandem reactions that are capable of controlling both newly formed stereocenters in a relative and absolute sense, using substoichiometric amounts of catalyst, would be very advantagous. Furthermore, this process would be complementary to existing reactions if the tandem reaction could be performed on acyclic systems, where the diastereoselectivity was not governed by the constraints of the ring system.

2.5.2 Enantio- and Diastereoselective Intramolecular Stetter Reaction

All the data gathered in the asymmetric intramolecular Stetter reaction suggests that the electrophilic nature of the aldehyde and the Michael acceptor affect the rate and thus outcome of the reaction. We reasoned that slowing down addition to the aldehyde or carbon-carbon bond formation allows the nucleophilic carbene to undergo unproductive side-reactions. A mechanistic investigation of the asymmetric intramolecular Stetter was initiated in order to gain insight into the reaction with an eye toward designing more active catalysts with a broader substrate scope.

The currently accepted mechanism of the Stetter reaction is an adaptation of the well-documented benzoin reaction (Scheme 23). According to the proposed

mechanism, intermediate **VI** would result from nucleophilic attack of the carbene into the aldehyde. Subsequent proton transfer would afford the acyl anion equivalent **VII**, whose resonance structure is the triazole-enamine. Carbon-carbon bond formation results from nucleophilic attack of the enamine **VII** into a Michael acceptor, generating enolate **VIII**. Enolate protonation would generate the 1,4-dicarbonyl compound and release the catalyst, closing the catalytic cycle.

Scheme 23.

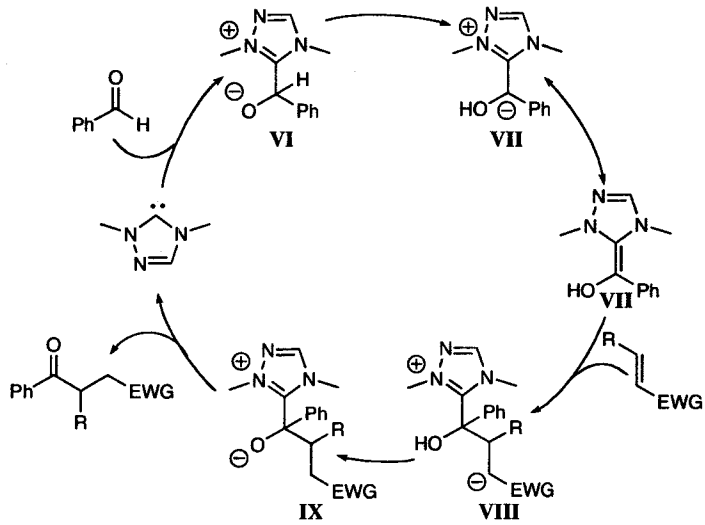

The carbon-carbon bond-forming step is reasoned to be the rate-limiting since cyclization occurrs when the electrophilic nature of the Michael acceptor is increased (Table 10, entries 5-7). If this is the case, the reaction should exhibit no deuterium isotope effect. If, however, addition of carbene to the aldehyde is rate-determining, the reaction should show an inverse isotope effect, while if proton transfer is rate-limiting the isotope effect should be primary.

Deuteroaldehyde **96** was synthesized as part of an effort to answer this question. Before we discuss the results of the kinetic isotope effect obtained while

monitoring the reaction by ^{1}H NMR (these results will be presented later in Chapter 3) the results that lead to the unpredictable discovery of reaction conditions that were capable of performing a highly enantio- and diastereoselective intramolecular Stetter reaction will be discussed.[47]

Subjection of deuteroaldehyde **96** to the reaction conditions afforded the desired product with 60-80% deuterium incorporation at the α-position of the Michael acceptor, as expected according to the proposed mechanism. The Stetter reaction of **96** was monitored by ^{2}H NMR to determine the fate of the remaining 20-40% deuterium. We noted the formation of three new deuterium peaks during the course of the reaction, two of which corresponded to deuteration of the enolate after carbon-carbon bond formation as suggested by intermediate **VIII** of the proposed mechanism, while the third peak corresponded to the proton-deuteron exchange with the conjugate acid of our base, HMDS (hexamethyldisilazane) (Scheme 24).

Scheme 24.

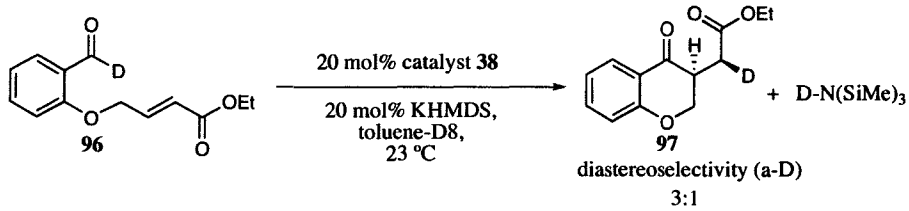

A close examination of the relative ratios revealed some selectivity in the deuteration event (3:1). It was speculated that the HMDS may be acting as the proton/deuteron shuttle in this reaction and we wondered whether selectivity of deuteron transfer would be improved by removing the amine base. The experiment was repeated in the absence of HMDS, removed under high vacuum, and only the two resonances corresponding to deuteration at the diastereomeric α-positions of the

Michael acceptor were observed. More importantly, this protocol led to an increase in diastereoselectivity of deuteron transfer from 3:1 to 9:1.

Scheme 25.

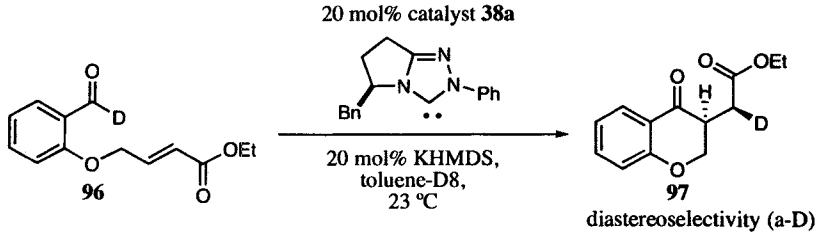

Having realized the viability of a diastereoselective deuteron transfer, our attention was turned to prochiral trisubstituted Michael acceptors. The cyclization of α-methyl α,β-unsaturated ethyl ester **98** was chosen as the model substrate for investigation. Cyclization of **98** under standard reaction conditions of 20 mol % salt and 20 mol% KHMDS in toluene afforded the desired product in good enantioselectivity although the diastereoselectivity varied from 3:1 to 13:1 (Table 11, entry 1). The reaction conducted in the presence of 100 mol% HMDS resulted in 12:1 diastereoselectivity albeit in lower yield (entry 2). To our gratification, the reaction run in the absence of HMDS resulted in an increase in diastereoselectivity without loss of enantioselectivity (entry 3). Further catalyst optimization revealed an increase in enantio- and diastereoselectivity utilizing the slightly more electron-deficient carbene **39a**. In addition to the phenylalanine-derived catalyst the aminoindanol catalyst **61a**, also developed in the Rovis lab, can be used to afford the opposite enantiomeric series of the desired product in high enantio- and diastereoselectivity with slightly lower yields (entry 5), resulting from its somewhat diminished reactivity relative to **39a**.

Table 11.

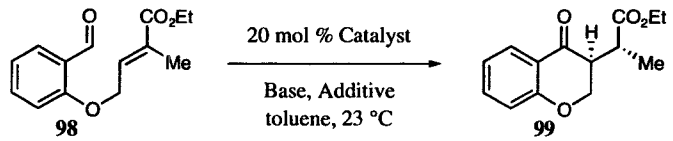

Entry	Catalyst	Base	HMDS	% Yield	% ee	dr (%)[a]
1	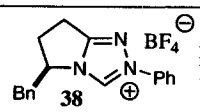 **38**	20 mol % KHMDS	—	85-88	90	3:1 to13:1
2	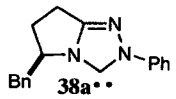 **38a**••	—	100 mol % HMDS	60	88	12:1
3	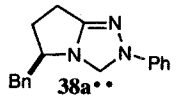 **38a**••	—	—	88	90	15:1
4	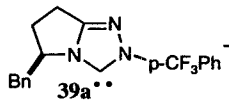 **39a**••	—	—	94	95	30:1
5	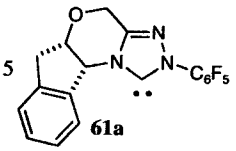 **61a**	—	—	80	- 99	150:1

[a] Enantiomeric excess of the major diasteromer and diastereomeric ratio determined by HPLC or GC analysis using a chiral stationary phase.

As highlighted in Table 11 the source of variable diastereoselectivity in entry 1 is unclear but suggests that there is a factor involved which is not understood. In an effort to determine if the basic reaction conditions affect the diastereoselectivity, the enantio- and diastereoenriched product **99** was subjected to the reaction conditions (Table 12). The standard reaction conditions of 20 mol% salt and 20 mol% KHMDS epimerized the product from 30:1 to 3:1 diastereoselectivity without loss of enantioselectivity (entry 1). Subjection of product **99** to 20 mol% carbene **38a** in the absence of HMDS or 20 mol% HMDS resulted in minor epimerization with no loss of enantioselectivity (entry 2 and 5). On the other hand, subjection of product **99** to 20 mol% carbene **39a** or **61a**, possessing an electron-withdrawing group on the triazolinylidene carbene, resulted in negligible erosion of diastereoselectivity and no

erosion of enantioselectivity (entry 3 and 4). The thermodynamic diastereomeric ratio was determined to be 1.5:1 by treating the enantio- and diastereoenriched product **99** to refluxing DBU in toluene (Table 12, entry 6). These results illustrate that varying degrees of epimerization can occur under the basic reaction conditions, while the free carbene protocol leads to minimal epimerization of the resultant product. In addition, the electronic nature of the chiral triazolinylidene carbenes can be tuned to reduce the amount of epimerization of the desired product. Utilization of the free carbene affords reproducible high enantio- and diastereoselectivity and therefore all subsequent reactions were performed utilizing these conditions.

Table 12.

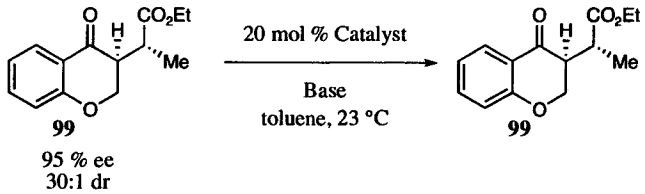

95 % ee
30:1 dr

Entry	Catalyst	Base	% ee[a]	% dr[a]
1	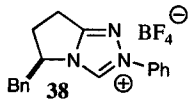 **38**	20 mol % KHMDS	94	3:1
2	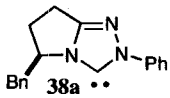 **38a** ••	—	94	10:1
3	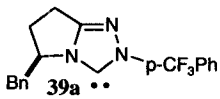 **39a** ••	—	95	28:1
4[b]	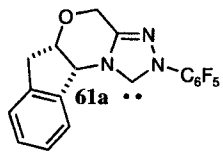 **61a** ••	—	- 99	150:1
5	—	20 mol % HMDS	95	20:1
6	—	10 equiv. of DBU	0	1.5:1

[a] Enantiomeric excess of the major diasteromer and diastereomeric ratio determined by HPLC or GC analysis using a chiral stationary phase. [b] The carbene was subjected to product with -99% ee and 150:1 dr.

With these optimized conditions in hand, a series of prochiral trisubstituted Michael acceptors were prepared to test the scope of the enantio- and diastereoselective Stetter reaction (Table 13). The reaction displays impressive generality with respect to nature and size of the α-substituted Michael acceptors. Moderate steric bulk can be tolerated at the α-position of various α-disubstituted α,β-unsaturated esters (entries 1-5). Alkylidene lactone and cyclopentanone each afford the desired product in high enantio- and diastereoselectivity (entries 6-7). Furthermore, aliphatic aldehydes are also viable substrates, affording the desired

product in >80% yield with good enantio- and diastereoselectivity (entries 9-10). An apparent advantage of utilizing the intramolecular Stetter reaction is illustrated by the formation of the bicyclic and tricyclic products (entries 6-7 and 9-10). Construction of 1,4-dicarbonyls that are joined by a single carbon-carbon bond each possessing a stereogenic center would typically be rather difficult utilizing other known carbon-carbon bond forming reactions. The intramolecular Stetter reaction allows for simple formation of these types of systems.

Table 13.

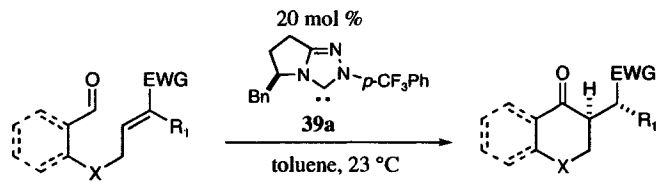

Entry	Substrate	Product	% Yield	% ee	% dr
1	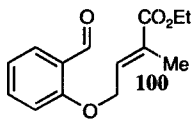 **100**	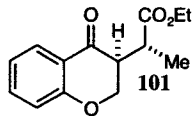 **101**	94	95	30:1
2	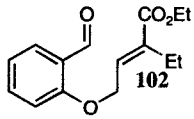 **102**	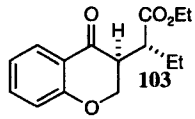 **103**	95	92	35:1
3[b]	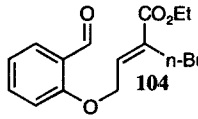 **104**	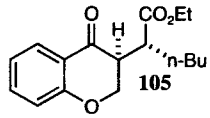 **105**	53	94	12:1
4	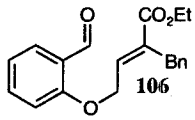 **106**	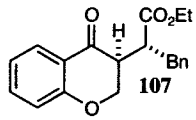 **107**	80	84	20:1[c]
5	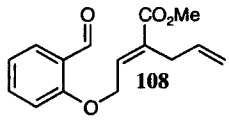 **108**	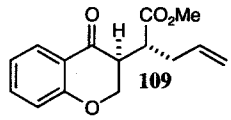 **109**	95	83	13:1
6	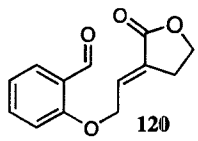 **120**	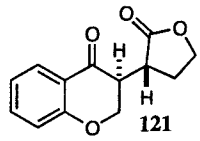 **121**	95	94	10:1
7	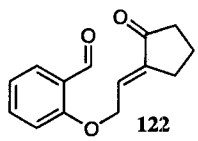 **122**	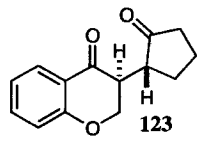 **123**	80	95	18:1
8	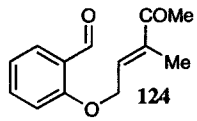 **124**	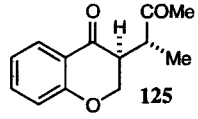 **125**	85	55	10:1
9	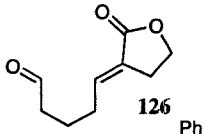 **126**	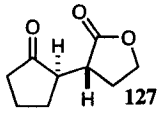 **127**	94	99	50:1
10	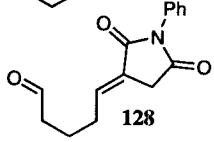 **128**	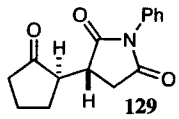 **129**	80	88	15:1

2.5.3 Stereochemical Model for the Diastereoselective Proton Transfer

The relative stereochemistry of the newly formed contiguous stereocenters was assigned as syn based on single crystal analysis for **101** and **121**.[48] This stereochemistry could arise from a diastereoselective proton transfer event from two possible enolate rotamers that result from the highly enantioselective carbon-carbon bond formation, **130** or **131** (Scheme 26). It is also conceivable that the α-hydroxy-α-azolium anion adds to the Michael acceptor in concerted fashion, analogous to the reverse Cope elimination mechanism seen with hydroxylamine additions.[49]

Scheme 26.

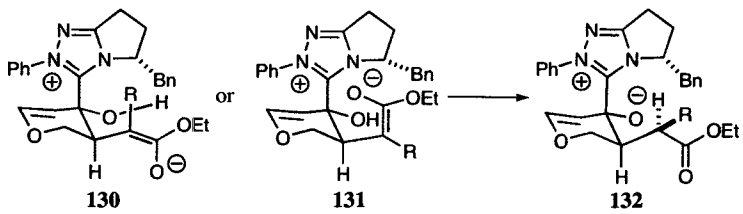

Rotamer **131** is governed by electrostatic interaction between the enolate and the azolium, where protonation from the less hindered face would result in the observed stereochemistry. Rotamer **130** is in accord with the Zimmerman model where the electrophile would be expected to approach from the less hindered face according to the general Scheme 22. If rotamer **130** undergoes an intermolecular protonation the minor diastereomer would be formed. However, Zimmerman has shown that in designed systems a pendant pyridine delivers a proton to the sterically more hindered face of enolates by intramolecular proton transfer. We hypothesize that the reaction proceeds by the Zimmerman model **130** to afford **132**, via an intramolecular proton transfer. Intramolecular proton transfer (intermediate **VIII** in Scheme 23) should be faster than a bi-molecular protonation event.

Support for the intramolecular proton transfer was gained by examining isomeric Michael acceptors. According to the Zimmerman model **130** or the electrostatic model **131** (where the electrophile approaches from the less hindered face in an intermolecular fashion), the relative diastereoselectivity should be independent of the olefin geometry of the Michael acceptor. On the other hand, an intramolecular proton transfer should result in opposite relative diastereoselectivity for the (E) vs. (Z) trisubstituted Michael acceptor assuming proton transfer is faster than bond rotation. Substrates **133** and **135** were subjected to the reaction conditions and found to provide complementary diastereoselectivity. The (E)-isomer proved highly enantio- and diastereoselective, affording **134** in 42:1 diastereoselectivity (Scheme 27), while the (Z)-isomer preferentially afforded **136** in 1:6 diastereoselectivity, albeit low enantioselectivity.

Scheme 27.

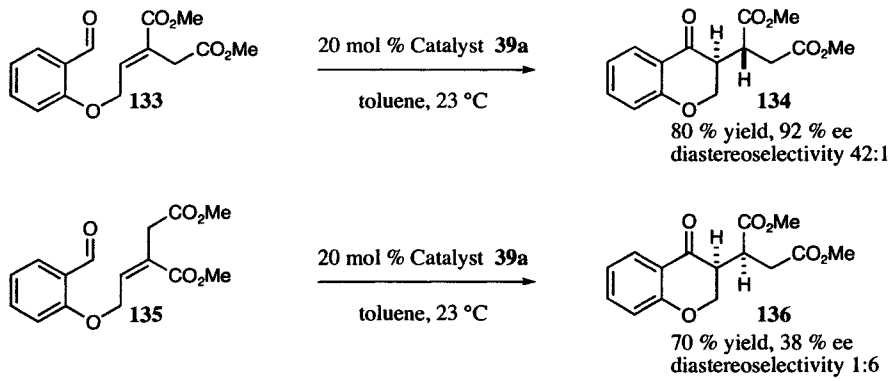

Further support for the intramolecular proton transfer event was gained by conducting the reactions at various concentrations. Presumably, high dilution conditions should favor an intramolecular proton transfer and more concentrated reaction conditions could favor an intermolecular proton transfer. To test this

hypothesis we conducted reaction at 0.3 M to 0.005 M and found that lowering the reaction concentration increased the diastereoselectivity from 10:1 to 30:1 (Scheme 28). The reactions were monitored by GC analysis over the course of 24 hours. The diastereoselectivity remained constant for each reaction, suggesting that a bimolecular event leads to a slight degradation of selectivity. However, it cannot be ruled out that higher concentration leads to a greater amount of epimerization.

Scheme 28.

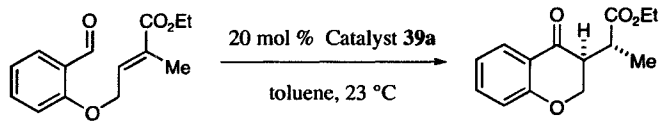

110 **101**

Entry	Molar Concentration	% Yield	% ee	% dr
1	0.3	94	95	10:1
2	0.1	94	95	15:1
3	0.02	94	95	30:1
4	0.006	80	95	30:1

The control of the relative diastereoselectivity suggests enolate protonation must occur prior to bond rotation (Scheme 29). As mentioned above, it is also possible that the α-hydroxy-α-azolium anion adds to the Michael acceptor in a concerted fashion, analogous to the reverse Cope elimination mechanism seen with hydroxylamine addition. Intramolecular protonation of enolate **130** or **131** would result in the observed diastereoselectivity. Bond rotation of either **130** or **131** would access a common enolate intermediate that would result in the same relative diastereoselectivity.

Scheme 29.

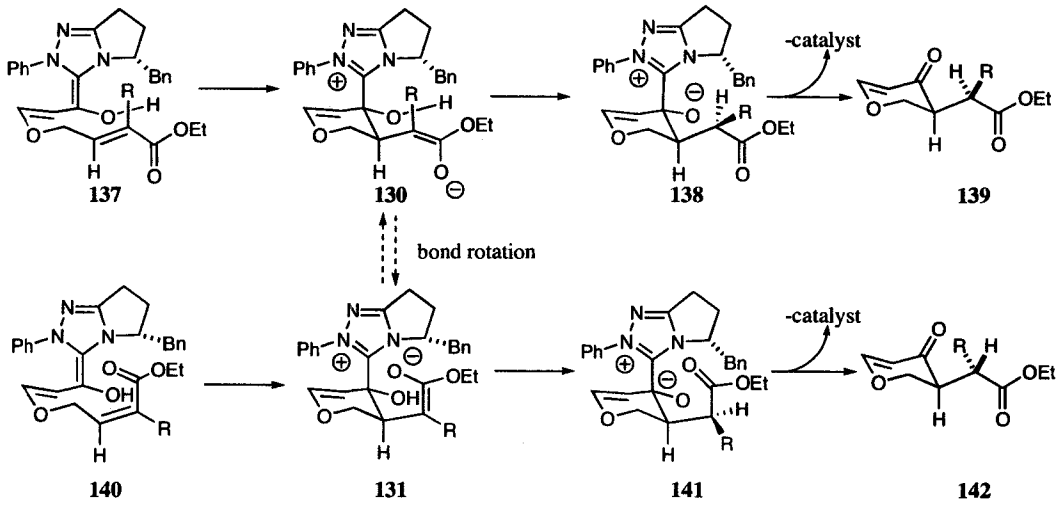

2.5.4 Limitation in the Scope of the α,α-Disubstituted Michael Acceptors

Successful employment of a variety of α,α-disubstituted Michael acceptors encouraged us to extend the scope of contiguous stereocenters via the asymmetric intramolecular Stetter reaction. Aliphatic aldehydes tethered to a variety of Michael acceptors were examined (Table 13). To our surprise and immense disappointment, attempts to cyclize the new aliphatic aldehydes were met with limited success. Increasing the steric bulk at the α-position of the Michael acceptor from hydrogen to methyl completely shuts down the reaction, (entry 1 in Table 10 and Table 13). This result indicates that possibly the intramolecular Stetter reaction occurs in a concerted fashion where carbon-carbon bond formation and proton transfer occur at the same time. Increasing the steric nature of the α-substituent resulted in only recovered starting material (Table 13, entires 2-4). Attempts to increase the electrophilic nature of the Michael acceptor by employing a α-chloro-α,β-unsaturated ethyl ester resulted in recovered starting material (Table 13, entry 5). Increasing the electrophilicity of

the Michael acceptor by switching to a α,β-unsaturated phenyl ketone **155** afforded the desired product in excellent yield and enantioselectivity, albeit 2:1 diastereoselectivity (Table 13, entry 7). No desired product was obtained utilizing a di-substituted methyl ketone **153**. Using different thiazolium or triazolium salts in the presence of KHMDS or TEA in different solvents afforded no benefit. The lack of reactivity of the α,α-disubstituted unsaturated ethyl esters compared to the previously studied α-substituted Michael acceptors caused us to question the alkene geometry of the Michael acceptors. Diminished reactivity was observed for *Z* alkene isomers; NOE experiments were conducted on the starting material **153** to rule out the possibility that *Z* alkenes were obtained during the synthesis of the starting materials. NOE experiments showed an interaction between the β-hydrogen of the Michael acceptor and the acyl methyl group supporting that the *E* alkene was synthesized. If the *Z* alkene was synthesized a NOE signal would be expected between the α-methyl group and the β-hydrogen of the Michael acceptor **153**. Unfortunately, these experiments did not provide an explanation as to why these substrates were unreactive. The difference between the reaction of α-methyl-α,β-unsaturated ethyl ester **143** and the α-methyl-α,β-unsaturated phenyl ketone **155** suggests that the reactions failed due to the electrophilic nature of the Michael acceptor.

Scheme 30.

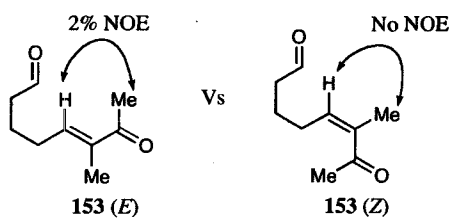

Table 13.

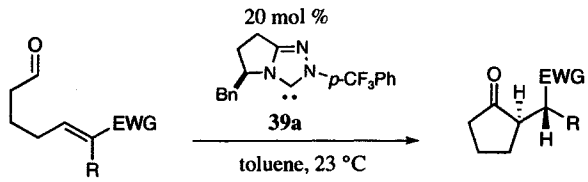

Entry	Substrate	Product	% Yield	% ee	% dr
1	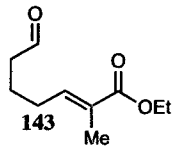 **143**	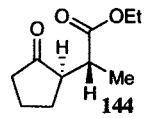 **144**	0	NA	NA
2	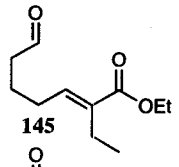 **145**	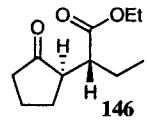 **146**	0	NA	NA
3	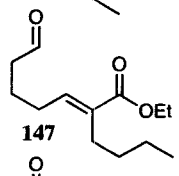 **147**	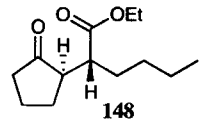 **148**	0	NA	NA
4	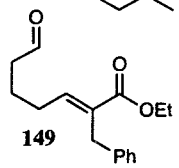 **149**	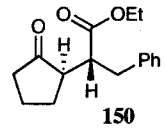 **150**	0	NA	NA
5	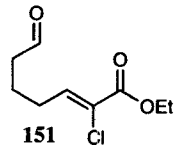 **151**	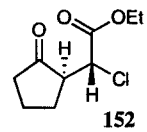 **152**	0	NA	NA
6	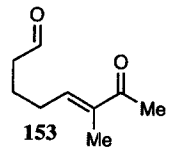 **153**	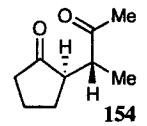 **154**	0	NA	NA
7	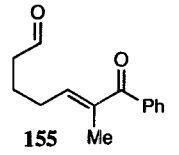 **155**	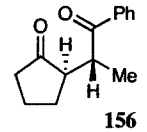 **156**	**90**	**95**	**2:1**

Analogous to the aliphatic series, employing an aromatic aldehyde tethered to a α-methyl-α,β-unsaturated phenyl ketone also resulted in good reactivity but poor enantio-and diastereoselectivity. The poor diastereoselectivity could be a result of the

basic reaction conditions and the increased acidity of the hydrogen α to the phenyl ketone.

Scheme 31.

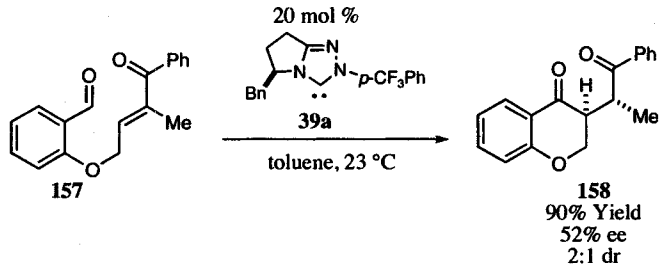

Further limitation in the formation of contiguous stereocenters with the intramolecular Stetter reaction, arises when a leaving group is placed at the α-position of the Michael acceptor. Treatment of aromatic aldehydes tethered to a di-substituted Michael acceptor containing a halogen or phenol substituent at the α-position resulted in the desired cyclization product. However, under the basic reaction conditions the elimination product was obtained (Table 14). The reaction of **164** can be monitored by TLC and stopped prior to completion to isolate the desired product; however, the diastereoselectivity was found to be a disappointing 1:1.5 and therefore the reaction was not optimized nor was the enantioselectivity determined.

Table 14.

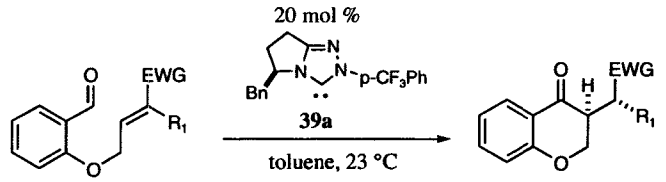

Entry	Substrate	Product	% Yield	% ee	% dr
1	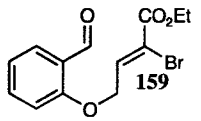 159	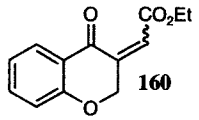 160	65	NA	NA
2[a]	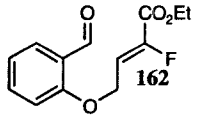 162	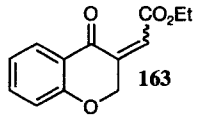 163	27	NA	NA
3	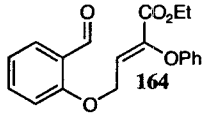 164	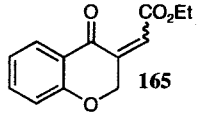 165	60	NA	NA
4	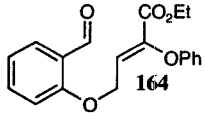 164	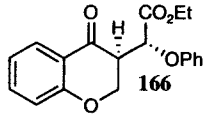 166	23	ND	1:1:5

[a] Reaction run at 0.1M because no reaction occured at 0.02 M

The synthetic utility of the intramolecular Stetter reaction has been extended to include the formation of contiguous stereocenters in high enantio- and diastereoselectivity. We are able to control both newly formed stereocenters in a relative and absolute sense using catalytic amounts of chiral triazolinylidene carbenes. Currently, the formation of contiguous stereocenters via the asymmetric intramolecular Stetter reaction is restricted to alkyl substituents at the α position of the Michael acceptor.

2.5.5 Asymmetric Intermolecular Stetter Reaction

The intermolecular Stetter reaction using achiral thiazolium salts or cyanide anion has been extensively studied and by and large the scope of the reaction is

extremely broad. Typically, protic solvents with amine bases are employed and the temperature is usually ambient or above. Michael acceptors that contain a β-substituent are normally chalcone derived and often result in diminished reactivity.

Consequently, the asymmetric intermolecular Stetter reaction has received less attention and has met with limited success. Enders and co-workers reported the only example of an intermolecular Stetter reaction utilizing a chiral thiazolium pre-catalyst **169** in a bi-phasic solution of CH_2Cl_2:H_2O that resulted in the desired 1,4-dicarbonyl **170** in 39% ee but only 4% overall yield (Scheme 32).[50]

Scheme 32.

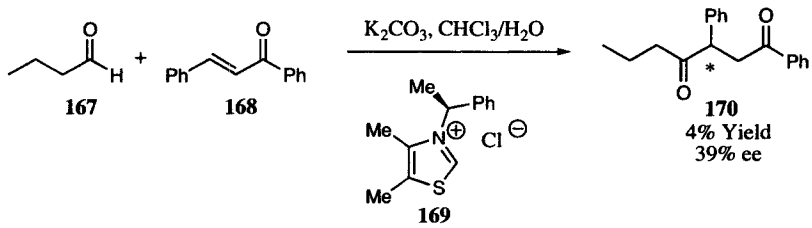

Recently, Johnson and co-workers have developed an elegant solution to the enantioselective intermolecular synthesis of 1,4-dicarbonyls by taking advantage of the umpolung reactivity of acyl silanes catalyzed by chiral metallophosphites (Scheme 33). Acyl silanes are effective aldehyde surrogates capable of forming an acyl anion equivalent that can add to a variety of electrophiles in the presence of nucleophilic catalysts. A key feature in the utility of acyl silanes is the [1,2] Brook rearrangement that offers unique advantages in the umpolung reactions.[51] Taking advantage of this concept Johnson was able to fashion the enantioselective synthesis of 1,4-dicarbonyls in 89-97% ee and good chemical yield for α,β-unsaturated amides that contained an aromatic substituent at the β-position (Scheme 33).[52] Simple

recrystallization leads to useful enantioselectivity upgrades in several cases. In spite of this example the asymmetric intermolecular Stetter reaction remains problematic.

Scheme 33.

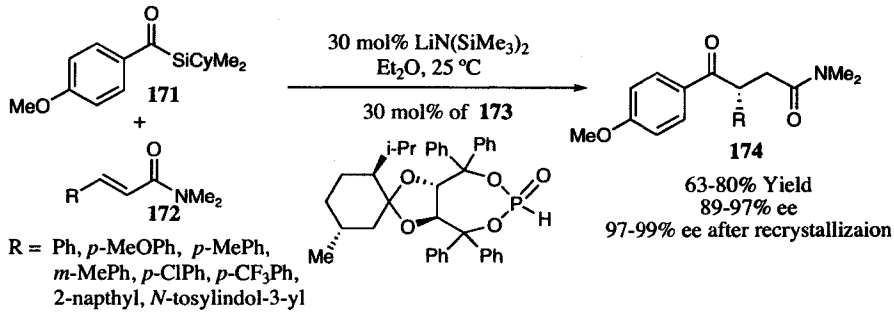

Optimistic from the success observed with the highly asymmetric intramolecular Stetter reaction, we turned our attention to the asymmetric intermolecular Stetter reaction. The initial intermolecular Stetter reaction was performed using thiazolium salt as the pre-catalyst and to no surprise afforded the desired product in 82% yield (Table 15, entry 1). With reaction conditions in hand, and with TLC and NMR of the product chiral triazolium salt **38** was tested. However, no desired product was observed by TLC or crude ^{1}H NMR. The electronic nature of the aldehyde component was varied from electron rich to electron poor to see if the aldehyde affected the outcome of the reaction and in each case only starting material was obtained (entries 2-5). The reaction conditions were switched to toluene, KHMDS and heat (23→110 °C), but still no desired reaction was observed.

Table 15.

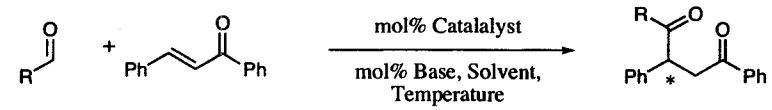

Entry	Aldehyde	Catalyst	Base	Solvent	Temp °C	% Yield	% ee
1	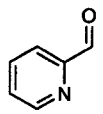 **175**	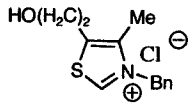	Et_3N	EtOH	78	82	NA
2	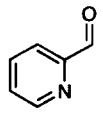 **176**	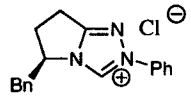	Et_3N	EtOH	78	0	NA
3	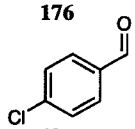 **177**	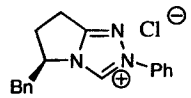	Et_3N	EtOH	78	0	NA
4	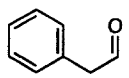 **178**	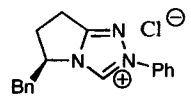	Et_3N	EtOH	78	0	NA
5	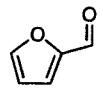 **179**	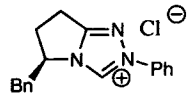	Et_3N	EtOH	78	0	NA
6	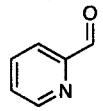 **180**	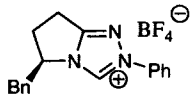	KHMDS	Toluene	23-110	0	NA
7	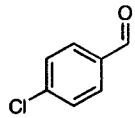 **181**	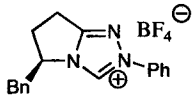	KHMDS	Toluene	23-110	0	NA

A closer examination of the reaction by ^{1}H NMR revealed a disappearance of the nucleophilic carbene and the α,β-unsaturated hydrogen signals of chalcone. It is known that nucleophilic triazolinylidene carbenes can add to the β-position of an appropriate Michael acceptor. [53] Treatment of the triazolium salt **38** with 1 equivalent of KHMDS and 1 equivalent of chalcone afforded a new product that corresponded to the addition of the nucleophilic carbene to chalcone (Scheme 33). To our surprise the

product was stable to column chromatography and eluted as a single diastereomer, whose structure remains to be conclusively determined. This irreversibly interaction between the carbene and chalcone could be responsible for the lack of reactivity in the intermolecular Stetter reaction. This unexpected result could also lead to a triazolium catalyzed umpolung reaction of α,β-unsaturated ketones if this reaction could be coupled with an appropriate electrophile.[54]

Scheme 34.

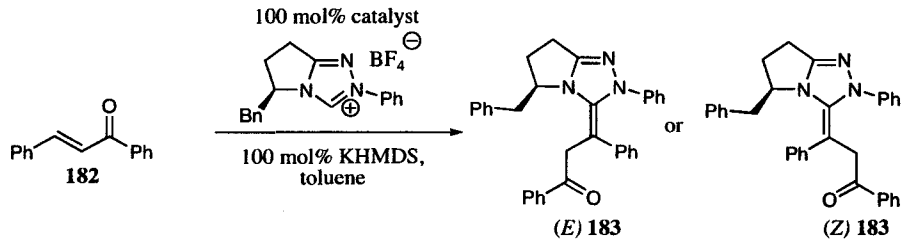

Since our triazolium carbene irreversibly interacts with chalcone, which is the most common pro-chiral Michael acceptor employed in the intermolecular Stetter reaction, acyl silanes were examined for their reactivity. Acyl silanes typically are used as aldehyde surrogates and they should irreversible interact with the carbene in preference to chalcone. Addition of chalcone and acyl silane **184** in 1 mL of THF to a solution of 30 mol% triazolium salt **38**, 33 mol% DBU and 400 mol% i-PrOH, followed by 24 hour reflux. To our gratification afforded the desired product in 41% yield (Scheme 35). Unfortunately, the isolated product was only 5% optically enriched and application of other available chiral triazolium salts did not improve the reactivity or selectivity.

Scheme 35.

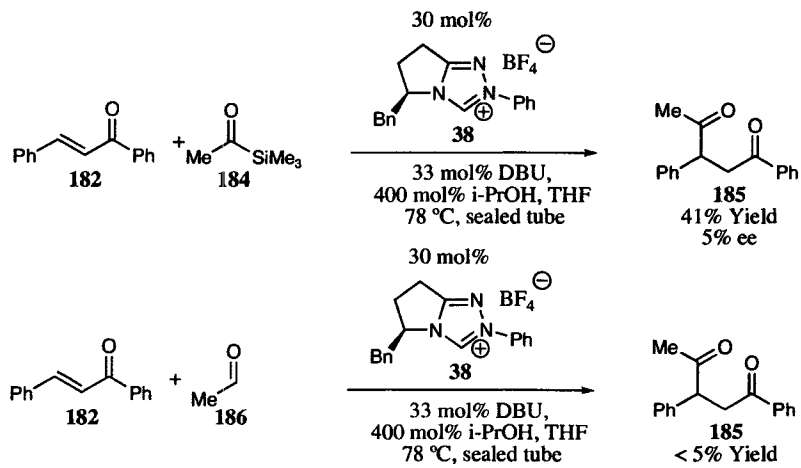

Acyl silanes appear to be advantageous for the intermolecular Stetter reaction, since acetaldehyde only afforded trace amounts of product. The exact role of the acyl silane is unclear, but addition of the carbene to the aldehyde is followed by an irreversible [1,2] Brook rearrangement to form the Breslow intermediate, this intermediate possibly being stabilized by the silyl group which helps facilitate carbon-carbon bond formation. It is not completely clear if *iso*-propanol desilates the Breslow intermediate, which in theory should generate the same intermediate as the reaction commencing from acetaldehyde, or the intermediate after carbon-carbon bond formation.

2.5.6 Conclusion

In conclusion, a highly enantioselective intramolecular Stetter reaction has been developed which utilized a variety of electron rich and electron poor aromatic aldehydes tethered to a variety of Michael acceptors. We extended this reaction manifold to include aliphatic aldehydes that contain acidic hydrogens α to the

aldehyde. Subsequently the synthetic utility of the intramolecular Stetter reaction has been extended with the development of a highly enantio- and diastereoselective version. We are able to control both newly formed stereocenters in a relative and absolute sense using catalytic amounts of chiral triazolinylidene carbenes. The initial carbon-carbon bond formation proceeds in excellent enantioselectivity and the available evidence suggests that proton transfer occurs at the sterically more hindered face in an intramolecular fashion. The relative diastereoselectivity can be controlled by the olefin geometry of the Michael acceptor, while varying the electronic nature of the chiral triazolinylidene carbene leads to increased enantio- and diastereoselectivity.

References

[1] For reviews see; (a) Enders, D.; Balensiefer, T. *Acc. Chem. Res.* **2004**, *37*, 534-541. (b) Johnson, J. S.; *Angew. Chem., Int. Ed.* **2004**, *43*, 1326-1328. (c) Pohl. M.; Lingen, B.; Muller, M. *Chem. Eur. J.* **2002**, *8*, 5288-5295.

[2] For review, see; (a) Albright, J. D. *Tetrahedron* **1983**, *39*, 3207-3233. (b) Aitken, R. A.; Thomas, A. W. *Adv. Heterocyclic Chem.* **2001**, *79*, 89-114.

[3] Wohler, F.; Liebig, J. *Annalen der Pharmacie* **1832**, 249-282.

[4] Lapworth, A. *J. Chem. Soc.* **1903**, *83*, 995-1005.

[5] Breslow, R. *J. Am. Chem. Soc.* **1958**, *80*, 3719-3726.

[6] Kluger, R. *Chem. Rev.* **1987**, *87*, 863-876.

[7] (a) Sheehan, J. C.; Hunneman, D. H. *J. Am. Chem. Soc.* **1966**, *88*, 3666-3667. (b) Sheehan, J. C.; Hara, T. *J. Org. Chem.* **1974**, *39*, 1196-1199.

[8] (a) Tagaki, W.; Tamura, Y.; Yano, Y. *Bull. Chem. Soc. Jpn.* **1980**, *53*, 478-480. (b) Martí, J.; Castells, J.; López-Calahorra, F. *Tetrahedron Lett.* **1994**, *35*, 699-702. (c)

[9] Enders, D.; Breuer, K. *Helv. Chim. Acta* **1996**, *79*, 1217-1221.

[10] Knight, R. L.; Leeper, F. J.*Tetrahedron Lett.* **1997**, *38*, 3611-3614.

[11] Gerhard, A. U.; Leeper, F. J. *Tetrahedron Lett.* **1997**, *38*, 3615-3618.

[12] Dvorak, C. A.; Rawal, V. H. *Tetrahedron Lett.* **1998**, *39*, 2925-2928.

[13] Knight, R. J.; Leeper, F. J. *J. Chem. Soc. Perkin Trans.* **1998**, 1891-1893.

[14] We had immediate success in the asymmetric intramolecular Stetter reaction and as mentioned in chapter 1, without our prior knowledge, Leeper and Knight had already reported that triazolium salts with a similar scaffold afforded moderate reactivity and selectivity in the asymmetric benzoin reaction.

[15] Dünkelmann, P.; Kolter-Jung, D.; Nitsche, A.; Demir, A. S.; Siegert, P.; Lingen, B.; Baumann, M.; Pohl, M.; Müller, M. *J. Am. Chem. Soc.* **2002**, *124*, 12084-12085.

[16] (a) Linghu, X.; Johnson, J. S. *Angew. Chem., Int. Ed.* **2003**, *42*, 2534-2536. (b) Linghu, X.; Johnson, J. S. *J. Am. Chem. Soc.* **2004**, *126*, 3070-3071. (c) Linghu, X.; Bausch, C. C. *J. Am. Chem. Soc.* **2005**, *127*,

[17] Stetter, H.; Kuhlmann, H. In *Organic Reactions*; Paquette, L. A., Ed.; Wiley: New York, 1991; Vol. 40, pp 407-496.

[18] Ciganek, E. *Synthesis* **1995**, 1311-1314. One prior example of a intramolecular Stetter reaction was reported see; Trost, B.; Shuey, C. D.; DiNinno, F.; McElvain, C. D. *J. Am. Chem. Soc.* **1979**, *101*, 1284.

[19] Enders and co-workers did report one other example of an asymmetric intermolecular Stetter reaction prior to 2002; however the reaction only went in 4% yield and 39% ee, see; Enders, D.; Balensiefer, T. Acc. Chem. Res. **2004**, *37*, 534-541.

[20] Enders, D.; Breuer, K.; Runsink, J. *Helv. Chim. Acta.* **1996**, *79*, 1899-1902.

[21] Kerr, M. S.; Read de Alaniz, J.; Rovis, T. *J. Am. Chem. Soc.* **2002**, *124*, 10298-10299.

[22] Pesch, J.; Harms, K.; Bach, T. *Eur. J. Org. Chem.* **2004**, 2025-2035.

[23] Mennen, S. M., Blank, J. T.; Tran, M. B.; Imbriglio, J. E.; Miller, S. J. *Chem. Commun.* **2005**, 195.

[24] Kerr, M. S.; Rovis, T. *J. Am. Chem. Soc.* **2004**, *126*, 8876-8877.

[25] Liu, Q.; Rovis, T. *J. Am. Chem. Soc.* **2006**, *128*, 2552-2553.

[26] Reynolds, N. T.; Rovis, T. *Tetrahedron* **2005**, *61*, 6368-6378.

[27] See reference 18a.

[28] Optically enriched product **51** was re-subjected to an intramolecular Stetter reaction conditions and racemic product was re-isolated.

[29] Reactions that contain an EWG on the aromatic backbone are typically done in 15-60 minutes. If the reaction is allowed to stir for 24 hours the product is isolated with enantiomeric excess between 67-80%. In addition we briefly examined if ee loss occurred during purification by column chromatography; see section 2.4.3 for details.

[30] Kerr, M. S.; Rovis, T. *Synlett* **2003**, 1934-1936.

[31] The absolute configuration of products **34** formed with catalyst **38** was determined to be S by comparison of the measured optical rotation value with the corresponding literature data (see reference 20). The absolute configuration of the other substrates was assigned by analogy.

[32] (a) Dudding, T.; Houk, K. N. *Proc. Natl. Acad. Sci.* USA **2004**, *101*, 5770-5775.

[33] The proposed transition state is further supported by a recent example by Enders and co-workers utilizing chiral triazolium salts in an asymmetric intramolecular crossed-benzoin reaction. Enders, D.; Niemeier, O.; Balensiefer, T. *Angew. Chem. Int. Ed.*, **2006**, *45*, 1463-1467.

[34] See reference 24.

[35] (a) Yamaguchi, M. In *Comprehensive Asymmetric Catalystis;* Jacobsen, E. N., Pfaltz, A., Yamamoto, H., Eds.; Springer: Berlin, 1999; Vol. 3, Chapter 31.2. (b) Sibi,

M. P.; Manyem, S. *Tetrahedron* **2000**, *56,* 8033-8061 and references therein. (c) Alexakis, A.; Benhaim, C. *Eur. J. Org. Chem.* **2002**, 3221-3236.

[36] For examples of copper catalyzed 1,4-addition–aldol reactions, see: (a) Kitamura, M.; Miki, T.; Nakano, K.; Noyori, R. *Tetrahedron Lett.* **1996**, *37*, 5141-5144. (b) Feringa, B. L.; Pineschi, M.; Arnold, L. A.; Imbos, R.; H. M. de Vries, A. *Angew. Chem., Int. Ed. Engl.* ***1997***, *36*, 2620-2623. (c) Naasz, R.; Arnold, L. A.; Pineschi, M.; Keller, E.; Feringa, B. L. *J. Am. Chem. Soc.* **1999**, *121*, 1104-1105. (d) Arnold, L. A.; Naasz, R.; Minnaard, A. J.; Feringa, B. L. *J. Am. Chem. Soc.* **2001**, *123*, 5841-5842. For an example of a halide and tosylate trap, see: (e) Mizutani, H.; Degrado, S. J.; Hoveyda, A. H. *J. Am. Chem. Soc.* **2002**, *124*, 779-781. (f) Degrado, S. J.; Mizutani, H.; Hoveyda, A. H. *J. Am. Chem. Soc.* **2001**, *124*, 755-756. For examples of a ketone, ester and nitrile trap, see: (g) Agapiou, K.; Cauble, D. F.; Krische, M. J. *J. Am. Chem. Soc.* **2004**, *126*, 4528-4529. For an example of oxocarbenium trap, see: (h) Alexakis, A.; Trevitt, G. P.; Bernardinelli, G. *J. Am. Chem. Soc.* **2001**, *123*, 4358-4359. For an example of a proton trap, see: (i) Degrado, S.; Mizutani, H.; Hoveyda, A. H. *J. Am. Chem. Soc.* **2002**, *124*, 13362-13363. (j) Augustin, M.; Palais, L.; Alexakis, A. *Angew. Chem., Int. Ed.* **2005**, *44*, 1376-1378.

[37] For examples of Rh-catalyzed 1,4-addition-aldol reaction, see: (a) Taylor, S. J.; Duffey, M. O.; Morken, J. P. *J. Am. Chem. Soc.* **2000**, *122*, 4528-4529. (b) Yoshida, K.; Ogasawara, M.; Hayashi, T. *J. Am. Chem. Soc.* **2002**, *124*, 10984-10985. (c) Cauble, D. F.; Gipson, J. D.; Krische, M. J. *J. Am. Chem. Soc.* **2003**, *125*, 1110-1111, and references therein.

[38] For selective examples of 1,4-addition/tandem reactions with chiral auxiliaries, see: (a) Chernaga, A. N.; Davies, S. G.; Lewis, C. N.; Todd, R. S. *J. Chem. Soc., Perkin Trans. 1,* **1999**, 3603-3608. (b) Miller, D. B.; Raychaudhuri, S. R.; Avasthi, K.; Lal, K.; Levison, B.; Salomon, R. G. *J. Org. Chem.* **1990**, *55*, 3164-3175.

[39] For selective examples of conjugate addition/tandem reactions of chiral nucleophiles, see: (a) Hanessian, S.; Gomtsyan, A.; Malek, N. *J. Org. Chem.* **2000**, *65*, 5623-5631. (b) Enders, D.; Vazquez, J.; Raabe, G. *Eur. J. Org. Chem.* **2000**, 893-901.

[40] For example of tandem radical reactions, see: Sibi, M. P.; Chen, J. *J. Am. Chem. Soc.* **2001**, *123*, 9472-9473.

[41] For examples of concerted conjugate addition to Michael acceptors, see: (a) Niu, D.; Zhao, K. *J. Am. Chem. Soc.* **1999**, *121*, 2456-2459. (b) Sibi, M. P.; Liu, M. *Org. Lett.* **2000**, *21*, 3393-3396. (c) Sibi, M. P.; Prabagaran, N.; Ghorpade, S. G.; Jasperse, C. P. *J. Am. Chem. Soc.* **2003**, *125*, 11796-11797.

[42] Sibi, M. P.; Petrovic, G.; Zimmerman, J. *J. Am. Chem. Soc.* **2005**, *127*, 2390-2391.

[43] (a) Reetz, M. T.; Moulin, D.; Gosberg, A. *Org. Lett.* **2001**, *25*, 4083-4085. (b) Navarre, L.; Darses, S.; Genet, J. P. *Angew. Chem., Int. Ed.* **2004**, *43*, 719-723. (c) Moss, R. J.; Wadsworth, K. J.; Chapman, C. J.; Frost, C. G. *Chem. Commun.* **2004**, 1984-1985. (d) For a related enantioselective hydrophosphination of methacrylonitrile, see: Sadow, A. D.; Haller, I.; Fadini, L.; Togni, A. *J. Am. Chem. Soc.* **2004**, *126*, 14704-14705.

[44] (a) Glese, B.; Hoffmann, U.; Roth, M.; Velt, A.; Wyss, C.; Zehnder, M.; Zipse, H. *Tetrahedron Lett.* **1993**, *34*, 2445-2448. (b) Taber, D. F.; Gorski, G. J.; Liable-Sands, L. M.; Rheingold, A. L. *Tetrahedron Lett.* **1997**, *38*, 6317-6318. (c) Sibi, M. P.; Asano, Y.; Sausker, J. B. *Angew. Chem., Int. Ed.* **2001**, *40*, 1293-1296 and references within. (d) Sibi, M. P.; Sausker, J. P. *J. Am. Chem. Soc.* **2002**, *124*, 984-991.

[45] (a) Zimmerman, H. E. *Acc. Chem. Res.* **1987**, *20*, 263-268. (b) Zimmerman, H. E.; Wang, P. *Org. Lett.* **2002**, *15*, 2593-2595. For an intramolecular proton transfer, see: (c) Berrada, S.; Metzner, P. *Tetrahedron Lett.* **1987**, *28*, 409-412.

[46] (a) Fleming, I.; Lewis, J. J. *J. Chem. Soc., Perkin Trans. 1,* **1992**, 3257-3266 and references therein. For related examples that study the approach of electrophiles on carbon-carbon double bond adjacent to a stereogenic center, see: (b) Row-Paddon, M. N.; Rondan, N. G.; Houk, K. N. *J. Am. Chem. Soc.* **1982**, *104*, 7162-7166. (c) Yamamoto, Y.; Maruyama, K. *J. Chem. Soc., Perkin Trans. 1,* **1984**, 904-905. (d) Kawasaki, H.; Tomioka, K.; Koga, K. *Tetrahedron Lett.* **1985**, *26*, 3031-3034. (e) Mohrig, J. R.; Rosenberg, R. E.; Apostol, J. W.; Bastienaansen, M.; Evans, J. W.; Franklin, S. J.; Frisbie, D. C.; Fu, S. S.; Hamm, M. L.; Hirose, C. B.; Hunstad, D. A.; James, T. L.; King, R. W.; Larson, C. J.; Latham, H. A.; Owen, D. A.; Stein, K. A.; Warnet, R. *J. Am. Chem. Soc.* **1997**, *119*, 479-486.

[47] Read de Alaniz, J.; Rovis, T. *J. Am. Chem. Soc.* **2005**, *127*, 6284-6289.

[48] See experimental section for crystal structure data.

[49] For examples of concerted conjugate addition to Michael acceptors, see: (a) Niu, D.; Zhao, K. *J. Am. Chem. Soc.* **1999**, *121*, 2456-2459. (b) Sibi, M. P.; Liu, M. *Org. Lett.* **2000**, *21*, 3393-3396. (c) Sibi, M. P.; Prabagaran, N.; Ghorpade, S. G.; Jasperse, C. P. *J. Am. Chem. Soc.* **2003**, *125*, 11796-11797.

[50] Enders, D.; Balensiefer, T. Acc. Chem. Res. **2004**, *37*, 534-541.

[51] For related examples of acyl silanes in the Stetter reaction see; (a) Mattson, A. E.; Bharadwaj, A. R.; Scheidt, K. A. *J. Am. Chem. Soc.* **2004**, *126*, 2314-2315. (b) Bharadwaj, A. R.; Scheidt, K. A. *Org. Lett.* **2004**, *6*, 2465-2468.

[52] Nahm, M. R.; Potnick, J. R.; White, P. S.; Johnson, J. S. *J. Am. Chem. Soc.* **2006**, and references within.

[53] (a) Enders, D.; Breuer, K.; Raabe, G.; Runsink, J.; Teles, H.; Melder, J-P.; Ebel, K.l Brode, S. *Angew. Chem., Int. Ed.* **1995**, *34*, 1021-1023. (b) Enders, D.; Breuer, K.; Teles, J. H.; Runsink, J. *Liebigs Ann. Chem.* **1996**, 2019-2028. (c) Enders, D.; Breuer, K.; Kallfass, U.; Balensiefer, T. *Synthesis*, **2003**, *8*, 1292-1295.

[54] Fischer, C.; Smith, S. W.; Powell, D. A.; Fu, G. C. *J. Am. Chem. Soc.* **2006**, *128*, 1472-1473.

Chapter 3

The Mechanism of the Intramolecular Stetter Reaction

3.1 Introduction

In 1953 Breslow reported a landmark paper entitled *On the mechanism of thiamine action* that elucidated the catalytic role of thiamine pyrophosphate.[1] In an account of the discovery, Breslow recalls the definitive moment when he discovered the acidity of the hydrogen atom sandwiched between the nitrogen and sulfur of the thiamine: "using a home-built 30 MHz instrument (tuned by inserting a screwdriver into the chassis) in the laboratory of Ben Dailey, I watched a single proton signal in the NMR of thiazolium salts disappear as that proton exchanged with D_2O."[2] Combining this observation with other experimental evidence, Breslow was able to postulate the currently accepted mechanism of the thiazolium catalyzed benzoin reaction. According to the proposed mechanism, intermediate **II** results from nucleophilic attack of the ylide **I** into the aldehyde. Subsequent proton transfer affords the acyl anion equivalent **III**, commonly known as the Breslow intermediate. Carbon-carbon bond formation results from nucleophilic attack of the Breslow intermediate **III** into another aldehyde molecule, generating the enolate **IV**. Alkoxide protonation followed by catalyst turnover generates the desired product. The benzoin reaction is fully reversible utilizing thiazolium derived catalysts.

Scheme 1.

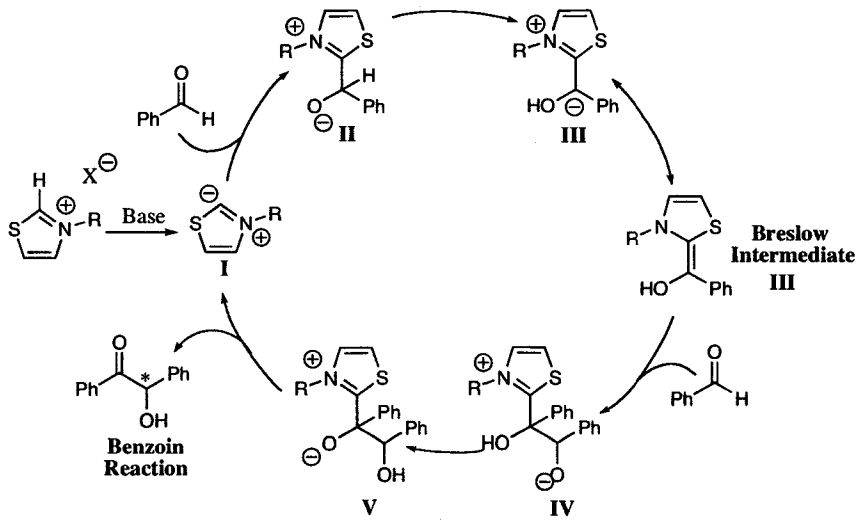

3.1 The Proposed Mechanism of the Stetter Reaction

A thorough study of the mechanism of the Stetter reaction has not, to our knowledge, been conducted. In its absence, the most reasonable mechanism (Scheme 2) is an adaptation of the related, and much better studied, benzoin reaction.[3] According to the proposed mechanism, intermediate **VI** results from nucleophilic attack of the carbene into the aldehyde. Subsequent proton transfer affords the acyl anion equivalent **VII**, whose resonance structure is the triazole-enamine. Carbon-carbon bond formation results from nucleophilic attack of the enamine **VII** into a Michael acceptor, generating enolate **VIII**. Enolate protonation generates the 1,4-dicarbonyl and releases the catalyst, closing the catalytic cycle.

Scheme 2.

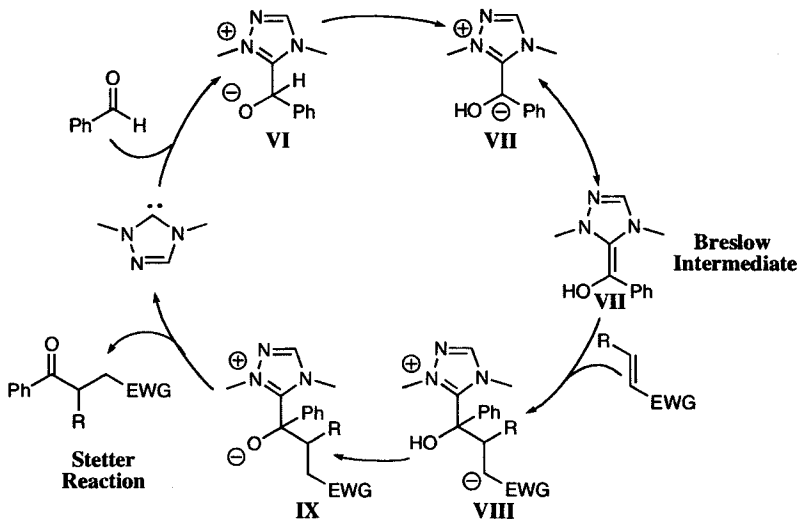

A highly enantioselective intramolecular Stetter reaction was developed with a limited understanding of the factors that affect the mechanism. There are still substrates that do not participate under the optimized reaction conditions. Furthermore, for reasons that are unclear, we are unable to perform an asymmetric intermolecular Stetter reaction. Driven by this lack of understanding and control, a thorough investigation of the mechanism of the intramolecular Stetter reaction was conducted with an overall goal of developing more general reaction conditions for the asymmetric Stetter reaction.

3.1 Uncovering the Rate-Determining Step

3.1.1 Deuterium Isotope Effect

To garner more information about the intramolecular Stetter reaction the kinetic isotope effect (KIE) of labeled aldehydes was examined. Comparison of rates of proton verses deuterium labeled aldehydes tethered to identical Michael acceptors should determine if there is an appreciable deuterium isotope effect. Based on our

experimental evidence (Chapter 2) it was initially believed that carbon-carbon bond formation was the rate-limiting step in the intramolecular Stetter reaction. If carbon-carbon bond formation is the rate-determining step, the reaction should exhibit no appreciable deuterium isotope effect ($k_H/k_D = \sim 1$). If, however, addition of carbene to the aldehyde is rate-determining, the reaction should show a secondary isotope effect. Secondary isotope effects are significant when the rate-determining step involves a hybridization change of the isotopically labeled atom and for hybridization changes from $sp^2 \rightarrow sp^3$ an inverse KIE is observed ($k_H/k_D < 1$). If either proton transfer is involved in the rate-determining step the isotope effect should be primary ($k_H/k_D >> 1$).[4]

To determine the kinetic isotope effect deuteroaldehyde **6** was synthesized. A three-step sequence was employed for the preparation of the required deuteroaldehyde. Salicylaldehyde **1** was protected as the dithioacetal **2**,[5] which was deprotonated with n-BuLi at –78 °C and quenched with deuterated methanol (MeOD).[6] Deprotection of the dithioacetal afforded the desired deuteroaldehyde **4**. Subsequent reaction with ethyl bromocrotonate in acetone resulted in the desired deuteroaldehyde tethered to an α,β-unsaturated ethyl ester (Scheme 3).[7]

Scheme 3.

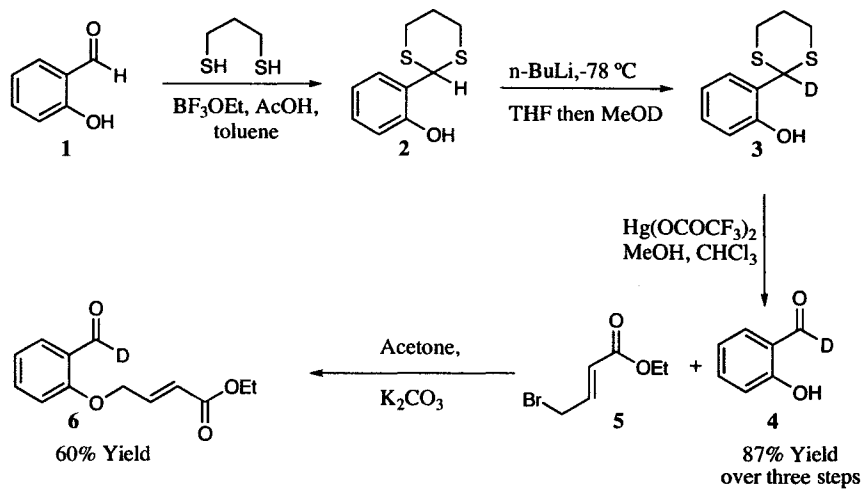

Mechanistic studies began with direct competition experiments between deuteroaldehyde **6** and protioaldehyde **7** (Scheme 4). My co-worker Mark S. Kerr performed the first reaction, where he treated a 1:1 mixture of the protio- and deuteroaldehyde to optimized reaction conditions and stopped the reaction at approximately 10-20% conversion or ^{1}H NMR integration of the isolated unreacted starting materials provided the KIE (Scheme 4).

Scheme 4.

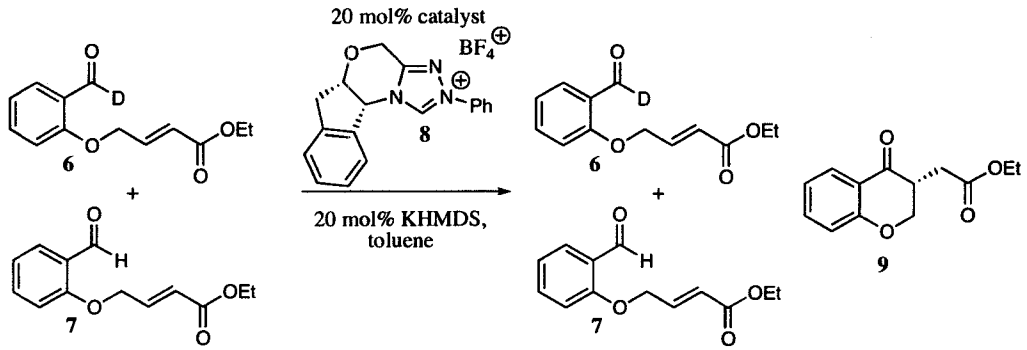

Comparing the conversion of the protio- and deuteroaldehydes, a KIE of approximately 4.0 was observed which implies a primary isotope effect. The primary isotope effect corresponds to either breaking the CH bond in the tetrahedral intermediate **VI** or breaking the OH bond in **VIII**. Worried about the error associated with the k_H/k_D value we wanted to unambiguously determine the deuterium isotope effect.[8] To that end, our attention was turned to monitoring the reaction *in situ* by ^{1}H NMR because the proton shift of the starting material and product of the Stetter reaction are easy to distinguish. With the assistance of Chris Rithner a ^{1}H NMR experiment was developed that recorded a proton spectrum every 30 seconds for 120 minutes. Difficulty in monitoring the reaction by ^{1}H NMR was experienced due to the rate of product formation (**9**) at ambient temperature; the reaction was complete in less than 5 minutes. Therefore, the reactions were run at 10 °C, which slowed the reaction down but caused fluctuations in the baseline of the initial ^{1}H NMR spectrum while the reaction temperature equilibrated. An additional problem arose from the inability to adequately mix the NMR solution during the course of the reaction that sometimes caused variation in the reaction rate. We experienced further complications with deuteroaldehyde **6** because the reaction rate decreased substantially, due, apparently, to catalyst decomposition. As a result reactions performed with deuteroaldehyde **6** often did not go to completion. Despite these setbacks we were able to obtain further support for a primary kinetic isotope effect (Figure 1).

Figure 1.

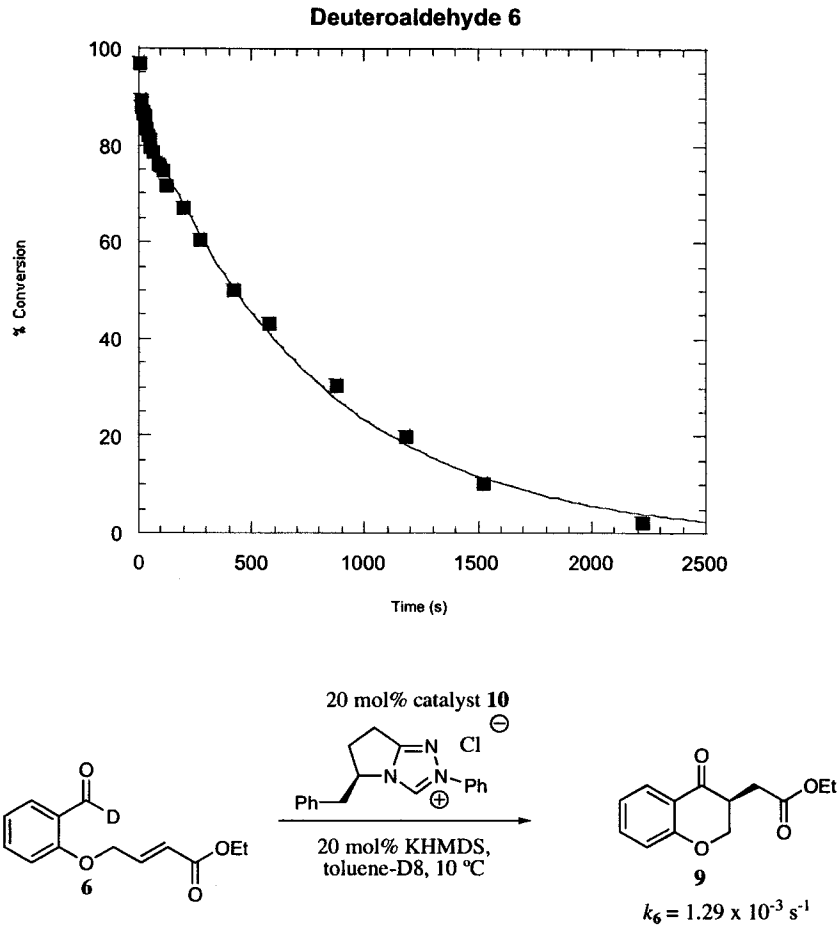

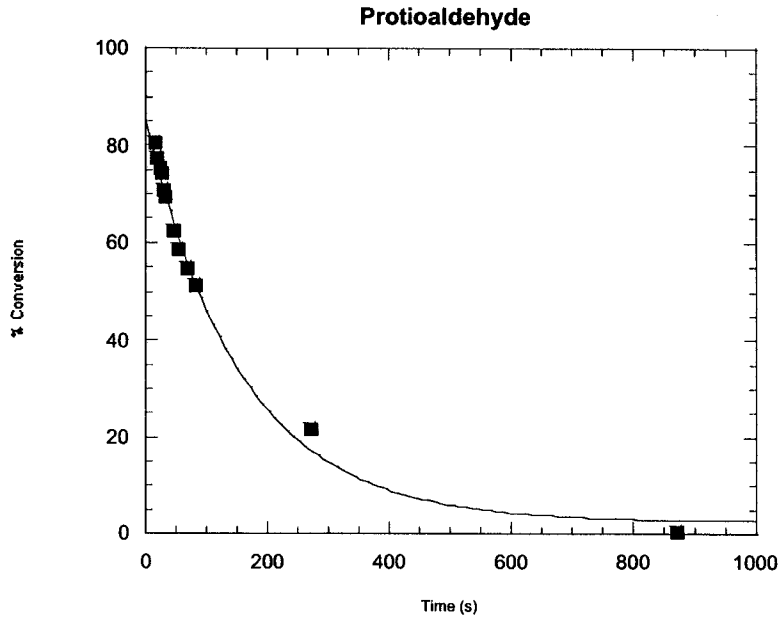

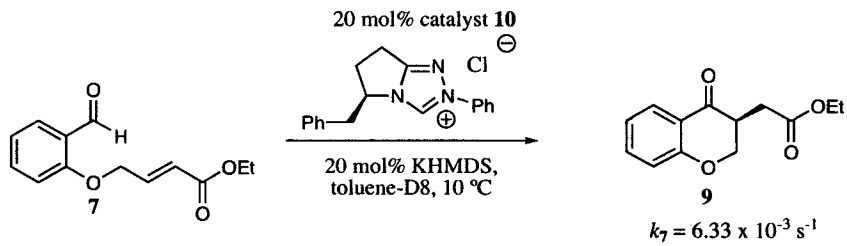

The observed rate constants for conversion of intramolecular Stetter reaction of **6** and **7** are $k_6 = 1.29 \times 10^{-3}\ s^{-1}$ and $k_7 = 6.33 \times 10^{-3}\ s^{-1}$, respectively. The kinetic isotope effect can be determined by k_7/k_6, which is the ratio of the rate constants. A primary deuterium isotope effect of 4.90 is observed, which corresponds to either breaking the CH bond of intermediate **VI** or breaking the OH bond of intermediate **VIII**.

Unfortunately it cannot be ruled out that the deuterium isotope effect obtained from the individual ^{1}H NMR was a result of decomposition of catalyst **10** or problems associated with the experimental technique. We knew from previous experiments

(discussed in the next section 3.3.2) that oxygen is detrimental to the catalytic reaction conditions, an effect especially prevalent for slow reactions such as those involving **6**. To minimize such problems the kinetic isotope reactions were conducted in a glove box and the percent of product formation was calculated by gas chromatography with di-*tert*-butyl-biphenyl as the internal standard. The observed rate constants for **6** and **7** are $k_6 = 1.32 \times 10^{-3}\ s^{-1}$ and $k_7 = 3.95 \times 10^{-3}\ s^{-1}$, respectively. The kinetic isotope effect was determined to be 2.99, indicating that breaking the CH bond of intermediate **VI** or breaking the OH bond of intermediate **VIII** is involved in the rate-determining step under these conditions.

The reaction of **6** or **7** with 5 mol% catalyst **10** was run in the absence of the conjugate acid hexamethyldisilazane (HMDS) at 27 °C (Scheme 5).

Scheme 5.

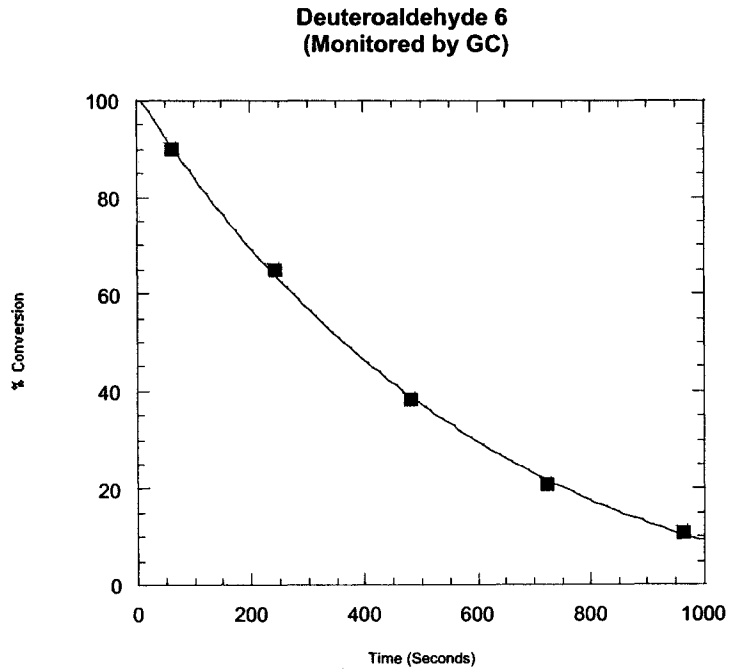

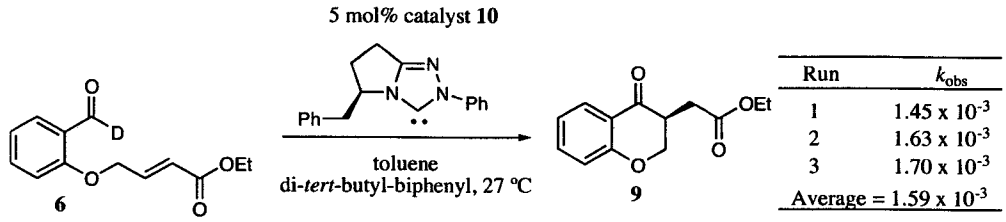

Run	k_{obs}
1	1.45×10^{-3}
2	1.63×10^{-3}
3	1.70×10^{-3}
Average = 1.59×10^{-3}	

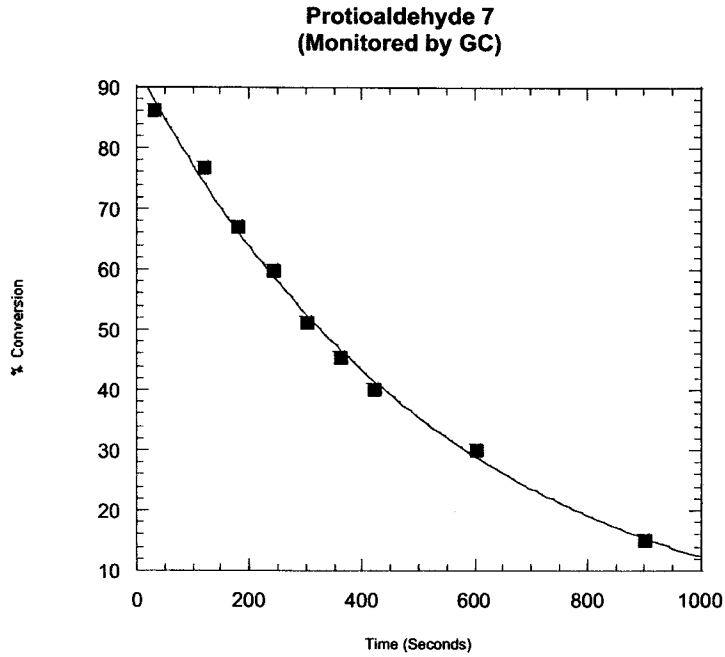

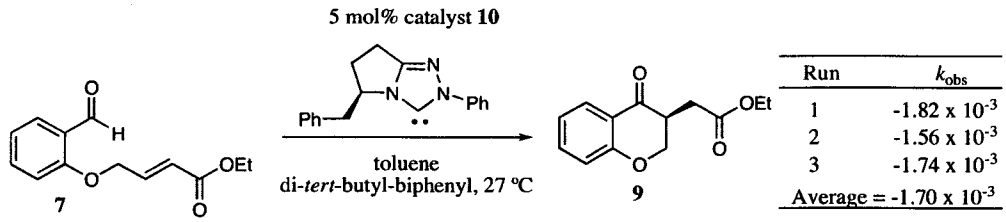

Run	k_{obs}
1	-1.82×10^{-3}
2	-1.56×10^{-3}
3	-1.74×10^{-3}
Average = -1.70×10^{-3}	

To our surprise the observed rate constants for conversion of intramolecular Stetter reaction of **6** and **7** are $k_6 = 1.59 \times 10^{-3}$ s^{-1} and $k_7 = 1.70 \times 10^{-3}$ s^{-1}, respectively. The kinetic isotope effect was determined to be 1.07, indicating that breaking the CH bond of intermediate **VI** or breaking the OH bond of intermediate **VIII** is presumably not involved in the rate-determining step under these conditions.

The deuterium isotope effect of 2.99 in the presence of HMDS strongly suggests a primary isotope effect. However, the deuterium isotope effect of 1.06 in the absence of HMDS combined with experimental evidence (increasing the electrophilic nature of the Michael acceptor can help cyclize difficult substrates) suggests that carbon-carbon bond formation is involved in the rate-determining step. It appears the rate-determining step changes with reaction conditions. In addition it has been suggested by us that the reaction might be operating in a concerted fashion, as illustrated in (Scheme 6),[9] analogous to the reverse Cope elimination mechanism seen with hydroxylamine additions.[10] It was speculated the high diastereoselectivity, up to 150:1, obtained during the intramolecular Stetter reaction of α-disubstituted Michael acceptors took place in a concerted fashion. In order to acquire additional information about the mechanism of the intramolecular Stetter reaction, we collaborated with Professor Singleton at Texas A&M.

Scheme 6.

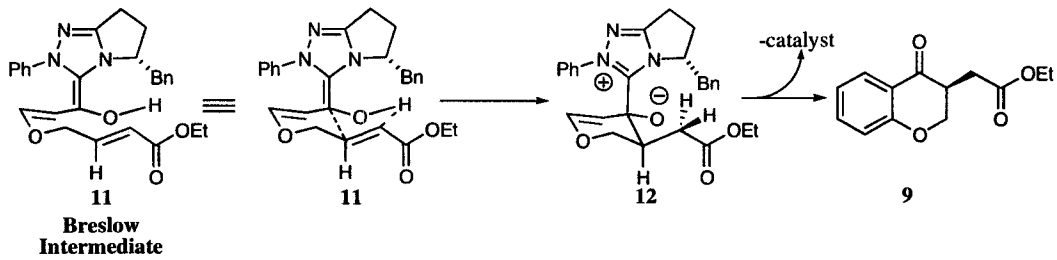

3.3.2 ^{13}C Isotope Effect

Singleton and co-workers have elucidated the mechanism of a number of concerted reactions by measuring ^{13}C kinetic isotope effects.[11] They have demonstrated that the kinetic isotope effect can be measured by integrating the natural abundance of ^{13}C in the starting material recovered from a reaction and comparing

these values to the ^{13}C of unreacted starting material. The accuracy of the integration values requires that there are no major side reactions and the reaction must be stopped at approximately 80% completion. In addition, at least 0.5 grams of recovered starting material must be isolated and must be compared to starting material not submitted to the reaction but prepared from the same batch of starting material. This required the preparation of gram quantities of starting material since the reaction would require at least 2.2 grams of **7**. Additionally, the development of reaction conditions that allowed the catalyst loading to be decreased was desirable since 20 mol% would be 0.620 grams of catalyst, which at the time was being prepared in 1 gram batches.

Experimental observations suggested that air and water both lead to decomposition pathways in the intramolecular Stetter reaction. A better understanding of these detrimental effects may allow for a decrease in the catalyst loading. To determine if oxygen is detrimental the carbene was prepared in an NMR tube and the spectrum was recorded under an atmosphere of argon. No change was observed over 8 hours; subsequently the NMR tube was purged with a balloon of oxygen and the carbene spectrum was monitored by ^{1}H NMR over 24 hours. Once again we observed no change in the proton spectrum by NMR. It is known that the Breslow intermediate is susceptible to oxidation[12] and it was hypothesized that the free carbene is stable to oxygen but unstable during catalytic conditions. In order to test this hypothesis triazolium salt **10** was treated with KHMDS open to air and allowed to stir for 5 minutes (Scheme 7). Starting material **7** was then added in 1mL of toluene and stirred open to air. The reaction prematurely stopped, indicating that

oxygen causes the reaction to shut down. However 42% conversion was observed, suggesting active catalyst is present after stirring open to air for 5 minutes. Presumably the carbene is oxidized during the catalytic cycle to an inactive species.

Scheme 7.

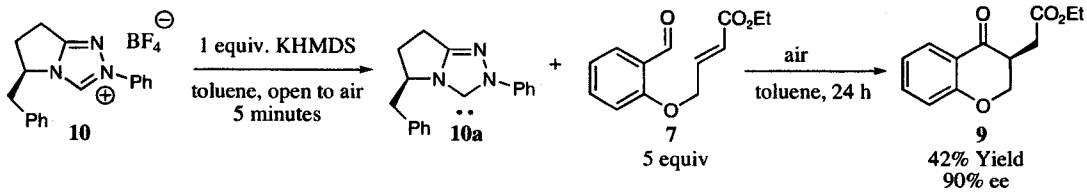

Clearly, oxygen is detrimental to the Stetter reaction, and we next turned our attention to the effects of water. The use of water-saturated toluene as solvent resulted in no reaction. Utilizing ACS grade toluene which contains trace amounts of water resulted in decreased efficiency and the formation of an undesired aldol product, providing **13** (Scheme 8).

Scheme 8.

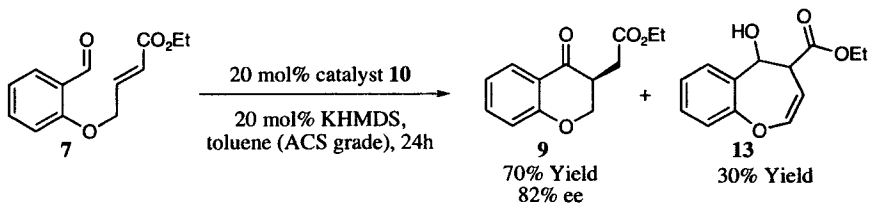

Assuming a trace amount of water in the ACS grade toluene is responsible for the decrease in efficiency, the addition of a water scavenger should help. To our gratification the addition of molecular sieves, sodium sulfate ($NaSO_4$), or magnesium sulfate ($MgSO_4$) resulted in a decrease in reaction time and increased the overall yield, albeit in slightly decreased enantioselectivity (Scheme 9).

Scheme 9.

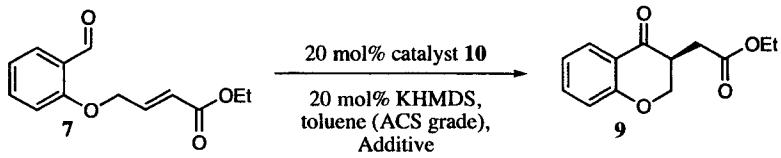

Entry	Additive	Time h	% Yield	% ee
1	—	24	70%	82%
2	molecular sieves 4Å	1.5	90%	85%
3	$NaSO_4$	2	80%	82%
4	$MgSO_4$	2	90%	87%

The decrease in reaction time and increase in yield in the presence of water scavengers implies that trace amounts of water can lead to catalyst decomposition. Despite the slight decrease in enantioselectivity, the utility of ACS grade toluene in the presence of $MgSO_4$ makes this process synthetically attractive, especially when anhydrous toluene is not readily available.

Knowing that oxygen is detrimental to the reaction it was decided to bubble argon through the solution of toluene before and during the course of the reaction in order to exclude fractional amounts of oxygen from inhibiting the reaction. To our delight subjection of 2.2 grams (9.4 mmol) of **7** to a solution of 3 mol% carbene **10** in toluene with bubbling argon resulted in 97% isolated yield of the desired product in 89% ee (Scheme 10).

Scheme 10.

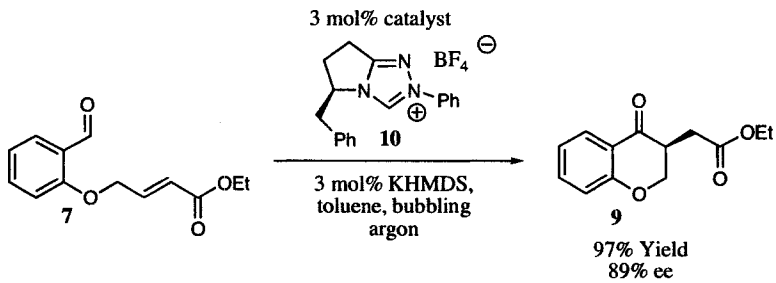

With a better understanding of the parameters that affect the intramolecular Stetter reaction, the reaction on 2.2 grams of starting material **7** was stopped at ~80% completion, required for determining the ^{13}C kinetic isotope effect. The starting material from these reactions was isolated and sent to Singleton along with a 0.5 gram sample of **7** not subjected to the reaction conditions. If the reaction proceeds in a concerted fashion (Scheme 6) an increase in the natural abundance of ^{13}C at the aldehyde carbon, the α and β carbon of the Michael acceptor is expected. If, however, addition to the aldehyde or proton transfer from the tetrahedral intermediate (**VI**) is the rate determining step an increase in the natural abundance of the ^{13}C would be observed at the aldehyde carbon. The results showed a kinetic isotope effect only at the aldehyde carbon illustrated by the increase in natural abundance of ^{13}C at this position (Scheme 11).

Scheme 11.

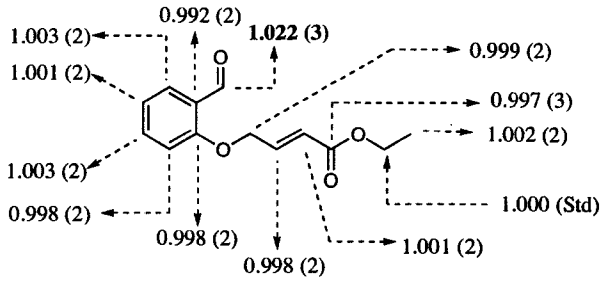

The KIE of 1.022 corresponds to a primary ^{13}C kinetic isotope effect. The primary kinetic isotope effect suggests two reasonable scenarios: carbene addition to the aldehyde is irreversible or proton transfer from the tetrahedral intermediate (**VI**) is irreversible. The results from the ^{13}C kinetic isotope effect cannot distinguish between these possible rate-limiting steps. However, combining this data with our previous calculations for the deuterium isotope effect in the presence of HMDS clearly suggests that proton transfer from the tetrahedral intermediate (**VI**) is the rate-limiting step in the intramolecular Stetter reaction under these reaction conditions. Since the irreversible step occurs prior to carbon-carbon bond formation we are unable to ascertain any information about the second half of the catalytic cycle with these experiments. Further ^{13}C kinetic isotope experiments need to be conducted on the reaction in the absence of HMDS in order to confirm the change in the rate-determining step in the absence of HMDS.

Probing the Second Half of the Catalytic Cycle

In the absence of further evidence, it was assumed that proton transfer from the tetrahedral intermediate is the rate-determining step in the intramolecular Stetter reaction. With this assumption the rate of the reaction should be dependent on the

nature of the tetrahedral intermediate (Scheme 2, **VI**). Therefore, two identical aldehydes tethered to different Michael acceptors (shown as tetrahedral intermediates **14** and **15**) should proceed at the same rate (Scheme 12). Furthermore, an electron poor aldehyde (**16**) is expected to react faster than an electron rich aldehyde (**17**) since the acidity of the hydrogen on the tetrahedral intermediate (**VI**) is affected by the nature of the aromatic aldehyde.

Scheme 12.

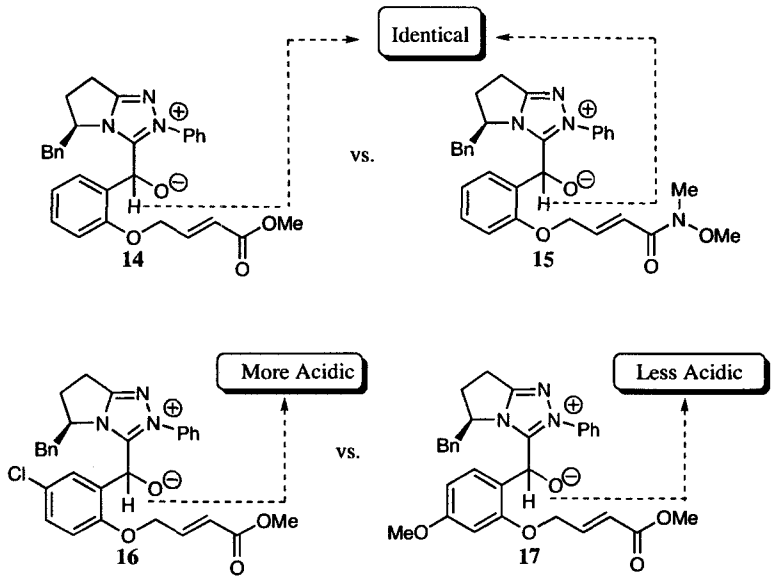

A direct competition between the two substrates was conducted. The direct competition should eliminate the variability associated with catalyst decomposition, since both substrates should be equally affected by catalyst decomposition.

To a flame dried flask was added 40 mol% triazolium salt **10** followed by 5 mL of toluene and 20 mol% KHMDS (0.5 M solution of KHMDS was prepared before each experiment); the resulting solution was stirred for 5 minutes at room temperature with bubbling argon. The mixture was cooled to 0 °C over five minutes, at which time a 1 mL toluene solution of **18**, **20**, and the internal standard di-*tert*-

butyl-biphenyl **21** was added. A 0.1 mL aliquot was taken at 1, 3, 5, 8, 10, 15, 20, 25, 30, 40, and 60 minutes and immediately worked up by passing through a small column and eluted with 100% ethyl acetate. Gas chromatography was used to determine the percent conversion of **18** and **20** relative to the internal standard (Scheme 13). To our gratification, identical aldehydes tethered to sterically different Michael acceptors proceed at approximately the same rate, as predicted from our proposed hypothesis (see Scheme 12).

Scheme 13.

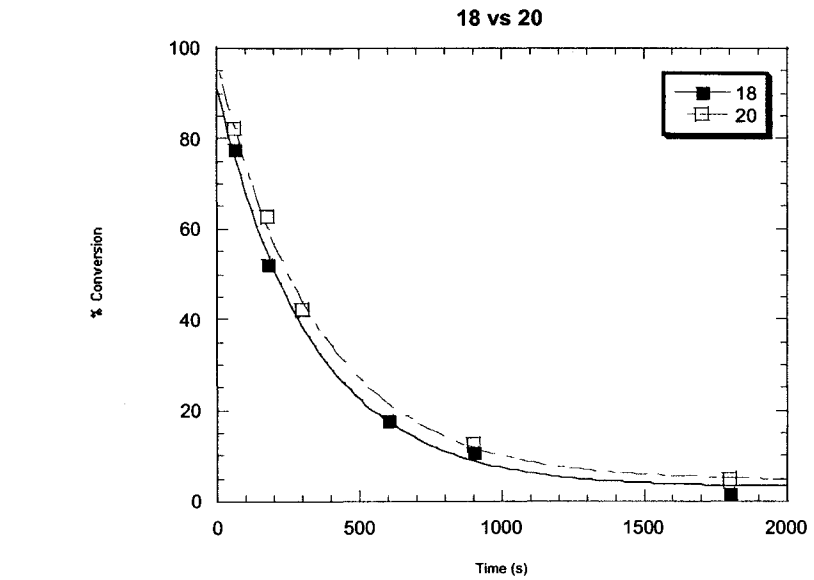

Scheme 13 illustrates that sterics of the α,β-unsaturated ester do not affect the overall rate of the reaction. With reaction and analysis conditions the rate of the reaction with electronically different Michael acceptors was investigated. According to the kinetic isotope effect, the reaction of two electronically different Michael acceptors should proceed at the same rate but experimental evidence suggests that increasing the electrophilicity of the Michael acceptor helps to cyclize difficult substrates. Subjection of **18** and **23** to identical reaction conditions as described above revealed that even electronically different Michael acceptors proceed at the same rate, in agreement with a rate-determining proton transfer event (Scheme 14).

Scheme 14.

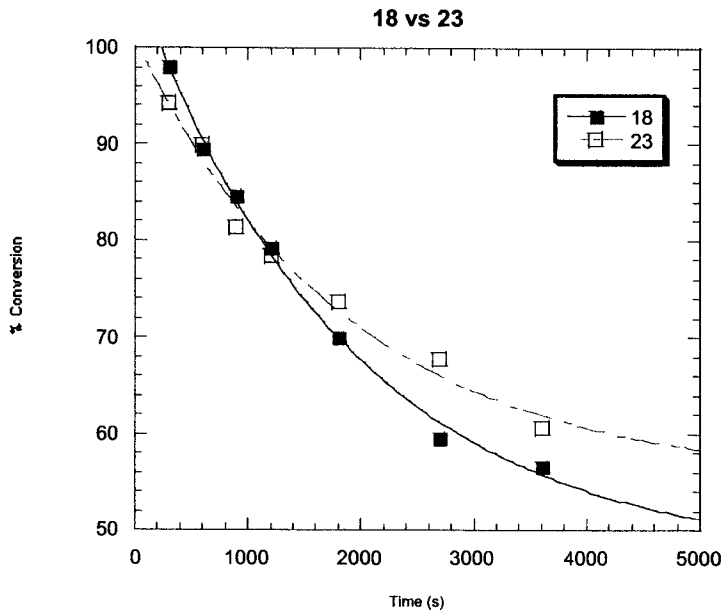

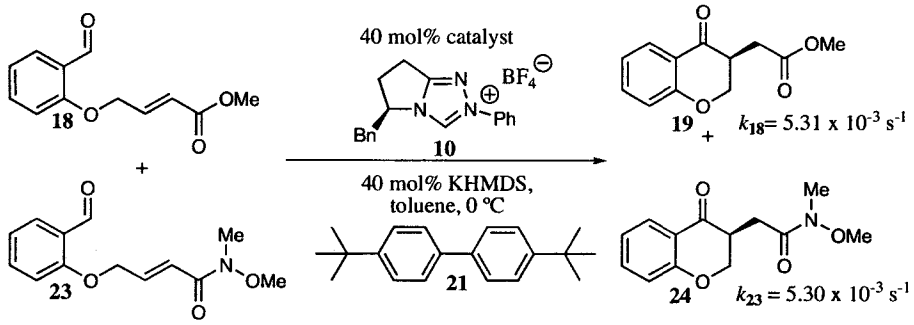

It is important to note slight catalyst decomposition is probably responsible for the observed rate decrease with the α,β-unsaturated methyl ester **18** and the α,β-unsaturated Weinreb amide substrate **23** because the reaction went to completion, but only after 24 hours.

According to the competition experiments, variation of the steric and electronic nature of the Michael acceptor should not play a decisive role in the success of an intramolecular Stetter reaction. It therefore should be no surprise that a broad range of electronically different tethered Michael acceptors work in the

intramolecular Stetter reaction. The competition experiments also suggest that there must be some other contributing factor that aids in cyclization of the difficult substrates when the electronics of the Michael acceptor are changed.

Judging from the results in the competition between different Michael acceptors we were optimistic that the competition experiments between different aromatic aldehydes would lead to different reaction rates. Treatment of an electron poor aldehyde **25** and electron neutral aldehyde **18** to the reaction conditions illustrates that the aldehyde that contains an electron-withdrawing group (**25**) reacts 6.7 times faster than **18**. The observed rates were k_{18}= 2.71 x 10^{-4} s^{-1} and k_{25} = 18.3 x 10^{-4} s^{-1}. Presumably the EWG group decreases the pKa of the tetrahedral intermediate and thus increases the rate of the reaction (Scheme 15).

Scheme 15.

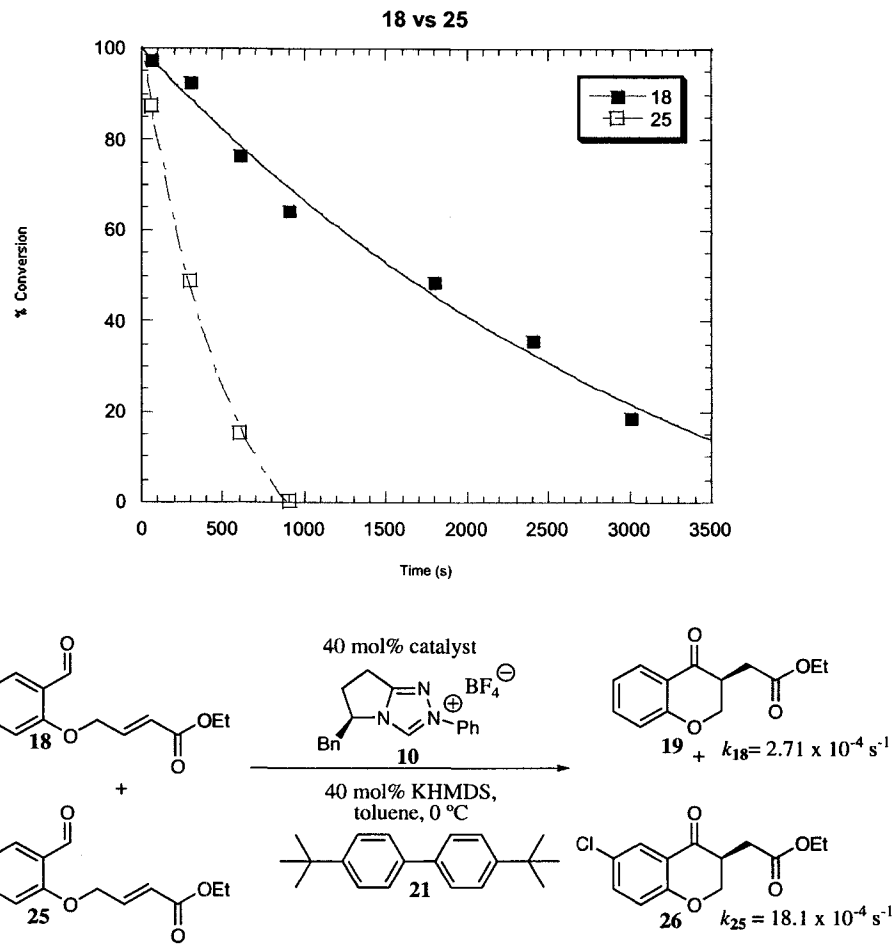

Due to the difficulty in cyclization of substrates that possess an electron donating substituent (EDG) at the 4-postion with triazolium salt **10**, reactions were performed with triazolium salt **28**. Unsurprisingly the aldehyde that contains a *para*-methoxy group proceeded slower than the parent substrate **18** (Scheme 16). The observed rates were k_{18}= 15.1 x 10^{-4} s^{-1} and k_{27} = 3.98 x 10^{-4} s^{-1}. The rate acceleration of **18** is 3.8 times faster than **27** which can be attributed to the decreases in pKa of the tetrahedral intermediate hydrogen formed with substrate **27**.

Scheme 16.

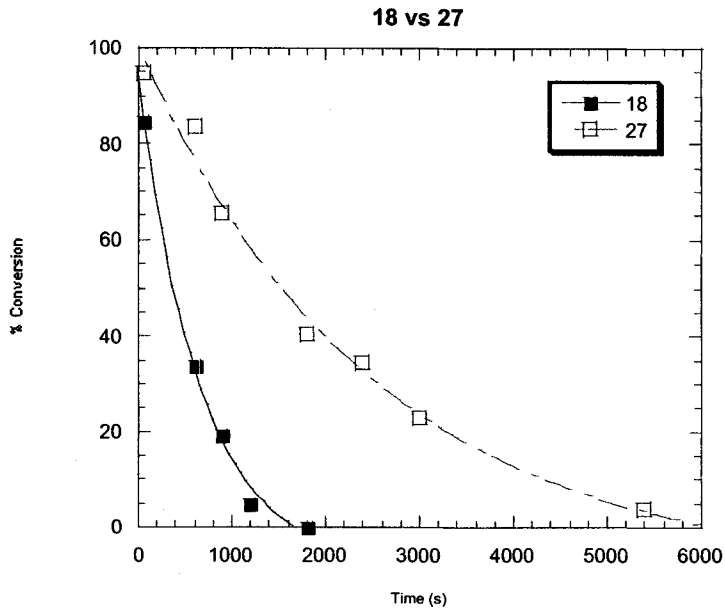

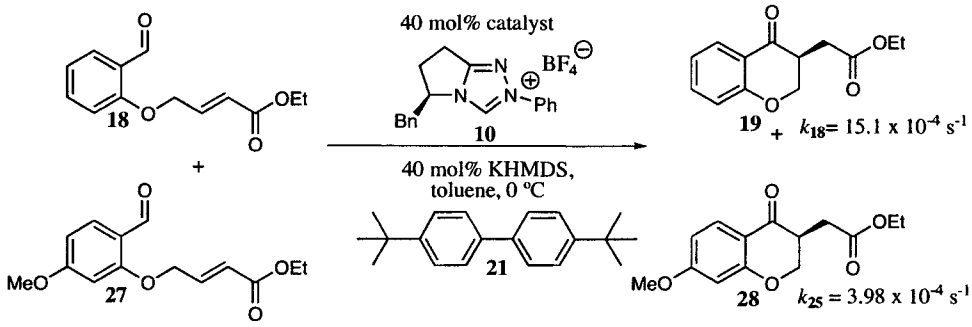

Comparing the rate of different Michael acceptors allowed us to probe the effects in the second half of the catalytic cycle. According to the competition experiments the nature of the Michael acceptor does not contribute significantly to the rate of the intramolecular Stetter reaction, which indicates that carbon-carbon bond formation is not involved in the rate-limiting step, as initially hypothesized. Modification to the nature of the aromatic aldehyde resulted in dramatic rate differences, especially when compared to the competition experiments with different Michael acceptors. The notable rate acceleration with electron poor aldehydes helps

support our previous evidence that proton transfer is the rate-limiting step in the intramolecular Stetter reaction. In addition, observed acceleration supports our experimental evidence that electron-poor triazolium catalysts are generally more reactive. Presumably, removing electron density from the triazolinylidene increases the rate of proton transfer, facilitating the formation of the acyl anion equivalent which leads to carbon-carbon bond formation. These generalizations are only relevant to reactions conducted in the presence of HMDS and do not take into account the possibility that the rates of the reactions might change under free carbene reaction conditions (in the absence of HMDS).

3.4 The Resting State of the Triazolinylidene Carbene

Under typical ^{1}H NMR experimental conditions, the presence of the free carbene after substrate addition was never observed, even after the reaction was complete by ^{1}H NMR. Conceivably, further NMR investigations could help identify the resting state of the nucleophilic carbene. NMR studies began by treating the triazolium salt **10** in toluene-D8 with a 0.5 M solution of KHMDS in toluene-D8. The resulting carbene proton spectrum is shown in Figure 3. The ^{1}H NMR of the free carbene is clear with several diagnostic signals.

Figure 3.

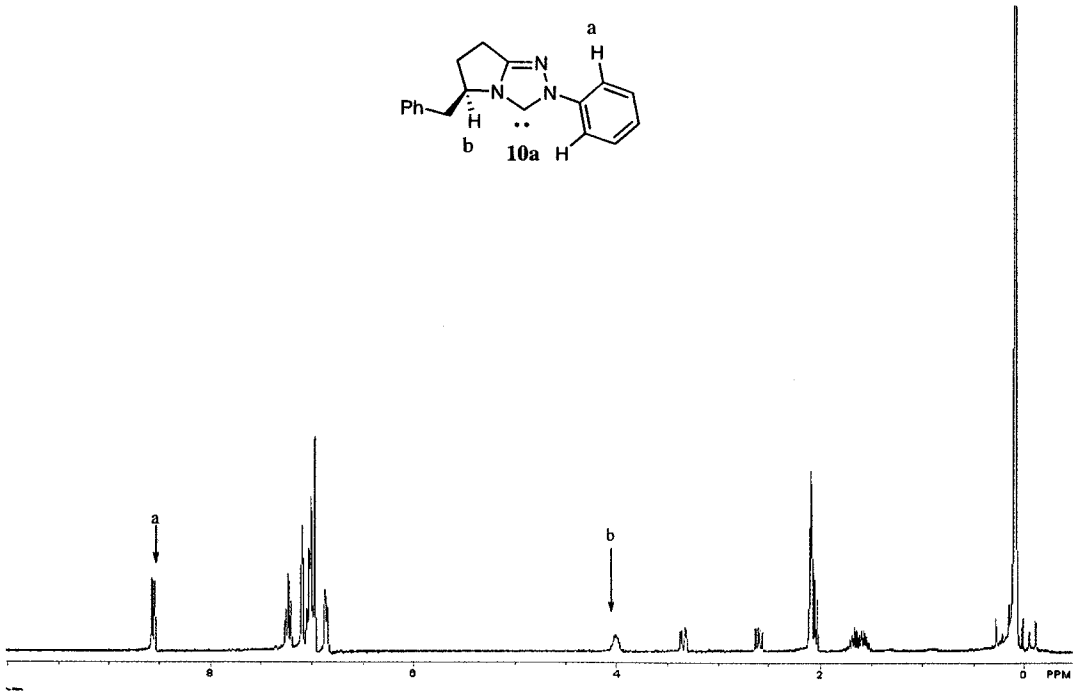

We were not able to observe any intermediate by ^{1}H NMR upon addition of starting material **7** at ambient temperature (Figure 4.) Instead only signals corresponding to product formation were observed with several unidentified signals in the baseline. Addition of another 5 equivalents of **7** to the NMR solution resulted in product **9**, a result which suggests that the active species is still present but does not rest as the free carbene.

Figure 4.

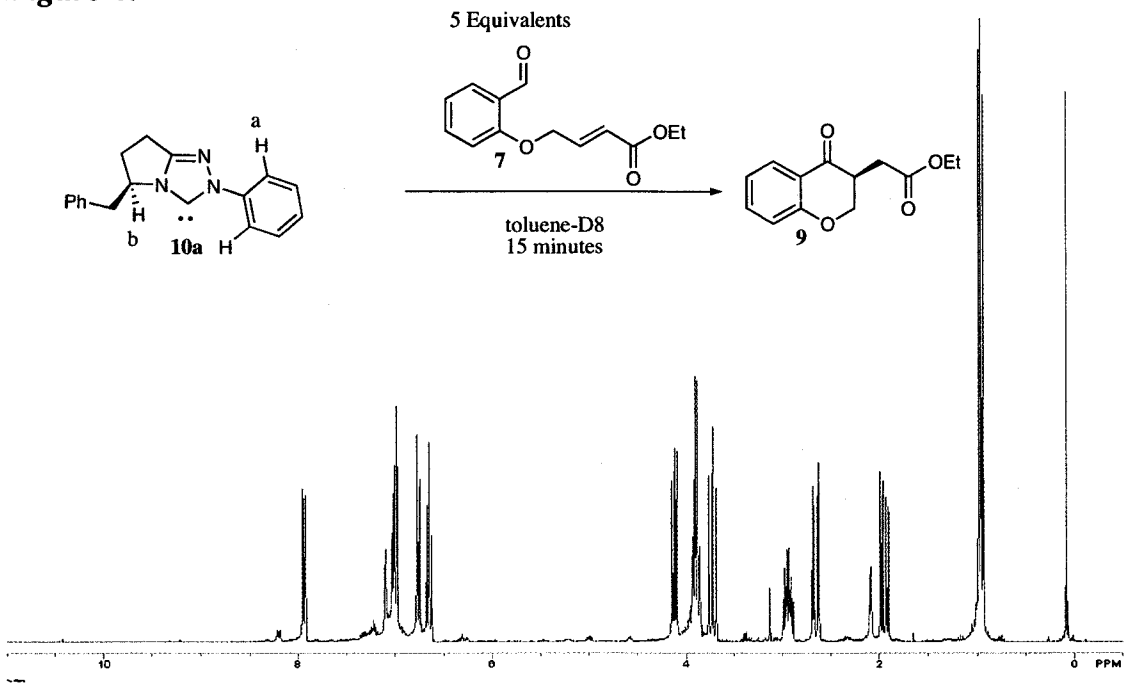

Unfortunately, repeating the NMR experiment with one equivalent of carbene **10a** to half an equivalent of substrate **7** still did not illuminate the resting state of the carbene, except to show that it is not sitting as the free carbene. It was speculated that the carbene was interacting with the product **9**. To test this hypothesis **9** was treated with carbene **10a** in a 1:1 ratio. The ^{1}H NMR clearly showed that carbene **10a** was not present, but there was no significant change to the proton spectrum of the product. (Figure 5 is the NMR spectrum expanded between 0-5 ppm).

Figure 5.

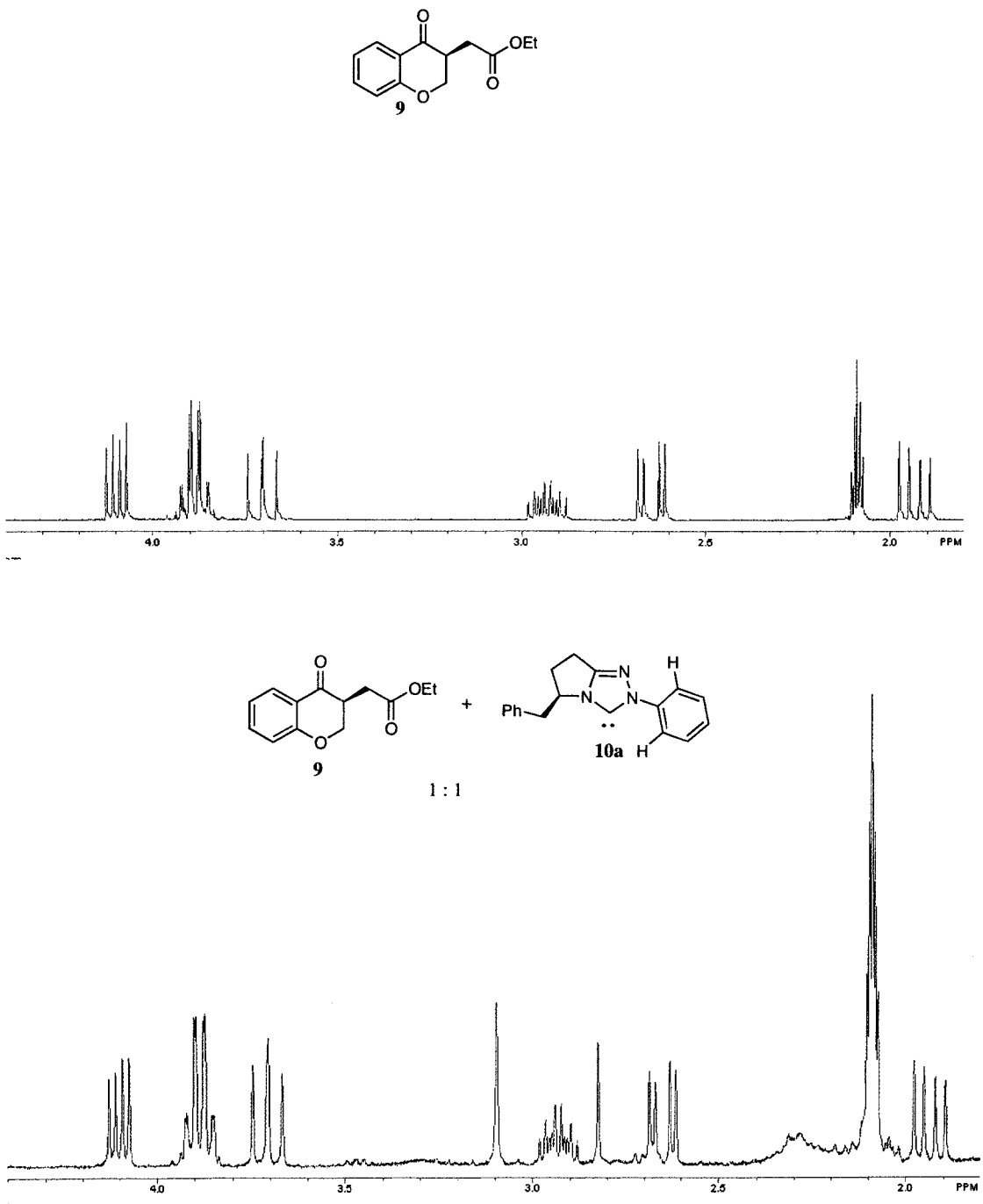

In order to gain further understanding of the resting state of the carbene and to determine if the carbene was decomposing under the reaction conditions, ^{13}C-labeled triazolium salt was synthesized. Upon inspection of our current synthetic route the most obvious location for the label was at the carbene center, which comes from triethylorthoformate. The only problem with the incorporation of a ^{13}C label in our current synthetic sequence is that trimethylorthoformate is used as a solvent and the price of 0.5 ml of ^{13}C enriched triethylorthoformate is ~ $300. Consequently, reducing the amount of triethylorthoformate without jeopardizing product formation was needed.

Optimization of catalyst preparation began with the known method for the formation of phenyl hydrazine adduct **32** from the chiral pyrrolidinone **30** (Scheme 17).[13]

Scheme 17.

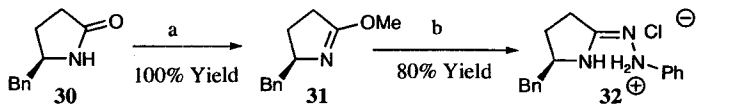

(a) $Me_3O^+BF_4^-$, CH_2Cl_2, 23 °C, 24 h,then ice-cold $NaHCO_3$ wash
(b) $PhNHNH_2HCl$,CH_2Cl_2

With access to large quantities of the required pre-cursor **32** in hand, we began to screen different reaction conditions that might help catalyze product formation. Almost certainly the active triethylorthoformate species formed reversibly via acid catalysis, liberating ethanol during the reaction. As a result the addition of acid or 5Å molecular sieves was expected to increase the formation of the active oxocarbenium intermediate and thus reduce the amount of triethylorthoformate required for the

reaction. The addition of 5Å molecular sieves did not afford any desired product with 2 equivalents of triethylorthoformate (Table 1, entry 1). Fortunately, the addition of 1 mL of methanolic hydrogen chloride (MeOH*HCl) permitted the reduction of triethylorthoformate from 20 equivalents to 5 equivalents (Table 1, entries 2-3). With optimized reaction conditions in hand the ^{13}C labeled triethylorthoformate was subjected to the reaction and to our satisfaction the reaction gave 70% yield of the desired ^{13}C-labeled product **10** (Table 1, entry 4).

Table 1.

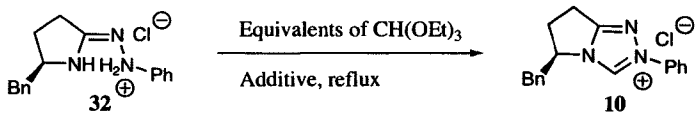

32 **10**

Entry	Equivalents	Additive	Yield
1	2	5 Å Molecular Sieves	0
2	20	MeOH HCl	90
3	5	MeOH HCl	92
4[a]	**5**	**MeOH HCl**	**70**

[a] Reaction run with ^{13}C labeled $CH(OEt)_3$

Formation of the ^{13}C labeled carbene in toluene-D8 was accomplished by addition of KHMDS (0.5 Molar solution of in toluene-D8) to ^{13}C-labeled triazolium salt **10**. A typical strong low-field carbene signal at 206 ppm is observed in the ^{13}C NMR spectrum with and without HMDS. This signal is typically found at 235-245 ppm for imidazolidinylidenes[14] **33**, at 235 ppm for benzimidazolinylidenes[15] **34**, between 210 and 220 ppm for imidazolinylidenes[16] **35** and 214 ppm for triazolinylidene[17] **36** (Scheme 18).

Scheme 18.

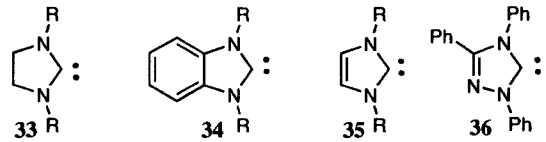

The addition of 3 equivalents of **7** to the NMR reaction mixture containing ^{13}C-labeled carbene **10** immediately led to two new ^{13}C NMR signals at 94 and 101 ppm (~3:1 ratio). The corresponding ^{1}H NMR spectrum of this reaction mixture showed complete product formation with no carbene signal. Assuming the carbene is bound to the product, ^{13}C-labeled carbene **10** was treated with 1 equivalent of product **9** and two signals at 94 and 101 ppm were observed (~3:1 ratio), in addition to the signal corresponding to the free carbene at 206 ppm. These results indicate that our carbene is interacting with the product. We have been unable to isolate the actual product that corresponds to the signals at 94 and 101 ppm but it is possible that they correspond to the diastereotopic products obtained from carbene addition to the ketone of the product (Scheme 19, **37** or **38**). After one hour of continued monitoring of the NMR mixture a new peak began to appear at 160 ppm and 24 hours later was the only ^{13}C signal observed. The ^{13}C signal at 160 ppm also resulted with the addition of one equivalent of water to the ^{13}C-labeled carbene, further supporting that the addition of water is one possible pathway for catalyst decomposition.

Scheme 19.

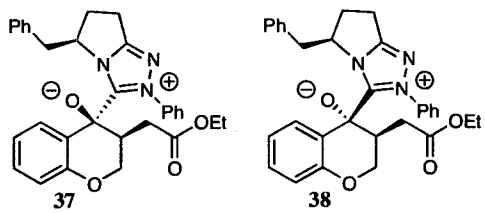

During investigations of the enantio- and diastereoselective intramolecular Stetter reaction in the absence of HMDS the free carbene was observed by ^{1}H NMR after completion of the reaction. It was therefore speculated that the resting state of the triazolinylidene might vary depending on the presence or absence of the conjugate acid hexamethyldisilazane. Subjection of carbene **10** to 2 equivalents of **7** in toluene-D8 resulted in the immediate product formation (**9**) and diagnostic signals at 3.3 and 1.6 ppm corresponding to the free carbene (Figure 6).

Figure 6.

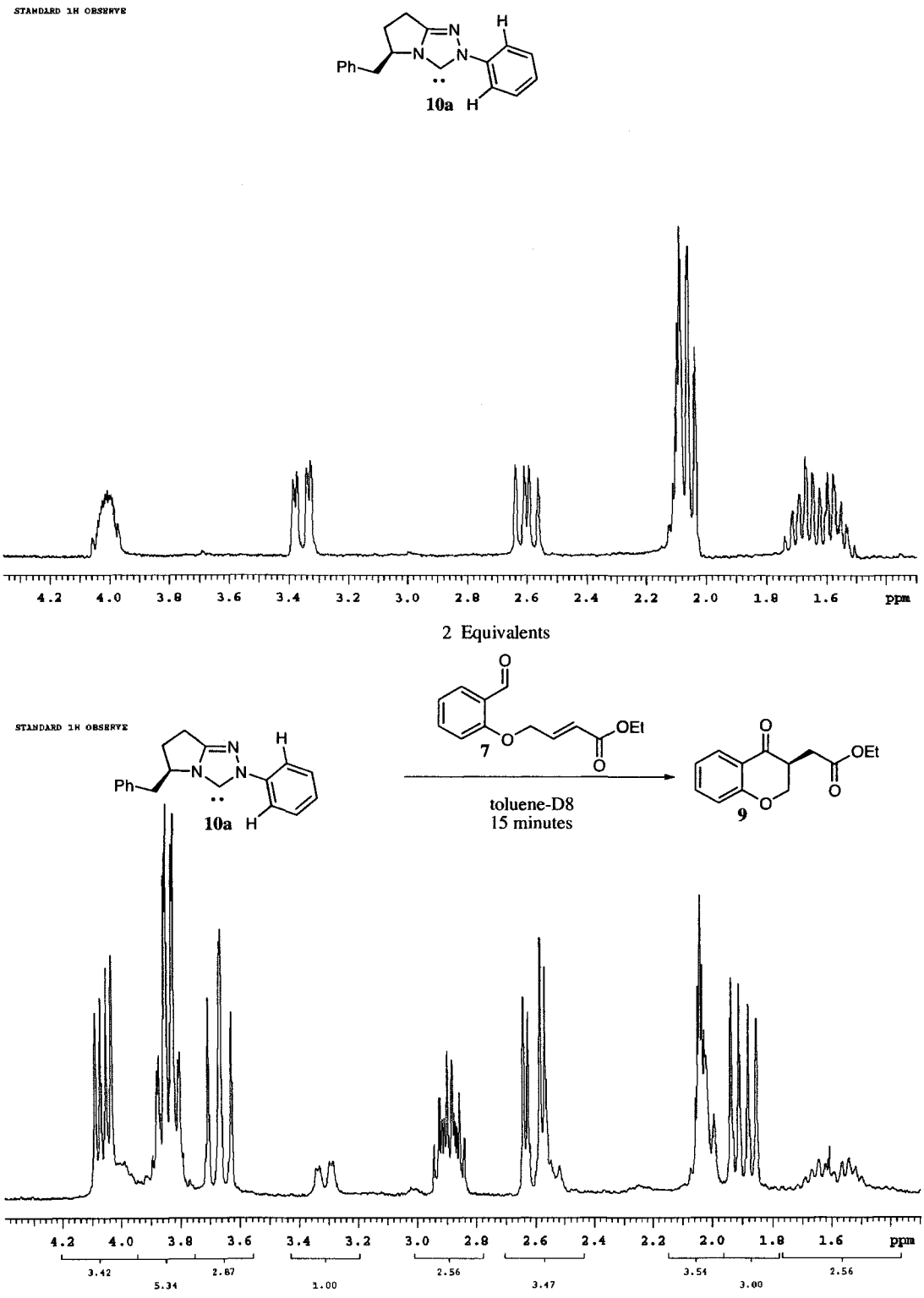

Having thoroughly examined the resting state of the ^{13}C-labeled carbene (**10**) we questioned if we could observe an intermediate on the catalytic cycle by utilizing an acyl silane as an aldehyde surrogate. When the reaction is performed utilizing acyl silane **39** and ^{13}C-labeled carbene **10** two new ^{13}C signals appear at 137 and 140 ppm. Cautiously, due to lack of sufficient evidence, these two new signals are presently tentatively attributed to the diastereotopic Breslow intermediates **40** or **41** (Scheme 20).

Scheme 20.

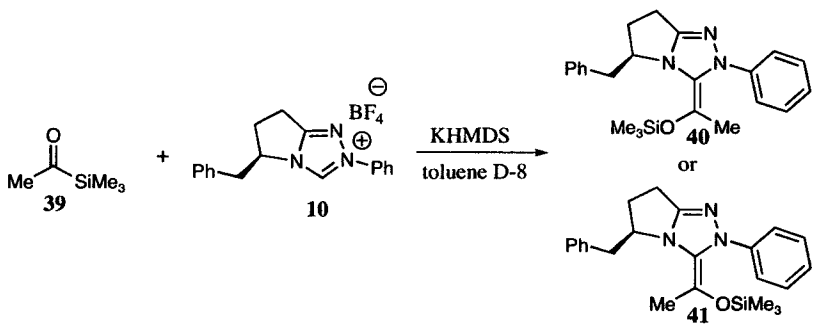

3.5 Rate Acceleration in the Absence of HMDS

To better understand the effect of HMDS on the rate of the intramolecular Stetter reaction, independent reactions in the presence and absence of HMDS were performed, and the rate of product formation was monitored by GC (Scheme 21).

Scheme 21.

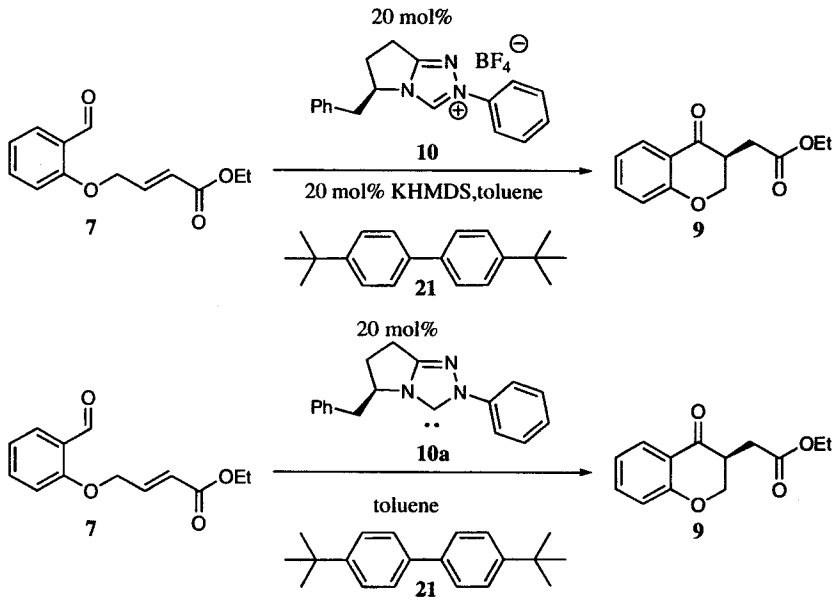

The reactions were performed at 0 °C at 0.025 M and aliquots were analyzed by GC. The observed rate constant for conversion of the intramolecular Stetter reaction in the presence of the conjugate acid HMDS is k_{HMDS}= 1.41 x 10^{-3} s^{-1}. The observed rate constant for conversion of intramolecular Stetter reaction in the absence of the conjugate acid HMDS is $k_{free\ carbene}$= 3.79 x 10^{-3} s^{-1}. There is a 2.6 fold rate acceleration in the absence of the conjugate acid HMDS. The rate acceleration could possibly be due to the difference in resting state of the carbene or the change in the rate-determining step, but other possibilities cannot be ruled out.

3.6 Crossover Experiment

According to the proposed mechanism there are two intermediates that require a proton transfer. Presumably the first proton transfer is intermolecular and, according to our experimental results in the enantio- and diastereoselective Stetter reaction, the second proton transfer is intramolecular. A crossover experiment

beginning with a protio- and deuteroaldehyde should generate two deuterium labeled products assuming there is an intermolecular component to the Stetter reaction. Deuteroaldehyde **6** and protioaldehyde **42** were chosen because the corresponding products are easily separable by column chromatography. Treatment of a 1:1 mixture of **6** and **42** under free carbene conditions led to 23-32% cross-over, depending on the concentration of the reaction (Scheme 22). The cross-over experiment provides good evidence for at least one intermolecular component to the Stetter reaction, although we can not distinguish between the two proton transfer events with this experiment.

Scheme 22.

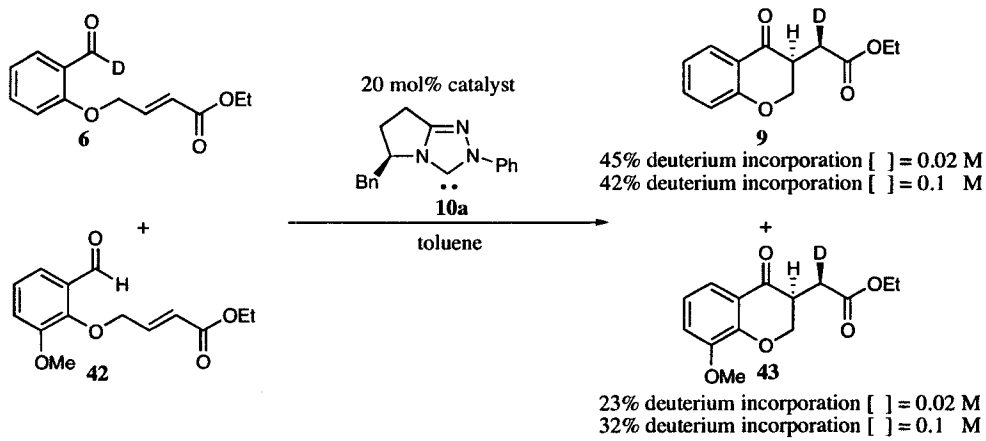

3.6 Conclusion

Our mechanistic studies provide an enhanced picture of the intramolecular Stetter reaction catalyzed by nucleophilic carbene **10**. The deuterium kinetic isotope effect, coupled with the ^{13}C kinetic isotope effect, imparts strong evidence that proton transfer from the first tetrahedral intermediate is the rate-determining step in the intramolecular Stetter reaction in the presence of HMDS. These results were further supported by the competition experiments, which illustrate a change in reaction rate due to the electronic nature of the aromatic aldehyde. Aided by ^{13}C labeled triazolium

salt **10**, we have unmasked the resting state of the carbene in the presence and absence of the conjugate acid HMDS. We have also been able to garner information about the decomposition pathways available during the catalytic cycle caused by exogenous water or oxygen. While the catalytic cycle is well understood (in the presence of HMDS), the cycle with free carbene remains under investigation.

References

[1] Breslow, R. L. *J. Am. Chem. Soc.* **1953**, *80,* 3719-3726.

[2] Breslow, R. *Current Contents* **1993**, *26*, 8.

[3] Mechanism of the thiamine-catalyzed benzoin condensation reaction, see: (a) Breslow, R.; Kim, R. *Tetrahedron Lett.* **1994**, *35*, 699-702. (b) White, M.; Leeper, F. *J. Org. Chem.* **2001**, *66*, 5124-5131. Mechanism of the cyanide catalyzed reaction, see: (c) Lapworth, A. *J. Am. Chem. Soc.* **1903**, *83*, 995. For the mechanism of the cyanide catalyzed crossed silyl benzoin reactions, see: (d) Linghu, X.; Bausch, C. C.; Johnson, J. S. *J. Am. Chem. Soc.* **2005**, *127*, 1833-1840.

[4] Advanced Organic Chemistry, F. A. Carey and R. J. Sundberg, Part A, 3rd Ed., Plenum Press, New York, 1990.

[5] Macleod, C.; McKiernan, G. J.; Guthrie, E. J.; Farrugia, L. J.; Hamprecht, D. H.; Macritchie, J.; Hartley, R. C. *J. Org. Chem.* **2003**, *68*, 387-401.

[6] Seebach, D.; Erickson, B. W.; Singh, G. *J. Org. Chem.* **1966**, *31*, 4303-4304.

[7] Ciganek, E. *Synthesis* **1995**, 1311-1314.

[8] The error associated with the observed k_H/k_D value of 4.0 is high due to low conversions and an approximate 1-2% error in the NMR integrations. Combining these effects compound to make error bars of up to +/- 40 at low conversions.

[9] Read de Alaniz, J.; Rovis, T. *J. Am. Chem. Soc.* **2005**, *127*, 6284-6289.

[10] (a) Niu, D.; Zhao, K. *J. Am. Chem. Soc.* **1999**, *121*, 2456-2459. (b) Sibi, M. P.; Liu, M. *Org. Lett.* **2000**, *21*, 3393-3396. (c) Sibi, M. P.; Prabagaran, N.; Ghorpade, S. G.; Jasperse, C. P. *J. Am. Chem. Soc.* **2003**, *125*, 11796-11797.

[11] For recent selected references, see; (a) Saettel, N. J.; Wiest, O.; Singleton, D. A.; Meyer, M. P. *J. Am. Chem. Soc.* **2002**,*124*, 11552-11559. (b) Singleton, D. A.; Hang, C.; Szymanski, M. J.; Meyer, M. P.; Leach, A. G.; Kuwata, K. T.; Chen, J. S.; Greer, A.; Foote, C. S.; Houk, K. N. *J. Am. Chem. Soc.* **2003**, *125*, 1319-1328. (c) Vo, L. K.; Singleton, D. A. *Org. Lett.* **2004**, *6*, 2469-2472. (d) Singleton, D. A.; Wang, Z. *J. Am. Chem. Soc.* **2005**, *127*, 6679-6685.

[12] Kluger, R. *Chem. Rev.* **1987**, *87*, 863-876.

[13] See chapter 1. (b) Kerr, M. S.; Read de Alaniz, J.; Rovis, T. *J. Org. Chem.* **2005**, *70*, 5725-5728.

[14] (a) Arduengo III, A. J.; Goerlich, J. R.; Marshall, W. J. *J. Am. Chem. Soc.***1995**, *117*, 11027-11028. (b) Denk, M. K.; Thadani, A.; Hatano, K.; Lough, A. J. *Angew. Chem., Int. Ed.* **1997**, *36*, 2607-2609.

[15] (a) Hahn, F. E.; Wittenbecher, L.; Boese, R.; Bläser, D. *J. Eur. Chem.* **1999**, *5*, 1931-1935. (b) Hahn, F. E.; Wittenbecher, L.; Le Van, D.; Fröhlich, R. *Angew. Chem., Int. Ed.* **2000**, *39*, 541-544.

[16] Arduengo III, A. J.; Harlow, L.; Kline, M. *J. Am. Chem. Soc.* **1991**, *113*, 361-363.

[17] Enders, D.; Breuer, K.; Raabe, G.; Runsink, J.; Teles, H. J.; Melder, J-P.; Ebel, K.; Brode, S. *Angew. Chem., Int. Ed.* **1995**, *34*, 1021-1023.

Chapter 4

Developing New Catalytic Reactions Utilizing Triazolinylidene Carbenes

4.1 Introduction

The development of new asymmetric carbon-carbon bond forming transformations is ubiquitous in organic chemistry; nevertheless they still remain a great challenge. Recently, new applications for NHCs in catalysis have been developed, which allow for nontraditional retrosynthetic bond disconnections.[1] The use of functionalized aldehydes in *N*-heterocyclic carbene-catalyzed umpolung reactions opens the door to new synthetic pathways via the Breslow intermediate **III** (Scheme 1). A common key feature in these transformations is the *in situ* generation of an electrophilic acyl azolium intermediate (**VI** or **X**).

Scheme 1.

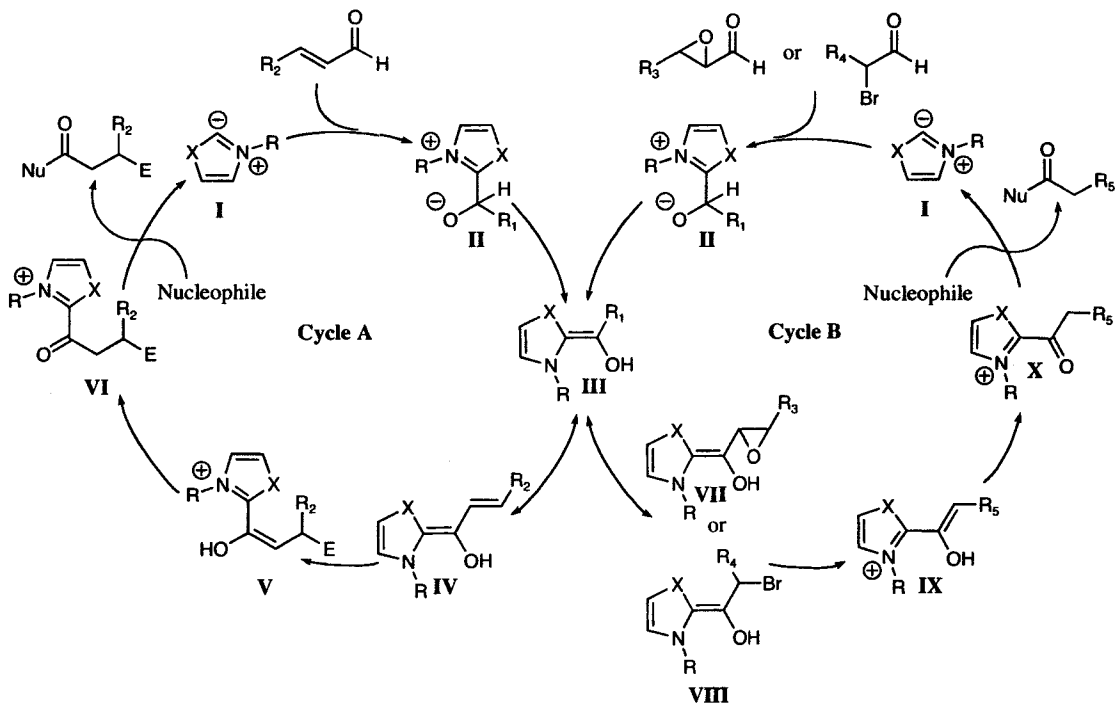

To date α,β-unsaturated aldehydes, α-halo- and α-epoxy aldehydes have been converted into acyl azolium species that can undergo subsequent reactions. In the case of the α,β-unsaturated aldehydes the key intermediate **VI** can be formed by coupling an α,β-unsaturated aldehyde with the nucleophilic carbene (cycle A), which generates **IV** a homologated version of the Breslow intermediate that can undergo electrophilic trapping followed by tautomerization to form the acyl azolium **VI**. Alternatively (cycle B), opening of the α-epoxy or elimination of the α-halogen leaving group from the Breslow intermediate **VII** and **VIII**, respectively, generates the acyl azolium **X** after tautomerization. Nucleophilic displacement of the acyl azolium affords the desired product and closes the catalytic cycle.

4.2 Synthetic Application of the Acyl Azolium Species

The formation of acyl azolium species plays an important biological role in the thiamine pyrophosphate-mediated reaction of the β-lactam carbons in clavulanic acid **6** (Scheme 2).[2] Townsend proposed that the thiamine pyrophosphate ylide form **2** undergoes addition to D-G3P (**1**) generating **3**. Elimination of hydroxide and ketonization to **4** may then be invoked. Elimination of phosphate followed by the addition on L-arginine and hydrolysis would afford acid **5** required for the biosynthesis of clavulanic acid **6**.

Scheme 2.

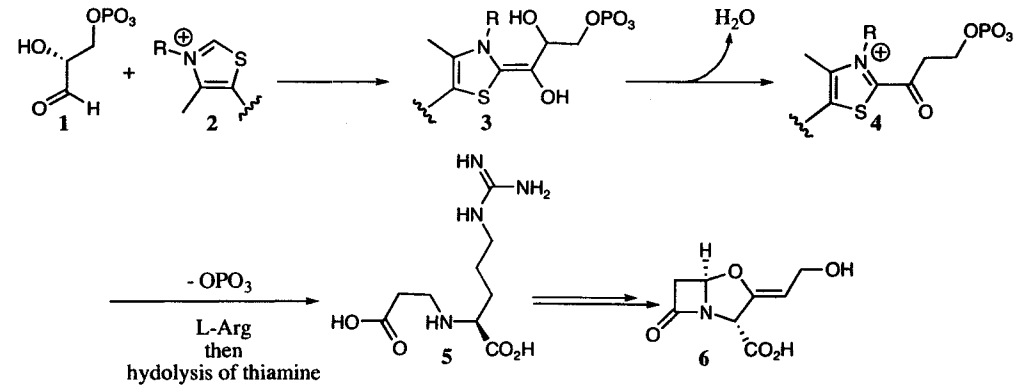

Recently, we developed a non-ezymatic method for the formation of esters from aldehydes that proceeds through an acyl azolium intermediate. The discovery of this new transformation occurred during our investigation towards the formation of contiguous stereocenters (Chapter 2.5.2) via the intramolecular Stetter reaction. To our surprise treatment of **7**, containing an α-phenol substituted aldehyde, did not result in the anticipated intramolecular Stetter reaction but instead product **8** was isolated in 95% yield (Scheme 3).

Scheme 3.

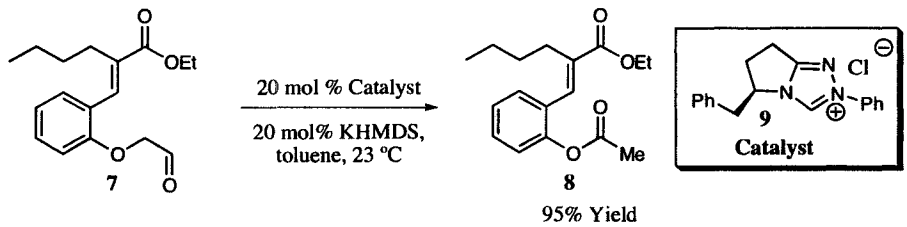

We reasoned that the formation of **8** proceeds through acyl azolium intermediate **XVI** (Scheme 4). Formation of the Breslow intermediate **XIV** proceeds in a fashion analogous to the benzoin or Stetter reaction. Elimination of the α-phenoxide group generates enol **XV**, which after tautomerization provides the acyl

azolium **XVI**. Recombination of the phenoxide with the acyl azolium intermediate generates **8**.

Scheme 4.

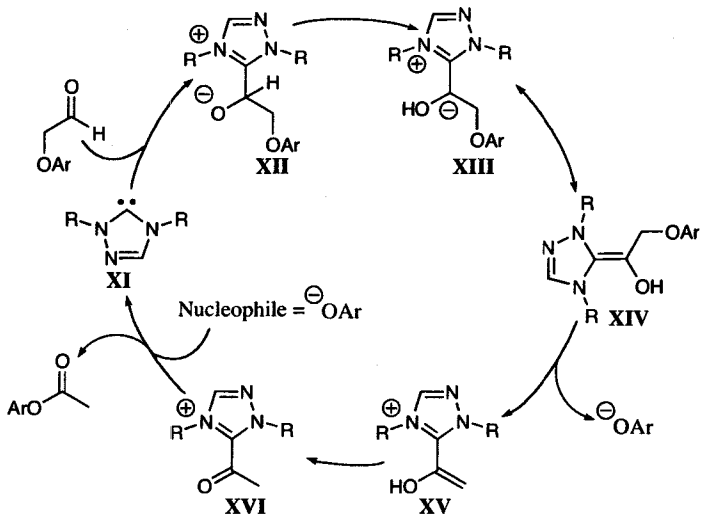

It was envisioned that we could transform this side reaction into a synthetically useful reaction by employing α-haloaldehydes in the presence of an appropriate nucleophile to regenerate the catalyst. To our gratification, secondary and tertiary bromides along with a range of nucleophiles participate in the reaction affording the desired ester in good yield.[3]

It was hypothesized that a kinetic resolution of secondary alcohols or desymmetrization of meso diols could be performed utilizing a chiral carbene, assuming the reaction goes through the proposed mechanism (Scheme 4). Investigation began with a kinetic resolution of phenethyl alcohol. Treatment of α-bromoaldehyde **10** with chiral triazolinylidene **9** in the presence of phenethyl alcohol **11** resulted in poor to good S values[4] (Table 1). Triethylamine afforded the modest results (entries 1-2) but the ee's of the recovered starting material were not consistent

from reaction to reaction. DBU afforded a synthetically useful S value of 16.3 (entry 3).

Table 1.

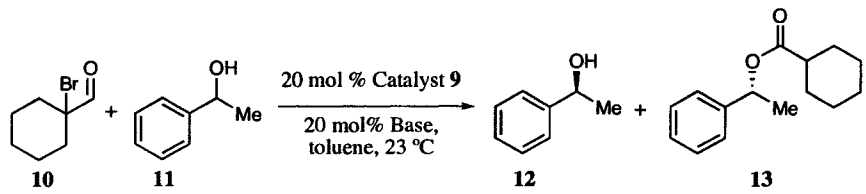

10 **11** **12** **13**

Entry	Base	12 % Yield	12 % ee	13 % Yield	S Value
1	TEA	45	44	55	3.2
2	TEA	60	34	40	4.2
3	**DBU**	**70**	**36**	**30**	**16.3**
4	Hunigs	63	10	37	1.5

The S value of the kinetic resolution is modest when a secondary α-bromoaldehyde is employed (Scheme 5).

Scheme 5.

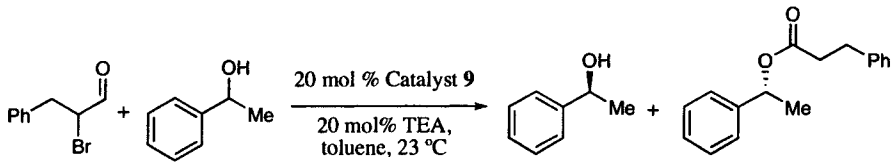

14 **11** **12** **15**

65% Yield
25% ee
S = 3.6

35% Yield

An increase in either the steric environment of the α-bromoaldehyde or the catalyst should increase the ability of the chiral acyl azolium intermediate to discriminate between the enantiomeric secondary alcohols. With this in mind, attention was turned to the desymetrization of meso diols. Meso diol **16** was subjected to the reaction and the desired product **17** was obtained in 83% ee and 75% isolated yield (Scheme 6).

Scheme 6.

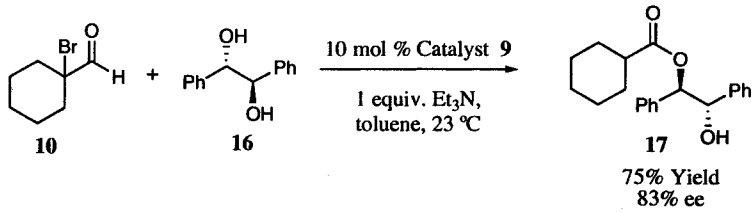

Concurrently, Bode and co-workers also developed a non-enzymatic method for the formation of β-hydroxyesters that proceeds through an acyl azolium intermediate.[5] Subjection of 2,3-epoxyaldehydes, such as **7**, to optimized reaction conditions afforded the desired *anti* product in greater than 10:1 diastereoselectivity and 89% isolated yield (Scheme 7).

Scheme 7.

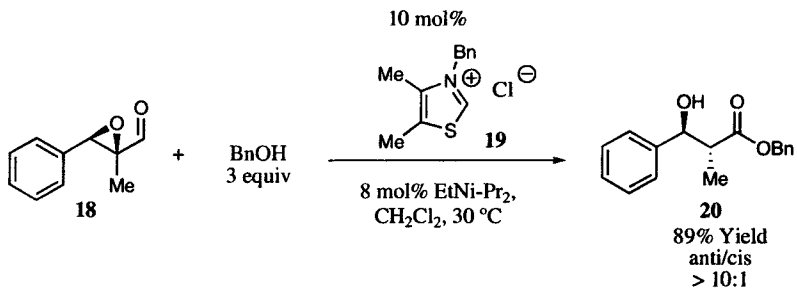

Since the development of this reaction a number of groups have extended the synthetic utility of the catalytic formation of the acyl azolium intermediate. Bode and Glorius have independently applied α,β-unsaturated aldehydes in the synthesis of lactones.[6] Subsequently Bode extended this methodology toward the synthesis of lactams.[7] Chiral imidazolylidenes have been applied to the kinetic resolution of secondary alcohols with modest to excellent success.[8] In addition, research from the Rovis laboratory has expanded this concept into the enantioselective synthesis of α-haloesters.[9] The unique reactivity of these catalytically generated nucleophilic species

and their subsequent electrophilic character offers a new dimension to aldehyde reactivity.

4.3 Transition Metal Catalyzed Reactions with Triazolinylidene Carbenes

Reactions of palladium π-allyl complexes with nucleophiles have attracted enormous attention since 1965.[10] The π-allylpalladium complexes are typically formed by an oxidative addition of Pd(0) with an allylic compound, which react *in situ* with nucleophiles. Remarkable progress has been made in the asymmetric variant of these reactions which either employs chiral ligands on the metal or makes use of enantioenriched allylic starting material.[11] Traditionally the reaction requires the incorporation of soft nucleophiles, such as malonates, phenols or enamines.

We wondered if the π-allylpalladium complex could serve as the electrophilic component for the acyl anion equivalents generated during a reaction between an aldehyde and a nucleophilic carbene (Scheme 8). There are a number of potential problems with the catalytic variant of this reaction. First, it is unclear if the acyl anion equivalent would be "soft" enough to attack the π-allylpalladium intermediate **XX**. Second, the catalytic reaction requires two different catalytic processes to occur simultaneously (the formation of the palladium π-allyl intermediate **XVII** and the formation of the acyl anion equivalent **XIX**). Last, the interaction between the palladium and the nucleophilic carbene must be weak or reversible in order to insure that each is available to catalyze its appropriate transformation.

Scheme 8.

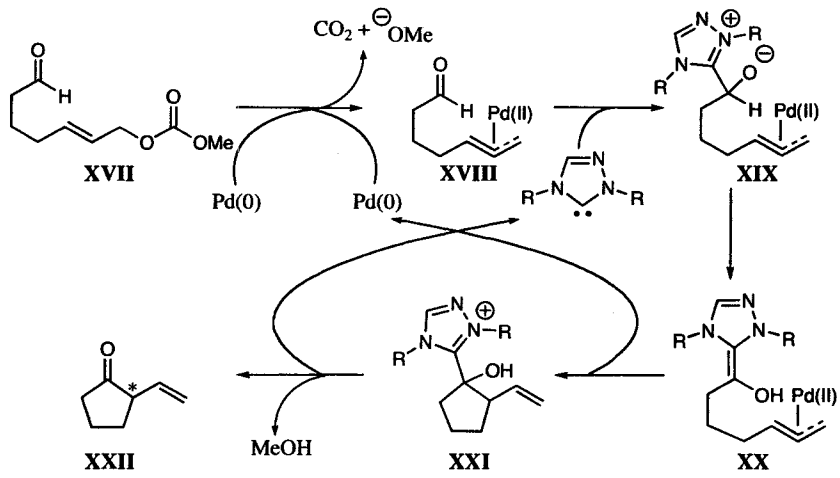

4.3.1 Addition of the Breslow Intermediate to Palladium π-allyl Species

Initial investigation began with model substrate **21** by screening various palladium sources, temperatures and solvents but each reaction either resulted in recovered starting material or multiple unidentified products.[12]

Scheme 9.

Owing to the difficulties associated with this reaction it was decided to take a few steps back and investigate the components of this reaction separately. To determine the effect of the carbene on the palladium π-allyl reactions, if any, a known reaction was conducted in the presence of 20 mol% carbene **26** and a slight decrease in yield was observed (Scheme 10).

Scheme 10.

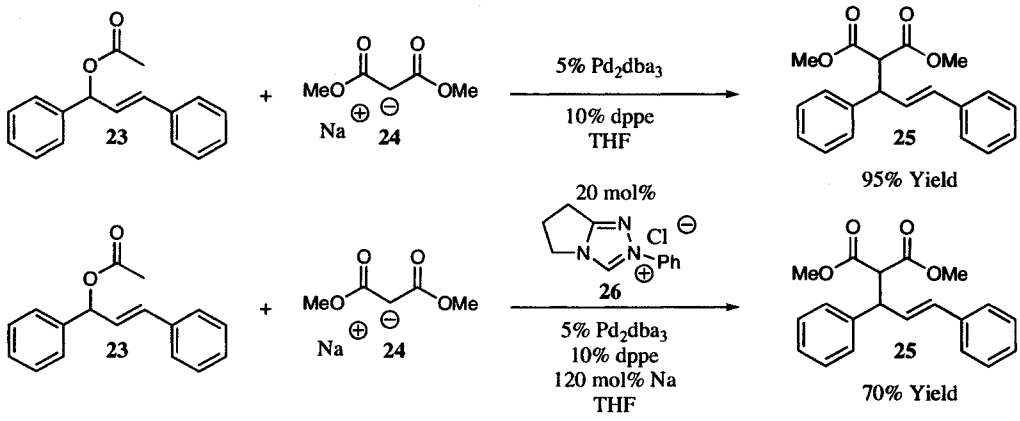

As suggested by Professor Hegedus, we turned our attention to evaluate if the acyl anion equivalent would be a suitable nucleophile. Treatment of stoichiometric palladium π-allyl[13] **27** with sodio dimethyl malonate in THF at 50 °C afforded 52% of the product **28**. Under identical reaction conditions no product corresponding to addition of the *in situ* generated acyl anion equivalent was detected (Scheme 11).

Scheme 11.

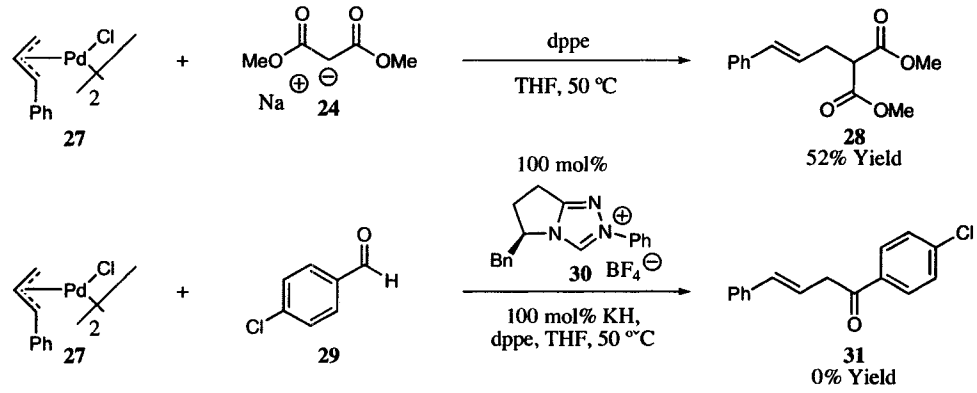

It is possible that the acyl anion equivalent is not being generated under these reaction conditions or is not a suitable nucleophile for the electrophilic palladium π-allyl species. Utilizing a thiazolium salt resulted in the formation of benzoin but no desired product was identified. Benzoin formation confirms that the acyl anion

equivalent is being formed in the presence of the palladium π-allyl species but is more reactive towards another aldehyde molecule.

The formation of the palladium π-allyl species from allyl carbonates is known to extrude carbon dioxide and an alkoxide. It was suggested by Professor Tunge that the *in situ* generated alkoxide could deprotonate the triazolium salt.[14] Employing allyl carbonates would insure the formation of nucleophilic carbene if, and only if, the palladium π-allyl is generated first. With this in mind **22** was added to a solution of 30 mol% Pd_2dba_3, 60 mol% dppe and 30 mol% triazolium salt **32** in toluene. The resulting solution was heated to 50 °C overnight and 35% of the desired product **33** was obtained.

Scheme 12.

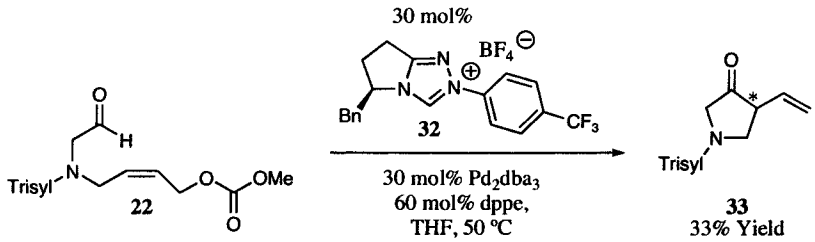

The enantioselectivity of this reaction has not been determined because all attempts to access **33** utilizing achiral triazolium salt **34** resulted in no desired product. It is unclear why the reaction does not proceed with the achiral triazolium salt.

Scheme 13.

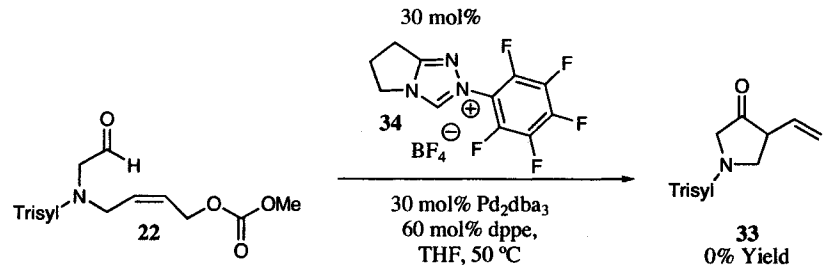

Aromatic aldehydes are typically easier to monitor and from previous experience in the asymmetric Stetter reaction were less problematic than the aliphatic aldehydes. Surprisingly, treatment of **35** to identical catalytic conditions did not afford the desired product **36** but instead generated the elimination product **37** in 70% yield (Scheme 14).

Scheme 14.

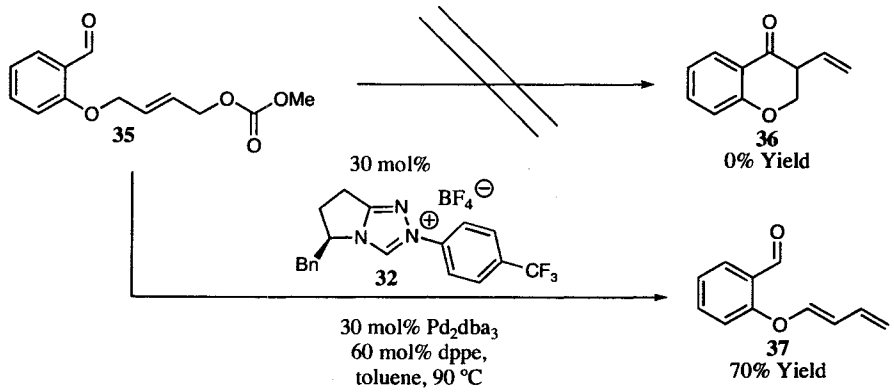

The elimination product has been observed in palladium π-allyl chemistry but often requires forcing conditions and the use of very electron rich ligands (t-Bu_3P). The elimination can occur by either β-hydride elimination or base induced elimination. We tried to curb this undesired reaction by varying the nature of the ligands on palladium but in every case only starting material or elimination product was obtained (Table 2). Unfortunately, the elimination product occurs even in the

absence of triazolium salt and presumably occurs before the acyl anion is generated (entry 4). No reaction occurs in the absence of palladium catalyst (entry 5).

Table 2.

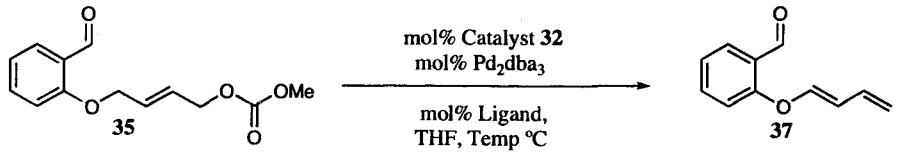

Entry	Catalyst	Pd_2dba_3	mol% Ligand	Temp	% Yield
1	30 mol% **32**	30 mol%	60% dppe	66	>80
2	15mol% **32**	5 mol%	10% 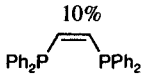	66	ST
3	20 mol% **32**	20 mol%	40% 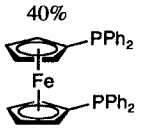	23	>80
4		20 mol%	40% 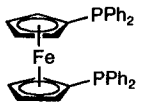	23	>80
5	20 mol% **32** + 40 % DBU			66	ST

The alkene geometry of the allyl carbonate was examined to determine if it plays a role in the undesired elimination reaction. Regrettably, reactions performed with a variety of ligands, metal sources and solvents all lead to the elimination product with the *Z* alkene (Scheme 15).

Scheme 15.

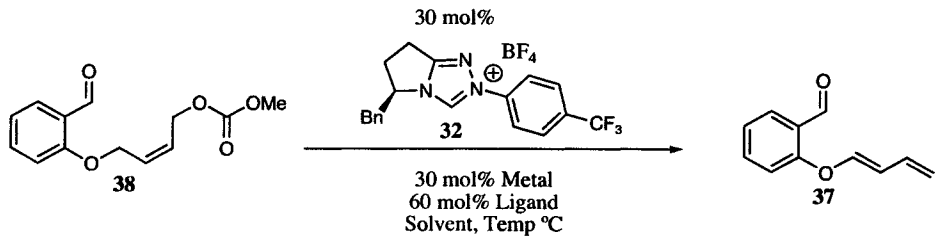

In light of the facile elimination of the palladium π-allyl species it appears that we chose a very poor model substrate to develop this reaction. Although we have not successfully developed an efficient reaction for utilizing palladium π-allyl intermediates with the *in situ* generated acyl anion equivalent, we have established the concept is feasible. Further reaction optimization is required.

4.3.2 Synthesis of Chiral Triazolinylidene-Gold(I) Complexes

The development of *N*-heterocyclic carbene (NHC) late-transition metal complexes has now become a well-established area of research.[15] In addition, catalysis with Au(I) or Au(III) complexes has undergone a renaissance in the last couple of years.[16] In contrast to the wealth of information available for late-transition-metal NHC compounds, NHC-gold(I) compounds are virtually unexplored.[17] In particular, to our knowledge, the synthesis of chiral NHC-gold(I) complexes did not exist at the start of this project. Furthermore, the catalytic activity of NHC-gold(I) complexes was unknown outside the arena of ligand exchange. This prompted us to investigate the synthesis of new NHC-gold(I) complexes and evaluate their catalytic activity.

In 2005, Nolan and co-workers reported a straightforward preparation of imidazole- and triazole-derived carbene complexes of Au(I).[18] We were particularly interested in the synthesis of complex **41**, which commenced from the corresponding triazolium salt (Scheme 16). Nolan noted that treatment of **39** directly with $Au(SMe_2)Cl$ resulted in undesired side reactions.

Scheme 16.

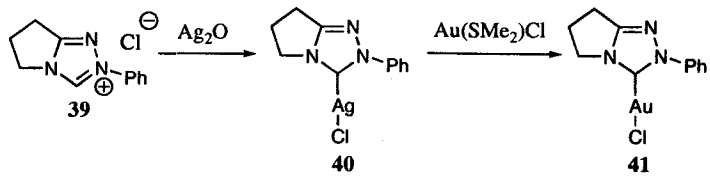

Based on precedent we began the synthesis of chiral triazolinylidene-derived gold(I) complexes. Reaction of triazolium salt **42** with silver oxide resulted in the isolation of the required triazolium-silver complex **43** that could be transmetallated with the $Au(SMe_2)Cl$ to afford the chiral triazolium-gold(I) chloride complex as an off white solid (Scheme 17).[19]

Scheme 17.

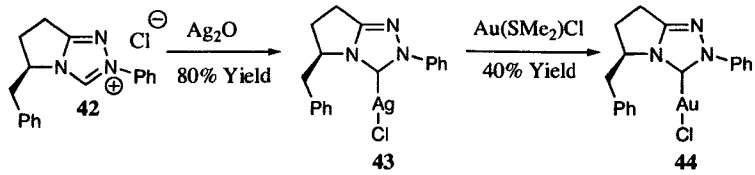

To unambiguously characterize the new triazolinylidene-derived gold(I) complex and to gain insight into its size and structure, X-ray quality crystals were grown and analyzed. ORTEP representation is shown in Figure 1.

Figure 1.

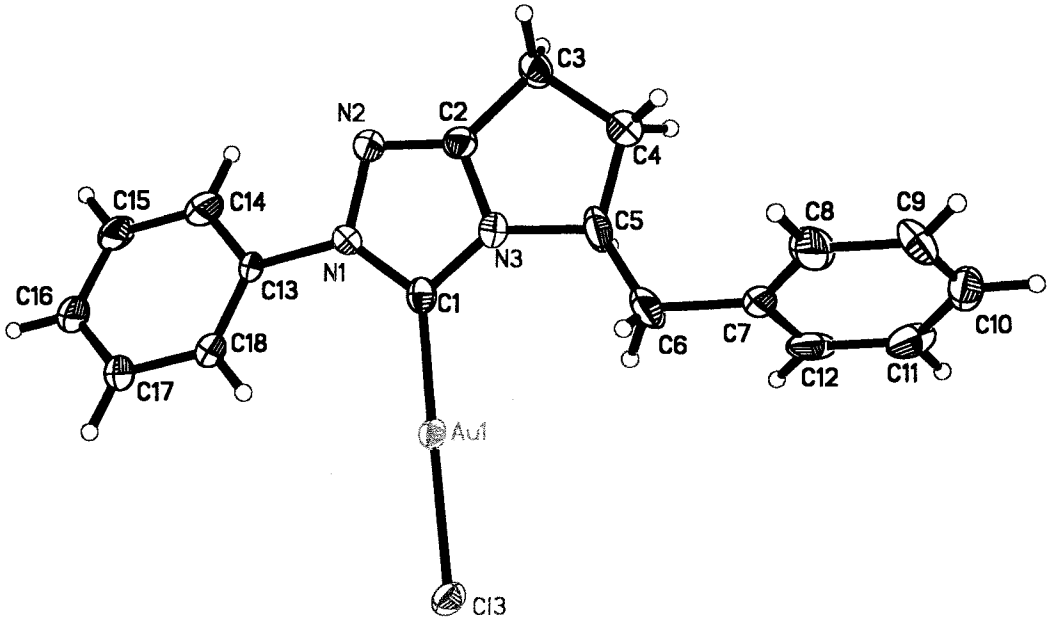

The triazolinylidene-derived gold(I) complex has a two-coordinate gold(I) atom, in an essentially linear arrangement with a C-Au-Cl bond angle of 178.1° (2). The gold-carbene (Au-C(1)) and gold-chloride (Au-Cl) bond distances were found to be 1.969 (7) Å and 2.2830 (17) Å, respectively. The bond distance and angle are in agreement with other reported imidazole- and triazole-derived gold complexes (Table 3).[20]

Table 3.

Entry	Complex	Au-C(1)	Au-Cl	C(1)-Au(1)-Cl
1	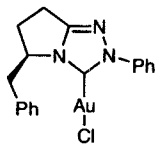 **44**	1.969 (7)	2.2830 (17)	178.1 (2)
2[a]	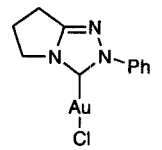 **41**	1.979 (5)	2.2880 (13)	175.59 (15)
3[a]	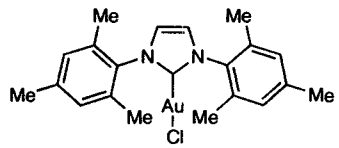 **45**	1.998 (5)	2.2756 (12)	180
4[a]	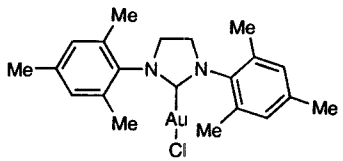 **46**	1.983 (4)	2.2766 (10)	177.68 (11)

[a] Reference 15.

4.3.3 Reactivity of the Chiral Triazolium-derived Gold(I) Complex

The thermal cyclization of ketones onto alkynes, commonly known as the Conia-ene reaction, provides access to α-vinlylated ketones. Recently, Toste and co-workers reported the first catalytic version of this reaction at ambient temperature and under neutral conditions utilizing a phosphine gold(I) complex as the catalyst (Scheme 18).[21]

Scheme 18.

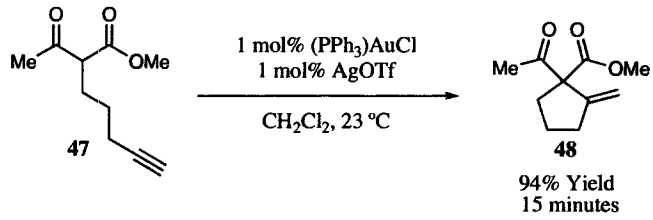

NHC-metal complexes display reactivity comparable to phosphine-metal complexes and, therefore, we felt the Conia-ene reaction would be a good model reaction to test the reactivity of the new chiral triazolium-derived gold(I) complex. To our delight **44** catalyzed the Conia-ene reaction at ambient temperature in near quantitative conversion (Scheme 19). Unfortunately, the chiral triazolium-derived gold(I) complex was unable to translate chirality into the product.

Scheme 19.

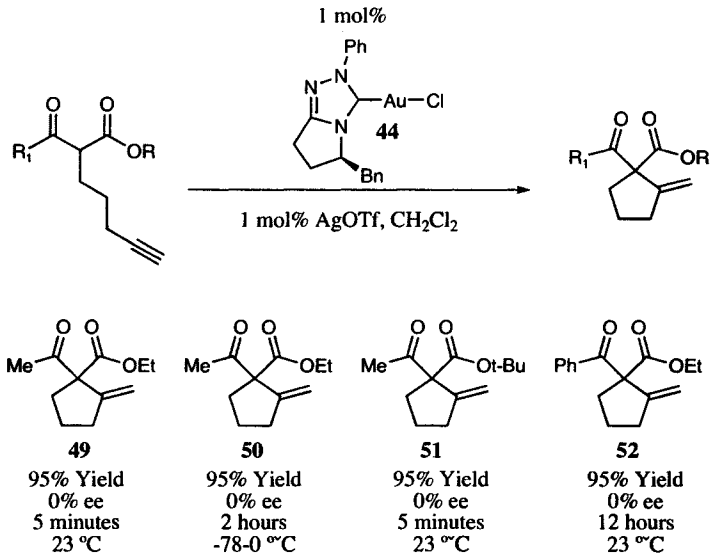

Toste has probed the mechanism of the gold catalyzed Conia-ene reaction. These deuterium-labeling experiments support a mechanism involving enol addition to an Au-alkyne complex (Scheme 20). As illustrated in structure **53** the ligand on the gold is ~180 ° away from the carbon-carbon bond formation. Transition state **53**

offers a possible explanation why 0% ee was obtained, since the chiral scaffold is presumably not in proximity of the carbon-carbon bond formation.

Scheme 20.

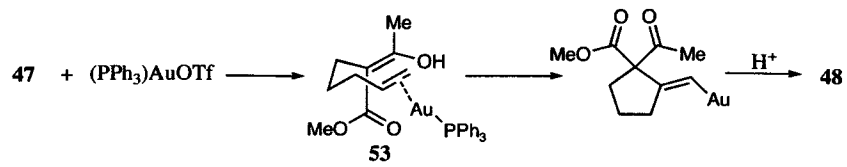

Despite the lack of enantioselectivity in the Conia-ene reaction, we were encouraged by the reactivity of the NHC-gold(I) complex. The reactivity of other gold catalyzed reactions were evaluated and the NHC-gold(I) complex was capable of activating alkenes toward nucleophilic attack from either phenol[22] **54** or 1,3-dicarbonyl[23] **57** (Scheme 21).

Scheme 21.

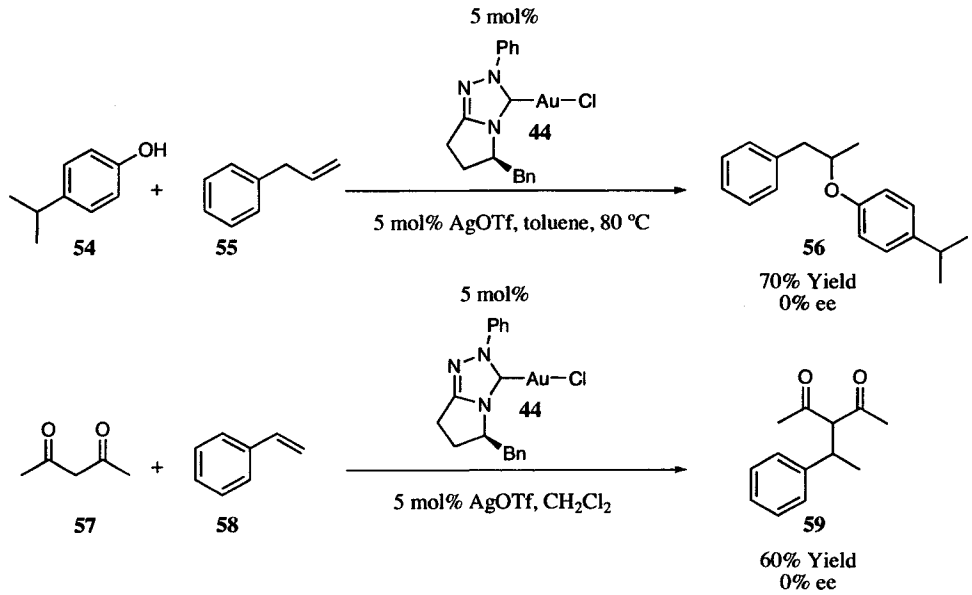

While the majority of developed reactions rely on the gold complex to activate the alkene or alkyne by Lewis acid coordination for subsequent nucleophilic attack,

more recent studies have suggested that carbene-like intermediates may be involved in a number of gold(I)-catalyzed reactions. Toste and co-workers recently reported that a variety of propargyl acetates undergo a 1,2-migration to generate a proposed vinyl carbene that participates in olefin cyclopropanation reactions.[24,25]

Toste reported the reaction of propargyl pivaloate **60** with styrene, catalyzed by 5 mol% cationic triphenylphosphinegold(I), afforded cyclopropane **62** in 74% yield and a 6:1 mixture of *cis:trans* diastereomers (Scheme 22).

Scheme 22.

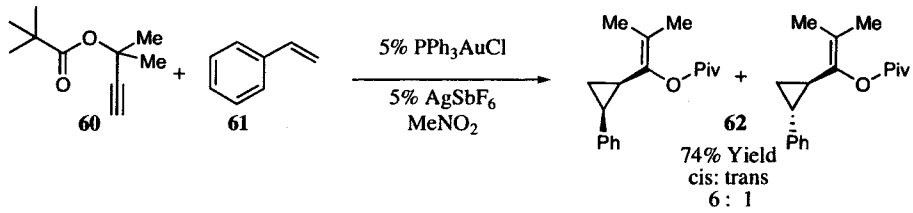

They attribute the high diastereoselectivity observed in the formation of *cis*-cyclopropane to the unfavorable interaction between the phenyl substituent and the gold(I)-carbenoid (Scheme 22, path b).

Scheme 22.

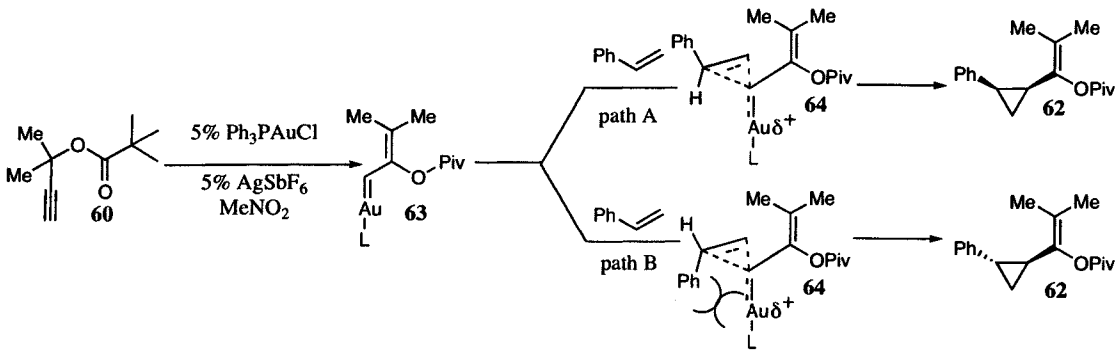

This provided the impetus for the development of an asymmetric gold-catalyzed cyclopropanation reaction. After substantial catalyst optimization Toste identified (*R*)-DTBM-SEGPHOS as the ligand of choice for enantioselective cyclopropanation (Scheme 23). The reaction is sensitive to the size of the propargyl ester with pivaloate esters resulting in the highest enantiomeric excess. A variety of styrene-derived olefins afford the desired products in high cis selectivity and enantioselectivities.

Scheme 23.

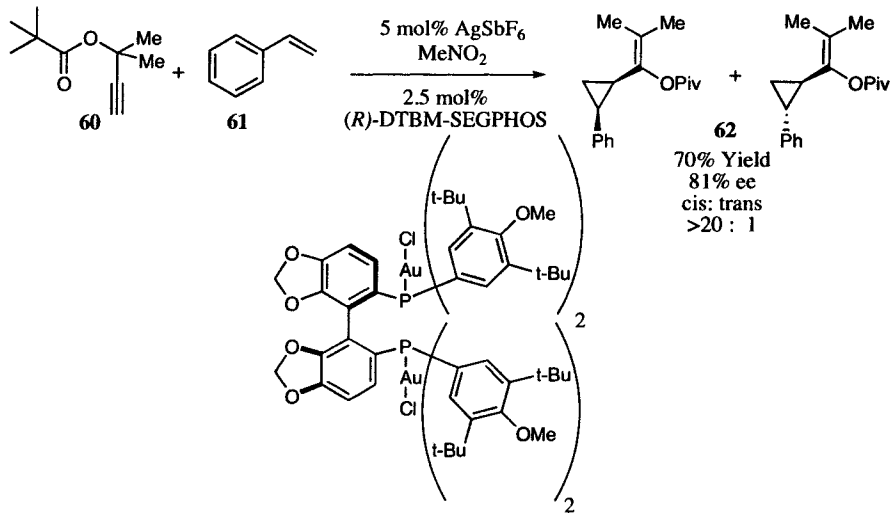

It was envisioned that the gold(I)-catalyzed cyclopropanation of olefins using propargyl esters as gold(I)-carbene precursors would be an excellent reaction to test our chiral triazolium-derived gold(I) complex. Propargyl pivaloate **61** and propargyl acetate **63** were prepared and subjected to various reaction conditions (Table 4). The formation of cyclopropane **62** was achieved in 80% yield and 13:1 *cis:trans* diastereoselectivity, albeit 0% ee. Attempts to increase the enantioselectivity of the reaction by varying the solvent failed (Table 4, entries 1-4). Secondary propargyl

acetate afforded the desired product in good yield and diastereoselectivity but 0% ee (Table 4, entry 5). Optimized reaction conditions described by Toste resulted in 80% yield of the desired cyclopropane in 13:1 *cis:trans* diastereoselectivity but 0% ee (Table 4, entry 6).

Table 4.

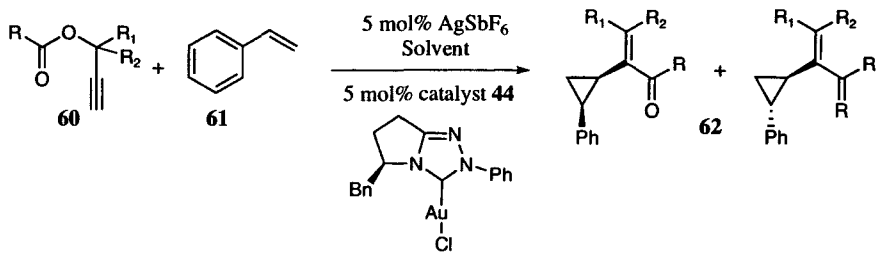

Entry	R	R_1	R_2	Solvent	% Yield	% ee	cis:trans
1	Me	Me	Me	$MeNO_2$	80	0	12:1
2	Me	Me	Me	toluene	ND	0	13:1
3	Me	Me	Me	THF	0	NA	NA
4	Me	Me	Me	CH_2Cl_2	0	NA	NA
5	Me	H	Ph	$MeNO_2$	80	0	12:1
6	t-Bu	Me	Me	$MeNO_2$	80	0	13:1

It was shocking that no enantioselectivity was observed and we wondered if the chiral carbene was dissociating from the gold during the reaction. Previous experiments had shown that triazolium-derived silver complex dissociated in toluene and that the liberated carbene was capable of catalyzing the intramolecular Stetter reaction (Scheme 24, entry 1). However, subjection of the intramolecular Stetter substrate **63** to the cyclopropanation reaction conditions only afforded the cyclopropane product **62** and unreacted aldehyde **63**, thus suggesting that the carbene does not dissociate from the cationic gold during the reaction.

Scheme 24.

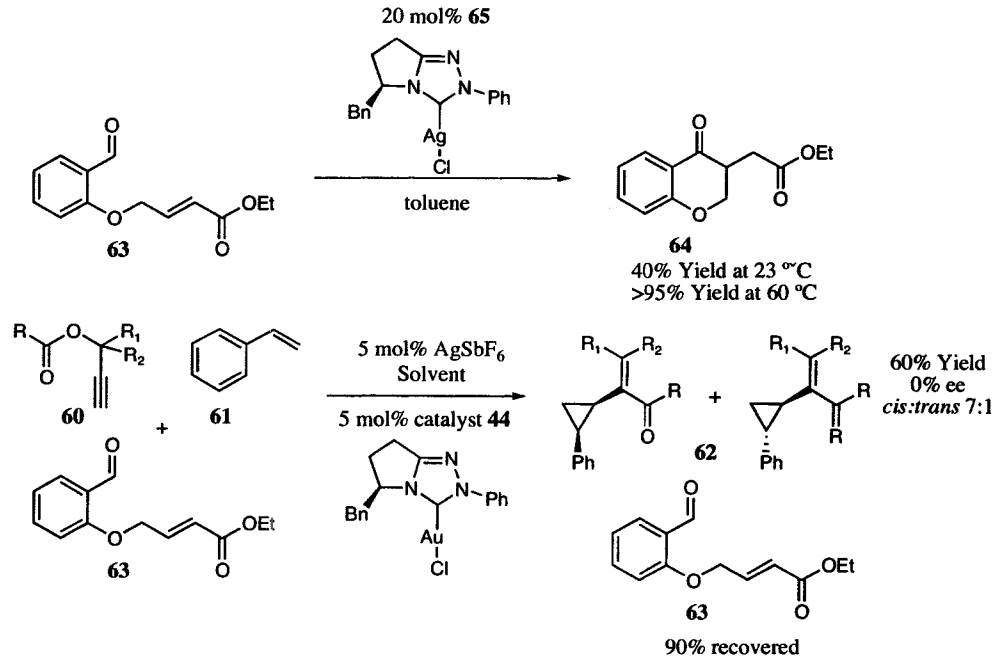

Presumably the lack of chiral induction observed in the cyclopropanation reaction is a result of the chiral ligand being too far from the reactive center. With this in mind the aminoindanol-derived triazolium-gold(I) complex was synthesized in 87% yield from the corresponding triazolium chloride salt **65** (Scheme 25).

Scheme 25.

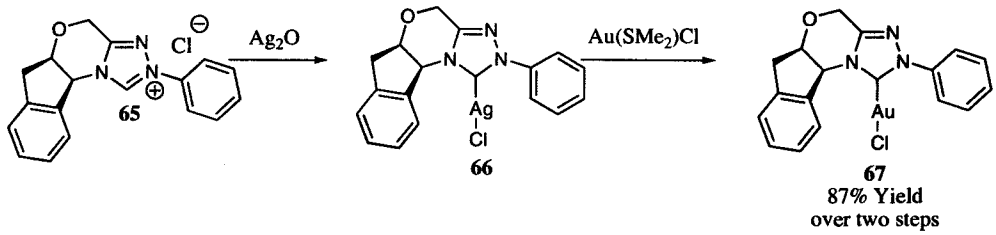

Application of **67** to the cyclopropanation reaction conditions afforded the desired product in 83% yield and 13:1 *cis:trans* diastereoselectivity but, once again, 0% ee. The cyclopropanation reactions can be performed in the absence of the silver

salt but the reaction is less efficient (Scheme 26, entry 2). In addition no increase in diastereoselectivity or enantioselectivity was observed.

Scheme 26.

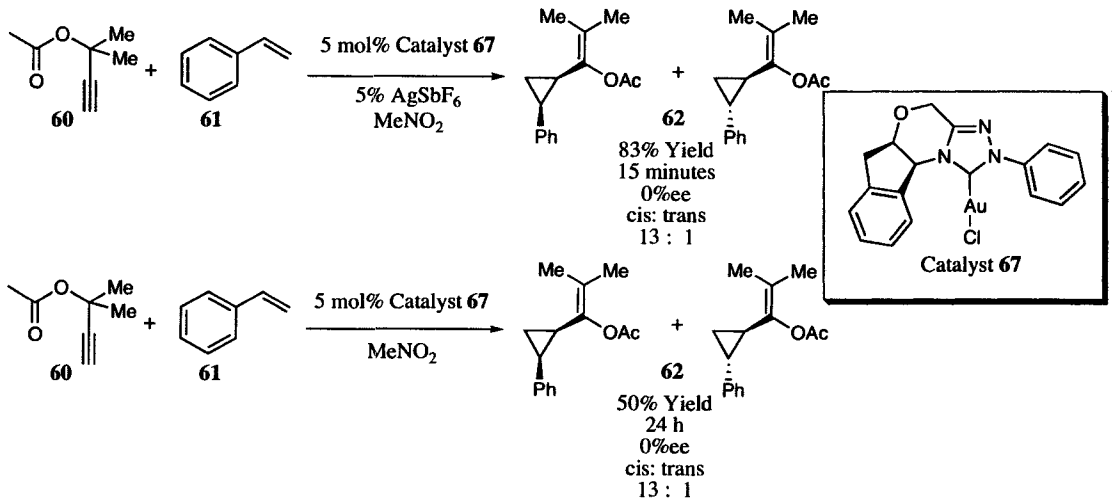

A broad range of transformations can be catalyzed by NHC-gold complexes, although the successful development of an asymmetric NHC-gold catalyzed reaction was not realized. It appears that the linear nature of the gold complex requires a very bulky chiral ligand in order to generate optically enriched products. Further work directed towards developing new chiral ligands might provide a solution to this problem.

4.3.4 The Catalytic Conversion of *N*-Tosylimines to Nitriles

Tertiary phosphine catalysts play an important role in a number of bond-forming transformations. For example, phosphonium ylides in the Wittig reaction, transition metal-catalyzed reactions in which phosphines act as ligands and fewer examples in which phosphine acts as a catalyst. Recently Lu reported the reaction of 2,3-butadienoates **68** with electron deficient *N*-tosylimines **69** in the presence of a

catalytic amount of triphenylphosphine which generates the corresponding [3+2] cycloaddition product **70** in high yield (Scheme 27).[26]

Scheme 27.

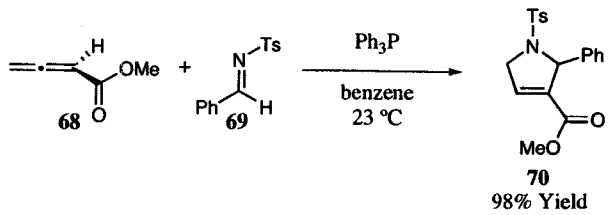

N-heterocyclic carbenes are excellent surrogates for phosphines in metal complexes. However, it was unclear if NHCs could mimic the catalytic role of triphenylphosphine and catalyze the [3+2] cycloadditions of allenoates and *N*-tosylimines. Treatment of **68** and **69** in the presence of triazolium-derived carbene **30**, generated using different bases, results exclusively in **73** (Table 5, entries 1-3). To ensure the isopropyl substituent on the allenoate does not interfere in the [3+2] cycloaddition a control experiment using tributylphosphine was conducted and resulted in excellent yield of **72** with no formation of **73** (Table 5, entry 4).

Table 5.

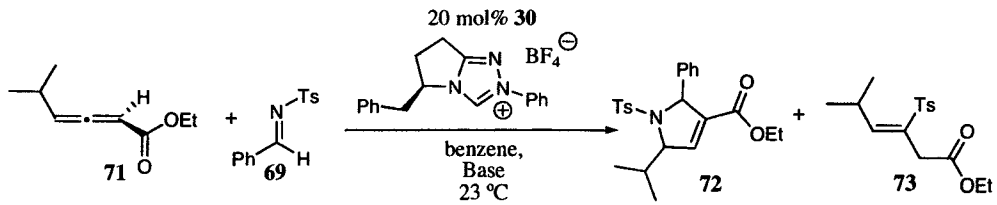

Entry	20 mol% Base	% Yield **72**	% Yield **73**
1	KHMDS	0	55
2	DBU	0	60
3	KO-t-Bu	0	63
4[a]		85	0

[a] 20 mol% PBu_3 was used as the catalyst.

It is believed that the formation of **73** proceeds by nucleophilic attack of the carbene into the *N*-tosylimine to generate a tetrahedral intermediate **XXIV** (Scheme 28). Subsequent proton transfer generates **XXV** that eliminates the stabilized tosyl anion, which subsequently attacks the allenoate to afford product **78**. The completion of the catalytic cycle occurs with the formation of benzonitrile and the release of the carbene.

Scheme 28.

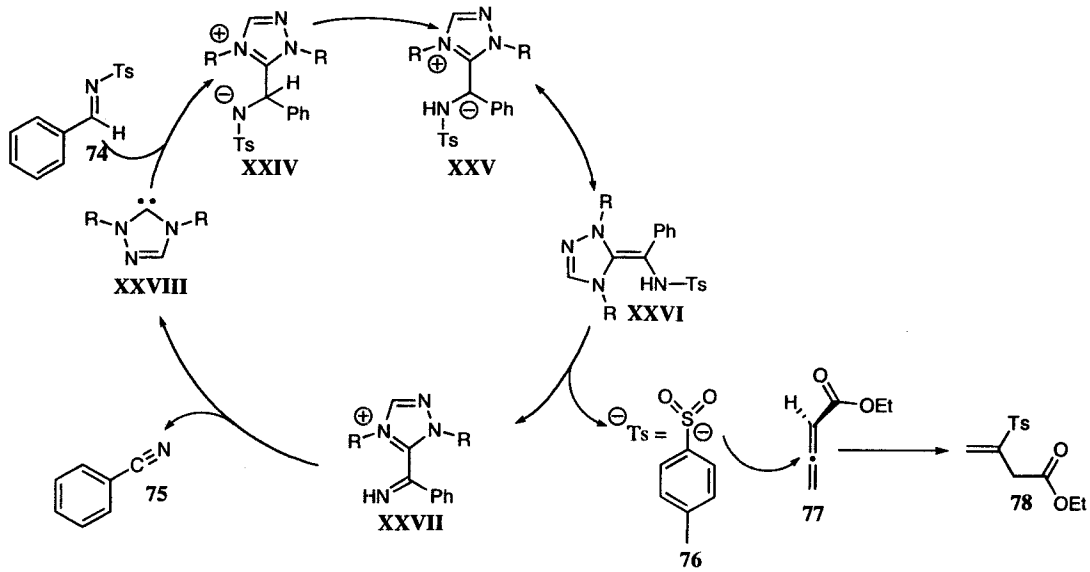

Glass reported the conversion of N-tosylimines to nitriles utilizing superstoichiometric potassium cyanide as the catalyst in 1977.[27] The types of NHCs that are capable of catalyzing this reaction were briefly surveyed; thiazolium, imidazolium and triazolium-derived carbenes were all found to be competent catalysts for the conversion of *N*-tosylimines to nitriles (Table 6). Due to the volatility of benzonitrile allenoates were added to trap the liberated tosyl anion. Reaction success was judged by the formation of **73** which we assumed corresponded to the formation of the benzonitrile. A variety of *N*-tosylimines were converted into

the corresponding nitriles (Table 6, entries 1-4). Reducing the electophilicity of the imine results in only recovered starting material (Table 6, entry 5).

Table 6.

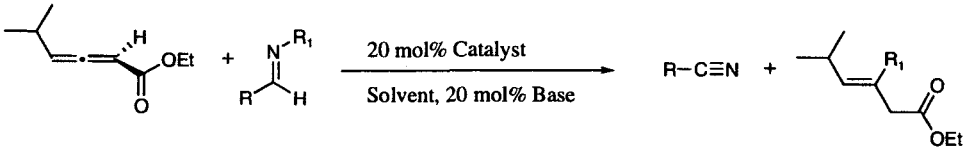

Entry	Catalyst	Imine	Base	Solvent	Yield of **73**
1	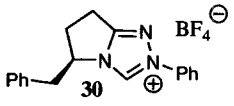 **30**	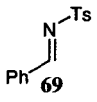 **69**	KHMDS	toluene	55
2	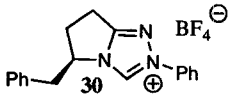 **30**	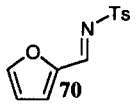 **70**	KHMDS	toluene	65
3	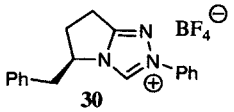 **30**	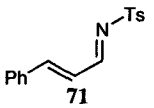 **71**	DBU	toleune	21
4	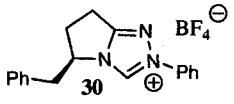 **30**	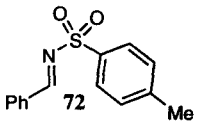 **72**	KHMDS	benzene	70
5	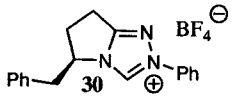 **30**	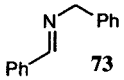 **73**	KHMDS	toleune 110 °C	ST
6	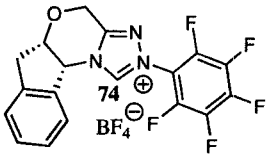 **74**	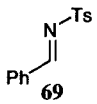 **69**	KHMDS	toluene	>50
7	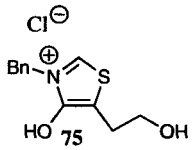 **75**	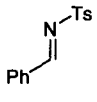 **69**	DBU	benzene	>50
8	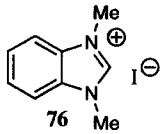 **76**	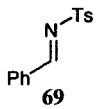 **69**	KOt-Bu	benzene	>50

To ensure nitrile formation during the reactions *N*-tosylimine **71** was subjected to the reaction conditions in the absence of allenoate and 45% of the desired product **72** was isolated (Scheme 29).

Scheme 29.

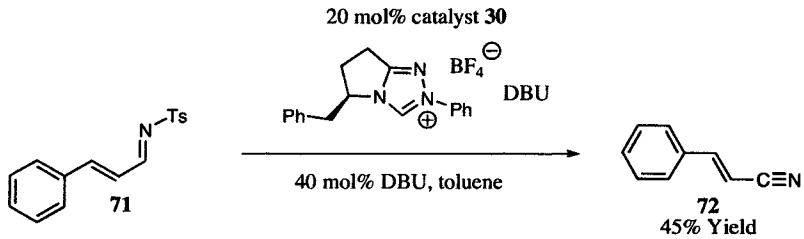

In an attempt to conduct a [3+2] cycloaddition we discovered a mild and catalytic conversion of *N*-tosylimines to nitriles. Thiazolium, imidazolium and triazolium-derived carbenes can catalyze this transformation, thereby making it a convenient method for the formation of nitriles. Further optimization is required in order to increase the isolated yields of the desired product.

4.3.5 Conclusion

The broad range of chemistry that can be catalyzed by *N*-heterocyclic carbenes underlines the enormous potential of these species in organic chemistry. We have been able to take advantage of the *in situ* generated acyl anion equivalent in the conversion of α-haloaldehdyes to esters and *N*-tosylimines to nitriles. In addition, we have successfully demonstrated that palladium π-allyl intermediates can serve as the electrophilic partner for the nucleophilic acyl anion equivalent. Furthermore, we have synthesized a new family of chiral triazolinylidene-gold(I) complexes and illustrated their reactivity in a variety of different carbon bond forming reactions.

[1] (a) Nair V.; Bindu, S.; Sreekumar, V. *Angew. Chem., Int. Ed.* **2005**, *44*, 5130-515. (b) Zeitler, K. *Angew. Chem., Int. Ed.* **2005**, *44*, 7506-7510.

[2] Khaleeli, N.; Li, R.; Townsend, C. A. *J. Am. Chem. Soc.* **1999**, *121*, 9223-9224.

[3] Reynolds, N. T.; Read de Alaniz, J.; Rovis, T. *J. Am. Chem. Soc.* **2004**, *126*, 9518-9519.

[4] Goodman, J. M.; Köhler, A-K.; Alderton, S. C. M. *Tetrahedron Lett.* **1999**, *40*, 8715-8718.

[5] Yu-Kin, K.; Bode, J. W. *J. Am. Chem. Soc.* **2004**, *126*, 8126-8127.

[6] (a) Sohn, S. S.; Rosen, E. L.; Bode, J. W. *J. Am. Chem. Soc.* **2004**, *116*, 6331-6334. (b) Glorius, F.; Burstein, C. *Angew. Chem., Int. Ed.* **2004**, *43*, 6205-6208. (c) Chan, A.; Scheidt, K. A. *Org. Lett.* **2005**, *7*, 905-908. (d) Sohn, S. S.; Bode, J. W. *Org. Lett.* **2005**, *7*, 3873-3876.

[7] He, M.; Bode, J. W. *Org. Lett.* **2005**, *7*, 3131-3134.

[8] (a) Suzuki, Y.; Yamauchi, K.; Muramatsu, K.; Sato, M. *Chem. Commun.* **2004**, 2770-2771. (b) Kano, T.; Sasaki, K.; Maruoka, K. *Org. Lett.* **2005**, *7*, 1347-1349.

[9] Reynolds, N.; Rovis, T. *J. Am. Chem. Soc.* **2005**, *127*, 16406-16407.

[10] (a) Trost, B. M. *Accts. Chem. Res.* **1980**, *13*, 385-393. (b) Tsuji, J. *Tetrahedron* **1986**, *42*, 4361-4401.

[11] Trost, B. M.; Crawley, M. L. *Chem. Rev.* **2003**, *103*, 2921-2943.

[12] This project initiated in collaboration with Professor Krische at UT Austin, who donated two model substrates (**21** and **22**) for our initial investigation.

[13] Professor Hegedus generously provided us with compound **27** and suggested the idea of utilizing stoichiometric palladium π-allyl intermediate.

[14] Professor Tunge suggested this idea at the 39th National Organic Chemistry Symposium in Salt Lake City, June 12-16, 2005.

[15] (a) Herrmann, W. A. *Angew. Chem., Int. Ed.* **2002**, *41*, 1290-1309. (b) Bourissou, D.; Guerret, O.; Gabbaï, F. P. Bertrand, G. *Chem. Rev.* **2000**, *100*, 39-91. (c) Scott, N. M.; Nolan, S. P. *Eur. J. Inorg. Chem.* **2005**, (d) Crudden, C. M.; Allen, D. P. *Coord. Chem. Rev.* **2004**, *248*, 2247-2273.

[16] (a) Ito, Y.; Sawamura, M.; Hayashi, T. *J. Am. Chem. Soc.* **1986**, *108*, 6405-6406. (b) Müller, T. E.; Pleier, A. K. *J. Chem. Soc., Dalton Trans.* **1999**, *5*, 583-588. (c) Dai, L. X.; Lin, Y. R.; Hou, X. L.; Zhou, Y. G. *Pure Appl. Chem.* **1999**, *71*, 1033-1040. (d) Ito, H.; Yajima, T.; Tateiwa, J.; Hosomi, A. *Chem. Commun.* **2000**, *11*, 981-982. (e) Shi, F.; Deng, Y. *Chem. Commun.* **2001**, *5*, 443-444. (f) Hashmi, A. S. K.; Schwarz, L.; Choi, J.-H.; Frost, T. M.; *Angew. Chem., Int. Ed.* **2000**, *39*. 2285-2288. (f) Oberhuber, C. N.; Muñoz, M. P.; Buñuel, E.; Nevado, C.; Cárdenas, D. J.; Echavarren, A. M. *Angew. Chem., Int. Ed.* **2004**, *43*, 2402-2406. (g) Zhang, L.; Wang, S. *J. Am. Chem. Soc.* **2006**, *128*,1442-1443. (h) Zhang, L. *J. Am. Chem. Soc.* **2005**, *127*, 16804-16805. (i) Corkey, B. K.; Toste, D. F. *J. Am. Chem. Soc.* **2005**, *127*,17168-17169. (k) Shi, Z.; Gorin, D. J.; Toste, D. F. *J. Am. Chem. Soc.* **2005**, *127*,5802-5803. (j) Genin, E.; Toullec, P. Y.; Antoniotti, S.; Brancour, C.; Genet, J-P.; Michelet, V. *J. Am. Chem. Soc.* **2005**, *127*,3112-3113. (k) Georgy, M.; Boucard, V.; Campagne, J-M. *J. Am. Chem. Soc.* **2005**, *127*,14180-14181. (l) Markham, J. P.; Staben, S.T.; Toste, D. F. *J. Am. Chem. Soc.* **2005**, *127*,9708-9709. For a review see, (k) Hoffmann-Röder, A.; Krause, N. *Org. Biomol. Chem.*, **2005**, *3*, 387-391.

[17] Lin, I. J. B.; Vasam, C. S. *Can. J. Chem.* **2005**, *83*, 812-825, and references therein.

[18] Frémont, P.; Scott, N. M.; Stevens, E. D.; Nolan, S. P. *Organometallics* **2005**, *24*, 2411-2418.

[19] For a review on Ag(I) *N*-heterocyclic carbene complexes, see: Garrison, J. C.; Youngs, W. J. *Chem. Rev.* **2005**, *105*, 3978-4008.

[20] (a) Hu, X.; Castro-Rodriguez, I.; Olsen, K.; Meyer, K. *Organometallics* **2004**, *23*, 755-764. (b) Barnard, P. J.; Baker, M. V.; Berners-Price, S. J.; Skelton, B. W.; White, A. H. *Dalton Trans.* **2004**, 1038-1047. (c) Wang, H. M. J.; Vasam, C. S.; Tsai, T. Y. R.; Chen, S.-H.; Chang, A. H. H.; Lin, I. J. B. *Organometallics* **2005**, *24*, 486-493. (d) Britten, J. F.; Lock, C. J. L.; Wang, H. M. J. Z. *Acta Crystallogr.* **1992**, *C48*, 1600-1603. (e) Lee, K. M.; Lee, C. K.; Lin, I. J. B. *Chem. Commun.* **1997**, 899-900. (f) Kruger, G. J.; Olivier, P. J.; Lindeque, L.; Raubenheimer, H. G. *Acta Crystallgr.* **1995**, *C51*, 1814-1816. (g) Bovio, B.; Burini, A.; Pietroni, B. R. *J. Organomet. Chem.* **1993**, *452*, 287-291. (h) Boehler, C.; Stein, D.; Donati, N.; Gruetzmacher, H. *New. J. Chem.* **2002**, *26*, 1291-1295. (j) Wang, H. M. J.; Chen, C. Y. L.; Lin, I. J. B. *Organometallics* **1999**, *18*, 1216-1223.

[21] Kennedy-Smith, J. J.; Staben, S.; Toste, D. F. *J. Am. Chem. Soc.* **2004**, *126*, 4526-4527.

[22] Yang, C-G.; He, C. *J. Am. Chem. Soc.* **2005**, *127*, 6966-6967.

[23] Yao, X.; Li, C-J. *J. Am. Chem. Soc.* **2004**, *126*, 6884-6885.

[24] Johansson, M. J.; Gorin, D. J.; Staben, S. T.; Toste, D. F. *J. Am. Chem. Soc.* **2005**, *127*, 18002-18003. For a related gold(III)-catalyzed intramolecular cyclopropanation reaction, see; Fürstner, A.; Hannen, P. *Chem. Commun.* **2004**, 2546.

[25] For similar reactivity of other transition-metal catalyzed olefin cyclopropanation with propargyl acetates, see; (a) Miki, K.; Ohe, K.; Uemura, S. *Tetrahedron Lett.* **2003**, *44*, 2019. (b) Miki, K.; Ohe, K.; Uemura, S. *J. Org. Chem.* **2003**, *68*, 8505. (c) Miki, K.; Uemura, S.; Ohe, K. *Chem. Lett.* **2005**, *34*, 1968.

[26] Lu, X.; Zhang, C.; Xu, Z. *Acc. Chem. Res.* **2001**, *34*,535-544 and references therein.

[27] (a) Glass, R. S.; Hoy, R. C. *Tetrahedron Lett.* **1976**, *21*, 1777-1780. (b) Glass, R. S.; Hoy, R. C. *Tetrahedron Lett.* **1976**, *21*, 1781-1781.

Chapter 1 Experimental

The Development of Chiral Bicyclic Triazolium Salts

General Methods. All reactions were performed under an atmosphere of argon in flame-dried glassware with magnetic stirring. Toluene was degassed with argon and passed through one column of neutral alumina and one column of Q5 reactant. Column chromatography was performed on EM Science silica gel 60 (230-400 mesh). Thin layer chromatography was performed on EM Science 0.25 mm silica gel 60-F plates. Visualization was accomplished with UV light, $KMnO_4$, aqueous ceric ammonium molybdate, anisaldehyde, or bromocresol green dips followed by heating.

Melting points were measured with a MelTemp II melting point apparatus outfitted with a Fluke 51 thermocouple and are uncorrected. Infrared spectra were obtained on a Nicolet Avatar 320 FT-IR spectrometer. ^1H NMR and spectra were recorded on a Varian 400 MHz spectrometer at ambient temperature. Data are reported as follows: chemical shift in parts per million (δ ppm) from an internal [standard tetramethylsilane (TMS) or deuterated chloroform ($CDCl_3$)], multiplicity (s = singlet, d = doublet, t = triplet, q = quartet, and m = multiplet), integration, and coupling constant (Hz). ^{13}C NMR were recorded on a Varian 100 MHz spectrometer at ambient temperature. Chemical shifts are reported in ppm from ($CDCl_3$) taken as 77.0 ppm. Mass spectra were obtained on Fisons VG Autospec. Mass spectra were obtained on Fisons VG Autospec. Optical rotations were measured on an Autopol III automatic polarimeter in a 1 dm cell.

Starting material **24**, **32**, **33**, **34** and **53** were purchased from Aldrich Chemical Co. and used without purification. All other chemicals were purchased from Aldrich

Chemical Co. and used without purification. Spectral data of compounds **27**,[1] **41**,[2] **42**,[2] **43**, **49**[3] matched literature description.

Representative Procedure for the Synthesis of Pyrrolidinones

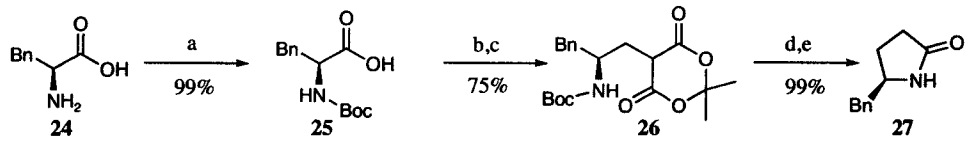

(a) Boc_2O, NaOH, THF/H_2O, 23 °C (b) Meldrum's acid, DMAP, DCC, CH_2Cl_2, 0 °C (c) AcOH, $NaBH_4$, CH_2Cl_2, 0 °C (d) Toluene, 110 °C (e) TFA, CH_2Cl_2, 0 °C.

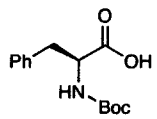

(S)-2-*tert*-Butoxycarbonylamino-3-phenyl-propionic acid (25): A 500 mL round bottom flask was charged with THF:H_2O (1:1, 200 mL) and (S)-phenylalanine (8.000 g, 48.43 mmol) at room temperature. 1.1 eq. Boc_2O (11.63 g, 53.27 mmol) was added to the reaction mixture followed by 2.2 equiv. sodium hydroxide (4.262 g, 106.55 mmol) and the reaction was stirred at room temperature overnight. The THF was removed *in vacuo* and CH_2Cl_2 (300 ml) was added to the reaction flask. 10 % HCl was added dropwise to this solution while stirring vigorously until the precipitate ceased forming (~ pH 4). The organic layer was separated and dried with ($MgSO_4$) and concentrated *in vacuo* to give **25** (12.681 g, 47.80 mmol, 99%) as clear thick oil, which was used without further purification. Spectral data matched literature description.[4]

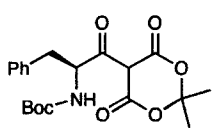

(S)-[1-Benzyl-2-(2,2-dimethyl-4,6-dioxo-[1,3]dioxan-5-yl)-2-oxo-ethyl]-carbamic acid *tert*-butyl ester: A 500 mL round bottom flask was charged with amino acid **25** (12.681 g, 47.80 mmol), Meldrum's acid (7.579 g, 52.59 mmol), DMAP (8.760 g, 71.70 mmol), and CH_2Cl_2 (200 ml) and cooled to -5 °C. To the reaction mixture was added a solution of DCC (10.851 g, 52.59 mmol) in CH_2Cl_2 (100 ml) via addition funnel over one hour. The reaction was

stirred at at -5 °C overnight. Upon warming to room temperature, the dicyclohexylurea was filtered off and the reaction mixture was washed with 5% $KHSO_4$ (4 X 100 ml) and brine (100 ml) and dried in the refrigerator with $MgSO_4$ for 5 hours. This was filtered and concentrated down to approximately 200 mL and used without further purification.

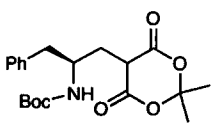

(R)-[1-Benzyl-2-(2,2-dimethyl-4,6-dioxo-[1,3]dioxan-5-yl)-ethyl]-carbamic acid *tert*-butyl ester (26): A 500 mL round bottom flask was charged with (S)-[1-Benzyl-2 (2,2-dimethyl-4,6-dioxo-[1,3]dioxan-5-yl)-2-oxo-ethyl]-carbamic acid *tert*-butyl ester (approx. 47 mmol, all of the material from the previous step) in CH_2Cl_2 (200 ml) and 98% AcOH (30 ml, 530.70 mmol). The solution was cooled to –5 °C and 36 equal portions (0.126 g) of $NaBH_4$ (4.521 g, 119.50 mmol total) were added over three hours every 5 minutes avoiding large exotherms. The reaction was stirred at –5 °C for 18 hours. The organic layer was washed with water (3 x 100 ml) and brine (2 x 100 ml) and the combined organic extracts were dried with $MgSO_4$ and concentrated down. The desired product was crystallized from diethyl ether (75 ml) to yield **26** (13.530 g, 35.85 mmol, 75% from **25**) as an analytically pure white solid. Spectral data matched literature description.[1]

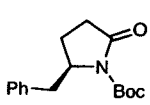

(R)-2-Benzyl-5-oxo-pyrrolidine-1-carboxylic acid *tert*-butyl ester: A 250 mL round bottom flask equipped with a reflux condenser was charged with **5** (8.700 g 23.00 mmol) and toluene (100 mL) and heated to 110 °C for 5 hours. Upon cooling, the organic layer was concentrated under vacuum and used without further purification.

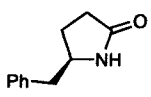

(R)-5-Benzyl-pyrrolidin-2-one (27): A flame-dried 500 mL round bottom flask was charged with (R)-2-Benzyl-5-oxo-pyrrolidine-1-carboxylic acid *tert*-butyl ester (6.325 g, 22.97 mmol) and dry CH_2Cl_2 (200 mL) and cooled to 0 °C. To this solution was added trifluoroacetic acid (3.9 mL, 50.71 mmol) dropwise. The reaction was allowed to warm to room temperature and stirred for 4 hours. The reaction was quenched slowly with $NaHCO_3$ and extracted with CH_2Cl_2. The organic layer was washed with water, brine and dried with $MgSO_4$ and concentrated down to yield **27** (3.989 g, 22.79 mmol) a yellow oil that matched literature spectral data.[1]

Representative One-Pot Synthesis of Triazolium Salts

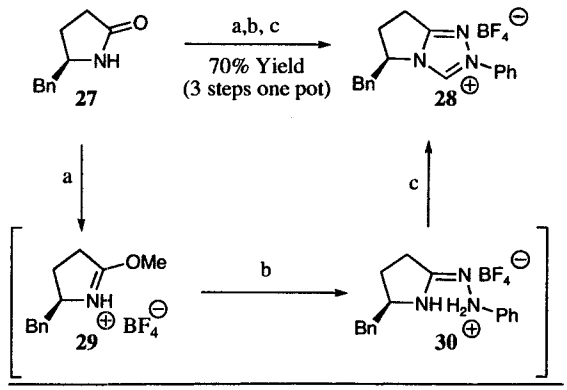

(a) $Me_3O^+BF_4^-$, CH_2Cl_2, 23 °C, 24 h (b) $PhNHNH_2$, CH_2Cl_2, 23 °C (c) $CH(OMe)_3$: MeOH (7 : 1), 80 °C

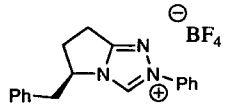

5-Benzyl-2-phenyl-6,7-dihydro-5*H*-pyrrolo[2,1-*c*][1,2,4]triazol-2-ium Tetrafluoroborate (28):[5] A flame-dried 100 mL round bottom flask was charged with **27** (1.000 g, 5.71 mmol) and CH_2Cl_2 (40 mL). Trimethyloxonium tetrafluoroborate (0.930 g, 6.29 mmol) was added and the reaction mixture stirred overnight at room temperature. To the pinkish solution was added phenylhydrazine (0.62 mL, 6.29 mmol) and stirred overnight. The solvent was

removed *in vacuo* and the product was used without further purification. To this was added methanol (2 mL) and trimethyl orthoformate (14 mL). The reaction mixture was heated to 80 °C and stirred at this temperature overnight. The solvent was removed *in vacuo* and the product was precipitated from ethyl acetate to give an off white/yellow powder. Recrystallization from hot MeOH affords **28** (0.890 g, 50%) as a white crystalline solid. Rf (3:1 acetone:CH_2Cl_2) = 0.16; ^{1}H NMR (400 MHz, $CDCl_3$), δ 10.02 (1H, s), 7.83-7.80 (2H, m), 7.53-7.51 (3H, m), 7.32-7.27 (3H, m), 7.23-7.20 (2H, m), 5.36-5.28 (1H, m), 3.54 (1H, dd, *J*=13.5, 5.0 Hz), 3.20-3.0 (1H, m), 3.15 (1H, dd, *J*=13. 5, 8.8 Hz), 3.01-2.85 (1H, m), 2.07-2.55 (1H, m); ^{13}C NMR (100 MHz, acetone-D6) δ 163.9, 138.3, 137.0, 136.7, 131.6, 131.1, 130.4, 129.9, 128.3, 122.1, 62.9, 40.3, 33.4, 22.1; IR (NaCl, neat) 1585, 1513, 1222, 1062cm^{-1}; m.p. 195.1-196.5 °C; $[\alpha]_D^{23}$ = + 9.1° (acetonitrile); HRMS (FAB+) calcd for $C_{18}H_{18}N_3$ 276.1499, Found 276.1498.

Representative Three Step Synthesis of Triazolium Salts

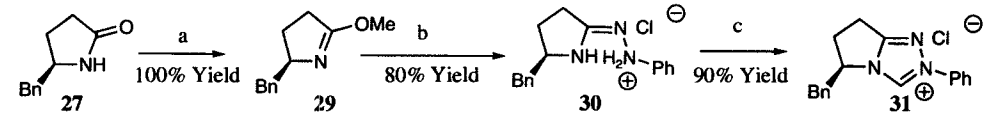

(a) $Me_3O^+BF_4^-$, CH_2Cl_2, 23 °C, 24 h,then ice-cold $NaHCO_3$ wash (b) $PhNHNH_2HCl$,CH_2Cl_2
(c) $CH(OMe)_3$: MeOH (7 : 1), 80 °C

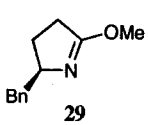

29

(R)-2-Benzyl-5-methoxy-3,4-dihydro-2*H*-pyrrole (29): A flame-dried 100 mL round bottom flask was charged with **27** (1.000 g, 5.71 mmol) and CH_2Cl_2 (40 mL). Trimethyloxonium tetrafluoroborate (0.840 g, 5.71 mmol) was added and the reaction mixture stirred overnight at room temperature. The mixture was then diluted with CH_2Cl_2 and washed with ice-cold saturated aqueous sodium bicarbonate (3 x 3 mL per mmol^{-1} of pyrrolidinone **27**).[6] The solution was dried over

anhydrous magnesium sulfate and concentrated *in vacuo* to afford **29** as a liquid in quantitative yield. The product was used in the next step without further purification.

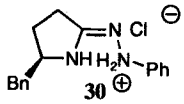

(*R*)-*N*'-(5-Benzyl-pyrrolidin-2-ylidene)-*N*-phenyl-hydrazinium Chrlorid (30): A flame-dried 100 mL round bottom flask was charged with **29** (0.89 g, 4.23 mmol) and CH_2Cl_2 (30 mL). Phenylhydrazine hydrochloride (0.610 g, 4.23 mmol) was added and the reaction mixture stirred overnight at room temperature. The solvent was removed *in vacuo* to afford 1.25 g (98%) of the desired salt **30** as an orange solid. ^{1}H NMR (400 MHz, DMSO), δ 11.41 (1H, s), 10.30 (1H, s), 8.67 (1H, s), 7.33-7.18 (7H, m), 6.92-6.80 (3H, m), 4.2-4.17 (1H, m), 3.00-2.94 (1H, m), 2.90-2.72 (2H, m), 2.65-2.49 (1H, m), 2.11-2.06 (1H, m), 1.92-1.81 (1H, m); ^{13}C NMR (100 MHz, $CDCl_3$) δ 169.7, 146.0, 136.3, 129.4, 128.8, 128.2, 126.5, 120.6, 113.2, 113.2, 60.1, 27.7, 25.1; m.p. 204.6-205.9 °C;(HRMS (FAB+) calcd for $C_{17}H_{20}N_3$ 266.1660, Found 266.1657.

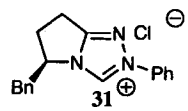

5-Benzyl-2-phenyl-6,7-dihydro-5*H*-pyrrolo[2,1-*c*][1,2,4]triazol-2-ium Chloride (31): To a flame dried flask was added **30** (1.25 g, 4.14 mmol) followed by methanol (2 mL) and trimethyl orthoformate (14 mL). The reaction mixture was heated to 80 °C and stirred at this temperature overnight. The solvent was removed *in vacuo* and the product was precipitated from ethyl acetate to give 1.25 g (97%) of **31** an off white/yellow powder. ^{1}H NMR (400 MHz, $CDCl_3$), δ 10.02 (1H, s), 7.83-7.80 (2H, m), 7.53-7.51 (3H, m), 7.32-7.27 (3H, m), 7.23-7.20 (2H, m), 5.36-5.28 (1H, m), 3.54 (1H, dd, *J*=13.5, 5.0 Hz), 3.20-3.0 (1H, m), 3.15 (1H, dd, *J*=13. 5, 8.8 Hz), 3.01-2.85 (1H, m), 2.07-2.55 (1H, m); ^{13}C NMR (100 MHz, acetone-D6) δ 163.9, 138.3, 137.0, 136.7, 131.6, 131.1, 130.4, 129.9, 128.3,

122.1, 62.9, 40.3, 33.4, 22.1; m.p. 195.1-196.5 °C ;$[\alpha]_D^{23}$ = + 7.4° (acetonitrile); HRMS (FAB+) calcd for $C_{18}H_{18}N_3$ 276.1499, Found 276.1498.

Representative Counter Ion Exchange Reaction of Triazolium Salts

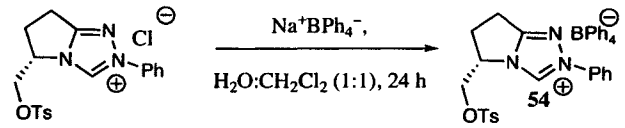

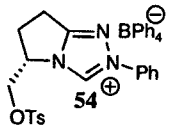

2-Phenyl-5-(toluene-4-sulfonyloxymethyl)-6,7-dihydro-5*H*-pyrrolo[2,1-*c*][1,2,4]triazol-2-ium-tetraphenyl borate (54): To a round bottom flask containing **54** chloride salt (0.8 g, 1.975 mmol, yellow oil) was added 20 mL of a 1:1 mixture of H_2O:CH_2Cl_2 followed by 0.8 g (2.37 mmol) of sodium tetraphenyl borate and the resulting solution was stirred overnight. The mixture was diluted with CH_2Cl_2 and separated. The solution was dried over anhydrous magnesium sulfate and concentrated *in vacuo* to afford **54** as orange solid in quantitative yield. ^{1}H NMR (400 MHz, $CDCl_3$), δ 7.53-7.44 (11H, m), 6.99-6.95 (7 H, m), 6.85-6.81 (3H, m), 4.20 (1H, m), 3.75 (1H, m), 3.38 (1H, m), 3.0-2.7 (2H, m), 2.46 (1H, m), 2.25 (1H, m); ^{13}C NMR (100 MHz, $CDCl_3$) δ 164.6, 164.2, 163.7, 163.2, 162.1, 135.8, 135.4, 134.7, 134.7, 131.2, 131.0, 130.1, 128.7, 128.3, 127.9, 127.3, 127.2, 127.1, 127.0, 122.1, 121.0, 59.0,45.9, 30.2, 21.6.

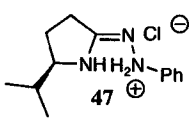

^{1}H NMR (400 MHz, DMSO), δ 11.44 (1H, s), 10.09 (1H, s), 8.66 (1H, s), 7.24 (2H, dd, *J*= 7.4, 7.7 Hz), 6.90-6.82 (3H, m), 3.81 (1H, m), 2.99-2.93 (2H, m), 2.13 (1H, m), 1.97-181 (2H, m), 0.82 (6H, dd, *J*= 6.7, 6.4 Hz); ^{13}C NMR (100 MHz, $CDCl_3$) δ 169.8, 146.1, 129.0, 120.6, 113.2, 64.9, 30.6, 28.1, 22.1, 18.3, 16.46; m.p. 220.2 °C

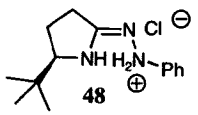

48

^{1}H NMR (400 MHz, DMSO), δ 11.41 (1H, s), 10.30 (1H, s), 8.67 (1H, s), 7.33-7.18 (7H, m), 6.92-6.80 (3H, m), 4.2-4.17 (1H, m), 3.00-2.94 (1H, m), 2.90-2.72 (2H, m), 2.65-2.49 (1H, m), 2.11-2.06 (1H, m), 1.92-1.81 (1H, m); ^{13}C NMR (100 MHz, $CDCl_3$) δ 169.7, 146.0, 136.3, 129.4, 128.8, 128.2, 126.5, 120.6, 113.2, 113.2, 60.1, 27.7, 25.1; m.p. 204.6-205.9 °C;(HRMS (FAB+) calcd for $C_{17}H_{20}N_3$ 266.1660, Found 266.1657.

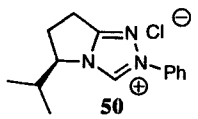

50

^{1}H NMR (400 MHz, DMSO), δ 12.87 (1H, s), 8.13-8.10 (2H, m), 7.58-7.43 (3H, m), 5.10 (1H, m), 3.28-3.1 (2H, m), 2.94-2.74 (3H, m), 2.65-2.54 (2H, m), 1.11 (6H, dd, *J*= 8.6, 9.1 Hz); ^{13}C NMR (100 MHz, $CDCl_3$) δ 161.2, 138.7, 135.4, 130.2, 129.9, 120.1, 65.8, 30.9, 28.1, 21.8, 18.6, 16.1; m.p. 73.2-75.4 °C;(HRMS (FAB+) calcd for $C_{14}H_{18}N_3$ 228.1499, Found 228.1500.

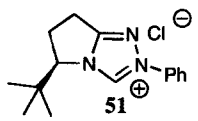

51

^{1}H NMR (400 MHz, $CDCl_3$), δ 10.06 (1H, s), 7.92-7.89 (2H, m), 7.57-7.52 (3H, m), 4.82 (1H, dd, *J*= 3.5, 3.2 Hz), 3.31-2.95 (3H, m), 2.65 (1H, m), 1.07 (9H, s); ^{13}C NMR (100 MHz, $CDCl_3$) δ137.4, 130.7, 130.9, 120.9, 70.4, 34.7, 29.1, 25.1, 21.8; m.p. 146.7-149.2 °C;(HRMS (FAB+) calcd for $C_{15}H_{20}N_3$ 242.1655, Found 242.1657.

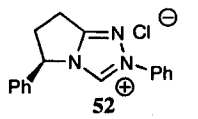

52

^{1}H NMR (400 MHz, $CDCl_3$), δ 10.06 (1H, s), 7.92-7.89 (2H, m), 7.57-7.52 (3H, m), 4.82 (1H, dd, *J*= 3.5, 3.2 Hz), 3.31-2.95 (3H, m), 2.65 (1H, m), 1.07 (9H, s); ^{13}C NMR (100 MHz, $CDCl_3$) δ161.72, 136.7, 135.3,

135.2, 130.3, 129.6, 129.3, 129.1, 128.3, 126.7, 126.6, 120.7, 119.35, 63.6, 35.8, 21.9;(HRMS (FAB+) calcd for $C_{17}H_{16}N_3$ 262.1345, Found 262.1345.

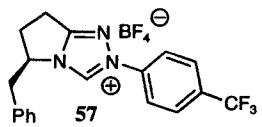

5-Benzyl-2-(4-trifluoromethyl-phenyl)-6,7-dihydro-5*H*-pyrrolo[2,1-*c*][1,2,4]triazol-2-ium tetrafluoroborate (37): Rf (9:1 CH_2Cl_2: MeOH) = 0.4; ^{1}H NMR (400 MHz, $CDCl_3$), δ 10.18 (1H, s), 7.93 (2H, d, *J*= 8.5 Hz), 7.60 (2H, d, *J*= 8.6 Hz), 7.23-7.13 (5H, m), 5.18 (1H, m), 3.56 (1H, dd, *J*=4.3, 13.5 Hz), 3.15-2.92 (3H, m), 2.78 (1H, m), 2.53 (1H, m); ^{13}C NMR (100 MHz, $CDCl_3$) δ 162.3, 137.9, 137.7, 134.4, 132.6, 132.2, 129.2, 129.0, 127.7, 127.3, 127.2, 124.4, 121.0, 61.9, 39.5, 32.1, 21.4; IR (NaCl, neat) 1662, 1588, 1325, 1069 cm^{-1}; m.p. 196.2-198.4 °C; $[\alpha]_D^{23}$ = + 6.2° (acetonitrile); HRMS (FAB+) calcd for $C_{19}H_{17}F_3N_3$ 344.1364, Found 344.1373.

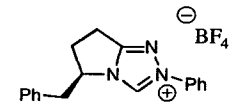

28

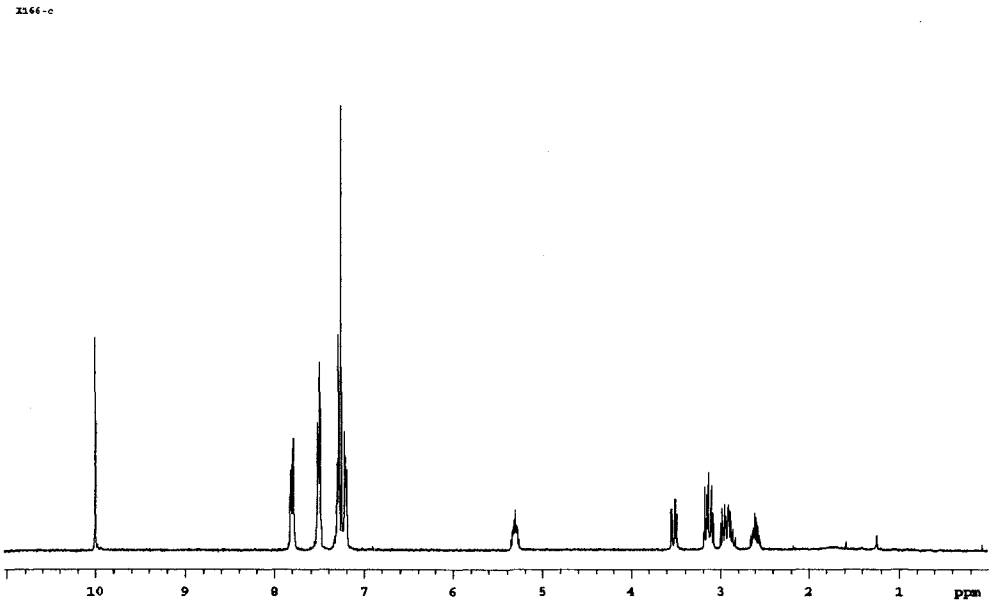

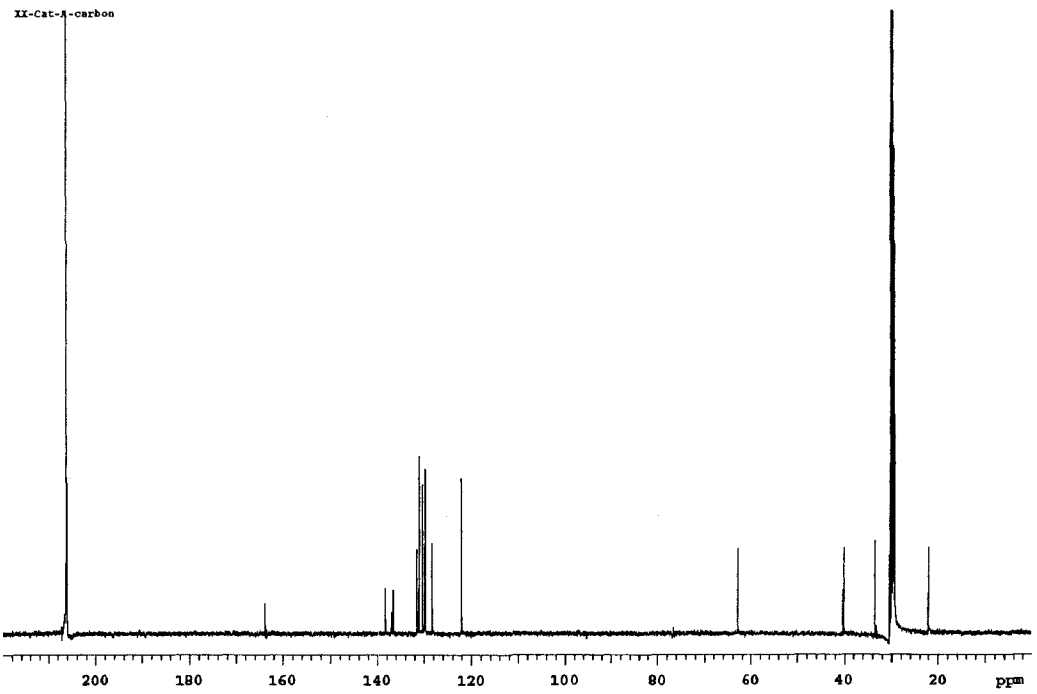

References

[1]Smrcina, M.; Majer, P.; Majerová, E.; Guerassina, T.; Eissenstat, M. A. *Tetrahedron*, 1997, *53*, 12867-12874.

[2] Burgess, L. E.; Meyers, A. I. *J. Org. Chem. Soc.* **1992**, *57*, 1656-1662.

[3] Lettau, H.; Buege, A.; Harenberb, P.; Haertel, S.; Jarmer, K.; Kock, K.; Poeppel, W.; Schikora, A.; Schneider, R. *Pharmazie* **1993**, *48*, 410-414.

[4] Meyers, A. I.; Tavares, F. X. *J. Org. Chem.* **1996**, *61*, 8207-8215.

[5] Kerr, M. S.; Read de Alaniz, J.; Rovis, T. *J. Org. Chem.* **2005**, *70*, 5725-5728.

[6] Enders, D.; Kallfass, U. *Angew. Chem., Int. Ed.* **2002**, *41*, 1743-1745.

Chapter 2 Experimental

The Development of Chiral Bicyclic Triazolium Salts

General Methods. All reactions were performed under an atmosphere of argon in flame-dried glassware with magnetic stirring. Toluene was degassed with argon and passed through one column of neutral alumina and one column of Q5 reactant. Column chromatography was performed on EM Science silica gel 60 (230-400 mesh). Thin layer chromatography was performed on EM Science 0.25 mm silica gel 60-F plates. Visualization was accomplished with UV light, $KMnO_4$, aqueous ceric ammonium molybdate, anisaldehyde, or bromocresol green dips followed by heating.

Infrared spectra were obtained on a Nicolet Avatar 320 FT-IR spectrometer. ^1H NMR and spectra were recorded on a Varian 400 MHz spectrometer at ambient temperature. Data are reported as follows: chemical shift in parts per million (δ ppm) from an internal [standard tetramethylsilane (TMS) or deuterated chloroform ($CDCl_3$)], multiplicity (s = singlet, d = doublet, t = triplet, q = quartet, and m = multiplet), integration, and coupling constant (Hz). ^{13}C NMR were recorded on a Varian 100 MHz spectrometer at ambient temperature. Chemical shifts are reported in ppm from ($CDCl_3$) taken as 77.0 ppm. Mass spectra were obtained on Fisons VG Autospec. Analytical high performance liquid chromatography (HPLC) was performed on a Dynamax model SD-200 HPLC equipped with a Dynamax model UV-1 variable wavelength UV detector using a Chiracel OD-H (0.46 cm X 25 cm) chiral column. Optical rotations were measured on an Autopol III automatic polarimeter in a 1 dm cell.

Toluene was degassed with argon and passed through one column of neutral alumina and one column of Q5 reactant. KHMDS was purchased from Aldrich Chemical Co. and 0.5 M solutions in toluene were prepared prior to each reaction. All other chemical were purchased from Aldrich Chemical Co. and used without further purification.

Racemic material was prepared by the method of Ciganek[1] with the following modifications; CH_2Cl_2 was used as the solvent. Preparation of chiral triazolium salts **12, 31, 32, 35, 36, 37, 38, 39, 40, 41** and **42** were prepared according to chapter 1. Triazolium salts **60** and **61** were obtained from Mark S. Kerr and prepared according to literature method and lab precedent.[2] Starting materials were prepared known literature methods.[3] The absolute configuration of **25** was assigned by optical rotation and compared to literature value.[4] Relative configuration of **110** and **120** has been assigned based on single crystal X-ray analysis. The others were assigned by analogy.

General procedure for the asymmetric intramolecular Stetter reaction: A flame dried round bottom flask was charged with triazolium salt (0.2 eq) and 5 mL of toluene. To this solution was added KHMDS (0.5 M in toluene prepared prior to use from 0.05 g of KHMDS in 0.5 mL of toluene) (0.2 eq) via syringe and the solution was stirred at ambient temperature for 5 minutes. A solution of the substrate (1 eq 0.12 mmol) in 2 mL of toluene was added. The resulting solution was allowed to stir at ambient temperature and monitored by TLC. The reaction was worked up by placing directly onto a column and purified. The desired product was purified by

flash column chromatography and eluted with a suitable solution of hexane and ethyl acetate (typically 4:1). Evaporation of solvent afforded analytically pure product.

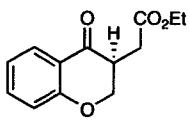

(2*S*)-(4-Oxo-chroman-3-yl)-acetic acid ethyl ester (34): According to the general procedure, 10.0 mg (0.028 mmol) of **38** and 57.0 μL (0.028 mmol) of KHMDS and 33.0 mg (0.140 mmol) of **33** were reacted for1 hour. Upon work-up 31 mg (94%) of desired ester was isolated as a colorless oil: Spectral data matched literature description;[1] HPLC analysis - Chiracel AD column, 97:3 hexanes to isopropanol 0.5 ml/ min. Minor enantiomer 30.2 minutes, major enantiomer 40.2 minutes.

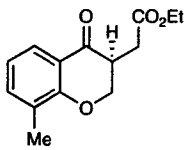

(2*S*)-(8-Methyl-4-oxo-chroman-3-yl)-acetic acid ethyl ester (44): According to the general procedure, 10.0 mg (0.028 mmol) of **38** and 57.0 μL (0.028 mmol) of KHMDS and 35.0 mg (0.14 mmol) of **43** were reacted for1 hour. Upon work-up 28 mg (80%) of desired ester was isolated as a colorless oil: Spectral data matched literature description;[1] HPLC analysis - Chiracel AD column, 97:3 hexanes to isopropanol 0.5 ml/ min. Minor enantiomer 19.4 minutes, major enantiomer 25.1 minutes.

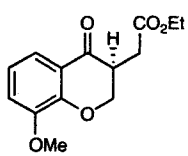

(2*S*)-(8-Methoxy-4-oxo-chroman-3-yl)-acetic acid ethyl ester (46): According to the general procedure, 10.0 mg (0.028 mmol) of **38** and 57.0 μL (0.028 mmol) of KHMDS and 37.0 mg (0.14 mmol) of **45** were reacted for1 hour. Upon work-up 29 mg (80%) of desired ester was isolated as a

colorless oil: Spectral data matched literature description;[1] HPLC analysis - Chiracel AD column, 97:3 hexanes to isopropanol 1.0 ml/ min. Minor enantiomer 27.8 minutes, Major enantiomer 42.2 minutes.

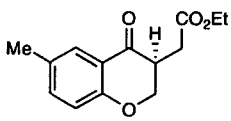

(2*S*)-(6-Methyl-4-oxo-chroman-3-yl)-acetic acid ethyl ester (48): According to the general procedure, 11.6 mg (0.032 mmol) of **38** and 64.0 μL (0.032 mmol) of KHMDS and 50.0 mg (0.160 mmol) of **47** were reacted for 60 minutes. Upon work-up 40 mg (80%) of desired ester was isolated as a colorless oil: Spectral data matched literature description;[1]HPLC analysis -Chiracel AD column, 97:3 hexanes to isopropanol 0.5 ml/ min. Minor enantiomer 25.7 minutes, major enantiomer 39.2 minutes.

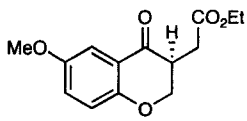

***(2S)*-(6-Methoxy-4-oxo-chroman-3-yl)-acetic acid ethyl ester (50).** According to the general procedure, 10.0 mg (0.028 mmol) of **49** and 57.0 μL (0.028 mmol) of KHMDS and 38.0 mg (0.143 mmol) of **38** were reacted for 24 hours. Work-up afforded 35.7 mg (94%) of the desired product as colorless oil. R_f (1:1 hexane to ethyl acetate) = 0.6; $[\alpha]_D^{23}$ = +23.75° ($CHCl_3$); HPLC analysis – Chiracel AD column 95:5 hexanes to isopropanol 1.0 mL/min. Minor enantiomer: 14.0 minutes. Major enantiomer: 19.0 minutes; ^{1}H NMR (400 MHz, $CDCl_3$) δ 7.29 (1H, m), 7.07 (1H, m), 6.89 (1H, m), 4.54 (1H, dd, *J*= 5.2, 11.2 Hz), 4.25 (1H, dd, *J*= 11.2, 11.7 Hz), 4.17 (2H, q, *J*= 7.2 Hz), 3.78 (3H, s) 3.29 (1H, dddd, *J*= 5.1, 8.1, 11.0, 13.0 Hz), 2.90 (1H, dd, *J*=5.0, 17.0 Hz), 2.40 (1H, dd, *J*=7.8, 17.0 Hz), 1.27 (3H, t, *J*= 7.2 Hz); ^{13}C NMR (100 MHz, $CDCl_3$) δ 192.5, 171.2, 153.9,

125.1, 119.0, 107.5, 70.3, 61.0, 55.8, 42.5, 30.5, 14.3; IR (NaCl, CH_2Cl_2) 1723, 1687, 1490, 1432, 1272 cm^{-1}; HRMS (FAB+) calcd for $C_{14}H_{16}O_5$ 264.0998, Found 265.1068.

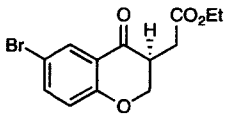

***(2S)*- (6-Bromo-4-oxo-chroman-3-yl)-acetic acid ethyl ester (52)** According to the general procedure, 11.6 mg (0.032 mmol) of **38** and 64.0 μL (0.032 mmol) of KHMDS and 50.0 mg (0.160 mmol) of **51** were reacted for 20 minutes. Work-up afforded 47.5 mg (95%) of the desired product as colorless oil. R_f (1:1 hexane to ethyl acetate) = 0.6; $[\alpha]_D^{23}$ = + 10.22 ($CHCl_3$); HPLC analysis – Chiracel OD-H column 97:3 hexanes to isopropanol 0.5 mL/min. Major enantiomer: 24.6 minutes, Minor enantiomer: 26.3 minutes; ^1H NMR (400 MHz, $CDCl_3$) δ 7.95(1H, d, *J*= 2.5 Hz), 7.51 (1H, dd, *J*= 2.5, 8.7 Hz), 6.85 (1H, d, *J*= 8.9 Hz), 4.58 (1H, dd, *J*= 5.3, 11.3 Hz), 4.26 (1H, dd, *J*= 11.1, 11.5 Hz), 4.15 (2H, q, *J*=7.2 Hz), 3.28 (1H, dddd, *J*= 5.1, 8.7, 9.8, 13.0 Hz), 2.87 (1H, dd, *J*= 4.6, 17.0 Hz), 2.39 (1H, dd, *J*= 7.8, 17.0 Hz), 1.25 (3H, t, *J*= 7.2 Hz); ^{13}C NMR (100 MHz, $CDCl_3$) δ 191.3, 171.0, 160.5, 138.5, 129.7, 121.7, 119.9, 114.1, 70.2, 61.0, 42.2, 30.1, 14.1; IR (NaCl, CH_2Cl_2) 1723, 1687, 1600, 1469 cm^{-1}; HRMS (FAB+) calcd for $C_{13}H_{13}BrO_4$ 311.9997, Found 313.0059.

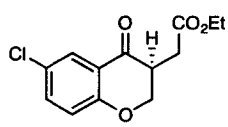

***(2S)*- (6-Chloro-4-oxo-chroman-3-yl)-acetic acid ethyl ester (54)** According to the general procedure, 13.5 mg (0.037 mmol) of **38** and 76.0 μL (0.037 mmol) of KHMDS and 50.0 mg (0.186 mmol) of **53** were reacted for 20 minutes. Work-up afforded 47 mg (94%) of the desired product as

colorless oil. R_f (1:1 hexane to ethyl acetate) = 0.6; $[\alpha]_D^{23}$ = + 1.4 ($CHCl_3$); HPLC analysis–Chiracel AD column 95:5 hexanes to isopropanol 1 mL/min. Major enantiomer: 10.9 minutes, Minor enantiomer: 15.0 minutes; ^1H NMR (400 MHz, $CDCl_3$) δ 7.80(1H, d, *J*= 2.5 Hz), 7.38 (1H, dd, *J*= 2.5, 8.9 Hz), 6.90 (1H, d, *J*= 8.9 Hz), 4.57 (1H, dd, *J*= 5.3, 11.1 Hz), 4.26 (1H, dd, *J*= 11.5, 11.9 Hz), 4.15 (2H, q, *J*=7.2 Hz), 3.28 (1H, dddd, *J*= 5.1, 8.1, 10.2, 13.0 Hz), 2.88 (1H, dd, *J*= 4.6, 17.0 Hz), 2.39 (1H, dd, *J*= 8.1, 17.0 Hz), 1.25 (3H, t, *J*= 7.2 Hz); ^{13}C NMR (100 MHz, $CDCl_3$) δ 191.5, 171.1, 160.1, 138.8, 127.0, 126.6, 121.2, 119.6, 70.3, 61.0, 42.3, 30.2, 14.1; IR (NaCl, CH_2Cl_2) 1730, 1701, 1469, 1418 cm^{-1}; HRMS (FAB+) calcd for $C_{13}H_{13}ClO_4$ 268.0502, Found 269.0580.

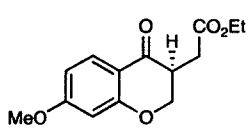

***(2S)*- (7-Methoxy-4-oxo-chroman-3-yl)-acetic acid ethyl ester (56)** According to the general procedure, 10.0 mg (0.028 mmol) of **38** and 57.0 μL (0.028 mmol) of KHMDS and 38.0 mg (0.143 mmol) of **55** were reacted for 60 minutes. Work-up afforded 17.1 mg (45%) of the desired product as colorless oil. R_f (1:1 hexane to ethyl acetate) = 0.7; ; $[\alpha]_D^{23}$ = + 8.0 ($CHCl_3$); HPLC analysis – Chiracel AD-H column 95:5 hexanes to isopropanol 1.0 mL/min. Major enantiomers: 36.24 minutes: Minor Enantiomer: 27.61 minutes; ^1H NMR (400 MHz, $CDCl_3$) δ 7.89(1H, d, *J*= 8.7 Hz), 6.55 (1H, dd, *J*= 2.3, 8.7 Hz), 6.38 (1H, d, *J*= 2.3 Hz), 4.55 (1H, dd, *J*= 5.3, 11.0 Hz), 4.24 (1H, dd, *J*= 11.2, 11.2 Hz), 4.15 (2H, q, *J*=7.1 Hz), 3.80 (3H, s), 3.24 (1H, dddd, *J*= 4.9, 8.3, 9.8, 11.7 Hz), 2.90 (1H, dd, *J*= 4.7, 17.0 Hz), 2.35 (1H, dd, *J*= 8.5, 17.0 Hz), 1.25 (3H, t, *J*= 7.2 Hz); ^{13}C NMR (100 MHz, $CDCl_3$) δ 191.2, 171.5, 165.9, 163.6, 129.0, 114.3, 110.0, 100.6, 70.5, 60.9,

55.6, 42.0, 30.4, 14.1; IR (NaCl, CH_2Cl_2) 1730, 1680, 1600, 1265 cm^{-1}; HRMS (FAB+) calcd for $C_{14}H_{16}O_5$ 264.0998, Found 265.1062.

(56)

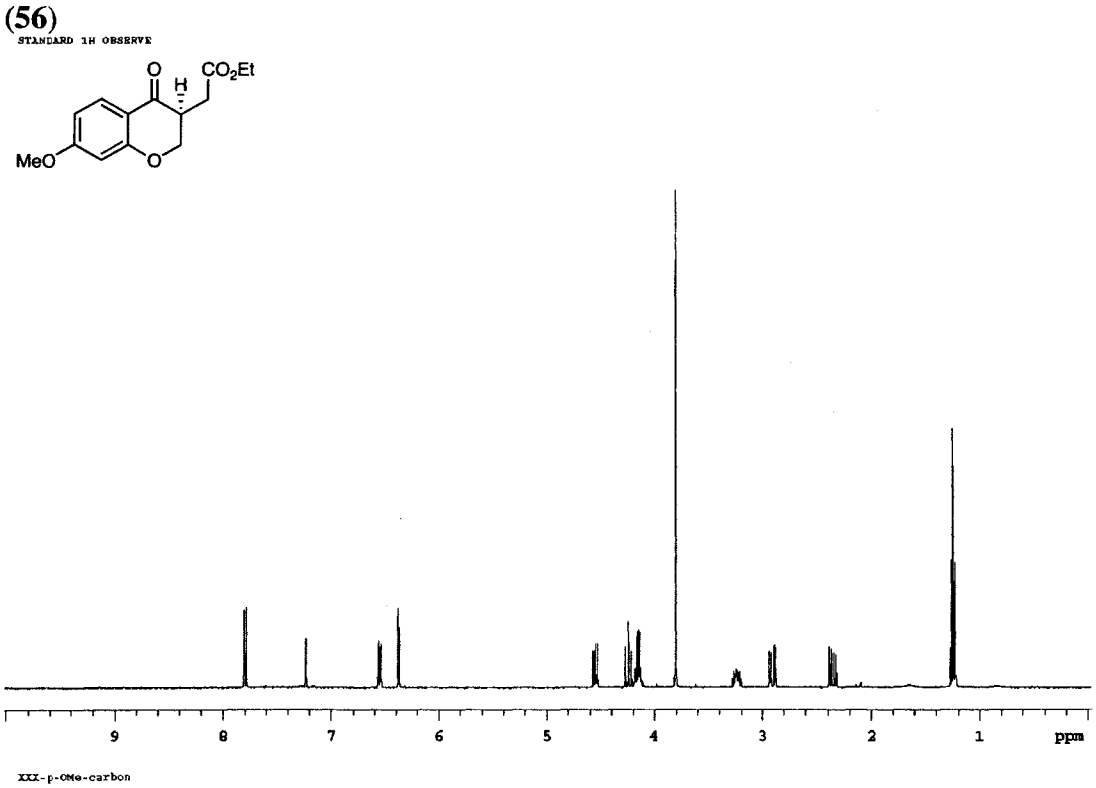

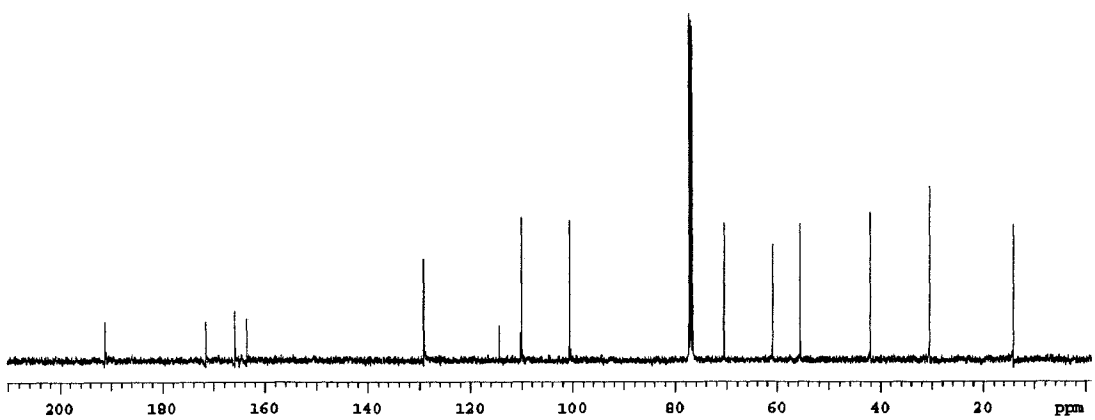

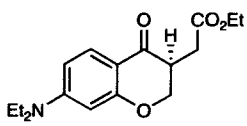

***(2R)*-(7-Diethylamino-4-oxo-chroman-3-yl)-acetic acid ethyl ester (58).** According to the general procedure, 8.5 mg (0.019 mmol) of **57** and 40.0 μL (0.019 mmol) of KHMDS and 30.0 mg (0.098 mmol) of **38** were reacted for 24 hours. Work-up afforded 16.5 mg (55%) of the desired product as colorless oil. R_f (1:1 hexane to ethyl acetate) = 0.3; $[\alpha]_D^{23}$ = -1.86 ($CHCl_3$); HPLC analysis – Chiracel AD-H column 90:1 hexanes to isopropanol 1.0 mL/min. Major enantiomer: 17.3 minutes, Minor enantiomer: 15.9 minutes; ^{1}H NMR (400 MHz), δ 7.72 (1H, d, *J*= 8.9 Hz), 6.35 (1H, d, *J*= 8.5 Hz), 6.07 (1H, s), 4.50 (1H, dd, *J*= 5.0, 10.9 Hz), 4.2 (1H, dd, *J*= 11.0, 11.0 Hz), 4.15 (2H, q, *J*= 7.2 Hz), 3.36 (4H, q, *J*= 7.2 Hz), 3.18 (1H, m), 2.91 (1H, dd, *J*= 4.5, 16.8 Hz), 2.33 (1H, dd, *J*=4.5, 16.8 Hz), 1.25 (3H, t, *J*= 7.2 Hz), 1.17 (6H, t, *J*= 7.2 Hz); ^{13}C NMR (100 MHz, $CDCl_3$) δ 190.1, 171.8, 163.5, 129.2, 106.7, 70.3, 60.7, 45.0, 41.9, 30.7, 14.1, 12.4; IR (NaCl, CH_2Cl_2) 1730, 1665, 1600; HRMS (FAB+) calcd for $C_{17}H_{23}NO_4$ 305.1627. Found 306.1694.

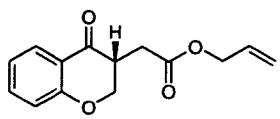

***(2R)*-(4-Oxo-chroman-3-yl)-acetic acid allyl ester (62)** According to the general procedure, 11.3 mg (0.024 mmol) of **61** and 48.0 μL (0.024 mmol) of KHMDS and 30.0 mg (0.122 mmol) of **61** were reacted for 60 minutes. Work-up afforded 28.2 mg (94%) of the desired product as colorless oil. R_f (4:1 hexane to ethyl acetate) = 0.4; $[\alpha]_D^{23}$ = - 3.97 ($CHCl_3$); HPLC analysis – Chiracel AD-H column 90:1 hexanes to isopropanol 1.0 mL/min. Major enantiomer: 8.78 minutes, Minor enantiomer: 11.67 minutes; ^{1}H NMR (400 MHz, $CDCl_3$) δ 7.89(1H, d, *J*= 8.7 Hz), 6.55 (1H, dd, *J*= 2.3, 8.7 Hz), 6.38 (1H, d, *J*= 2.3

Hz), 4.55 (1H, dd, *J*= 5.3, 11.0 Hz), 4.24 (1H, dd, *J*= 11.2, 11.2 Hz), 4.15 (2H, q, *J*=7.1 Hz), 3.80 (3H, s), 3.24 (1H, dddd, *J*= 4.9, 8.3, 9.8, 11.7 Hz), 2.90 (1H, dd, *J*= 4.7, 17.0 Hz), 2.35 (1H, dd, *J*= 8.5, 17.0 Hz), 1.25 (3H, t, *J*= 7.2 Hz); ^{13}C NMR (100 MHz, $CDCl_3$) δ 192.5, 171.0, 136.0, 131.8, 127.3, 121.5, 120.4, 118.6, 117.8, 117.8, 70.1, 65.6, 42.4, 30.2; IR (NaCl, CH_2Cl_2) 1738, 1690, 1612, 1474 cm^{-1}; HRMS (FAB+) calcd for $C_{14}H_{16}O_5$ 246.0892, Found 247.0975.

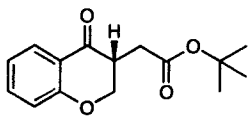

(*2R*)-(4-Oxo-chroman-3-yl)-acetic acid *tert*-butyl ester (65)

According to the general procedure, 9.0 mg (0.022 mmol) of **61** and 45.0 μL (0.022 mmol) of KHMDS and 30.0 mg (0.114 mmol) of **64** were reacted for 60 minutes. Work-up afforded 28.2 mg (94%) of the desired product as colorless oil. R_f (4:1 hexane to ethyl acetate) = 0.4; $[\alpha]_D^{23}$ = - 2.45 $CHCl_3$); HPLC analysis – Chiracel AD-H column 90:10 hexanes to isopropanol 1.0 mL/min. major enantiomer 5.64 minutes, minor enantiomer 5.96 minutes; ^1H NMR (400 MHz, $CDCl_3$) δ 7.86 (1H, m), 7.44 (1H, m), 6.99 (1H, m), 6.94 (1H, m), 4.54 (1H, dd, *J*= 5.3, 11.3 Hz), 4.26 (1H, dd, *J*= 11.5, 11.5 Hz), 3.25 (1H, dddd, *J*=4.9, 12.8, 17.0, 17.0 Hz), 2.82 (1H, dd, *J*= 4.7, 17.0 Hz), 2.35 (1H, dd, *J*= 8.5, 17.0 Hz), 1.25 (3H, t, *J*= 4.7, 16.8 Hz), 2.31 (1H, dd, *J*= 8.3, 16.8 Hz), 1.44 (9H, s); ^{13}C NMR (100 MHz, $CDCl_3$) δ 192.7, 170.5, 161.6, 135.9, 127.3, 121.4, 120.5, 117.7, 81.2, 70.2, 42.6, 31.5, 28.0; IR (NaCl, CH_2Cl_2) 1730, 1694, 1607, 1476 cm^{-1}; HRMS (FAB+) calcd for $C_{15}H_{18}O_4$ 262.1205, Found 263.1287.

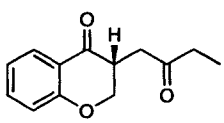

***(2R)*-(3-(2-Oxo-pentyl)-chroman-4-one (69)** According to the general procedure, 9.0 mg (0.019 mmol) of **61**and 37.0 μL (0.019 mmol) of KHMDS and 20.0 mg (0.0916 mmol) of **68** were reacted for 60 minutes. Work-up afforded 19.0 mg (94%) of the desired product as colorless oil. R_f (4:1 hexane to ethyl acetate) = 0.4; HPLC analysis – Chiracel AD-H column 90:1 hexanes to isopropanol 0.5 mL/min. Minor enantiomer: 18.62 minutes, Major enantiomer: 19.41 minutes; ^{1}H NMR (400 MHz, $CDCl_3$) δ 7.84 (1H, d, *J*= 7.6 Hz), 7.45 (1H, m), 6.99 (1H, dd, *J*= 7.5, 7.6 Hz), 6.94 (1H, d, *J*= 8.3 Hz), 4.51 (1H, dd, *J*= 5.3, 11.0 Hz), 4.21 (1H, dd, *J*= 11.5, 11.5 Hz), 3.40 (1H, dddd, *J*=4.9, 12.8, 17.0, 17.0 Hz), 2.99 (1H, dd, *J*= 4.6, 17.9 Hz), 2.61-2.41 (3H, m), 1.08 (3H, t, *J*= 7.2 Hz); ^{13}C NMR (100 MHz, $CDCl_3$) δ 208.3, 193.4, 161.7, 135.9, 127.2, 121.4, 120.5, 117.8, 70.2, 41.7, 37.6, 36.2, 7.7; IR (NaCl, CH_2Cl_2) 1715, 1687, 1605, 1437 cm^{-1}; HRMS (FAB+) calcd for $C_{13}H_{14}O_3$ 218.0943, Found 219.1026.

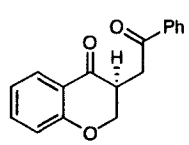

***(2S)*- 3-(2-Oxo-2-phenyl-ethyl)-chroman-4-one (71).** According to the general procedure, 14.0 mg (0.030 mmol) of **61** and 60.0 μL (0.030 mmol) of KHMDS and 40.0 mg (0.150 mmol) of **70** were reacted for 24 hours. Work-up afforded 37.2 mg (94%) of the desired product as colorless oil. R_f (1:1 hexane to ethyl acetate) = 0.7; $[\alpha]_D^{23}$ = -36.2 ($CHCl_3$); HPLC analysis – Chiracel OD-H column 90:10 hexanes to isopropanol 1.0 mL/min. Major enantiomer: 10.9 minutes, Minor enantiomer: 13.9 minutes; ^{1}H NMR (400 MHz, $CDCl_3$) δ 7.99-7.97 (2H, m), 7.88 (1H, m), 7.56 (1H, m), 7.49-7.44 (3H, m), 7.01 (1H, m), 6.97 (1H, m), 4.62 (1H, dd, *J*= 5.3, 11.1 Hz), 4.29 (1H, dd, *J*=11.3, 11.5 Hz), 3.69 (1H, dd, *J*= 3.8,

18.1 Hz), 3.58 (1H, dddd, *J*= 3.8, 5.3, 8.5, 11.9 Hz); ^{13}C NMR (100 MHz, $CDCl_3$) δ 197.2, 193.6, 162.0, 136.6, 136.2, 133.6, 128.9, 128.3, 127.6, 121.6, 120.8, 118.0, 70.6, 42.0, 34.5; IR (NaCl, CH_2Cl_2) 1680, 1607, 1483 cm^{-1}; HRMS (FAB+) calcd for $C_{17}H_{14}O_3$ 266.0943, Found 267.1028.

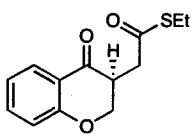

(*2S*)-(4-Oxo-chroman-3-yl)-thioacetic acid *S*-ethyl ester (73). According to the general procedure, 15 mg (0.032 mmol) of **61** and 65.0 μL (0.032 mmol) of KHMDS and 30.0 mg (0.159 mmol) of **72** were reacted for 2 hours. Work-up afforded 27.0 mg (90%) of the desired product as colorless oil. R_f (1:1 hexane to ethyl acetate) = 0.7; $[\alpha]_D^{23}$ = + 1.25 ($CHCl_3$); HPLC analysis–Chiracel AD-H column 90:1 hexanes to isopropanol 1.0 mL/min. Minor enantiomer: 8.1 minutes, Major enantiomer: 9.0 minutes; ^1H NMR (400 MHz, $CDCl_3$) δ 7.88 (1H, m), 7.47 (1H, m), 7.04-6.95 (2H, m), 4.58 (1H, dd, *J*= 5.1, 11.3 Hz), 4.25 (1H, dd, *J*=11.3, 11.3 Hz), 3.38 (1H, m), 3.21 (1H, dd, *J*= 4.4, 16.5 Hz), 2.92 (2H, q, *J*= 7.3 Hz), 2.64 (1H, dd, *J*= 8.8, 16.1 Hz), 1.27 (3H, t, *J*=7.3 Hz); ^{13}C NMR (100 MHz, $CDCl_3$) δ 196.8, 192.0, 161.5, 135.9, 127.3, 121.4, 120.3, 117.7, 70.0, 42.7, 39.4, 23.6, 14.7; IR (NaCl, CH_2Cl_2) 1680, 1607, 1476 cm^{-1}; HRMS (FAB+) calcd for $C_{13}H_{14}O_3S$ 250.0664, Found 251.0730.

(73)

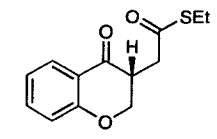

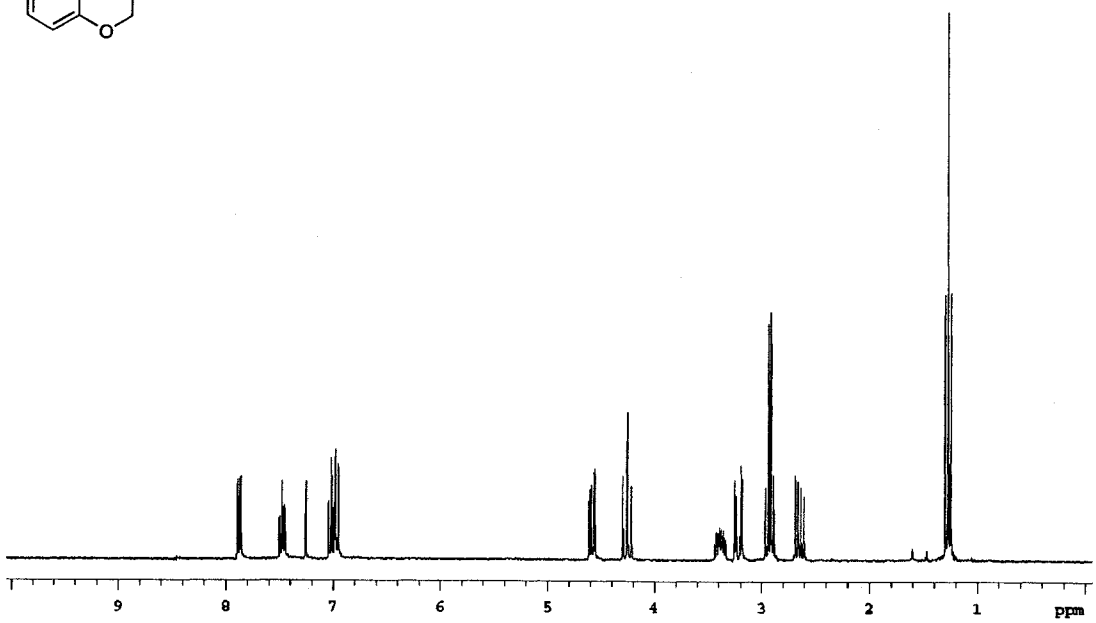

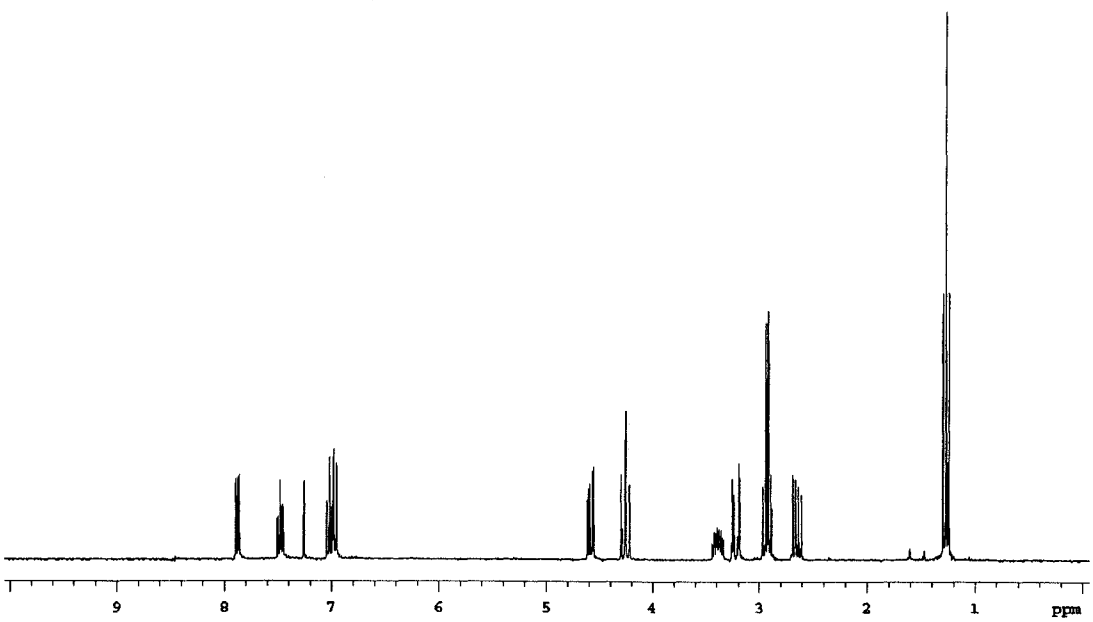

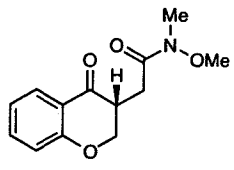

***(2R)*-(*N*-Methoxy-*N*-methyl-2-(4-oxo-chroman-3-yl)-acetamide (75).** According to the general procedure, 18.7 mg (0.040 mmol) of **61** and 80.0 μL (0.040 mmol) of KHMDS and 50.0 mg (0.200 mmol) of **74** were reacted for 8 hours. Work-up afforded 47.0 mg (94%) of the desired product as colorless oil. R_f (1:1 hexane to ethyl acetate) = 0.3; $[\alpha]_D^{23}$ = -12.9° ($CHCl_3$); GC analysis–Chiraldex AD-H column 90:1 hexanes to isopropanol 1.0 mL/min. Major enantiomer: 16.0 minutes, Minor enantiomer: 19.8 minutes;; ^1H NMR (400 MHz, $CDCl_3$) δ 9.86 (1H, s), 7.86 (1H, m), 7.46 (1H, m), 7.10 (1H, m), 6.95 (1H, m), 4.53 (1H, dd, *J*= 5.3, 11.3 Hz), 4.22 (1H, dd, *J*= 11.5, 11.7 Hz), 3.43 (1H, dddd, *J*= 5.1, 7.0, 12.4, 12.4 Hz), 3.06 (1H, dd, *J*=5.1, 18.5 Hz), 2.53 (1H, dd, *J*= 7.2, 18.5 Hz); ^{13}C NMR (100 MHz, $CDCl_3$) δ 193.5, 161.7, 135.8, 127.2, 121.3, 120.6, 117.7, 70.5, 61.2, 42.0, 32.2, 27.9; IR (NaCl, CH_2Cl_2) 1694, 1658, 1600, 1476 cm^{-1}. HRMS (FAB+) calcd for $C_{13}H_{15}NO_4$ 249.1001, Found 250.1067.

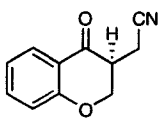

***(2S)*-(4-Oxo-chroman-3-yl)-acetonitrile (76).** According to the general procedure, 15.0 mg (0.032 mmol) of **61** and 64.0 μL (0.032 mmol) of KHMDS and 30.0 mg (0.160 mmol) of **75** were reacted for 24 hours. Work-up afforded 24.0 mg (88%) of the desired product as colorless oil. R_f (1:1 hexane to ethyl acetate) = 0.7; $[\alpha]_D^{23}$ = +7.0 ($CHCl_3$); HPLC analysis–Chiracel ADH column 90:1 hexanes to isopropanol 1.0 mL/min. Minor enantiomer: 14.8 minutes, Major

enantiomer: 15.6 minutes; ^{1}H NMR (400 MHz, $CDCl_3$) δ 7.87 (1H, m), 7.50 (1H, m), 7.04 (1H, m), 6.98(1H, m), 4.72 (1H, dd, *J*= 5.1, 11.5 Hz), 4.32 (1H, dd, *J*=11.5, 11.7 Hz), 3.17 (1H, dddd, *J*= 4.9, 9.4, 13.8, 13.8 Hz), 2.97 (1H, dd, *J*= 4.7, 17.5 Hz), 2.58 (1H, dd, *J*= 9.2, 17.5 Hz); ^{13}C NMR (100 MHz, $CDCl_3$) δ 190.0, 161.6, 136.7, 127.4, 122.0, 119.8, 118.0, 117.0, 69.4, 42.0, 14.1; IR (NaCl, CH_2Cl_2) 2247, 1687, 1607, 1287 cm^{-1}; HRMS (FAB+) calcd for $C_{11}H_9NO_2$ 187.0633, Found 188.0719.

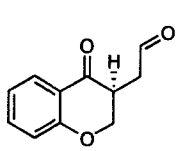

***(2S)*-(4-Oxo-chroman-3-yl)-acetaldehyde (78).** According to the general procedure, 20.0 mg (0.042 mmol) of **61** and 84.0 μL (0.042 mmol) of KHMDS and 40.0 mg (0.210 mmol) of **77** were reacted for 24 hours. Work-up afforded 20.0 mg (50%) of the desired product as colorless oil. R_f (1:1 hexane to ethyl acetate) = 0.7; HPLC analysis – Chiracel AD-H column 90:10 hexanes to isopropanol 1.0 mL/min. Major enantiomer: 12.0 minutes. Minor enantiomer: 12.7 minutes; ^{1}H NMR (400 MHz, $CDCl_3$) δ 9.86 (1H, s), 7.86 (1H, m), 7.46 (1H, m), 7.10 (1H, m), 6.95 (1H, m), 4.53 (1H, dd, *J*= 5.3, 11.3 Hz), 4.22 (1H, dd, *J*= 11.5, 11.7 Hz), 3.43 (1H, dddd, *J*= 5.1, 7.0, 12.4, 12.4 Hz), 3.06 (1H, dd, *J*=5.1, 18.5 Hz), 2.53 (1H, dd, *J*= 7.2, 18.5 Hz); ^{13}C NMR (100 MHz, $CDCl_3$) δ, 14.4; IR (NaCl, CH_2Cl_2) 1726, 1690, 1600, 1474 cm^{-1}.

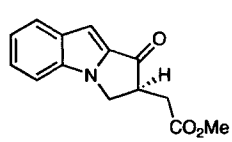

(*S*)-(1-Oxo-2,3-dihydro-1*H*-3a-aza-cyclopenta[*a*]inden-2-yl)-acetic acid methyl ester (80). According to the general procedure, 14.0 mg (0.038 mmol) of **79** and 77.0 μL (0.038 mmol) of KHMDS and 47.0 mg (0.192 mmol) of **40** were reacted for 24 hours. Work-up afforded 37.5 mg

(80%) of the desired product as colorless oil. R_f (1:1 hexane to ethyl acetate) = 0.4; $[\alpha]_D^{23}$ = -148.7 ($CHCl_3$); GC analysis– Chiraldex AD-H 90:1 hexanes to isopropanol 0.5 mL/min. Minor enantiomer: 28.34 minutes, Major enantiomer: 33.18 minutes; ^1H NMR (400 MHz), δ 7.72 (1H, d, *J*= 8.9 Hz), 6.35 (1H, d, *J*= 8.5 Hz), 6.07 (1H, s), 4.50 (1H, dd, *J*= 5.0, 10.9 Hz), 4.2 (1H, dd, *J*= 11.0, 11.0 Hz), 4.15 (2H, q, *J*= 7.2 Hz), 3.36 (4H, q, *J*= 7.2 Hz), 3.18 (1H, m), 2.91 (1H, dd, *J*= 4.5, 16.8 Hz), 2.33 (1H, dd, *J*=4.5, 16.8 Hz), 1.25 (3H, t, *J*= 7.2 Hz), 1.17 (6H, t, *J*= 7.2 Hz); ^{13}C NMR (100 MHz, $CDCl_3$) δ 190.1, 171.8, 163.5, 129.2, 106.7, 70.3, 60.7, 45.0, 41.9, 30.7, 14.1, 12.4; IR (NaCl, CH_2Cl_2) 1731, 1704, 1539, 1315; HRMS (FAB+) calcd for $C_{14}H_{13}NO_3$ 243.0895. Found 244.0973.

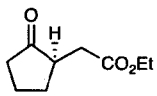

(2*R*)-(2-Oxo-cyclopentyl)-acetic acid ethyl ester (82): According to the general procedure, 10.0 mg (0.028 mmol) of **38** and 57.0 μL (0.028 mmol) of KHMDS and 24.0 mg (0.140 mmol) of **81** were reacted for1 hour. Upon work-up 19 mg (90%) of desired ester was isolated as a colorless oil: Spectral data matched literature description;[1] Gas chromatography analysis - B-DM column with constant 110 °C oven temperature. Major enantiomer 19.6 minutes, minor enantiomer, 20.5 min. $[\alpha]_D^{23}$ = -96.0 ($CHCl_3$).

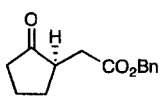

(2*R*)-(2-Oxo-cyclopentyl)-acetic acid benzyl ester (84): According to the general procedure, 15.6 mg (0.043 mmol) of **38** and 86.0 μL (0.043 mmol) of KHMDS and 50.0 mg (0.215 mmol) of **83** were reacted for 24 hours. Work-up afforded 42.2 mg (85%) of the desired product as colorless oil. R_f (1:1

hexane to ethyl acetate) = 0.7; $[\alpha]_D^{23}$ = -96.0 ($CHCl_3$); HPLC analysis–Chiracel AD-H column 90:10 hexanes to isopropanol 0.5 mL/min. Major enantiomer: 16.09 minutes. Minor enantiomer: 18.09 minutes; ^{1}H NMR (400 MHz, $CDCl_3$) δ 7.36-7.23 (5H, m), 5.09 (2H, s), 2.76 (1H, ddd, *J*= 7.6, 19.6, 22.1 Hz), 2.48-2.42 (2H, m), 2.35-2.22 (2H, m), 2.12 (1H, m), 2.01 (1H, m), 1.76 (1H, m), 1.58 (1H, m); ^{13}C NMR (100 MHz, $CDCl_3$) δ219.1, 171.9, 135.6, 128.5, 128.2, 128.1, 66.4, 45.5, 37.3, 33.8, 29.2, 20.5; IR (NaCl, CH_2Cl_2) 1730, 1454, 1265 cm^{-1}; HRMS (FAB+) calcd for $C_{14}H_{16}O_3$ 232.1099, Found 233.1178.

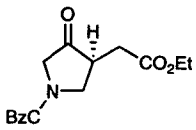

(2*S*)-(3-Ethoxycarbonylmethyl-4-oxo-pyrrolidine-1-carboxylic acid benzyl ester (88): According to the general procedure, 12.0 mg (0.032 mmol) of **38** and 65.0 μL (0.032 mmol) of KHMDS and 50.0 mg (0.164 mmol) of **87** were reacted for 24 hours. Work-up afforded 40.0 mg (80%) of the desired product as colorless oil. R_f (1:1 hexane to ethyl acetate) = 0.5; $[\alpha]_D^{23}$ = + 23.1 $CHCl_3$); ^{1}H NMR (400 MHz, $CDCl_3$) δ 7.36-7.23 (5H, m), 5.09 (2H, s), 2.76 (1H, ddd, *J*= 7.6, 19.6, 22.1 Hz), 2.48-2.42 (2H, m), 2.35-2.22 (2H, m), 2.12 (1H, m), 2.01 (1H, m), 1.76 (1H, m), 1.58 (1H, m); ^{13}C NMR (100 MHz, $CDCl_3$) δ219.1, 171.9, 135.6, 128.5, 128.2, 128.1, 66.4, 45.5, 37.3, 33.8, 29.2, 20.5; IR (NaCl, CH_2Cl_2) 1760, 1709, 1418 cm^{-1}; HRMS (FAB+) calcd for $C_{16}H_{19}NO_5$ 305.1263, Found 306.1333.

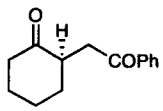

(2*R*)- 2-(2-Oxo-2-phenyl-ethyl)-cyclohexanone (94): According to the general procedure, 17.0 mg (0.046 mmol) of **38** and 92.0 μL (0.046

mmol) of KHMDS and 50.0 mg (0.231 mmol) of **93** were reacted for 24 hours. Work-up afforded 30.0 mg (60%) of the desired product as colorless oil. R_f (4:1 hexane to ethyl acetate) = 0.4; $[\alpha]_D^{23}$ = -24.3 $CHCl_3$); HPLC analysis-Chiracel OD-H column 95:5 hexanes to isoproponal 0.5 ml/min. Major enantiomer: 10.94 minutes, Minor enantiomer: 13.97 minutes; ^{1}H NMR (400 MHz, $CDCl_3$) δ 7.96 (2H,m), 7.53 (1H, m), 7.43 (2H, m), 3.75 (1H, dd, *J*= 6.6, 17.7 Hz), 3.14 (1H, dddd, *J*= 5.9, 12.1, 12.1, 18.5 Hz), 2.65 (1H, dd, *J*= 5.8, 17.7 Hz), 2.43-2.39 (2H, m), 2.20-2.08 (2H, m), 1.89-1.60 (3H, m), 1.42 (1H, m); ^{13}C NMR (100 MHz, $CDCl_3$) δ 211.5, 198.6, 136.9, 132.9, 128.4, 128.0, 46.4, 41.9, 38.3, 34.2, 27.9, 25.3; IR (NaCl, CH_2Cl_2) 1712, 1684, 1441 cm^{-1}; HRMS (FAB+) calcd for $C_{14}H_{16}O_2$ 216.1150, Found 217.1226.

(94)

xxx-350

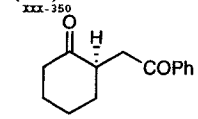

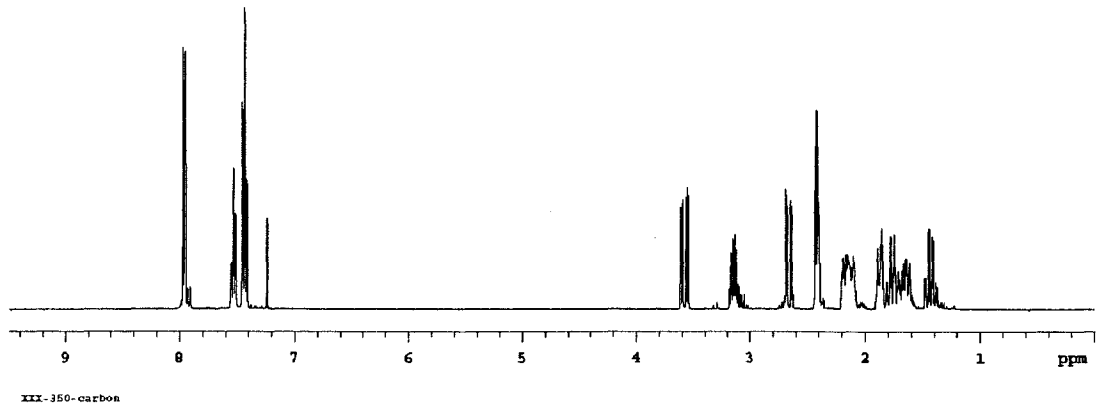

xxx-350-carbon

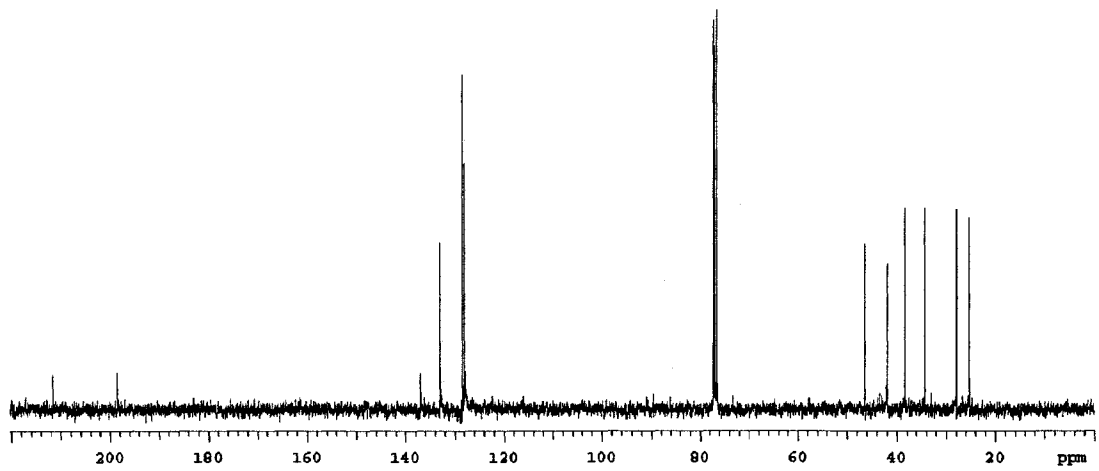

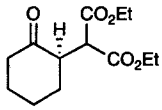

(*2R*)-*2*-(2-Oxo-cyclohexyl)-malonic acid diethyl ester (96): According to the general procedure, 14.1 mg (0.039 mmol) of **38** and 78.0 μL (0.039 mmol) of KHMDS and 50.0 mg (0.195 mmol) of **96** were reacted for 24 hours. Work-up afforded 49.0 mg (97%) of the desired product as colorless oil. R_f (4:1 hexane to ethyl acetate) = 0.4; $[\alpha]_D^{23}$ = -41.8 $CHCl_3$); ^1H NMR (400 MHz, $CDCl_3$) δ 4.16 (4H, dq, *J*= 2.3, 7.2 Hz), 3.61 (1H, d, *J*= 9.6 Hz), 3.16 (1H, ddd, *J*=5.5, 9.6, 13.2 Hz), 2.41-2.37 (2H, m), 2.11-1.99 (2H, m), 1.88 (1H, m), 1.74-1.46 (3H, m), 1.23 (6H, dt, *J*=2.5, 7.2 Hz); ^{13}C NMR (100 MHz, $CDCl_3$) δ 209.7, 168.5, 168.3, 61.4, 52.2, 50.2, 41.8, 31.1, 27.7, 25.0, 14.0, 13.9; IR (NaCl, CH_2Cl_2) 1750, 1728, 1452 cm^{-1}; HRMS (FAB+) calcd for $C_{13}H_{20}O_5$ 256.1311, Found 257.1399.

General procedure for the asymmetric intramolecular Stetter reaction of α,α-disubstituted Michael acceptors: A flame dried round bottom flask was charged with triazolium salt (0.2 eq) and 2 mL of toluene. To this solution was added KHMDS (0.5 M in toluene) (0.2 eq) via syringe and the solution was stirred at ambient temperature for 5 minutes. Toluene and HMDS was removed *in vacuo* by being placed under high vacuum for 1 hour.[5] Toluene (3 mL) was added followed by a solution of the substrate (1 eq 0.12 mmol) in 2 mL of toluene and the resulting solution was allowed to stir at ambient temperature for 24 hours. The reaction was quenched with 15% AcOH/toluene (2 mL) and the resulting solution was purified by

flash column chromatography and eluted with a suitable solution of hexane and ethyl acetate (typically 6:1). Evaporation of solvent afforded analytically pure product.

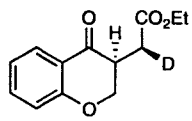

***(2S, 3'R)*-(4-Oxo-chroman-3-yl-deuterio)-acetic acid ethyl ester (97).** According to the general procedure, 13.0 mg (0.031 mmol) of **38** and 61.0 μL (0.031 mmol) of KHMDS and 35.0 mg (0.148 mmol) of **96** were reacted for 24 hours. Work-up afforded 31.5 mg (90%) of the desired product as colorless oil in 90% ee and 9:1 dr. R_f (1:1 hexane to ethyl acetate) = 0.7; $[\alpha]_D^{23}$ = +5.27° ($CHCl_3$); HPLC analysis – Chiracel AD column 97:3 hexanes to isopropanol 0.5 mL/min. Minor enantiomer: 22.95 minutes. Major enantiomer: 32.22 minutes; ^1H NMR (400 MHz, $CDCl_3$) δ 7.86 (1H, d, *J*=7.9 Hz), 7.45 (1H, dd, *J*= 8.6, 8.6 Hz), 6.99 (1H, dd, *J*= 7.5, 7.5 Hz), 6.94 (1H, d, *J*= 8.3 Hz), 4.57 (1H, dd, *J*= 5.3, 11.1 Hz), 4.27 (1H, dd, *J*= 11.6, 11.6 Hz), 4.16 (2H, q, *J*= 7.0 Hz), 3.3 (1H, m), 2.90 (0.2H, dd, *J*=4.8, 16.9 Hz), 2.38 (1H, m), 1.25 (3H, t, *J*= 7.0 Hz); ^{13}C NMR (100 MHz, $CDCl_3$) δ 192.8, 171.6, 161.9, 136.2, 127.6, 121.7, 120.7, 116.0, 70.4, 61.2, 42.6, 30.2 (t, *J*= 20.1 Hz), 14.4; IR (NaCl, CH_2Cl_2) 1738, 1694, 1600 cm^{-1}; HRMS (FAB+) calcd for $C_{13}H_{13}DO_4$ 235.0954, Found 236.1034.

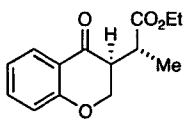

***(2R, 3'S)*-(4-Oxo-chroman-3-yl)-propionic acid ethyl ester (101).** According to the general procedure, 13.0 mg (0.031 mmol) of **39** and 61.0 μL (0.031 mmol) of KHMDS and 38.0 mg (0.153 mmol) of **100** were reacted for 24 hours. Work-up afforded 35.7 mg (94%) of the desired product as colorless oil in 95% ee and 30:1 dr. R_f (1:1 hexane to ethyl acetate) = 0.7; $[\alpha]_D^{23}$ = +7.85° ($CHCl_3$);

HPLC analysis – Chiracel OB-H column 97:3 hexanes to isopropanol 0.3 mL/min. Minor enantiomer: 98.1 minutes. Major enantiomer: 54.9 minutes; GC analysis – CP Wax 52CB column 130 °C at 3 ml/min. Minor diastereomer: 16.7 minutes, Major diastereomer: 19.0 minutes; ^{1}H NMR (400 MHz, $CDCl_3$) δ 7.86 (1H, d, *J*=7.9 Hz), 7.45 (1H, m), 6.99 (1H, m), 6.94 (1H, d, *J*= 8.3 Hz), 4.59 (1H, dd, *J*= 5.3, 11.3 Hz), 4.34 (1H, dd, *J*= 11.7, 11.7 Hz), 4.16 (2H, q, *J*= 7.0 Hz), 3.26 (1H, ddd, *J*= 5.3, 5.3, 12.2 Hz), 3.10 (1H, dq, *J*= 6.0, 7.1 Hz), 1.25 (3H, t, *J*=7.1 Hz), 1.2 (3H, d, *J*=7.2 Hz); ^{13}C NMR (100 MHz, $CDCl_3$) δ 192.6, 174.9, 161.8, 136.1, 127.6, 121.7, 122.2, 117.9, 68.7, 61.1, 47.8, 36.6, 14.4, 13.7; IR (NaCl, CH_2Cl_2) 1723, 1701, 1600 cm^{-1}; HRMS (FAB+) calcd for $C_{14}H_{16}O_4$ 248.1049, Found 249.1119.

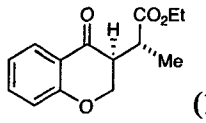

(101)

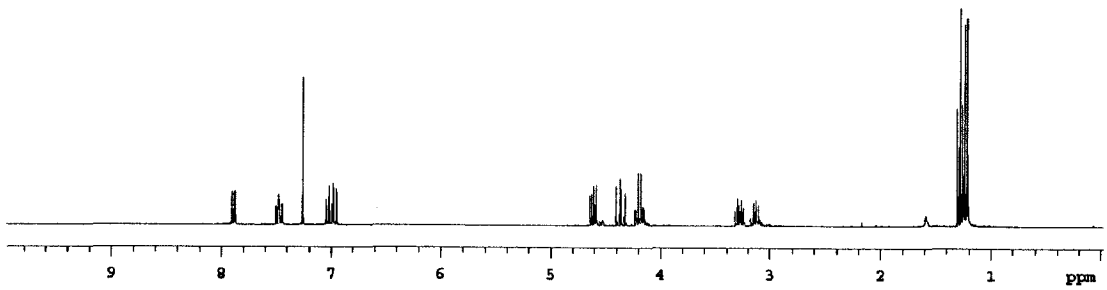

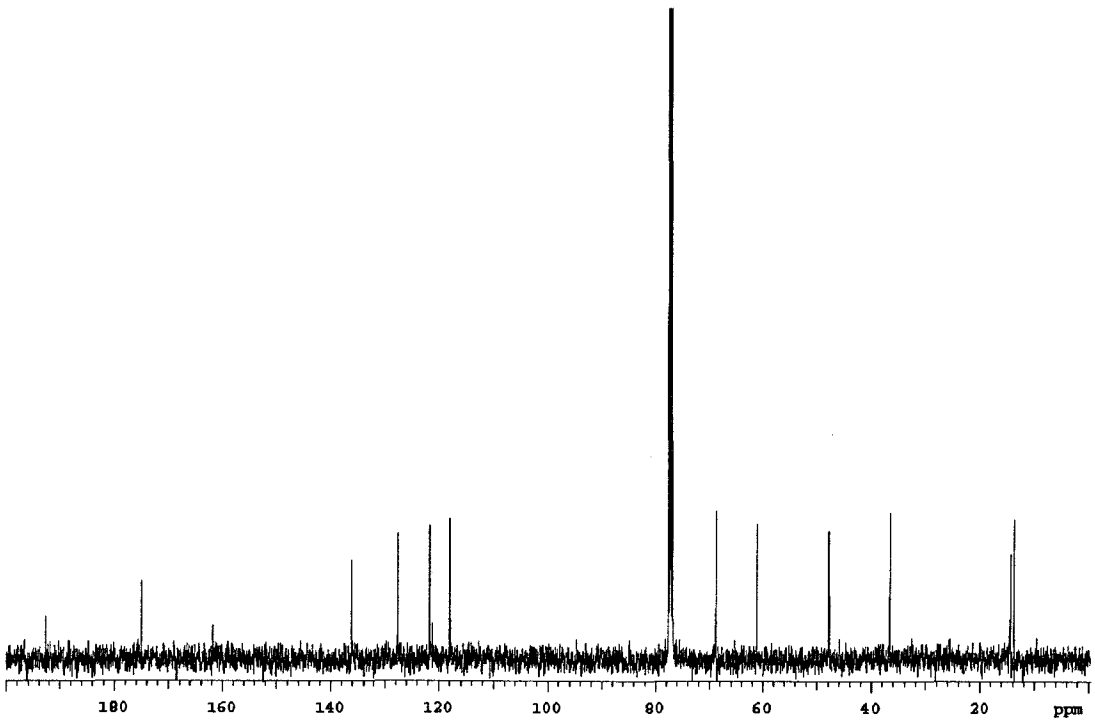

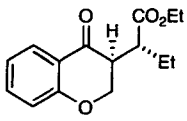

***(2R, 3'S)*-(4-Oxo-chroman-3-yl)-butyric acid ethyl ester (103).** According to the general procedure, 10.0 mg (0.023 mmol) of **39** and 46.0 μL (0.023 mmol) of KHMDS and 30.0 mg (0.116 mmol) of **102** were reacted for 24 hours. Work-up afforded 28.2 mg (94%) of the desired product as colorless oil in 92% ee and 35:1 dr. R_f (1:1 hexane to ethyl acetate) = 0.7; $[\alpha]_D^{23}$ = + 8.0° ($CHCl_3$); HPLC analysis – Chiracel AS column 95:5 hexanes to isopropanol 0.5 mL/min. Minor enantiomer: 12.7 minutes. Major enantiomer: 13.6 minutes; GC analysis – CP Wax 52CB column 130°C at 3ml/min. Major diastereomer: 26.5 minutes, Minor diastereomer: 23.2 minutes; ^{1}H NMR (400 MHz, $CDCl_3$) δ 7.85 (1H, d, *J*=7.9 Hz), 7.44 (1H, m), 6.99 (1H, m), 6.92 (1H, d, *J*= 8.3 Hz), 4.49 (1H, dd, *J*= 5.1, 11.5 Hz), 4.32 (1H, dd, *J*=11.5, 11.5 Hz), 4.16 (2H, q, *J*=7.0 Hz), 3.17 (1H, ddd, *J*= 5.1, 6.4, 11.7 Hz), 2.85 (1H, ddd, *J*= 4.7, 6.2, 10.3 Hz), 1.71-1.51 (2H, m), 1.24 (3H, t, *J*=7.1 Hz), 0.93 (3H, t, *J*=7.4 Hz); ^{13}C NMR (100 MHz, $CDCl_3$) δ 192.6, 174.4, 161.7, 136.1, 127.6, 121.7, 121.0, 117.9, 68.9, 60.9, 47.4, 43.9, 22.0, 14.4, 12.2; IR(NaCl, CH_2Cl_2) ;HRMS (FAB+) calcd for $C_{15}H_{18}O_4$ 262.1205, Found 263.1293.

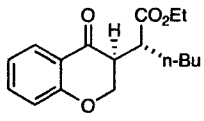

***(2R, 3'S)*-(4-Oxo-chromoan-3yl)-hexanoic acid ethyl ester (105).** According to the general procedure, 5.0 mg (0.012 mmol) of **39** and 23.0 μL (0.012 mmol) of KHMDS and 33.0 mg (0.116 mmol) of **104** were reacted for 12 hours. A second portion of a solution of **39** prepared according to the general procedure was added and the reaction was reacted for 12 additional hours. Work-up afforded 17.5 mg (53%) of the desired product as colorless oil in 94% ee and 12:1 dr. R_f (4:1 hexane to ethyl acetate) = 0.5; $[\alpha]_D^{23}$ = + 7.0° ($CHCl_3$); GC analysis–

Chiraldex B-DM 150°C at 3mL/min. Major enantiomer: 158.4 minutes, Minor enantiomer: 155.9 minutes; GC analysis– CP Wax 52CB column 130°C at 3ml/min. Major diastereomer: 60.3 minutes, Minor diastereomer: 53.1 minutes; ^{1}H NMR (400 MHz), δ 7.86 (1H, dd, *J*= 1.5, 7.9 Hz), 7.45 (1H, m), 6.99 (1H, m), 6.94 (1H, d, *J*= 8.1 Hz), 4.60 (1H, dd, *J*= 5.0, 11.4 Hz), 4.34 (1H, d, 11.5 Hz), 4.16 (2H, qq, *J*= 1.7, 7.1 Hz), 3.16 (1H, ddd, *J*= 5.1, 11.5, 5.1 Hz), 2.95 (1H, ddd, *J*=5.9, 10.2, 10.2 Hz), 1.34-1.28 (6H, m), 1.25 (3H, t, *J*=7.2 Hz), 0.87 (3H, m); ^{13}C NMR (100 MHz, $CDCl_3$) δ 192.5, 174.6, 161.8, 136.1, 127.6, 121.7, 121.0, 117.9, 68.9, 60.9, 47.7, 42.4, 29.9, 28.5, 22.7, 14.4, 14.1; IR (NaCl, CH_2Cl_2) 1730, 1688, 1600, 1457; HRMS (FAB+) calcd for $C_{17}H_{22}O_4$ 290.1518. Found 291.1590.

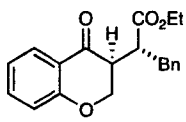

***(2R, 3'S)*-(4-Oxo-chromoan-3yl)-phenyl-propionic acid ethyl ester (107).** According to the general procedure, 10.0 mg (0.023 mmol) of **39** and 46.0 μL (0.023 mmol) of KHMDS and 37.0 mg (0.116 mmol) of **106** were reacted for 24 hours. Work-up afforded 30.0 mg (80%) of the desired product as colorless oil in 84% ee and 20:1 dr. R_f (1:1 hexane to ethyl acetate) = 0.6; $[\alpha]_D^{23}$ = + 39.5° ($CHCl_3$); HPLC analysis – Chiracel OJ column 90:10 hexanes to isopropanol 1.0 mL/min. Minor enantiomer: 13.83 minutes, Major enantiomer: 17.49 minutes; ^{1}H (400 MHz, $CDCl_3$) δ 7.89 (1H, dd, *J*=1.5, 7.9 Hz), 7.45 (1H, m), 7.27-7.18 (5H, m), 7.00 (1H, dd, *J*= 7.7, 7.7 Hz), 6.94, (1H, d, *J*= 8.4 Hz), 4.58 (1H, dd, *J*= 5.1, 11.5 Hz), 4.49 (1H, dd, *J*= 11.5, 15.4 Hz), 4.02 (2H, m), 3.19 (1H, m), 3.17 (1H, m), 3.00 (1H, m), 2.90 (1H, m), 1.07 (3H, t, *J*= 7.0 Hz); ^{13}C NMR (100 MHz, $CDCl_3$) δ 192.4, 174.8, 173.5, 161.8, 139.0, 136.2, 129.3, 129.2, 128.7, 127.6, 126.8, 122.8, 121.3,

117.9, 69.3, 61.0, 47.3, 45.1, 35.0, 14.2; IR (NaCl, CH_2Cl_2) 1730, 1687, 1607; HRMS (FAB+) calcd for $C_{20}H_{20}O_4$ 324.1362. Found 325.1439.

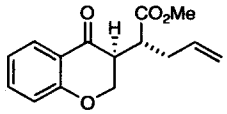

***(2R, 3'S)*-(4-Oxo-chroman-3-yl)-pent-4-enoic acid methyl ester (109).** According to the general procedure, 13.0 mg (0.030 mmol) of **39** and 61.0 μL (0.030 mmol) of KHMDS and 40.0 mg (0.154 mmol) of **108** were reacted for 24 hours. Work-up afforded 36.0 mg (90%) of the desired product as colorless oil in 83% ee and13:1 dr. R_f (1:1 hexane to ethyl acetate) = 0.6; $[\alpha]_D^{23}$ = + 40.4° ($CHCl_3$); HPLC anaylsis – Chiracel OD-H 97:3 hexanes to isopropanol 0.3 mL/min. Minor enantiomer: 17.4 minutes, Major enantiomer: 22.2 minutes; GC analysis – CP Wax 52CB column 130°C at 3ml/min. Major diastereomer: 27.3 minutes, Minor diastereomer: 24.3 minutes; ^1H (400 MHz, $CDCl_3$) δ 7.84 (1H, d, *J*=7.9 Hz), 7.44 (1H, m), 6.99 (1H, m), 6.93 (1H, d, *J*= 8.3 Hz), 5.73 (1H, dddd, *J*= 7.0, 10.2, 14.0, 17.2 Hz), 5.06 (2H, dd, *J*=17.0, 20.4), 4.59 (1H, dd, *J*= 5.1, 11.3) 4.37 (1H, dd, *J*=11.6, 11.6), 3.68 (3H, s), 3.21 (1H, ddd, *J*= 5.7, 11.7, 5.7), 3.0 (1H, m), 2.38 (1H, m); ^{13}C NMR (100 MHz, $CDCl_3$) δ 192.4, 174.1, 161.7, 136.1, 134.8, 127.6, 121.7, 121.0, 117.9, 68.9, 52.1, 46.9, 42.2, 33.3; IR (NaCl, CH_2Cl_2) 1731, 1690, 1603, 1480, 1209; HRMS (FAB+) calcd for $C_{15}H_{16}O_4$ 260.1049. Found 261.1138.

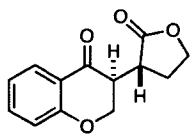

***(3R, 3'R)*-(2-Oxo-tetrahydro-furan-3yl)-chroman-4-one (121).** According to the general procedure, 10.0 mg (0.023 mmol) of **39** and 46.0 μL (0.023 mmol) of KHMDS and 27.0 mg (0.116 mmol) of **120** were reacted for

24 hours. Work-up afforded 25.6 mg (95%) of the desired product as a white solid in 94% ee and 10:1 dr. R_f (1:1 hexane to ethyl acetate) = 0.4; $[\alpha]_D^{23}$ = + 17.0° ($CHCl_3$); HPLC analysis – Chiracel OD-H column 90:10 hexanes to isopropanol 1.0 mL/minute Major enantiomer: 27.5 minutes, Minor enantiomer: 31.6 minutes; GC analysis – CP Wax 52CB column 130 °C at 3 ml/min. Minor diastereomer: 46.6 minutes, Major diastereomer: 49.9 minutes; ^{1}H (400 MHz, $CDCl_3$) δ 7.86 (1H, dd, *J*= 1.7, 7.9 Hz), 7.47 (1H, m), 7.01 (1H, m), 6.95 (1H, d, *J*= 8.3 Hz), 4.57-4.44 (3H, m), 4.25 (1H, ddd, *J*= 6.6, 9.8, 16.6 Hz), 3.42 (1H, ddd, *J*= 2.6, 6.4, 11.5 Hz), 3.19 (1H, ddd, *J*= 3.1, 9.1,11.9 Hz), 2.41 (1H, m), 2.25 (1H, m); ^{13}C NMR (100 MHz, $CDCl_3$) δ 192.4, 177.7, 161.9, 136.5, 127.5, 121.8, 121.0, 118.1, 68.6, 67.1, 45.3, 37.6, 25.9; IR (NaCl, CH_2Cl_2) 1760, 1680, 1600; HRMS (FAB+) calcd for $C_{13}H_{12}O_4$ 232.0736. Found 233.0819.

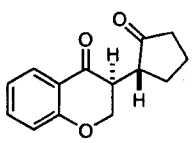

(*3R, 3'S*)-(2-Oxo-cyclopentyl)-chroman-4-one (123). According to the general procedure, 10.0 mg (0.023 mmol) of **39** and 46.0 μL (0.023 mmol) of KHMDS and 27.0 mg (0.115 mmol) of **122** were reacted for 24 hours. Work-up afforded 21.6 mg (80 %) of the desired product as a white solid in 95% ee and 18:1 dr. R_f (1:1 hexane to ethyl acetate) = 0.4; $[\alpha]_D^{23}$ = + 117° ($CHCl_3$); HPLC analysis – Chiracel AS column 95:5 hexanes to isopropanol 1 mL/min. Minor enantiomer: 13.5 minutes, Major enantiomer: 34.0 minutes; GC analysis – CP Wax 52CB column 130 °C at 3 ml/min. Minor diastereomer: 33.5 minutes, Major diastereomer: 32.6 minutes; ^{1}H NMR (400 MHz, $CDCl_3$) δ 7.86 (1H, dd, *J*= 1.5, 7.7 Hz), 7.46 (1H, m), 7.00 (1H, m), 6.95 (1H, d, *J*= 8.4 Hz), 4.52 (1H, dd, *J*= 10.9, 12.5

Hz), 4.39 (1H, dd, *J*=5.5, 10.9 Hz), 3.36 (1H, ddd, *J*= 2.6, 5.5 12.5 Hz), 2.65 (1H, m), 2.43-2.07 (4H, m), 1.94-1.78 (2H, m); ^{13}C NMR (100 MHz, $CDCl_3$) δ 219.3, 193.4, 161.8, 136.2, 127.5, 121.5, 121.2, 118.0, 69.2, 47.3, 45.6, 38.2, 27.1, 21.5; IR (NaCl, CH_2Cl_2) 1730, 1683, 1604; HRMS (FAB+) calcd for $C_{14}H_{14}O_3$ 230.094. Found 231.1009

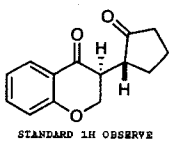

(123)

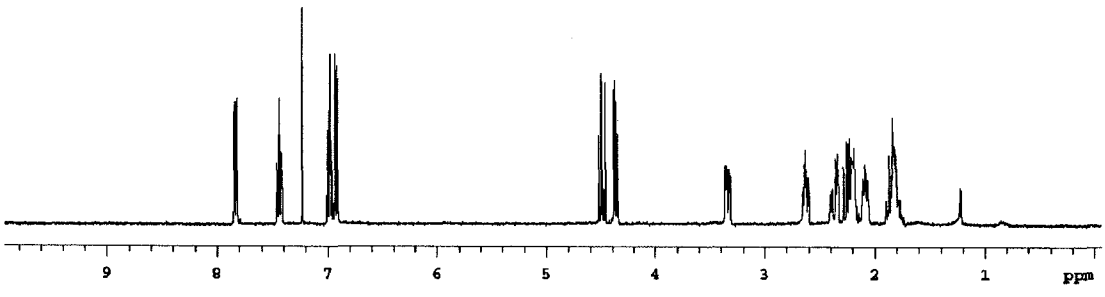

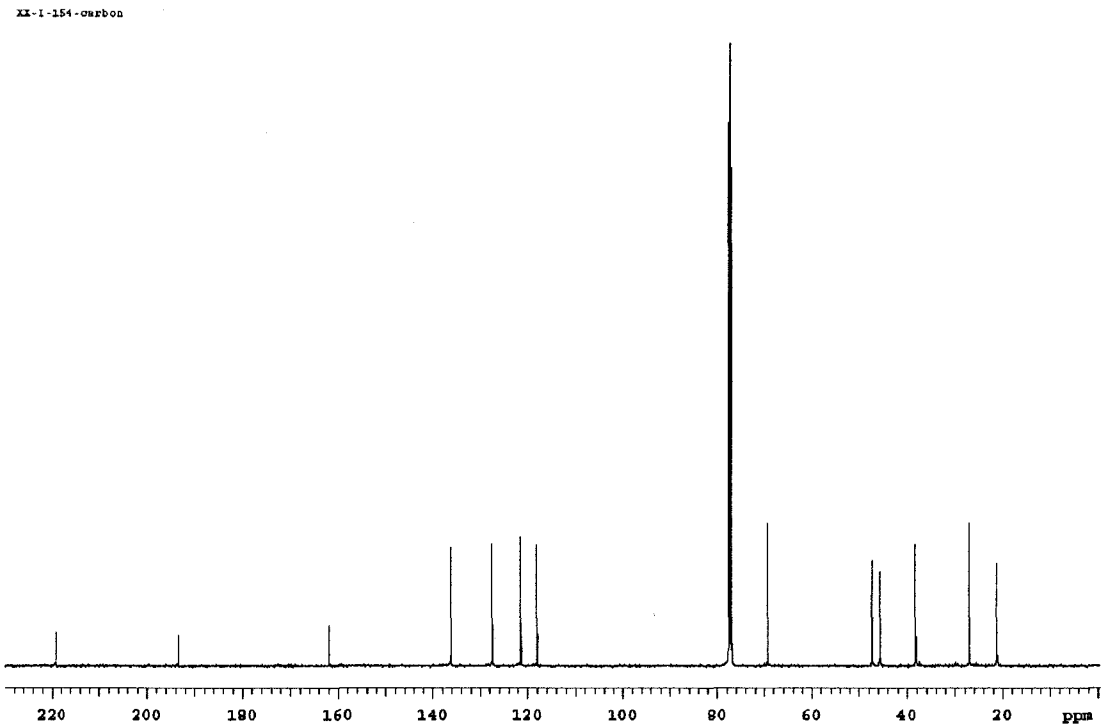

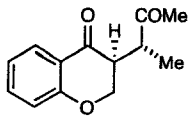

***(2R, 3'S)*-(1-Methyl-2-oxy-propy)-chroman-4-one (125).** According to the general procedure, 10.0 mg (0.023 mmol) of **39** and 46.0 μL (0.023 mmol) of KHMDS and 25.0 mg (0.116 mmol) of **124** were reacted for 24 hours. Work-up afforded 21.0 mg (85%) of the desired product as a white solid in 55% ee and 10:1 dr. R_f (1:1 hexane to ethyl acetate) = 0.4; $[\alpha]_D^{23}$ = -9.5° ($CHCl_3$); GC analysis – Chiraldex B-DM column 150 °C at 1.5 mL/min. Minor: 57.0 minutes, 58.0 minutes, Major: 75.0 minutes, 76.0 minutes; ^{1}H (400 MHz, $CDCl_3$) δ 7.82 (1H, dd, *J*= 1.6, 7.9 Hz), 7.45 (1H, m), 6.98 (1H, m), 6.94 (1H, d, *J*= 8.7 Hz), 4.58 (1H, dd, *J*= 5.4, 11.1 Hz), 4.22 (1H, dd, *J*= 11.1, 13.2 Hz), 3.37 (1H, ddd, *J*= 5.3, 6.9, 12.8 Hz), 3.07 (1H, dq, *J*= 7.2, 14.5 Hz), 2.31 (3H, s), 1.12 (3H, d, *J*= 7.3 Hz); ^{13}C NMR (100 MHz, $CDCl_3$) δ 210.2, 193.5, 174.8, 161.9, 136.2, 127.5, 121.6, 117.9, 68.8, 47.5, 43.1, 28.9, 13.3; IR (NaCl, CH_2Cl_2)1716, 1688, 1609; HRMS (FAB+) calcd for $C_{13}H_{14}O_3$ 218.0943. Found 219.1027.

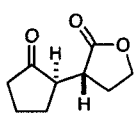

***(3R, 2'R)*-(2-Oxo-cyclopentyl)-dihydro-furan-2-one (127).**[6] According to the general procedure, 10.0 mg (0.023 mmol) of **39** and 46.0 μL (0.023 mmol) of KHMDS and 20.0 mg (0.116 mmol) of **126** were reacted for 24 hours. Work-up afforded 19.0 mg (94%) of the desired product as colorless oil in 99% ee and 50:1 dr. R_f (1:1 hexane to ethyl acetate) = 0.2; $[\alpha]_D^{23}$ = -104.4° ($CHCl_3$); GC analysis – Chiraldex B-DM column 150 °C at 3 mL/min. Major: 20.3 minutes, 24.23 minutes, Minor: 25.0 minutes, 26.7 minutes; ^{1}H (400 MHz, $CDCl_3$) δ 4.36 (1H, ddd, *J*= 1.9, 8.9, 10.8 Hz), 4.18 (1H, ddd, *J*= 6.6, 9.2, 10.3 Hz), 3.13 (1H, ddd, *J*= 3.2, 9.2, 11.9 Hz), 2.37 (1H, m), 2.26-2.13 (2H, m), 2.10-2.02 (3H, m), 1.84-1.69 (2H,m); ^{13}C

NMR (100 MHz, $CDCl_3$) δ 218.6, 178.6, 66.9, 49.0, 38.5, 37.9, 25.1, 24.7, 20.6; IR (NaCl, CH_2Cl_2) 1781, 1730; HRMS (FAB+) calcd for $C_9H_{12}O_3$ 168.0786. Found 169.0865.

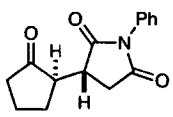

***(3R, 2'R)*-(2-Oxo-cyclopentyl)-1-phenyl-pyrrolidine-2,5-dione (129).** According to the general procedure, 15.0 mg (0.035 mmol) of **39** and 68.0 μL (0.035 mmol) of KHMDS and 44.0 mg (0.174 mmol) of **128** were reacted for 24 hours. Work-up afforded 35.0 mg (80%) of the desired product as white solid in 88% ee and 15:1 dr. R_f (ethyl acetate) = 0.5; $[\alpha]_D^{23}$ = -111.64° ($CHCl_3$); GC analysis – Chiraldex B-DM column 170 °C at 4 mL/min for 60 minutes then ramp to 180°C over 15 minutes, Major enantiomer: 123.2 minutes, Minor enantiomer: 128.2 minutes. GC analysis – CP Wax 52CB column 130°C at 3ml/min. Minor diastereomer: 48.5 minutes, Major diastereomer: 38.3 minutes; ^{1}H (400 MHz, $CDCl_3$) δ 7.46-7.42 (2H, m), 7.36 (1H, m), 7.24-7.22 (2H, m) 3.43 (1H, ddd, *J*=3.2, 5.1, 9.4 Hz), 2.96 (1H, dd, *J*= 9.6, 18.3), 2.82 (1H, m), 2.56 (1H, dd, *J*=5.3, 23.6 Hz), 2.39 (1H, m), 2.22-2.04 (3H, m), 1.92-1.80 (2H, m); ^{13}C NMR (100 MHz, $CDCl_3$) δ 218.3, 178.2, 175.3, 131.9, 129.4, 128.9, 126.7, 50.3, 38.9, 37.9, 32.5, 25.5, 20.5; IR (NaCl, CH_2Cl_2) 1703, 1507, 1382, 1181; HRMS (FAB+) calcd for $C_{15}H_{15}NO_3$ 257.1052. Found 258.1122.

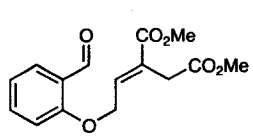

(E)-2-[2-(2-Formyl-phenoxy)-ethylidene]-succinic acid dimethyl ester (133). ^{1}H (400 MHz, $CDCl_3$) δ 10.48 (1H, s), 7.86 (1H, dd, *J*= 1.8, 7.7 Hz), 7.54 (1H, m), 7.17 (1H, t, *J*= 5.5 Hz), 7.07 (1H, dd, *J*=

7.7, 7.7 Hz), 6.95 (1 H, d, *J*=8.4 Hz), 4.87 (2H, d, *J*=5.5 Hz), 3.79 (3H, s), 3.70 (3H, s); R_f (1:1 hexane:ethyl acetate) = 0.7.

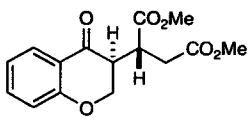

***(2R, 3'S)*-(4-Oxo-chroman-3-yl)-succinic acid dimethyl ester (134).** According to the general procedure, 10.0 mg (0.023 mmol) of **39** and 46.0 μL (0.023 mmol) of KHMDS and 34.0 mg (0.115 mmol) of **133** were reacted for 24 hours. Work-up afforded 27.0 mg (80%) of the desired product as oil in 92% ee and 42:1 dr. R_f (1:1 hexane:ethyl acetate) = 0.8; $[\alpha]_D^{23}$ = +48.5° ($CHCl_3$); HPLC analysis – Chiracel AS column 95:5 hexanes to isopropanol 0.5 mL/min. Major enatiomer: 45.9 minutes, Minor enantiomer: 43.3 minutes; GC analysis – CP Wax 52CB column 130 °C at 3 ml/min. Minor diastereomer: 71.0 minutes, Major diastereomer: 75.0 minutes; ^{1}H (400 MHz, $CDCl_3$) δ 7.84 (1H, dd, *J*=1.7, 7.9 Hz), 7.45 (1H, m), 6.99 (1H, m), 6.93 (1H, d, *J*=8.3 Hz), 4.54-4.43 (2H, m), 3.69 (3H, s), 3.66 (3H, s), 3.47 (1H, ddd, *J*=3.8, 5.3, 8.7 Hz), 3.24 (1H, ddd, *J*=3.6, 5.5, 11.7 Hz), 2.88 (1H, dd, *J*=8.7, 16.8 Hz), 2.58 (1H, dd, *J*= 5.3, 16.8 Hz); ^{13}C NMR (100 MHz, $CDCl_3$) δ 191.9, 173.1, 172.0, 161.6, 136.2, 127.3, 121.6, 120.8, 117.8, 69.0, 52.4, 47.0, 38.4, 33.1; IR (NaCl, CH_2Cl_2) 1730, 1687, 1600, 1483; HRMS (FAB+) calcd for $C_{15}H_{16}O_6$ 292.0947. Found 293.1015.

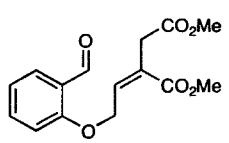

(Z)-2-[2-(2-Formyl-phenoxy)-ethylidene]-succinic acid dimethyl ester (135). ^{1}H (400 MHz, $CDCl_3$) δ 10.49 (1H, s),

7.83 (1H, dd, *J*= 1.8, 7.7 Hz), 7.52 (1H, m), 7.03 (1H, dd, *J*= 7.7, 7.7 Hz), 6.97 (1 H, d, *J*=8.4 Hz), 6.39 (1H, t, 4.5 Hz), 5.21 (2H, d, *J*=4.4 Hz), 3.78 (3H, s), 3.69 (3H, s); R_f (1:1 hexane:ethyl acetate) = 0.8.

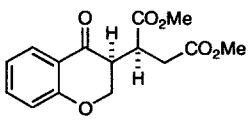

***(2S, 3'S)*-(4-Oxo-chroman-3-yl)-succinic acid dimethyl ester (136).** According to the general procedure, 10.0 mg (0.023 mmol) of **39** and 46.0 μL (0.023 mmol) of KHMDS and 34.0 mg (0.115 mmol) of **135** were reacted for 24 hours. Work-up afforded 23.8 mg (70%) of the desired product as oil in 38% ee and 1:6 dr. R_f (1:1 hexane:ethyl acetate) = 0.8; $[\alpha]_D^{23}$ = + 9.2° ($CHCl_3$); HPLC analysis – Chiracel AS column 95:5 hexanes to isopropanol 0.5 mL/min. Major enatiomer: 59.5 minutes, Minor enantiomer: 55.6 minutes; GC analysis – CP Wax 52CB column 130°C at 3ml/min. Minor diastereomer: 75.0 minutes, Major diastereomer: 71.5 minutes; ^{1}H (400 MHz, $CDCl_3$) δ 7.85 (1H, d, *J*=7.9 Hz), 7.46 (1H, m), 7.00 (1H, m), 6.94 (1H, d, *J*=9.2 Hz), 4.49 (1H, dd, *J*= 5.2, 11.2 Hz), 4.41 (1H, dd, *J*= 11.8, 22.9 Hz), 3.68 (3H, s), 3.65 (3H, s), 3.46 (1H, m), 3.17 (1H, ddd, *J*=*5.3*, 5.3, 10.0 Hz), 2.91 (1H, dd, *J*=8.6, 17.0 Hz), 2.52 (1H, dd, *J*= 5.5, 17.0 Hz); ^{13}C NMR (100 MHz, $CDCl_3$) δ 191.8, 172.8, 172.0, 161.4, 136.2, 127.5, 1201.7, 117.8, 68.8, 52.4, 46.9, 38.2, 33.3; IR (NaCl, CH_2Cl_2) 1735, 1681, 1600; HRMS (FAB+) calcd for $C_{15}H_{16}O_6$ 292.0947. Found 293.1015.

References

[1] Ciganek, E. *Synthesis* **1995**, 1311-1314.

[2] Kerr, M. S.; Read de Alaniz, J.; Rovis, T. *J. Org. Chem.* **2005**, *70*, 5725-5728.

[3] (a) Ciganek, E. *Synthesis* **1995**, 1311-1314. (b) Bjornestedt, R.; Zhong, G.; Lerner, R.; Barbas III, C. *J. Am. Chem. Soc.* **1996**, *118*,11720. (c) Claus, R.; Schreiber, S. *Organic Syntheses*, **1986**, *64*, 150.

[4] Enders, D.; Breuer, K. *Helv. Chim. Acta* **1996**, *79*, 1217-1221.

[5] A control experiment was run in the absence of KBF_4 salt and the enantio and diastereoselectivity of the reaction was not affected. The KBF_4 salt was removed by passing a solution of toluene containing the carbene and KBF_4 salt, which was prepared according to general procedure, through a Gelman 0.45 μm filter.

[6] Asselin, A. A.; Dionne, G.; Humber, L. G. U.S. Patent 79 64343, 1980; *American Home Products Corp.*, **1980**, 12.

Chapter 3

The Mechanism of the Intramolecular Stetter Reaction

General Methods. All reactions were performed under an atmosphere of argon in flame-dried glassware with magnetic stirring. Toluene was degassed with argon and passed through one column of neutral alumina and one column of Q5 reactant. Column chromatography was performed on EM Science silica gel 60 (230-400 mesh). Thin layer chromatography was performed on EM Science 0.25 mm silica gel 60-F plates. Visualization was accomplished with UV light, $KMnO_4$, and aqueous ceric ammonium molybdate dips followed by heating.

KHMDS was purchased from Aldrich Chemical Co. and 0.5 M solutions in toluene were prepared prior to each reaction. All other chemical were purchased from Aldrich Chemical Co. and used without further purification.

Infrared spectra were obtained on a Nicolet Avatar 320 FT-IR spectrometer. ^1H NMR and spectra were recorded on a Varian 400 MHz spectrometer at ambient temperature. Data are reported as follows: chemical shift in parts per million (δ ppm) from an internal [standard tetramethylsilane (TMS) or deuterated chloroform ($CDCl_3$)], multiplicity (s = singlet, d = doublet, t = triplet, q = quartet, and m = multiplet), integration, and coupling constant (Hz). ^{13}C NMR were recorded on a Varian 100 MHz spectrometer at ambient temperature. Chemical shifts are reported in ppm from ($CDCl_3$) taken as 77.0 ppm. Mass spectra were obtained on Fisons VG Autospec. Analytical high performance liquid chromatography (HPLC) was performed on a Dynamax model SD-200 HPLC equipped with a Dynamax model

UV-1 variable wavelength UV detector using a Chiracel OD-H (0.46 cm X 25 cm) chiral column. Optical rotations were measured on an Autopol III automatic polarimeter in a 1 dm cell.

Procedure for the preparation of starting materials 6 and 7: Deuteroaldehyde **6** was prepared according to literature precedent commencing from the commercially available salicylaldehyde **1** (scheme 1).

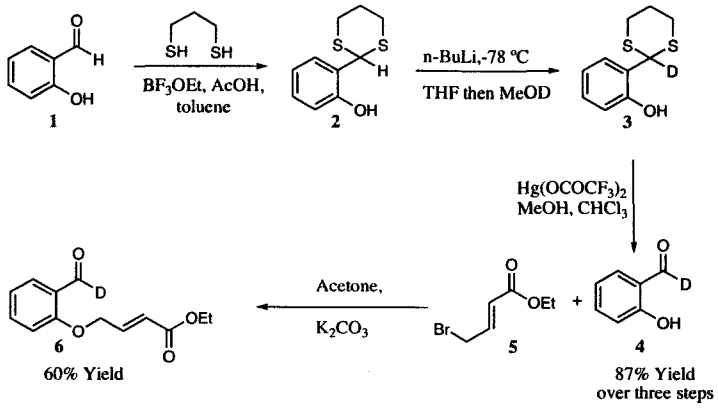

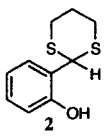

2-(2'-hydroxyphenyl)-1,3-dithiane (2). [1] $BF_3 \cdot OEt_2$ (12.8 mL, 89.6 mmol, 1.1 equiv) was added to a solution of salicylaldehyde **1** (10.00 g, 81.90 mmol), AcOH (80 mL), and 1,3-propanedithiol (9.00 mL, 89.6 mmol, 1.1 equiv) in toluene (160 mL), and the resulting mixture was stirred overnight at room temperature. The reaction mixture was diluted with Et_2O (200 mL) and quenched by addition of water, then the organic layer was washed with water (2x), $NaHCO_3$ solution (3x), and brine (2x). The organic solution was dried over $MgSO_4$ and concentrated *in vacuo* to give the crude product as an off-white solid that could be used without further purification. Spectral data matched literature data discribed. Yield: 17.00 g (98%).

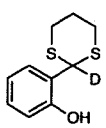

2-(2'-hydroxyphenyl)-1,3-dithiane (3).[2] A solution of dithiane **2** (2.18 g, 10.27 mmol) in anhydrous tetrahydrofuran (100 mL) was treated under argon at –60 to –75 °C with a solution of *n*-butyllithium in hexane (15.4 mL). After stirring at –78 °C for 1 hour the reaction was warmed to 0 °C for 5 minutes and then re-cooled to –78 °C. After stirring at –78 °C for 1 hour the solution was treated with 5 equivalents deuterated methanol (2 mL of MeOD, 51.35 mmol) and warmed to room temperature; 0.05 M hydrochloric acid was added and the tetrahydrofuran was removed in vacuo. The residue was shaken with 1:1 (v/v) dichlromethane-pentane; the organic phase was washed with $NaHCO_3$ solution (2x), water (2x) and brine. The organic solution was dried over $MgSO_4$ and concentrated *in vacuo* to give the desired product that could be used without further purification. Yield: 2.16 g (99%).

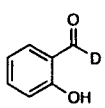

2-Hydroxy-benzaldehyde-1-*d* (4). A solution of **3** (0.5 g, 1.54 mmol) in chloroform (20 mL) and methanol (0.2 mL) was added mercury trifluoroacetate (0.982 g, 2.30 mmol, 1.5 equiv) and the resulting cloudy solution was stirred until reaction complete by TLC. After completion by TLC the reaction mixture was filtered and the resulting solution was concentrated *in vacuo*. The desired product was purified by flash column chromatography and eluted with a solution of hexane and ethyl acetate (4:1). Evaporation of solvent afforded analytically pure product. Yield: 0.25 g (90%).

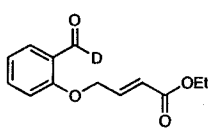

4-(2-Formyl-phenoxy)-but-2-enoic acid ethyl ester (6).[3] Ethyl 4-bromocrotonate (3.29 g, 17.05 mmol, 1.05 equiv) was added to a

mixture of **4** (2.00 g, 16.24 mmol), 3.36 g (24.36 mmol, 1.5 equiv) of K_2CO_3 in 30 mL of acetone. The reaction was stirred overnight and quenched with water and the organic layer was extracted with Et_2O. The organic layer was washed with 5% NaOH, water (2x) and brine (2x) and dried over $MgSO_4$ and concentrated *in vacuo*. The desired product was purified by flash column chromatography and eluted with a solution of hexane and ethyl acetate (4:1). Evaporation of solvent afforded analytically pure product. Yield: 1.2 g (60%). ^1H NMR (400 MHz, $CDCl_3$) δ 7.86 (1H, m), 7.54 (1H, m), 7.14-7.04 (2H, m), 6.94 (1H, m), 6.20 (1H, m), 4.83 (2H, dd, *J*= 1.8, 5.8 Hz), 4.22 (2H, q, *J*= 7.3 Hz), 1.30 (3H, t, *J*= 7.3 Hz); ^{13}C NMR (100 MHz, $CDCl_3$) δ 189.2, 165.7, 160.1, 141.1, 135.9, 128.7, 124.9, 122.4, 121.4, 112.4, 66.7, 60.7, 14.1; IR (NaCl, CH_2Cl_2) 1738, 1694, 1600 cm^{-1}; HRMS (FAB+) calcd for $C_{13}H_{13}DO_4$ 235.0954, Found 235.0941.

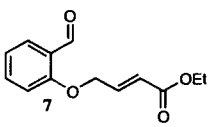

4-(2-Formyl-phenoxy)-but-2-enoic acid ethyl ester (6).[3] Ethyl 4-bromocrotonate (3.31 g, 17.19 mmol, 1.05 equiv) was added to a mixture of **4** (2.00 g, 16.37 mmol), 3.4 g (24.56 mmol, 1.5 equiv) of K_2CO_3 in 30 mL of acetone. The reaction was stirred overnight and quenched with water and the organic layer was extracted with Et_2O. The organic layer was washed with 5% NaOH, water (2x) and brine (2x) and dried over $MgSO_4$ and concentrated *in vacuo*. The desired product was purified by flash column chromatography and eluted with a solution of hexane and ethyl acetate (4:1). Evaporation of solvent afforded analytically pure product. Yield: 1.2 g (60%), spectral data match literature data described.

General procedure for the asymmetric intramolecular Stetter reaction on 10 mmol scale: A flame dried round bottom flask was charged with triazolium salt (0.102 g, 0.28 mmol, 0.03 equiv) and 500 mL of toluene. The solution was degassed for 15 minutes with argon bubbling through the toluene solution. To this solution was added 0.055 g of solid KHMDS (0.28 mmol, 0.03 equiv) and the solution was stirred at ambient temperature for 5 minutes with bubbling argon. Aldehyde **7** (2.2 g, 9.39 mmol) was added as solution in toluene (100 mL) via cannula and the resulting solution was allowed to stir at ambient temperature with bubbling argon. The reaction was monitored by TLC and ^{1}H NMR and quenched at ~80% completion with 15% AcOH in toluene (10 mL) and the reaction mixture was placed directly on the column. The desired product was purified by flash column chromatography and eluted with a solution of hexane and ethyl acetate (4:1 to 1:1). Evaporation of solvent afforded 1.83 g of analytically pure product and 0.365 g of analytically pure starting material that each matched literature description **7**.[3]

General procedure for the asymmetric intramolecular Stetter reaction monitored by ^{1}H NMR: A dry NMR tube was charged with triazolium salt (0.0105 g, 0.029 mmol, 0.20 equiv) and KHMDS (0.0057 g, 0.029 mmol, 0.02 equiv) in the glove box and 0.6 mL of toluene-D8 was added to the mixture. A ^{1}H NMR of the carbene was recorded at 10 °C. To this solution was added aldehyde **6** (0.034 g, 0.145 mmol) as solution in toluene-D8 (0.2 mL) pre-cooled to 10 °C. The resulting solution was shaken for 5 seconds then immediately placed in the NMR and data collection was commenced without further shimming.

General procedure for the asymmetric intramolecular Stetter reaction monitored by gas chromatography conducted in the box: A flame dried round bottom flask was charged with triazolium salt (0.0105 g, 0.029 mmol, 0.20 equiv) and 1 mL of toluene. The solution was degassed for 5 minutes with argon bubbling through the toluene solution. To this solution was added 60 μL of KHMDS (0.029 mmol, 0.02 equiv, 0.5 M solution in toluene prepared freshly prior to each reaction) and the resulting solution was stirred at ambient temperature for 5 minutes with bubbling argon, upon which the solvent was removed *in vacuo* for 30 minutes. The reaction vessel was sealed under vacuum and taken into the box upon which 5 mL of toluene was added and the resulting solution was stirred for 5 minutes at 25 °C. To this solution was added aldehyde **7** (0.034 g, 0.145 mmol) and di-*tert*-butyl-biphenyl **10** (0.0077 g, 0.029 mmol, 0.02 equiv) as solution in toluene (1mL). The resulting solution was stirred and 0.1 mL aliquots were taken at 1, 2, 4, 6, 8, 10, 15, 20, 25, 30, 35, 45, and 60 minutes. The aliquots were immediately worked up by passing through a small pipet column and the eluted with 100% ethyl acetate. GC-analysis was performed on a wax-cp column at 150 °C with 3 mL flow rate. GC analysis – CP Wax 52CB column 150 °C at 3ml/min. Product **9**: 2.1 minutes, Starting material **7**: 3.1 minutes, Standard **10**: 4.8 minutes.

General procedure for the asymmetric intramolecular Stetter reaction monitored by gas chromatography conducted on the bench top: A flame dried round bottom flask was charged with triazolium salt (0.0105 g, 0.029 mmol, 0.20 equiv) and 5 mL of toluene. The solution was degassed for 5 minutes with argon

bubbling through the toluene solution. To this solution was added 60 μL of KHMDS (0.029 mmol, 0.02 equiv, 0.5 M solution in toluene prepared freshly prior to each reaction) and the resulting solution was stirred at ambient temperature for 5 minutes with bubbling argon, upon which the solution was cooled to 0 °C over five minutes. To this solution was added aldehyde **7** (0.034 g, 0.145 mmol) and di-tertbutyl-di-phenyl **10** (0.0077 g, 0.029 mmol, 0.02 equiv) as solution in toluene (1mL) pre-cooled to 0 °C. The resulting solution was stirred at 0 °C under bubbling argon and 0.1 mL aliquots were taken at 1, 2, 4, 6, 8, 10, 15, 20, 25, 30, 35, 45, and 60 minutes. The aliquots were immediately worked up by passing through a small pipet column and the eluted with 100% ethyl acetate. GC analysis – CP Wax 52CB column 150 °C at 3ml/min. Product **9**: 2.1 minutes, Starting material **7**: 3.1 minutes, Standard **10**: 4.8 minutes.

References

[1] Macleod, C.; McKiernan, G. J.; Guthrie, E. J.; Farrugia, L. J.; Hamprecht, D. H.; Macritchie, J.; Hartley, R. C. *J. Org. Chem.* **2003**, *68*, 387-401.

[2] Seebach, D.; Erickson, B. W.; Singh, G. *J. Org. Chem.* **1966**, *31*, 4303-4304.

[3] Ciganek, E. *Synthesis* **1995**, 1311-1314.

Chapter 4

Developing New Catalytic Reactions Utilizing Triazolinylidene Carbenes

General Methods. All reactions were performed under an atmosphere of argon in flame-dried glassware with magnetic stirring. Toluene was degassed with argon and passed through one column of neutral alumina and one column of Q5 reactant. Column chromatography was performed on EM Science silica gel 60 (230-400 mesh). Thin layer chromatography was performed on EM Science 0.25 mm silica gel 60-F plates. Visualization was accomplished with UV light, $KMnO_4$, and aqueous ceric ammonium molybdate dips followed by heating.

KHMDS was purchased from Aldrich Chemical Co. and 0.5 M solutions in toluene were prepared prior to each reaction. All other chemical were purchased from Aldrich Chemical Co. and used without further purification.

Infrared spectra were obtained on a Nicolet Avatar 320 FT-IR spectrometer. ^1H NMR and spectra were recorded on a Varian 400 MHz spectrometer at ambient temperature. Data are reported as follows: chemical shift in parts per million (δ ppm) from an internal [standard tetramethylsilane (TMS) or deuterated chloroform ($CDCl_3$)], multiplicity (s = singlet, d = doublet, t = triplet, q = quartet, and m = multiplet), integration, and coupling constant (Hz). ^{13}C NMR were recorded on a Varian 100 MHz spectrometer at ambient temperature. Chemical shifts are reported in ppm from ($CDCl_3$) taken as 77.0 ppm. Mass spectra were obtained on Fisons VG Autospec. Analytical high performance liquid chromatography (HPLC) was performed on a Dynamax model SD-200 HPLC equipped with a Dynamax model UV-1 variable wavelength UV detector

using a Chiracel OD-H (0.46 cm X 25 cm) chiral column. Optical rotations were measured on an Autopol III automatic polarimeter in a 1 dm cell.

General procedure for the conversion of α-halo-aldehydes to esters. A flame-dried round-bottomed flask was charged with triazolium salt **9** (0.2 eq). Toluene triethylamine (1.0 eq), and alcohol (1.0 eq) were added via syringe and the solution was stirred at ambient temperature for 10minutes. α–Halo-aldehyde was then added via syringe and the reaction was stirred at room temperature for the time indicated. The reaction mixture was then subjected directly to column chromatography eluting with 4:1 hexane to ethyl acetate affording the pure product.

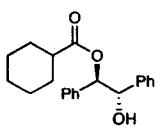

Cyclohexanecarboxylic acid 2-hydroxy 1,2-diphenyl-ethyl ester (17). According to the general procedure, 7.0 mg (0.023 mmol) of **9** in 2 mL of toluene was treated with 0.016 mL (0.117 mmol) of triethylamine and allowed to stir at ambient temperature. 14 mg (0.117 mmol) of **10** in 1 mL toluene was added via syringe and upon which 0.025 g (0.117 mmol) of **16** was added and the reaction was stirred for at 23 °C. The reaction was quenched by directly placing on a column and product was eluted with 4:1 hexane to ethyl acetate. Rf (4:1 hexane: ethyl acetate) = 0.5; $[\alpha]_D^{23}$ = + 5.8° ($CHCl_3$); HPLC analysis – Chiracel AD column 90:10 hexanes to isopropanol 0.5mL/min. Major: 23.3 minutes, Minor: 29.0 minutes; ^{1}H NMR (400 MHz, $CDCl_3$) δ 7.26 (10H, m), 5.87 (1H, d, J= 6.4 Hz), 4.93 (1H, d, J= 6.4 Hz), 2.24-2.10 (2H, m) 1.78-1.56 (5H, m) 1.30-1.11(5H, m); ^{13}C NMR (400 MHz, CDCl3) δ 174.9, 139.8, 137.1, 128.5, 128.5, 128.3, 127.8, 127.3, 78.5, 76.8, 43.4, 28.9, 28.9, 25.9, 25.5; IR (NaCl, CH_2Cl_2) 3480, 2929, 2854, 1727, 1445; HRMS (FAB+) calcd for $C_{21}H_{24}O_3$ 324.1725.

Found 324.1759.

General procedure for palladium π-allyl reactions. A flame-dried round-bottomed flask was charged with Pd_2dba_3 (0.039 mmol, 0.2 eq), dppe (0.079 mmol, 0.4 eq) and triazolium salt (0.039 mmol, 0.2 eq) in an inert atmosphere (N_2) glove box. Upon removal from the glove box, 1 to 2 mL of THF was added via syringe and the solution was stirred at ambient temperature for 5 minutes. To this solution was added the allyl carbonate as a solution in THF (1 mL) via syringe. The resulting solution was then brought to 50 °C and stirred overnight. Upon cooling to room temperature the reaction was worked-up by extraction with diethyl ether or directly placed on the column and eluted with hexane and ethyl acetate.

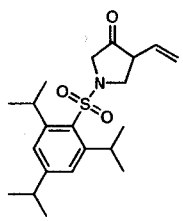

1-(2,4,6-Triisopropyl-benzenesulfonyl)-4-vinyl-pyrrolidin-3-one (33). According to the general procedure, 0.017 g (0.0186 mmol) of Pd_2dba_3, 0.015 g (0.0373 mmol) of dppe and 0.031 g (0.0186 mmol) of **32** was added 1 mL of THF. Followed by 0.047 g (0.1244 mmol) of **22**. Reaction cooled to ambient temperature and placed directly on the column and eluded with 2:1 hexane to ethyl acetate to afford 0.015 g (33%) of desired product **33**. Rf (2:1 hexane: ethyl acetate) = 0.85; HRMS (FAB+) calcd for $C_{21}H_{31}NO_3S$ 377.2025. Found 377.2026. ^1H NMR (400 MHz, $CDCl_3$) δ 7.70-7.68 (2H, m), 7.28-7.26 (2H, m), 6.87 (1H, d, J = 10.6 Hz), 3.84 (2H, q, J= 7.2 Hz) 3.27 (2H, s), 2.51 (1H, m), 2.39 (3H, s), 1.06 (3H, t, J = 7.2 Hz), 1.06 (6H, d, J= 6.6 Hz); ^{13}C NMR (400 MHz, CDCl3) δ 168.4, 150.8, 144.1, 136.1, 132.3, 129.6, 128.3, 61.1, 31.7, 28.8, 21.5, 21.5, 13.8.

Representative procedure for synthesis of chiral carbene-gold(I) complex.[1]

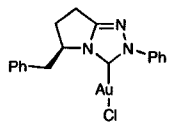

Triazolinylidene-gold(I) complex (44). 0.043 g (0.186 mmol) of silver(I) oxide was added round bottom flask charged with 0.1 g (0.321 mmol) of **42** in 10 mL of dichlormethane and the resulting solution was stirred for 4 hours. The mixture was filtered, and 0.115 g (0.389 mmol) of (dimethyl sulfide)gold(I) chloride was added and stirred for 3 h. The resulting mixture was filtered, and activated carbon was added to the filtrate and the mixture was then filtered over Celite, the solvent removed *in vacuo* to afford desired solid.

General procedure for the carbene-gold(I) catalyzed reactions. The gold reactions were conducted according to literature methods.[2]

General procedure for the conversion of *N*-tosylimines to nitriles. To a flame dried flask charged with azolium salt (0.2 eq) and 5 mL of benzene or toluene. To the solution was added 0.2 eq of base, followed by a solution of allenoate (1.1 eq) and *N*-tosylimine (1 eq) in 1 mL of benzene or toluene. The resulting solution was stirred at ambient temperature and solvent removed *in vacuo* and purified by column chromatography.

References

[1] Frémont, P.; Scott, N. M.; Stevens, E. D.; Nolan, S. P. *Organometallics* **2005**, *24*, 2411-2418.

[2] (a) Kennedy-Smith, J. J.; Staben, S.; Toste, D. F. *J. Am. Chem. Soc.* **2004**, *126*, 4526-4527. (b) Yang, C-G.; He, C. *J. Am. Chem. Soc.* **2005**, *127*, 6966-6967. (c) Yao, X.; Li, C-J. *J. Am. Chem. Soc.* **2004**, *126*, 6884-6885. (d) Johansson, M. J.; Gorin, D. J.; Staben, S. T.; Toste, D. F. *J. Am. Chem. Soc.* **2005**, *127*, 18002-18003.

Appendix 1:

Chapter 1 Crystal Structure Data for 28

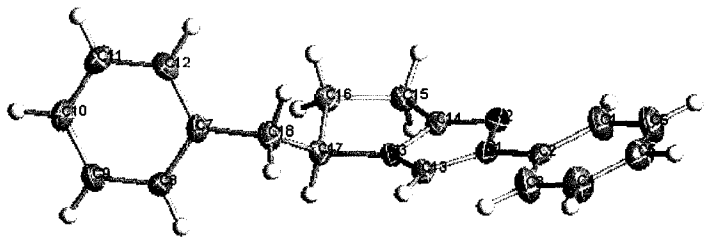

Table 1. Crystal data and structure refinement for **28**.

Identification code	rovis2m	
Empirical formula	C12 H13.33 Cl0.67 N2 O0.67	
Formula weight	219.88	
Temperature	173(2) K	
Wavelength	0.71073 Å	
Crystal system	Orthorhombic	
Space group	p2(1)2(1)2(1)	
Unit cell dimensions	a = 5.5724(8) Å	α= 90°.
	b = 12.1744(18) Å	β= 90°.
	c = 24.426(4) Å	γ = 90°.
Volume	1657.0(4) Å^3	
Z	6	

Density (calculated)	1.322 Mg/m^3
Absorption coefficient	0.239 mm^{-1}
F(000)	696
Crystal size	0.42 x 0.5 x 0.5 mm^3
Theta range for data collection	3.34 to 23.25°.
Index ranges	-6<=h<=6, -13<=k<=13, -27<=l<=27
Reflections collected	10362
Independent reflections	2367 [R(int) = 0.0435]
Completeness to theta = 23.25°	99.5 %
Refinement method	Full-matrix least-squares on F^2
Data / restraints / parameters	2367 / 0 / 221
Goodness-of-fit on F^2	1.030
Final R indices [I>2sigma(I)]	R1 = 0.0380, wR2 = 0.0913
R indices (all data)	R1 = 0.0392, wR2 = 0.0921
Absolute structure parameter	0.04(8)
Extinction coefficient	0.090(5)
Largest diff. peak and hole	0.269 and -0.306 $e.Å^{-3}$

Table 2. Atomic coordinates (x 10^4) and equivalent isotropic displacement parameters ($Å^2$x 10^3) for rovis2m. U(eq) is defined as one third of the trace of the orthogonalized U^{ij} tensor.

	x	y	z	U(eq)
C(1)	7277(5)	5131(2)	9812(1)	37(1)
C(2)	5648(4)	5471(2)	9431(1)	23(1)
C(3)	3647(5)	6066(2)	9580(1)	39(1)
C(4)	3317(5)	6331(3)	10127(1)	43(1)
C(5)	4958(6)	6004(2)	10512(1)	38(1)
C(6)	6925(5)	5397(3)	10357(1)	43(1)
C(7)	5151(5)	6845(2)	6654(1)	25(1)
C(8)	3406(5)	6411(2)	6311(1)	31(1)
C(9)	3399(5)	6663(2)	5757(1)	35(1)
C(10)	5111(5)	7351(2)	5541(1)	34(1)
C(11)	6868(5)	7776(2)	5874(1)	35(1)
C(12)	6887(5)	7515(2)	6427(1)	31(1)
C(13)	4805(5)	5599(2)	8437(1)	24(1)
C(14)	7903(4)	4680(2)	8164(1)	23(1)
C(15)	9358(4)	4328(2)	7686(1)	28(1)
C(16)	8423(4)	5112(2)	7234(1)	28(1)
C(17)	5834(4)	5431(2)	7390(1)	25(1)
C(18)	5112(5)	6607(2)	7263(1)	30(1)
N(1)	6041(3)	5234(2)	8862(1)	23(1)
N(2)	8045(4)	4643(2)	8696(1)	25(1)
N(3)	5932(3)	5248(2)	7995(1)	23(1)
Cl(1)	75(1)	7199(1)	8274(1)	29(1)
O(1)	5182(5)	8516(2)	8493(1)	60(1)

Table 3. Bond lengths [Å] and angles [°] for rovis2m.

C(1)-C(2)	1.364(3)
C(1)-C(6)	1.385(4)
C(2)-C(3)	1.378(4)
C(2)-N(1)	1.437(3)
C(3)-C(4)	1.387(4)
C(4)-C(5)	1.372(4)
C(5)-C(6)	1.376(4)
C(7)-C(12)	1.382(4)
C(7)-C(8)	1.389(4)
C(7)-C(18)	1.514(3)
C(8)-C(9)	1.387(3)
C(9)-C(10)	1.374(4)
C(10)-C(11)	1.374(4)
C(11)-C(12)	1.386(4)
C(13)-N(3)	1.319(3)
C(13)-N(1)	1.323(3)
C(14)-N(2)	1.304(3)
C(14)-N(3)	1.361(3)
C(14)-C(15)	1.485(3)
C(15)-C(16)	1.550(3)
C(16)-C(17)	1.542(3)
C(17)-N(3)	1.495(3)
C(17)-C(18)	1.520(3)
N(1)-N(2)	1.388(3)
C(2)-C(1)-C(6)	119.4(2)
C(1)-C(2)-C(3)	121.2(2)
C(1)-C(2)-N(1)	119.8(2)
C(3)-C(2)-N(1)	119.0(2)
C(2)-C(3)-C(4)	119.0(3)
C(5)-C(4)-C(3)	120.4(3)
C(6)-C(5)-C(4)	119.8(2)
C(5)-C(6)-C(1)	120.3(3)
C(12)-C(7)-C(8)	118.2(2)
C(12)-C(7)-C(18)	121.2(2)
C(8)-C(7)-C(18)	120.6(2)
C(9)-C(8)-C(7)	120.4(2)
C(10)-C(9)-C(8)	120.5(2)
C(9)-C(10)-C(11)	119.8(2)
C(10)-C(11)-C(12)	119.7(2)
C(7)-C(12)-C(11)	121.4(2)
N(3)-C(13)-N(1)	106.5(2)
N(2)-C(14)-N(3)	111.6(2)
N(2)-C(14)-C(15)	137.8(2)
N(3)-C(14)-C(15)	110.45(18)
C(14)-C(15)-C(16)	101.46(18)
C(15)-C(16)-C(17)	107.03(18)
N(3)-C(17)-C(18)	110.69(18)
N(3)-C(17)-C(16)	100.01(18)
C(18)-C(17)-C(16)	115.7(2)
C(7)-C(18)-C(17)	112.23(18)
C(13)-N(1)-N(2)	111.43(18)
C(13)-N(1)-C(2)	127.7(2)
N(2)-N(1)-C(2)	120.53(17)
C(14)-N(2)-N(1)	102.86(18)
C(13)-N(3)-C(14)	107.57(18)
C(13)-N(3)-C(17)	137.89(19)
C(14)-N(3)-C(17)	113.82(18)

Symmetry transformations used to generate equivalent atoms:

Table 4. Anisotropic displacement parameters ($Å^2 x\ 10^3$) for rovis2m. The anisotropic
displacement factor exponent takes the form: $-2\pi^2[\ h^2\ a^{*2}U^{11} + ... + 2\ h\ k\ a^*\ b^*\ U^{12}\ ]$

	U^{11}	U^{22}	U^{33}	U^{23}	U^{13}	U^{12}
C(1)	39(2)	47(2)	24(1)	-4(1)	-5(1)	11(1)
C(2)	28(1)	22(1)	19(1)	0(1)	1(1)	-5(1)
C(3)	40(2)	52(2)	26(1)	2(1)	-2(1)	14(1)
C(4)	41(2)	56(2)	32(1)	-4(1)	9(1)	15(2)
C(5)	50(2)	42(1)	22(1)	-7(1)	5(1)	-5(2)
C(6)	47(2)	59(2)	23(1)	-3(1)	-7(1)	10(2)
C(7)	26(1)	27(1)	21(1)	1(1)	2(1)	8(1)
C(8)	28(1)	41(2)	26(1)	7(1)	0(1)	-7(1)
C(9)	33(2)	49(2)	25(1)	5(1)	-6(1)	-4(1)
C(10)	43(2)	38(1)	22(1)	5(1)	2(1)	1(2)
C(11)	38(1)	34(1)	34(1)	5(1)	9(1)	-4(1)
C(12)	31(1)	33(1)	30(1)	-5(1)	-5(1)	2(1)
C(13)	22(1)	30(1)	21(1)	2(1)	0(1)	4(1)
C(14)	26(1)	21(1)	23(1)	1(1)	-2(1)	-1(1)
C(15)	25(1)	30(1)	27(1)	-2(1)	3(1)	3(1)
C(16)	28(1)	35(1)	21(1)	-3(1)	4(1)	1(1)
C(17)	27(1)	36(1)	13(1)	-1(1)	0(1)	-1(1)
C(18)	32(1)	39(1)	19(1)	-1(1)	0(1)	6(1)
N(1)	24(1)	24(1)	20(1)	1(1)	0(1)	1(1)
N(2)	26(1)	25(1)	25(1)	1(1)	2(1)	2(1)
N(3)	23(1)	30(1)	16(1)	1(1)	-2(1)	2(1)
Cl(1)	26(1)	30(1)	31(1)	-1(1)	-1(1)	3(1)
O(1)	48(1)	45(1)	89(2)	-6(1)	-13(1)	5(1)

Table 5. Hydrogen coordinates (x 10^4) and isotropic displacement parameters ($Å^2$x 10^3)
for rovis2m.

	x	y	z	U(eq)
H(1)	8640	4715	9704	44
H(3)	2512	6291	9312	47
H(4)	1947	6741	10235	52
H(5)	4736	6197	10886	46
H(6)	8048	5159	10625	52
H(8)	2210	5937	6456	38
H(9)	2202	6359	5525	42
H(10)	5080	7531	5163	41
H(11)	8064	8246	5727	43
H(12)	8119	7803	6654	38
H(13)	3385	6031	8447	29
H(15A)	9054	3549	7591	33
H(15B)	11095	4434	7753	33
H(16A)	8444	4739	6873	34
H(16B)	9446	5775	7212	34
H(18A)	3477	6743	7406	36
H(18B)	6223	7116	7451	36
H(20)	6770(110)	7850(50)	8430(20)	129(18)
H(19)	3270(120)	8000(60)	8340(30)	160(20)
H(17)	4720(50)	4920(20)	7245(9)	23(6)

Appendix 2:

Chapter 2 Crystal Structure Date for 101 and 121

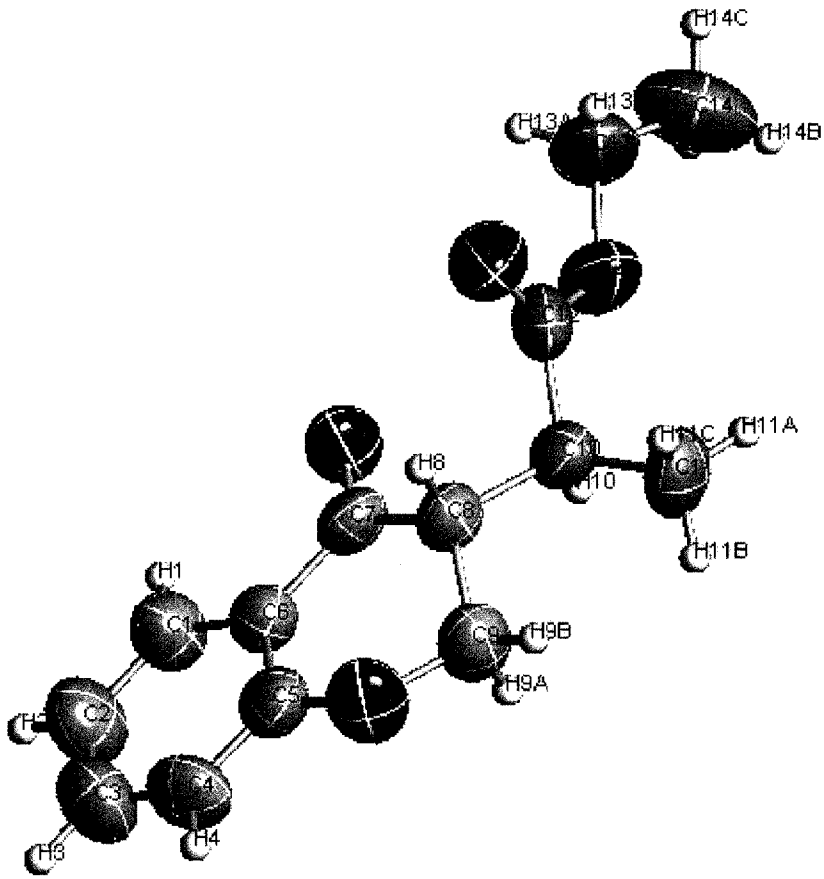

Table 1. Crystal data and structure refinement for try.

Identification code	try
Empirical formula	C14 H16 O4
Formula weight	248.27
Temperature	298(2) K
Wavelength	0.71073 Å

Crystal system	Monoclinic	
Space group	P2(1)	
Unit cell dimensions	a = 8.945(18) Å	α= 90°.
	b = 6.826(14) Å	β= 95.07(4)°.
	c = 10.57(2) Å	γ = 90°.
Volume	643(2) $Å^3$	
Z	2	
Density (calculated)	1.283 Mg/m^3	
Absorption coefficient	0.094 mm^{-1}	
F(000)	264	
Crystal size	0.08 x 0.20 x 0.40 mm^3	
Theta range for data collection	1.93 to 18.83°.	
Index ranges	-8<=h<=8, -6<=k<=6, -9<=l<=9	
Reflections collected	2519	
Independent reflections	1015 [R(int) = 0.0543]	
Completeness to theta = 18.83°	100.0 %	
Refinement method	Full-matrix least-squares on F^2	
Data / restraints / parameters	1015 / 1 / 165	
Goodness-of-fit on F^2	1.045	
Final R indices [I>2sigma(I)]	R1 = 0.0419, wR2 = 0.0980	
R indices (all data)	R1 = 0.0531, wR2 = 0.1073	
Absolute structure parameter	0(2)	
Largest diff. peak and hole	0.137 and -0.120 $e.Å^{-3}$	

Table 2. Atomic coordinates (x 10^4) and equivalent isotropic displacement parameters ($Å^2$x 10^3)
for try. U(eq) is defined as one third of the trace of the orthogonalized U^{ij} tensor.

	x	y	z	U(eq)
O(1)	6875(4)	-1605(5)	5222(3)	83(1)
O(2)	9116(3)	3157(5)	4046(3)	86(1)
O(3)	7555(5)	-61(7)	8126(3)	104(1)
O(4)	5072(5)	-203(6)	7769(3)	98(1)
C(1)	8250(5)	-1783(9)	2900(6)	82(2)
C(2)	8983(6)	-1774(10)	1821(6)	97(2)
C(3)	9786(6)	-141(13)	1530(6)	97(2)
C(4)	9838(6)	1469(10)	2276(6)	85(2)
C(5)	9067(6)	1475(8)	3350(5)	68(1)
C(6)	8276(5)	-188(8)	3689(5)	59(1)
C(7)	7544(5)	-165(8)	4880(4)	63(1)
C(8)	7679(5)	1650(6)	5658(4)	63(1)
C(9)	7877(6)	3387(8)	4810(5)	81(1)
C(10)	6328(5)	1873(6)	6455(4)	65(1)
C(11)	6196(6)	3918(7)	7048(5)	85(2)
C(12)	6438(7)	421(8)	7518(5)	82(2)
C(13)	5001(9)	-1522(11)	8830(6)	144(3)
C(14)	3578(8)	-1391(13)	9295(6)	150(3)

Table 3. Bond lengths [Å] and angles [°] for try.

O(1)-C(7)	1.222(6)
O(2)-C(5)	1.362(6)
O(2)-C(9)	1.436(6)
O(3)-C(12)	1.186(6)
O(4)-C(12)	1.343(6)
O(4)-C(13)	1.444(7)
C(1)-C(2)	1.364(7)
C(1)-C(6)	1.370(7)
C(2)-C(3)	1.376(9)
C(3)-C(4)	1.351(8)
C(4)-C(5)	1.379(7)
C(5)-C(6)	1.401(7)
C(6)-C(7)	1.469(7)
C(7)-C(8)	1.486(6)
C(8)-C(9)	1.506(7)
C(8)-C(10)	1.540(6)
C(10)-C(12)	1.494(7)
C(10)-C(11)	1.539(7)
C(13)-C(14)	1.407(8)
C(5)-O(2)-C(9)	114.0(4)
C(12)-O(4)-C(13)	117.1(4)
C(2)-C(1)-C(6)	121.4(5)
C(1)-C(2)-C(3)	119.3(5)
C(4)-C(3)-C(2)	121.4(5)
C(3)-C(4)-C(5)	119.2(5)
O(2)-C(5)-C(4)	116.9(6)
O(2)-C(5)-C(6)	122.5(5)
C(4)-C(5)-C(6)	120.6(5)
C(1)-C(6)-C(5)	118.0(4)
C(1)-C(6)-C(7)	123.0(5)
C(5)-C(6)-C(7)	119.0(5)
O(1)-C(7)-C(6)	120.8(5)
O(1)-C(7)-C(8)	121.7(4)

C(6)-C(7)-C(8)	117.5(5)
C(7)-C(8)-C(9)	109.6(4)
C(7)-C(8)-C(10)	110.8(4)
C(9)-C(8)-C(10)	112.8(4)
O(2)-C(9)-C(8)	112.7(4)
C(12)-C(10)-C(11)	107.3(4)
C(12)-C(10)-C(8)	110.1(4)
C(11)-C(10)-C(8)	113.8(4)
O(3)-C(12)-O(4)	122.9(5)
O(3)-C(12)-C(10)	126.0(6)
O(4)-C(12)-C(10)	111.0(5)
C(14)-C(13)-O(4)	109.6(6)

Symmetry transformations used to generate equivalent atoms:

Table 4. Anisotropic displacement parameters ($Å^2 x\ 10^3$) for try. The anisotropic displacement factor exponent takes the form: $-2\pi^2[\ h^2\ a^{*2}U^{11} + ... + 2\ h\ k\ a^*\ b^*\ U^{12}\ ]$

	U^{11}	U^{22}	U^{33}	U^{23}	U^{13}	U^{12}
O(1)	100(2)	55(2)	95(2)	2(2)	26(2)	-11(2)
O(2)	84(3)	69(3)	107(3)	-1(2)	27(2)	-23(2)
O(3)	106(3)	116(3)	89(2)	13(2)	7(2)	37(3)
O(4)	99(3)	86(3)	115(3)	36(2)	35(2)	16(2)
C(1)	95(4)	68(4)	83(4)	-9(4)	16(3)	-7(3)
C(2)	120(5)	87(4)	86(4)	-19(4)	25(4)	-10(5)
C(3)	87(4)	117(5)	90(4)	-4(5)	28(3)	-1(4)
C(4)	75(4)	96(6)	87(4)	14(4)	23(3)	-14(3)
C(5)	63(3)	66(5)	76(4)	5(4)	4(3)	5(3)
C(6)	56(3)	52(3)	69(3)	1(4)	6(2)	-7(3)
C(7)	64(3)	46(3)	78(4)	10(3)	3(3)	1(3)
C(8)	74(4)	45(3)	72(3)	-1(3)	9(3)	0(3)
C(9)	93(4)	60(3)	94(3)	1(3)	23(3)	0(3)
C(10)	62(3)	63(4)	72(3)	8(3)	8(3)	7(3)
C(11)	90(4)	57(4)	110(4)	-13(3)	20(3)	11(3)
C(12)	80(5)	88(5)	81(4)	3(4)	25(3)	27(4)
C(13)	187(7)	110(5)	147(5)	66(5)	87(5)	48(5)
C(14)	172(7)	171(7)	111(5)	35(5)	37(5)	-38(6)

Table 5. Hydrogen coordinates (x 10^4) and isotropic displacement parameters ($Å^2$x 10^3)
for try.

	x	y	z	U(eq)
H(1)	7721	-2895	3104	98
H(2)	8939	-2861	1288	116
H(3)	10304	-146	805	116
H(4)	10387	2561	2067	102
H(8)	8585	1535	6246	76
H(9A)	6964	3577	4257	98
H(9B)	8036	4551	5331	98
H(10)	5408	1607	5908	79
H(11A)	5337	3953	7531	128
H(11B)	6084	4883	6386	128
H(11C)	7085	4192	7596	128
H(13A)	5178	-2855	8562	172
H(13B)	5772	-1183	9498	172
H(14A)	2831	-1893	8671	225
H(14B)	3360	-46	9470	225
H(14C)	3571	-2145	10062	225

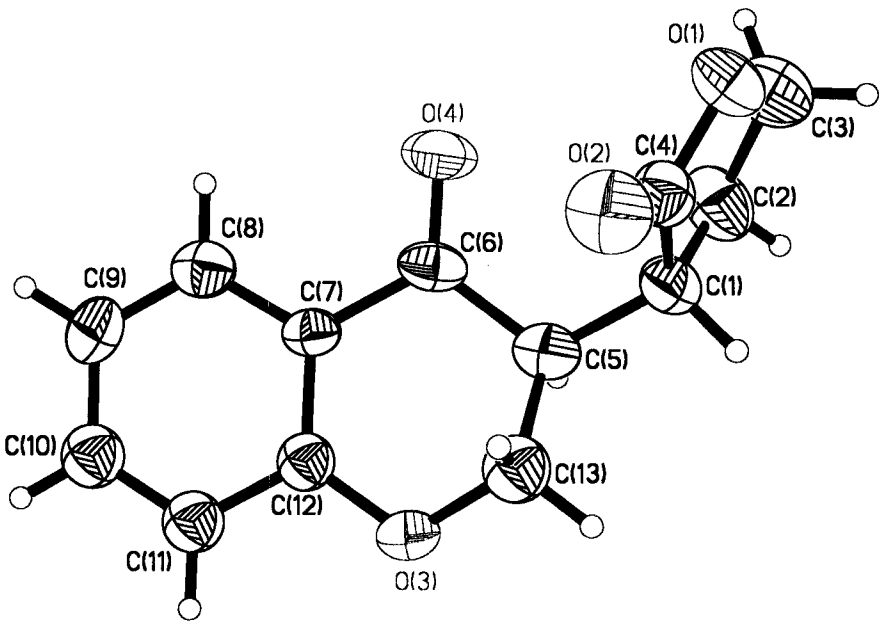

Table 1. Crystal data and structure refinement for Rovis7.

Identification code	ROVIS7	
Empirical formula	C13 H12 O4	
Formula weight	232.23	
Temperature	298(2) K	
Wavelength	0.71073 Å	
Crystal system	Orthorhombic	
Space group	P2(1)2(1)2(1)	
Unit cell dimensions	a = 6.4729(10) Å	α= 90°.
	b = 8.1736(13) Å	β= 90°.
	c = 21.179(3) Å	γ = 90°.
Volume	1120.5(3) $Å^3$	
Z	4	
Density (calculated)	1.377 Mg/m^3	
Absorption coefficient	0.102 mm^{-1}	
Absorption correction	SADABS	

F(000)	488
Crystal size	0.40 x 0.38 x 0.35 mm^3
Theta range for data collection	1.92 to 20.81°.
*High-resolution data truncated at 1.0 Å	
Index ranges	-6<=h<=6, -8<=k<=8, -21<=l<=21
Reflections collected	5636
Independent reflections	1179 [R(int) = 0.0331]
Completeness to theta = 20.81°	100.0 %
Refinement method	Full-matrix least-squares on F^2
Data / restraints / parameters	1179 / 0 / 134
Goodness-of-fit on F^2	1.016
Final R indices [I>2sigma(I)]	R1 = 0.0446, wR2 = 0.1066
R indices (all data)	R1 = 0.0603, wR2 = 0.1162
Largest diff. peak and hole	0.191 and -0.118 e.$Å^{-3}$

Table 2. Atomic coordinates (x 10^4) and equivalent isotropic displacement parameters ($Å^2$x 10^3) for rovis7. U(eq) is defined as one third of the trace of the orthogonalized U^{ij} tensor.

	x	y	z	U(eq)
O(1)	2022(5)	4053(4)	7368(1)	90(1)
O(2)	3655(6)	5720(5)	8006(2)	104(1)
O(3)	4123(4)	4004(3)	10027(1)	78(1)
O(4)	-487(5)	4500(4)	8735(1)	98(1)
C(1)	3127(8)	2874(6)	8308(2)	78(1)
C(2)	1674(10)	1689(7)	7996(2)	106(2)
C(3)	1324(9)	2369(8)	7364(2)	108(2)
C(4)	2999(7)	4400(7)	7900(2)	76(1)
C(5)	2696(7)	3177(6)	9008(2)	79(1)
C(6)	837(7)	4270(5)	9123(2)	70(1)
C(7)	726(6)	4977(5)	9764(2)	58(1)
C(8)	-1010(8)	5804(5)	9969(2)	73(1)
C(9)	-1194(8)	6342(5)	10584(2)	82(1)
C(10)	401(7)	6069(6)	10994(2)	81(1)
C(11)	2126(7)	5309(5)	10810(2)	77(1)
C(12)	2342(7)	4761(5)	10186(2)	66(1)
C(13)	4478(8)	3879(6)	9358(2)	86(1)

Table 3. Bond lengths [Å] and angles [°] for rovis7.

O(1)-C(4)	1.323(5)
O(1)-C(3)	1.449(6)
O(2)-C(4)	1.181(5)
O(3)-C(12)	1.351(5)
O(3)-C(13)	1.439(5)
O(4)-C(6)	1.203(4)
C(1)-C(2)	1.503(7)
C(1)-C(4)	1.520(6)
C(1)-C(5)	1.528(6)
C(2)-C(3)	1.467(6)
C(5)-C(13)	1.487(6)
C(5)-C(6)	1.519(6)
C(6)-C(7)	1.476(5)
C(7)-C(8)	1.381(6)
C(7)-C(12)	1.387(5)
C(8)-C(9)	1.379(6)
C(9)-C(10)	1.369(6)
C(10)-C(11)	1.336(6)
C(11)-C(12)	1.403(5)

C(4)-O(1)-C(3)	110.9(4)	O(4)-C(6)-C(7)	122.2(4)
C(12)-O(3)-C(13)	114.5(3)	O(4)-C(6)-C(5)	123.1(4)
C(2)-C(1)-C(4)	104.2(4)	C(7)-C(6)-C(5)	114.7(4)
C(2)-C(1)-C(5)	114.6(4)	C(8)-C(7)-C(12)	118.2(4)
C(4)-C(1)-C(5)	114.1(4)	C(8)-C(7)-C(6)	121.4(4)
C(3)-C(2)-C(1)	104.7(4)	C(12)-C(7)-C(6)	120.4(4)
O(1)-C(3)-C(2)	107.9(4)	C(7)-C(8)-C(9)	121.6(4)
O(2)-C(4)-O(1)	121.9(5)	C(10)-C(9)-C(8)	118.9(4)
O(2)-C(4)-C(1)	128.5(5)	C(11)-C(10)-C(9)	121.4(4)
O(1)-C(4)-C(1)	109.5(4)	C(10)-C(11)-C(12)	120.4(4)
C(13)-C(5)-C(6)	107.9(4)	O(3)-C(12)-C(7)	122.8(4)
C(13)-C(5)-C(1)	113.9(4)	O(3)-C(12)-C(11)	117.7(4)
C(6)-C(5)-C(1)	113.3(4)	C(7)-C(12)-C(11)	119.5(4)

O(3)-C(13)-C(5)	113.3(4)

Table 4. Anisotropic displacement parameters ($Å^2 x\ 10^3$) for rovis7. The anisotropic displacement factor exponent takes the form: $-2\pi^2[\ h^2\ a^{*2}U^{11} + ...\ + 2\ h\ k\ a^*\ b^*\ U^{12}\ ]$

	U^{11}	U^{22}	U^{33}	U^{23}	U^{13}	U^{12}
O(1)	108(2)	102(3)	59(2)	8(2)	-2(2)	-8(2)
O(2)	113(3)	81(2)	118(3)	1(2)	-4(2)	-21(2)
O(3)	74(2)	91(2)	69(2)	3(2)	-18(2)	22(2)
O(4)	76(2)	151(3)	68(2)	15(2)	-19(2)	11(2)
C(1)	91(4)	83(3)	59(3)	0(3)	-8(3)	7(3)
C(2)	142(5)	94(4)	80(4)	1(3)	3(4)	-11(4)
C(3)	120(5)	108(4)	96(4)	1(3)	-16(4)	-21(4)
C(4)	72(3)	88(4)	67(3)	0(3)	7(3)	-3(3)
C(5)	80(3)	82(3)	77(3)	4(2)	-14(3)	-3(3)
C(6)	69(3)	83(3)	57(3)	20(2)	-13(3)	-8(3)
C(7)	57(2)	53(2)	64(3)	8(2)	-14(2)	0(2)
C(8)	77(3)	63(3)	80(3)	9(3)	-11(2)	-5(3)
C(9)	82(3)	65(3)	99(4)	-5(3)	8(3)	10(3)

Table 5. Hydrogen coordinates (x 10^4) and isotropic displacement parameters ($Å^2$x 10^3) for rovis7.

	x	y	z	U(eq)
H(1A)	4529	2432	8271	93
H(2A)	2288	609	7970	127
H(2B)	387	1613	8229	127
H(3A)	2088	1745	7052	129
H(3B)	-133	2319	7259	129
H(5A)	2388	2113	9199	95
H(8A)	-2079	6003	9686	88
H(9A)	-2382	6882	10717	99
H(10A)	281	6419	11411	98
H(11A)	3191	5142	11098	92
H(13A)	5683	3199	9286	103
H(13B)	4776	4959	9192	103

Appendix 3:

Chapter 4 Crystal Structure Data 44

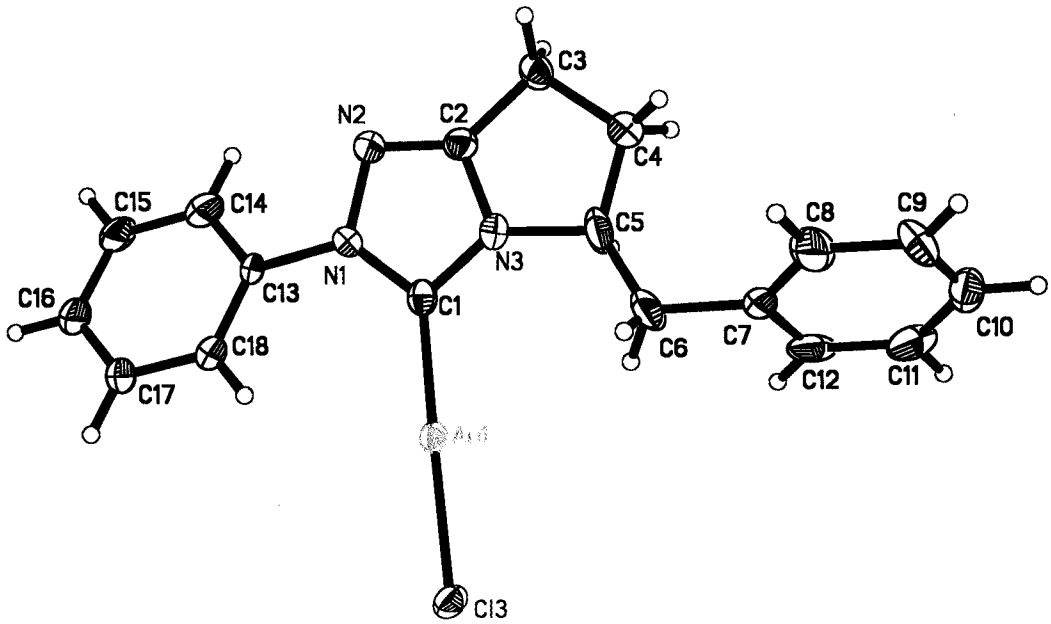

Crystal data and structure refinement for rovis14.		
Identification code	14p1bar	
Empirical formula	C18 H17 Au Cl N3	
Formula weight	507.76	
Temperature	100(2) K	
Wavelength	0.71073 Å	
Crystal system	Triclinic	
Space group	P-1	
Unit cell dimensions	a = 9.7511(15) Å	α= 62.392(2)°.
	b = 10.3347(16) Å	β= 62.942(2)°.
	c = 10.5311(16) Å	γ = 86.758(3)°.
Volume	821.3(2) $Å^3$	
Z	2	
Density (calculated)	2.053 Mg/m^3	

Absorption coefficient	9.120 mm^{-1}
F(000)	484
Crystal size	0.45 x 0.30 x 0.15 mm^3
Theta range for data collection	2.27 to 28.27°.
Index ranges	-12<=h<=12, -13<=k<=13, -13<=l<=13
Reflections collected	5150
Independent reflections	3550 [R(int) = 0.0199]
Completeness to theta = 28.27°	87.5 %
Absorption correction	multi-scan
Max. and min. transmission	0.3416 and 0.1050
Refinement method	Full-matrix least-squares on F^2
Data / restraints / parameters	3550 / 0 / 208
Goodness-of-fit on F^2	1.040
Final R indices [I>2sigma(I)]	R1 = 0.0387, wR2 = 0.0967
R indices (all data)	R1 = 0.0431, wR2 = 0.0982
Largest diff. peak and hole	3.778 and -2.378 e.$Å^{-3}$

Table 2. Atomic coordinates (x 10^4) and equivalent isotropic displacement parameters ($Å^2$x 10^3) for rovis14. U(eq) is defined as one third of the trace of the orthogonalized U^{ij} tensor.

	x	y	z	U(eq)
Au(1)	3187(1)	3261(1)	2543(1)	18(1)
Cl(3)	1458(2)	4030(2)	1562(2)	26(1)
C(1)	4681(9)	2542(8)	3374(9)	21(1)
N(1)	4764(8)	2445(8)	4661(8)	25(1)
N(3)	5946(7)	1963(7)	2747(7)	20(1)
C(2)	6722(9)	1598(9)	3615(9)	23(2)
N(2)	6018(8)	1866(9)	4839(8)	30(2)
C(18)	2272(10)	3120(11)	6086(10)	33(2)
C(17)	1415(11)	3653(11)	7148(10)	35(2)
C(14)	4441(12)	3285(12)	6571(11)	40(2)
C(13)	3788(9)	2950(9)	5798(9)	25(2)
C(15)	3557(12)	3795(11)	7631(11)	39(2)
C(16)	2031(12)	3989(12)	7931(11)	42(2)
C(3)	8148(9)	1026(10)	2936(9)	26(2)
C(4)	8079(12)	1075(12)	1479(11)	42(2)
C(5)	6686(12)	1630(16)	1382(14)	54(3)
C(7)	7011(15)	1586(16)	-1042(15)	63(4)
C(6)	6060(20)	1820(30)	430(20)	145(11)
C(10)	8778(10)	1219(11)	-3743(11)	34(2)
C(11)	8583(12)	2630(11)	-3955(12)	39(2)
C(9)	8092(10)	34(11)	-2207(11)	36(2)
C(12)	7714(14)	2810(13)	-2610(15)	52(3)
C(8)	7222(13)	216(15)	-861(12)	57(3)

Table 3. Bond lengths [Å] and angles [°] for rovis14.

Au(1)-C(1)	1.969(7)
Au(1)-Cl(3)	2.2830(17)
C(1)-N(1)	1.352(9)
C(1)-N(3)	1.363(9)
N(1)-N(2)	1.381(8)
N(1)-C(13)	1.449(9)
N(3)-C(2)	1.353(9)
N(3)-C(5)	1.480(10)
C(2)-N(2)	1.308(10)
C(2)-C(3)	1.480(11)
C(18)-C(13)	1.386(11)
C(18)-C(17)	1.386(11)
C(17)-C(16)	1.379(12)
C(14)-C(15)	1.373(12)
C(14)-C(13)	1.394(11)
C(15)-C(16)	1.397(13)
C(3)-C(4)	1.544(11)
C(4)-C(5)	1.472(12)
C(5)-C(6)	1.331(14)
C(7)-C(8)	1.355(17)
C(7)-C(12)	1.389(18)
C(7)-C(6)	1.527(13)
C(10)-C(9)	1.355(13)
C(10)-C(11)	1.384(13)
C(11)-C(12)	1.376(14)
C(9)-C(8)	1.378(13)

C(1)-Au(1)-Cl(3)	178.1(2)
N(1)-C(1)-N(3)	101.1(6)
N(1)-C(1)-Au(1)	132.3(6)
N(3)-C(1)-Au(1)	126.6(5)
C(1)-N(1)-N(2)	114.6(6)
C(1)-N(1)-C(13)	128.9(6)
N(2)-N(1)-C(13)	116.3(6)

C(2)-N(3)-C(1)	110.7(6)
C(2)-N(3)-C(5)	112.2(7)
C(1)-N(3)-C(5)	137.1(6)
N(2)-C(2)-N(3)	110.9(7)
N(2)-C(2)-C(3)	136.4(7)
N(3)-C(2)-C(3)	112.7(6)
C(2)-N(2)-N(1)	102.7(6)
C(13)-C(18)-C(17)	118.5(8)
C(16)-C(17)-C(18)	121.4(8)
C(15)-C(14)-C(13)	118.9(8)
C(18)-C(13)-C(14)	121.2(7)
C(18)-C(13)-N(1)	121.3(7)
C(14)-C(13)-N(1)	117.5(7)
C(14)-C(15)-C(16)	121.0(8)
C(17)-C(16)-C(15)	118.9(8)
C(2)-C(3)-C(4)	101.0(6)
C(5)-C(4)-C(3)	110.9(7)
C(6)-C(5)-C(4)	134.6(9)
C(6)-C(5)-N(3)	122.3(8)
C(4)-C(5)-N(3)	103.1(7)
C(8)-C(7)-C(12)	118.7(9)
C(8)-C(7)-C(6)	121.7(14)
C(12)-C(7)-C(6)	119.5(13)
C(5)-C(6)-C(7)	117.6(10)
C(9)-C(10)-C(11)	119.2(8)
C(12)-C(11)-C(10)	119.7(9)
C(10)-C(9)-C(8)	121.0(9)
C(11)-C(12)-C(7)	120.6(9)
C(7)-C(8)-C(9)	120.8(10)

Symmetry transformations used to generate equivalent atoms:

Table 4. Anisotropic displacement parameters ($Å^2 x\ 10^3$) for rovis14. The anisotropic displacement factor exponent takes the form: $-2\pi^2[\ h^2\ a^{*2}U^{11} + ...\ + 2\ h\ k\ a^*\ b^*\ U^{12}\ ]$

	U^{11}	U^{22}	U^{33}	U^{23}	U^{13}	U^{12}
Au(1)	21(1)	18(1)	16(1)	-10(1)	-9(1)	5(1)
Cl(3)	35(1)	29(1)	27(1)	-18(1)	-21(1)	14(1)
C(1)	23(4)	19(3)	19(3)	-11(3)	-8(3)	3(3)
N(1)	22(3)	35(4)	22(3)	-17(3)	-12(3)	14(3)
N(3)	21(3)	21(3)	17(3)	-10(2)	-6(3)	0(3)
C(2)	20(4)	27(4)	22(3)	-10(3)	-11(3)	5(3)
N(2)	23(4)	48(4)	25(3)	-21(3)	-14(3)	15(3)
C(18)	36(5)	48(5)	23(4)	-21(4)	-18(4)	21(4)
C(17)	38(5)	55(6)	27(4)	-29(4)	-19(4)	26(5)
C(14)	50(6)	57(6)	36(5)	-30(5)	-32(5)	27(5)
C(13)	27(4)	39(4)	17(3)	-18(3)	-12(3)	16(4)
C(15)	55(6)	58(6)	37(5)	-36(5)	-36(5)	30(5)
C(16)	52(6)	64(7)	31(4)	-34(5)	-27(4)	35(5)
C(3)	16(4)	32(4)	25(4)	-15(3)	-7(3)	4(3)
C(4)	43(6)	60(6)	34(5)	-29(5)	-23(4)	31(5)
C(5)	40(6)	111(10)	56(6)	-70(7)	-30(5)	43(6)
C(7)	81(8)	116(11)	68(7)	-79(8)	-65(7)	81(8)
C(6)	145(15)	330(30)	157(16)	-220(20)	-136(14)	203(19)
C(10)	28(5)	50(5)	33(4)	-28(4)	-14(4)	7(4)
C(11)	52(6)	36(5)	46(5)	-18(4)	-38(5)	12(4)
C(9)	26(5)	38(5)	39(5)	-24(4)	-8(4)	14(4)
C(12)	82(8)	64(7)	96(9)	-69(7)	-82(8)	59(6)
C(8)	46(6)	85(9)	26(5)	-23(5)	-13(5)	36(6)

Table 5. Hydrogen coordinates (x 10^4) and isotropic displacement parameters ($Å^2$x 10^3) for rovis14.

	x	y	z	U(eq)
H(18A)	1830	2876	5567	39
H(17A)	381	3790	7340	42
H(14A)	5480	3161	6368	48
H(15A)	3990	4020	8168	47
H(16A)	1428	4347	8662	50
H(3A)	8094	-2	3741	31
H(3B)	9110	1676	2566	31
H(4A)	9038	1732	448	50
H(4B)	8043	63	1609	50
H(5A)	7312	2670	616	65
H(6A)	5854	2842	21	174
H(6B)	5035	1126	1124	174
H(10A)	9385	1084	-4662	41
H(11A)	9047	3470	-5025	47
H(9A)	8213	-938	-2055	43
H(12A)	7594	3780	-2756	63
H(8A)	6764	-629	206	69